Conference Paper

by Prof.Dr. Lukas Novotny, University of Rochester

NFO-7:7th International Conference on Near-Field Optics and Related Techniques

University of Rochester, Rochester, NY (August 24 –28, 2002)

The seventh conference in the NFO conference series, held here in Rochester, provided to be the principal forum for advances in sub-wavelength optics, near-field optical microscopy, local field enhancement, instrumental developments and the ever-increasing range of applications. This conference brought together the diverse scientific communities working on the theory and application of near-field optics (NFO) and related techniques.

Many of the technologies earmarked for significant growth in the coming decades are critically dependent on credible nanometer-scale measurements and analysis. Therefore, physicists, chemists, biologists, and engineers are joining forces to observe, and understand, and control nanometer scale structures and events through the use of NFO. Efforts in the NFO over the past ten years have demonstrated that spatial resolution down to approximately 20nm can be achieved, offering significant improvement over conventional optical methods such as tunneling and force microscopy. The broad range of capabilities, including high spatial resolution spectroscopy, orientational sensitivity, ultra-fast detection, and the ability of operating in UHV, ambient and even liquid conditions while maintaining molecular sensitivity and resolution, leads to the assumption that the NFO communities are joining forces for a *breakthrough* technology.

At the conference, we were able to create an environment for open exchange or topical research information and to stimulate discussion on novel concepts and fields of application. Nearly 250 international scientists participated, as well as the leading manufacturers of scanning probe techniques and optical microscopy. New application areas were presented and various novel ideas emerged. I would also like to emphasize three factors which added to the overall success of the conference and proved that the mission of the NFO-7 has been fulfilled. Those factors were: 1) the quality of the presented work, 2) the quality of the presentations, and 3) the comradeship within the NFO community. I am positive that these factors will carry over to the next NFO conference in Seoul 2004, which hopefully will bring together the same quality of scientific work.

I would like to express my gratitude to the DOE, Chemical Sciences, Geosciences and Biosciences Division, Office of Basic Energy Sciences, Office of Science for supporting this very successful conference with the award DE-FG-02-ER15371 and hope that the DOE will be continuously involved and interested in the field of near-field optics. I apologize for any delays in the submission of this conference paper.

DISCLAIMER

NFO7

The 7th International Conference on
Near-field Optics and Related Techniques

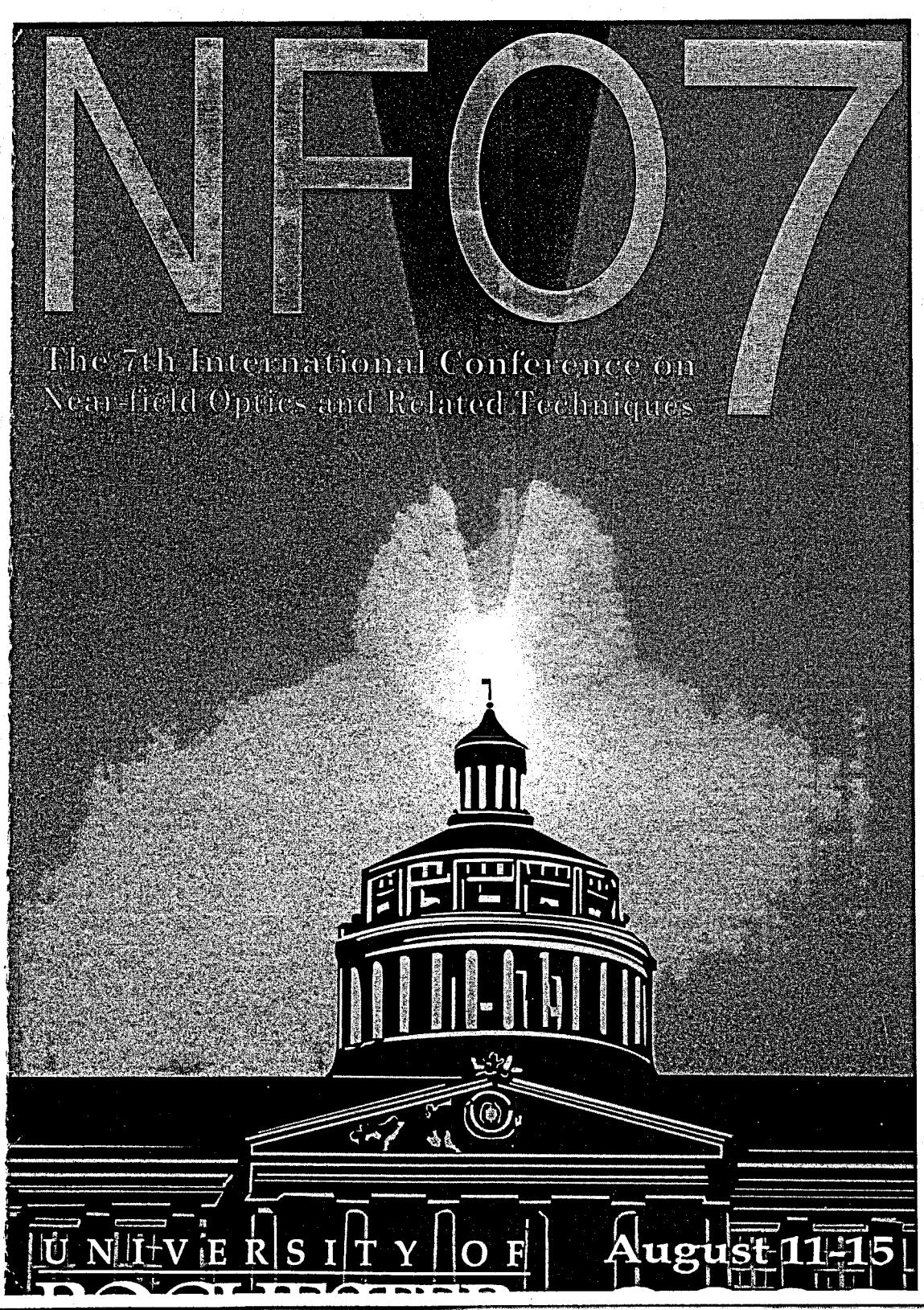

UNIVERSITY OF

August 11-15

Conference Organization

Novotny, Lukas, University of Rochester, Rochester, NY, USA
Stranick, Stephan J., National Institute of Standards and Technology (NIST), Gaithersburg, MD, USA

NFO-7 International Advisory Committee

Adams, David M., Columbia University, USA
Boccara, A. Claude, ESPCI, France
De Schryver, Frans, University of Leuven, Belgium
Dereux, Alain, University of Burgundy, France
Dunn, Robert C., University of Kansas, USA.
Fischer, Ulrich, University of Muenster, Germany
Goldberg, Bennett, Boston University, USA.
Greffet, Jean-Jacques, Ecole Centrale Paris, France
Hecht, Bert, University of Basel, Switzerland
Hell, Stefan, Max Planck Institute, Germany
Heinzelmann, Harry, CSEM, Switzerland
Jhe, Wonho, Seoul National University, Korea
Kawata, Satoshi, Osaka University, Japan
Keilmann, Fritz, Max Planck Institute, Germany
Lienau, Christoph, Max Born Institute, Germany
Meixner, Alfred, University of Siegen, Germany
Nesbitt, David J., NIST, USA
Ohtsu, Motoichi, Tokyo Inst. of Technology, Japan
Paesler, Michael, North Carolina State University, USA
Pohl, Dieter W., University of Basel, Switzerland
Sandoghdar, Vahid, ETH Zurich, Switzerland
Van Hulst, Niek F., University of Twente, The Netherlands
Van Labeke, Daniel, University of Franche-Comte, France
Xie, Sunney X., Harvard University, USA.

Publications Chairman

Adams, David M., Columbia University, USA

Local Organizing Committee

Novotny, Lukas
Albee, Mary A.
Benedict, Elisabeth L.
Beversluis, Michael R.
Bouhelier, Alexandre
Hartschuh, Achim
Ignatovitch, Filipp
Zurita-Sanchez, Jorge

Hotel Accomodations

Special room rates, for single or double occupancy, are being extended to NFO-7 conference attendees at the Holiday Inn Rochester Airport ($79/night + tax) and the Radisson Hotel Rochester Airport ($85/night + tax). To make your reservations and receive the special conference rate please follow instructions on the NFO-7 website.

Transportation

Bus service will be provided during the conference from the contracted hotels to the University campus, as well as to the George Eastman House, conference excursion, and conference banquet.

Local Map

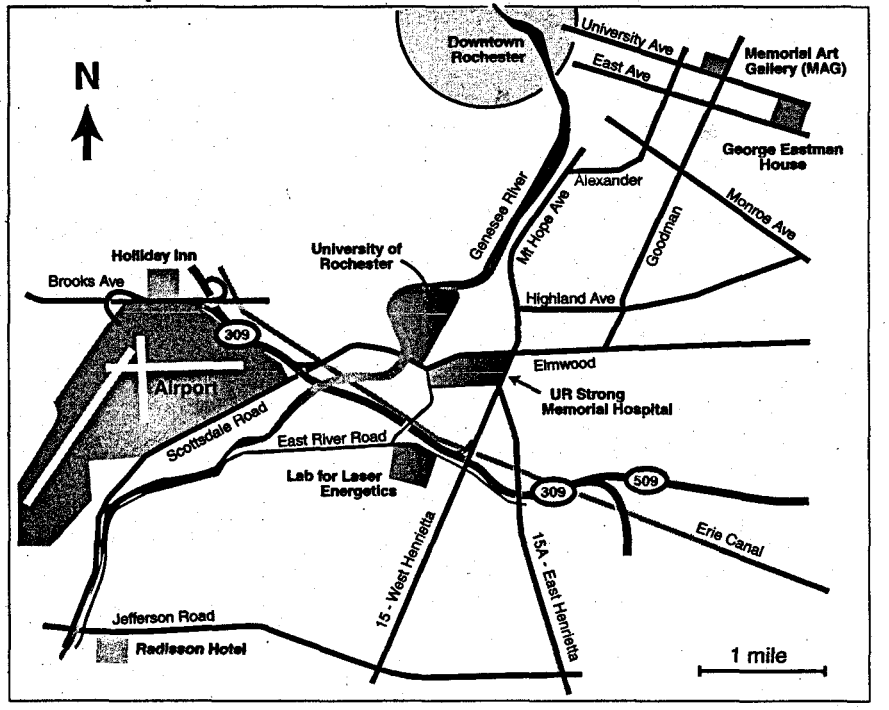

NFO-7 Contact Information

Registration and Logistics:

University of Rochester
Conference & Events Office
Re: NFO-7 Conference
33A Wallis Hall
Rochester, NY 14627, USA.

Phone: (716) 275-4111
Fax: (716) 275-8531
E-Mail: nfo7@services.rochester.edu

Submissions:

Betsy Benedict
University of Rochester
NFO-7, The Institute of Optics
Box 270186
Rochester, NY 14627, USA.

Phone: (716) 275-7720
Fax: (716) 244-4936
E-Mail: nfo7@optics.rochester.edu

Objective

The current trend towards nanoscience and nanotechnology makes it necessary to address the key issues of optics on the nanometer scale. The interaction of light with matter renders unique information about the structural and dynamic properties of matter and is of great importance for the study of biological and solid-state nano-structures. Near-field optics and nano-optics in general address the key issues of optics on the nanometer scale covering technology and basic sciences.

The NFO conference series is the principal forum for advances in sub-wavelength optics and the growing field of nano-optics in general. Scientists from different fields are joining forces to observe, understand, and control nanometer scale structures and phenomena through the use of NFO. The goal of this conference is to create an environment for open exchange of topical research information and to stimulate discussion on novel concepts and fields of application. All contributions relevant to NFO that are directed towards these goals will be welcomed for presentation.

Conference Topics

- o Light in confined structures
- o Novel concepts in near-field optics
- o Advances in instrumentation
- o Local field enhancement
- o Cavity nano-optics
- o Nonlinear and ultrafast phenomena
- o Nanofabrication and manipulation
- o Theory and modeling
- o Nano-optics of single molecules and quantum dots
- o Applications in material science
- o Applications in biology
- o Applications in chemistry
- o Industrial applications

Conference Program

The complete conference program and schedule of social events can be accessed through the NFO-7 website at **http://www.optics.rochester.edu/events/nfo7**.

Location

NFO-7 welcomes participants to Rochester, located in Upstate Western New York on Lake Ontario -- just 1.5 hours from Niagara Falls and 3 hours from Toronto by car. The conference will be held at the University of Rochester, which is only 10 minutes from the Rochester International Airport. Serviced by all major airlines, Rochester is roughly one hour from airports in New York City, Boston, Philadelphia, Baltimore, and Washington DC.

Registration Information

The NFO-7 conference kicks off with an evening reception at the famed George Eastman House on Sunday, August 11 at 6:00pm. The conference ends at noon on Thursday, August 15 and is immediately followed by an optional excursion to Niagara Falls. Registration fee includes the welcome reception, Genesee Country Museum excursion, conference banquet, abstract book, shuttle service, and meals (excl. breakfast). Please see the NFO-7 website for complete conference agenda and to obtain a registration form.

Registration Fees:

Early Bird (by June 1, 2002)	$ 400 (USD)
Regular (after June 1, 2002)	$ 600 (USD)
Student* Early Bird (by June 1, 2002)	$ 250 (USD)
Student* Regular (after June 1, 2002)	$ 450 (USD)
Guest**	$ 180 (USD)
Niagara Falls excursion	$ 80 (USD)

**Advisors of students (undergraduate or graduate) must sign and submit a "student status confirmation form" (available on NFO-7 website).*

***Guest fee covers welcome reception, conference banquet, Genesee Country Museum excursion, and shuttle service.*

Register directly online or download a registration form at:

http://www.optics.rochester.edu/events/nfo7

Cancellations

Written cancellations received before 15 July, 2002 will be subject to an administrative charge of $ 50 (USD). No refunds will be given after this date.

Submission of Abstracts

Conference participants are invited to submit abstracts for consideration for oral or poster presentation. Abstracts should be written electronically using the templates (Word or LaTeX) which are accessible through the NFO-7 webpage. Abstracts should be submitted electronically as e-mail attachments to **nfo7@optics.rochester.edu**. Further instructions can be found on the NFO-7 website. Your abstract should be received before **1 April, 2002**.

Manuscripts for NFO-7 Proceedings

The Journal of Microscopy will publish a limited number of papers presented at NFO-7. Authors of accepted abstracts are invited to submit a manuscript (6 page limit) which will be reviewed during the NFO-7 conference. Please refer to the instructions on the NFO-7 website for further information. Manuscript submission deadline is **11 August, 2002** (at the conference).

NFO7

The 7th International Conference on
Near-field Optics and Related Techniques

UNIVERSITY OF
ROCHESTER

August 11-15
2002

SUNDAY, AUGUST 11th

Registration & Reception	6:30pm – 8:30pm

Schlegel Hall Rotunda
Hubble Audiorium
Lander Auditorium
Wilson Commons

For other locations, see map on the back cover

MONDAY, AUGUST 12th

Effects Of Coherence on the Spectra of Optical Field — *E. Wolf*		8:00 – 9:00
Cavity Nano-optics & Novel Concepts in Near-Field Optics	Advances in Instrumentation	9:00 – 10:00
Coffee Break & Technical Exhibition		10:00 – 10:30
Light in Confined Structures	Advances in Instrumentation	10:30 – 12:10
Lunch		12:10 – 1:30
Light in Confined Structures	Advances in Instrumentation	1:30 – 3:30
Coffee Break & Technical Exhibition		3:30 – 4:00
Light in Confined Structures	Applications in Biology	4:00 – 6:00
Group Photo		6:00 – 7:00
Monday Poster Session		

TUESDAY, AUGUST 13th

Coherence and Manipulation of Spin States in Semiconductor nanostructures — *J. Gupta*		8:00 – 9:00
Theory & Modeling	Applications in Material Sciences	9:00 – 10:00
Coffee Break & Technical Exhibition		10:00 – 10:30
Novel Concepts in Near-Field Optics	Applications in Material Sciences	10:30 – 12:10
Lunch		12:10 – 1:30
Novel Concepts in Near-Field Optics	Industrial Applications & Applications in Chemistry	1:30 – 3:30
Coffee Break & Technical Exhibition		3:30 – 4:00
Novel Concepts in Near-Field Optics	Theory & Modeling	4:00 – 6:00
Tuesday Poster Session		6:00 – 7:00

WEDNESDAY, AUGUST 14th

Quantum Information Science

I. Walmsley

Theory and Modeling & Local Field Enhancement	Nanofabrication and Manipulation

Coffee Break & Technical Exhibition

Local Field Enhancement	Nanofabrication and Manipulation & Nano-Optics of SM and QD

Excursion to Genessee Village & Museums

Conference Banquet

8:00

9:00

10:00

10:30

12:50

1:30

7:00

THURSDAY, AUGUST 15th

Dynamics of Biophysical Processes Studied with Multiphoton Microscopy

A. Heikal

Non-linear and Ultrafast Phenomena	Theory & Modeling

Coffee Break & Technical Exhibition

Non-linear and Ultrafast Phenomena & Local field enhancement	Nano-Optics of SM and QD

Final Remarks

Excursion to Niagara Falls

Hubble Audiorium

Lander Auditorium

George Eastman House

Organizers of NFO7 gratefully acknowledge the following organizations and companies for their generous support:

The National Institute of Standards (NIST)

TM Microscopes, Veeco Metrology Group

US Department of Energy

The Institute of Optics, University of Rochester

JPK Instruments AG.

WITec Wissenschaftliche Instrumente und Technologie GmbH.

Coherent, Inc.

Organizing committee

This conference was made possible by

Lukas Novotny, Institute of Optics, University of Rochester, Rochester, NY, USA

Stephan J. Stranick, National Institute of Standards and Technology (NIST), Gaithersburg, MD, USA

NFO7 International Advisory Committee

David M Adams, Columbia University, USA
Claude A. Boccara, ESPCI, France
Frans De Schryver, University of Leuven, Belgium
Alain Dereux, University of Burgundy, France
Robert C .Dunn, University of Kansas, USA
Ulrich Fischer, University of Muenster, Germany
Bennett Goldberg, Boston University, USA
Jean-Jacques Greffet, Ecole Centrale Paris, France
Bert Hecht, University of Basel, Switzerland
Stefan Hell, Max Planck Institute, Germany
Harry Heinzelmann, CSEM, Switzerland
Wonho Jhe, Seoul National University, Korea
Satoshi Kawata, Osaka University, Japan
Fritz Keilmann, Max Planck Institute, Germany
Christoph Lienau, Max Bron Institute, Germany
Alfred Meixner, University of Siegen, Germany
David J. Nesbitt, NIST USA
Motoichi Ohtsu, Tokyo Inst. Of Technology, Japan
Michael Paesler, North Carolina State University, USA
Dieter W. Pohl, University of Basel, Switzerland
Vahid Sandoghdar, ETH Zurich, Switzerland
Niek F. Van Hulst, University of Twente, The Netherlands
Daniel Van Labeke, University of Franche-Comte, France
Sunney X. Xie, Harvard University, USA

Local Organizing Committee

Lukas Novotny *(chair)*
Neil Anderson
M. Andreas Lieb
Elizabeth L. Benedict *(abstract book)*
Michael R. Beversluis *(NFO7 website and logo)*
Alexandre Bouhelier *(submissions)*
Achim Hartschuh
Al Heaney
Filipp Ignatovich *(abstract book)*
Mi Young Molly Park *(abstract book)*
Nicole M. Putnam *(abstract book)*
Jorge Zurita-Sanchez

Conference and Events Office

Mary Albee
Celia Palmer
Amy Stark
Denise Soudan
Julie Blowers
Angie Coleman
Amy Webster
Andrew Snyder *(student)*

Proceedings publication chairman

David M Adams, Columbia University, USA

Table of Contents

112 Robin Hill Road • Santa Barbara, CA 93117 • Tel: 805-967-1400 • Fax: 805-967-7717 • Website: www.di.com, www.veeco.com

Digital Instruments, Veeco Metrology Group

Digital Instruments, Veeco Metrology Group
112 Robin Hill Road
Santa Barbara, CA 93117
805-967-1400
Fax: 805-967-7717
www.di.com and www.veeco.com

Digital Instruments, Veeco Metrology Group will exhibit its Aurora-3™ Near-Field Scanning Optical Microscope (NSOM), which significantly extends the capabilities of the standard-setting Aurora family of near-field microscopy systems. Digital Instruments Aurora-3, the most advanced NSOM platform available, combines industry-leading, patented tuning-fork technology with several new features to bring greater ease-of use to the researcher.

The Aurora-3 combines optical characterization with scanning probe microscopy (SPM) technology to overcome the diffraction limit of conventional optical equipment. A real-time linearized scanner provides accurate, one-step tip positioning, which is particularly important in such applications as single-molecule fluorescence. With its compatibility with the award winning Explorer SPM head, optional atomic force microscopy capabilities are also possible. Despite all of this, the Aurora-3 has a conveniently small footprint. These and the other ease-of-use features of the Aurora-3 will certainly bring the advantages of NSOM techniques to a greater number of general research studies.

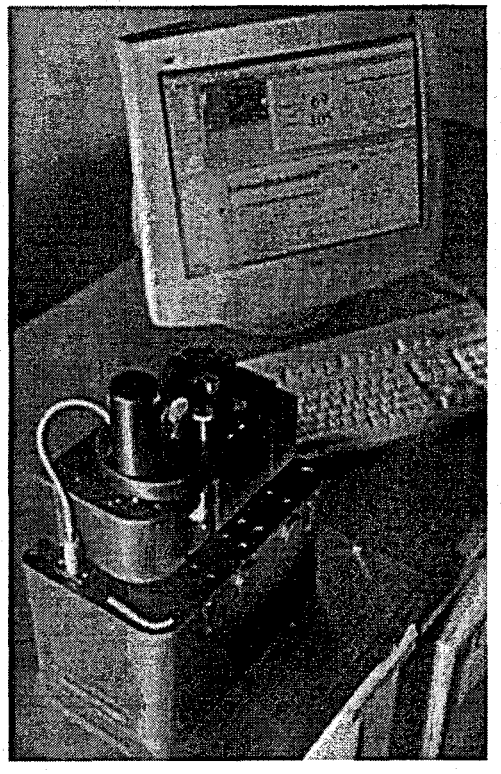

Aurora-3
Next-Generation NSOM

Alpha*SNOM*

3 high-resolution microscopes in one instrument

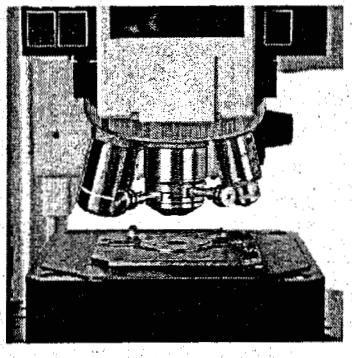

Confocal Laser Scanning Microscope (CLSM)
with sub µm-depth-resolution

Scanning Nearfield Optical Microscope (SNOM)
using unique Cantilever-SNOM-Sensors

Atomic Force Microscope (AFM)
providing local stiffness and adhesion

precise
versatile
easy to use

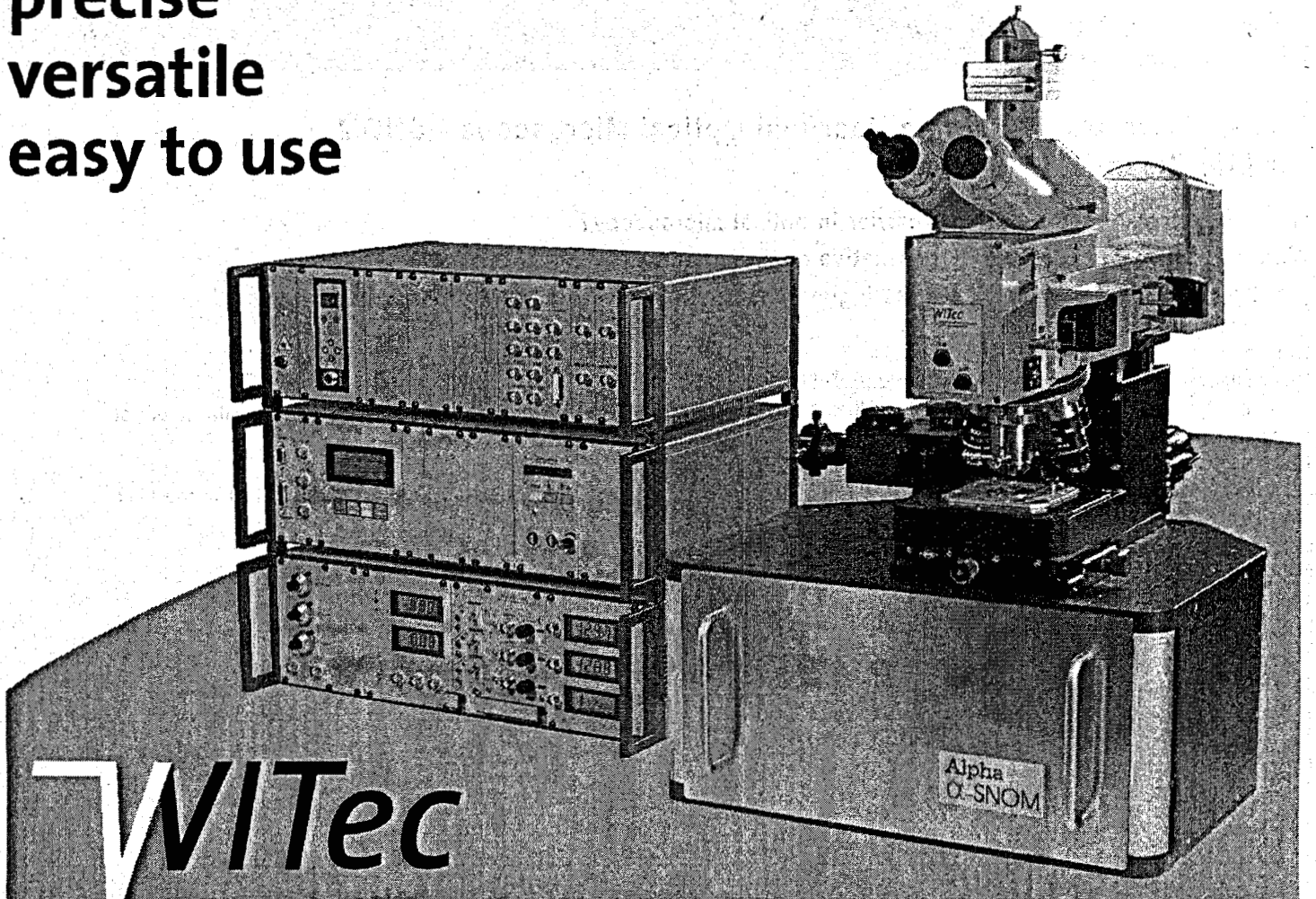

WITec

Wissenschaftliche Instrumente
und Technologie GmbH

Hörvelsinger Weg 6, D-89081 Ulm, Germany, email: info@WITec.de
fon +49 (0)700 94832-366, fax -329, www.WITec.de

jpk
INSTRUMENTS *Nanotechnology for Life Science*

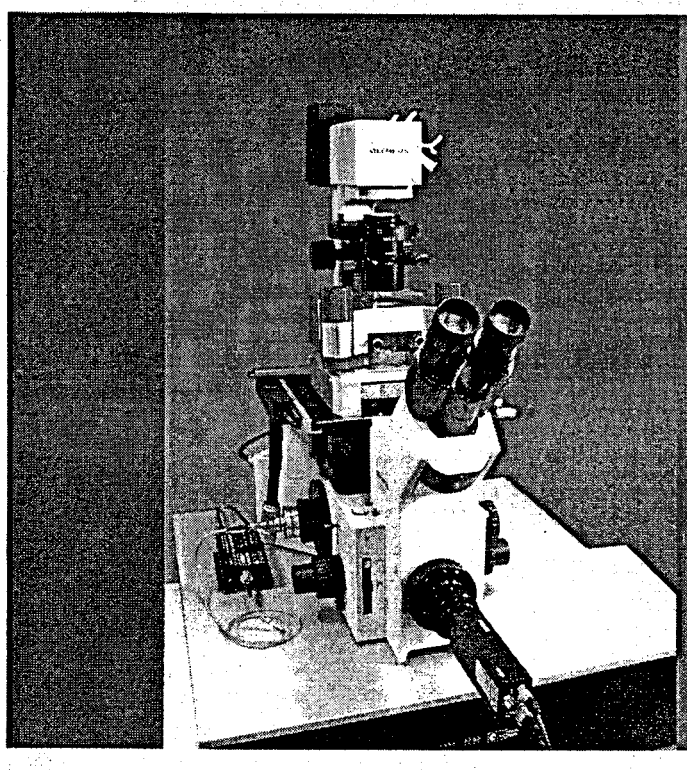

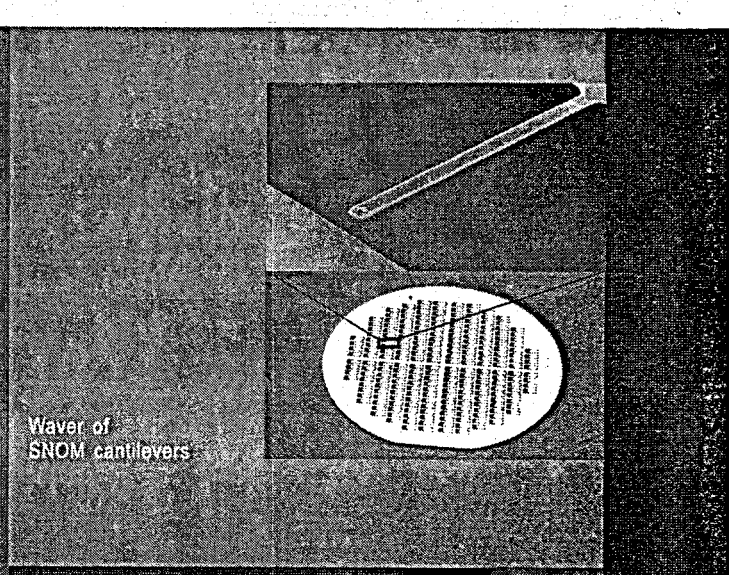

Waver of
SNOM cantilevers

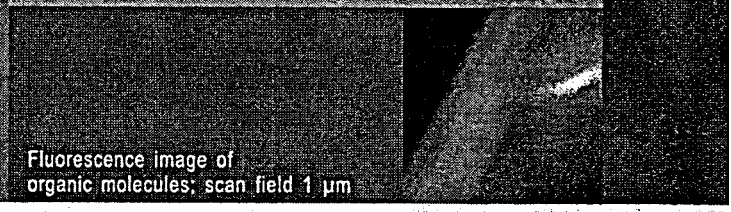

Fluorescence image of
organic molecules; scan field 1 µm

The *LightWizard*™ Scanning Nearfield Optical Microscope - SNOM for Life Science Research

Want to overcome the diffraction barrier in optical microscopy?
Want to study your samples in their native environments?
Want genuine 3D topography and the highest-resolution optical measurements simultaneously?

The solution

The cantilever-based JPK Instruments *LightWizard*™ Scanning Nearfield Optical Microscope (SNOM) is a breakthrough for soft matter and life science research.

The SNOM technology is a powerful microscopy technique that overcomes the Abbé diffraction limit. The fundamental advantage is that the user gets a molecularly resolved optical and topographical image of the same area simultaneously. Thus the comparison of optical and topographical features is easily possible.

Most important for the life scientist is that the *LightWizard*™ is able to work in air or fluids (e.g., buffers), but is also able to measure mechanical, chemical or other sample properties.

The combination of SNOM, AFM and inverted optical microscope with all features in one instrument makes the *LightWizard*™, the most powerful tool for your research.

On the trail of light

- measure the velocity of rotation of molecular rotors at different ATP concentrations
- see where single molecules fluoresce and image their topography
- do optical nanolithography in fluids
- detect material contrast by using sub-wavelength infrared illumination
- activate optical switches in cellular structures

Whatever your applications are:

There is unlimited space below the diffraction limit for your ideas. The *LightWizard*™ will help you to explore the nature of light in nanospace.

www.jpk.com
office@jpk.com

Jointly Producing Knowledge

Exhibitors

Nanonics Imaging, LTD. Dr. Eric Ammann
Manhat Technology Park, Malacha,
Jerusalem 914877, ISRAEL
972-2-6789-573
972-2-648-0827
info@nanonics.co.il

NIST – Advanced Technology Program.
Robert Bloksberg-Fireovid
100 Bureau Drive MS 4730, Gaithersburg, MD
20899-3571, USA
301-975-4787
301-548-1087
robert.b-f@nist.gov

Digital Instruments, Veeco.
Dr. Jeff Doran, Stefan Kaemmer
112 Robin Hill Road, Santa Barbara, CA 93117,
USA
805-967-1400
805-967-7717
Jeff.Doran@veeco.com,
Stefan.Kaemmer@veeco.com

RHK Technology, INC. Mark Flowers
1050 East Maple Road, Troy, MI 48083, USA
248-577-5426
248-577-5433
flowers@rhk-tech.com

Omicron Nanotechnology USA.
Dr. Fred Henn, Margit Walter
1226 Stoltz Road, Bethel Park, PA 15102, USA
412-831-2262
412-831-9828
infor@omicronus.com

JPK Instruments.
Torste Jaehnke, Joern Kamps, Mandy Rueckert
Bouchestrasse 12, 12435 Berlin, GERMANY
+49-30-5331-12073
+49-30-5331-1202
Jaehnke@jpk.com, Kamps@jpk.com,
Rueckert@jpk.com

WITec Wissens Instruments and Technology GmbH. Dr. KlausWeishaupt, Olaf Hollricher
Hoervelsinge Weg 6 D-89081, Ulm, GERMANY
+49-731-140-700
+49-731-140-7020
info@witec.de

The exhibit will be held in room 209 of the Computer Science Building.

Move in Monday, August 12 6:30 A.M. to 10:00 A.M.

Exhibit Hours
Monday, August 12 10:00 A.M. to 4:00 P.M.
Tuesday, August 13 10:00 A.M. to 4:00 P.M.
Wednesday, August 14 10:00 A.M. to 12:00 P.M.

Breakdown Wednesday, August 14 12:00 P.M. to 5:00 P.M.

Parallel sessions schedule

Monday August 12

	*Pick up at the hotels starting at **7:00am - 9:00am** every 1/2 hour and drop off at Hutchison Hall*
8:00 27	*Invited speaker. Hubble Auditorium* **Effects of Coherence on the Spectra of Optical Fields** Emil Wolf

Time/ Page	*Hubble auditorium* **Cavity Nano-Optics and Novel Concepts in Near-Field Optics** Chaired by Dieter Pohl	*Lander auditorium* **Advances in instrumentation** Chaired by David Adams
9:00 32*	*Single-molecule near-field optical energy transfer microscopy* B. Hecht, W. Trabesinger, A. Kramer, U.P. Wild, and M. Kreiter	*In-situ imaging of magnetic domains in ultra thin films by near-field and far-field magneto-optical microscopy* G. Meyer, T. Crecelius, G. Kaindl, and A. Bauer
9:20 34	*Optical switching due to whispering gallery modes in dielectric microspheres coated by a Kerr material* M. Haraguchi, M. Fukui, Y. Tamaki, and T. Okamoto	*Optical and mid-infrared scattering-type near-field optical microscopy at 10 nm resolution* T. Taubner, R. Hillenbrand, and F. Keilmann
9:40 36	*Spontaneous emission in nanoscopic dielectrics* H. Schniepp and V. Sandoghdar	*Development of photothermal near-field scanning optical microscope* Masanori Fujinami, Kiminori Toya, Hiromi Murakawa, and Tsuguo Sawada
10:00	*Coffee break outside on the plaza (see map). **Visit our technical exhibition room**, Computer Science Building room 209 (see map) for a chance to win a prize. The prize will be awarded at the conference banquet on Wednesday.*	

Time/ Page	*Hubble auditorium* **Light in confined structures.** Chaired by Joachim Krenn	*Lander auditorium* **Advances in instrumentation** Chaired by Lukas Eng
10:30 38	*Eigenfield patterns of optically resonant nanoparticles mapped by phase-contrast near-field microscopy* R. Hillenbrand and F. Keilmann	*Subsurface solid immersion microscopy for photonic nanostructures* Bennett Goldberg, Steven Ippolito, Zhiheng Liu, and M. Selim Ünlü
10:50 40	*Surface plasmon polariton waveguiding in random surface nanostructures* S. I. Bozhevolnyi, V. S. Volkov, and K. Leosson	*Bandwidth enhancement for shear-force feedback by exploiting the nonlinear probe-sample interaction* C.L. Jahncke and H.D Hallen
11:10 42	*Mapping the intensity distribution in a photonic crystal microcavity* P. Kramper and V. Sandoghdar	*Polymer NFO probe made by a nanomolding method.* G. M. Kim, E. ten Have, F. Segerink, B.J. Kim, N. F. van Hulst, and J. Brugger

* Abstracts of the talks given in Hubble auditorium are located on even pages, abstracts of the talks in Lander auditorium are on odd pages.

11:30 44	*Ultrafast spectroscopy in the spatial domain: sub-10 fs radiative decay times of surface plasmons in plasmonic band gap structures* D. S.Kim, S.C.Hohng, Y.H.Ahn, V. Malyarchuk, R.Muller, Ch.Lienau, J.W.Park, J.H.Kim, and Q. H. Park	*Fast optical dual-beam technique to characterize thermal axial elongation of near-field probes* A. La Rosa, B. Biehler, and A. Sinharay
11:50 46*	*Waveguiding through a two dimensional metallic photonic crystal* Fadi Baida, Daniel Van Labeke, and Y. Pagani	*Scanning probe microscopy using quartz crystal resonator* Yongho Seo and Wonho Jhe
12:10	*Lunch. Lunch boxes can be picked up at the outside plaza.* ***Visit our technical exhibition room,*** *Computer Science Building room 209 (see map).*	
Time/ Page	*Hubble auditorium* **Light in confined structures** Chaired by Christoph Lienau	*Lander auditorium* **Advances in instrumentation** Chaired by Bennett Golberg
1:30 48	*Near-field measurement of short range correlation in optical waves transmitted through random media* V.Emiliani, F.Intonti, D.Wiersma, M.Colocci, M.Cazayous, A.Lagendijk, and F.Aliev	*Absorption of evanescent light by Cs atoms of an optically forbidden transition* S. Tojo, M. Hasuo, and T. Fujimoto
1:50 50	*Optical characterization of holey fibers using NSOM techniques* C.W.J Hillman, W.S. Brocklesby, T.M Monro, W. Belardi, and D.J Richardson	*Near-field probe characterization by nanoscopic holes* M. Wellhofer, O. Hollricher, and O. Marti
2:10 52	*Light wave propagation through submicrometer high-dielectric contrast systems* R. Quidant, J. C. Weeber, and A. Dereux	*Characterization and fabrication of fully metal coated scanning near-field optical microscopy SiO_2 tips* L. Aeschimann, T. Akiyama, R. Eckert, H. Heinzelmann, U. Staufer, and N. F. De Rooij
2:30 54	*3-dimensional field distribution from nanometer single slit studied by NSOM* C. H. Wei, W. S. Fann, J. Tegenfeldt, and R. Austin	*A compact sensor-head for near-field optical microscopy and spectroscopy* H. U. Danzebrink, C. Dal Savio, Th. Dziomba, D. Kazantsev, B. Güttler, and H.-A. Fuß
2:50 56	*Mapping evanescent field of integrated waveguide with an apertureless scanning near-field optical microscope* S. Aubert, A. Bruyant, R. Bachelot, G. Lérondel, P. Royer, V. Minier, and J. Broquin	*Subwavelength-sized aperture fabrication in aluminum by a self terminated corrosion process in the evanescent field* D. Haefliger and A. Stemmer
3:10 58	*Study of the influence of the optical impedance matching onto near-field optical microscopy imaging in polarization mode* A. Gademann, I. V. Shvets, and C. Durkan,	*Highly efficient near-field probes* Shu-Guo Tang and Tom D. Milster
3:30	*Coffee Break. Exhibitions are open.*	

* Abstracts of the talks given in Hubble auditorium are located on even pages, abstracts of the talks in Lander auditorium are on odd pages.

Monday Schedule

Time/ Page	*Hubble auditorium* **Light in confined structures** Chaired by Fritz Keilmann	*Lander auditorium* **Applications in biology** Chaired by Hans Danzebrink
4:00 60	*Experimental studies of surface plasmon polariton band gap effect* V. S. Volkov and S. I. Bozhevolnyi	*Quantitative fluorescence microscopy on single molecules at the cell membrane performed with a near-field scanning optical microscope.* Bärbel I. de Bakker, M.F. García-Parajó, N.F. van Hulst, F. de Lange, A. Cambi, B.Joosten, and C.G. Figdor
4:20 62	*Novel near-field aperture on the AgO_x thin film* Fu-Han Ho, Hsun-Hao Chang, Yu-Hsaun Lin, and Din-Ping Tsai	*Unraveling the fluorescence emission of the red fluorescent protein DsRed using NSOM* M. Koopman, E.M.H.P. van Dijk, M.F. Garcia-Parajo, and N.F. van Hulst
4:40 64	*Nanometer-sized metal clad optical waveguides* T. Onuki, T. Tani, T. Tokizaki, Y. Watanabe, K. Nishio, and T. Tsuchiya	*Watching single molecule DNA synthesis with zero-mode waveguides* M. Levene, J. Korlach, S. Turner, H. Craighead, and W. W. Webb
5:00 66	*Plasmonic band gap structures as spatial sine wave generators* S. C. Hohng, Y. C. Yoon, D. S. Kim, V. Malyarchuk, Ch. Lienau, J. W. Park, J. H. Kim, and Q. H. Park	*Surface-enhanced Raman spectroscopy of single biomolecules* Thomas Huser, Chad E. Talley, Christopher W. Hollars, and Stephen M. Lane
5:20 68	*Surface plasmon propagation in structured metal films* Jan Seidel, Stefan Grafström, and Lukas M. Eng	*The observation of PC12 with non-optically probing near-field microscopy* Y. Kawata, M. Murakami, C. Egami, T. Tsuboi, and S. Terakawa
5:40 70	*A light source for nano-optical devices: electric current excitation of 2-dimensional optical wave in nano metal-gap* J. Takahara, A. Eda, K. Nakamura, M. Yokoyama, and Tetsuro Kobayashi	*Fluorescence apertureless near-field optical microscope for biological imaging* J. M. Gerton, L. A. Wade, G. A. Lessard, and S. R. Quake
6:00	*Group photo. Please proceed to the photo location (see map on the back)*	
7:00	**Monday poster session.** *See page 20. Wilson Commons May room (see map). Dinner will be provided.*	

Buses to hotels. Pick up at Hutchison Hall starting at 6:00pm - 9:30pm and drop off at hotels every 1/2 hours. Last bus leaves at 9:30pm.

Tuesday August 13

Pick up at Hotels starting at ***7:00am - 9:00am*** and drop off at Hutchison Hall	
8:00 29	*Invited speaker. Hubble Auditorium* **Coherence and manipulation of spin states in semiconductor nanostructures.** Jay Gupta

Time/ Page	*Hubble auditorium* **Theory and modeling** Chaired by Sergey Bozhevolnyi	*Lander auditorium* **Applications in material science** Chaired by Wonho Jhe
9:00 72*	*Near-field optics and quantum optics: an assignation arranged by four kinds of photons* Ole Keller	*Spontaneous coherent emission of light* R. Carminati, K. Joulain, J.P. Mulet, and J.J. Greffet
9:20 74	*Principle of apertureless near-field optical microscopy: Tip vibration and global illumination* R. Fikri, D. Barchiesi, and P. Royer	*A novel scanning near-field microwave microscope* Steven M. Anlage, Atif Imtiaz, Sheng-Chiang Lee, and Alexandre Tselev
9:40 76	*Dissipative shear force on nanoscale probes induced by electromagnetic field fluctuations* Jorge R. Zurita-Sanchez, Jean-Jacques Greffet, and Lukas Novotny	*Mesoscopic structures and dynamics of MEH-PPV thin films by picosecond scanning near-field optical microscopy* N. Tamai, Y. Nabetani, Y. Ma, and J. Shen
10:00	*Coffee break / Technical exhibition.* *If you have not done so or would like to increase your winning chances,* ***visit our technical exhibition room.***	

Time/ Page	*Hubble auditorium* **Novel concepts in near-field optics** Chaired by Ulrich Fischer	*Lander auditorium* **Applications in material science** Chaired by Bert Hecht
10:30 78	*Characterization and modification of the plasmon resonances in a single gold nanoparticle* T. Kalkbrenner and V. Sandoghdar	*Fourier polarimetry of mesostructure in thin polymer films* Lori S. Goldner, Michael J. Fasolka, Jeeseong Hwang, Kathryn Beers, Garnett W. Bryant, Augustine M Urbas, Peter DeRege, Timothy Swager, and Edwin L. Thomas
10:50 80	*Realization of evanescent and propagating Bessel beams: the role of the E_z component of the electric field on confinement* T. Grosjean and D. Courjon	*Anisotropy and periodicity in the electron density distribution and the well width fluctuations in a quantum well* Y. Yayon, M. Rappaport, V. Umansky, and I. Bar-Joseph
11:10 82	*Detection of local density of states using near-field emission measurements. Application to local spectroscopy.* R. Carminati, K. Joulain, J.P. Mulet, and J.J. Greffet	*Optical microscopic studies of nanoscale dynamics in polymer-dispersed liquid crystal films* D. A. Higgins, X. Liao, J. E. Hall, and E. Mei

* Abstracts of the talks given in Hubble auditorium are located on even pages, abstracts of the talks in Lander auditorium are on odd pages.

Tuesday Schedule

11:30 84	*A new generation of near-field probes fabricated by focused ion beams* Erik J. Sánchez, John T. Krug, II, and X. Sunney Xie	*Crystallization study of organic light emitting devices by polarization modulation near-field optical microcopy* Pei-Kuen Wei, Shen-Yu Hsu, Hsieh-Li Chou, and Wun Shain Fann
11:50 86*	*Three-dimensional imaging in near-field optics* P Scott Carney, John C Schotland, and Vadim A Markel	*Clustering of photoluminescence in InGaN films grown by MOCVD and MBE* J.O. White, M.S. Jeong, J.Y. Kim, K. Samiee, Y.W. Kim, J.M. Myoung, K. Kim, E.K. Suh, M.G. Cheong, C.S. Kim, C.-H. Hong, and H.J. Lee
12:10	*Lunch. Please pick up your lunch box.* ***Visit our technical exhibition room*** *(see map).*	
Time/ Page	*Hubble auditorium* **Novel concepts in near-field optics** Chaired by Vahid Sandoghdar	*Lander auditorium* **Industrial applications and Applications in chemistry** Chaired by Sunney Xie
1:30 88	*SNOM imaging of photonic nanopatterns, metal islands and molecular aggregates* U. C. Fischer, J. Heimel, H J. Maas, A. Naber, H. Fuchs, J. C. Weeber, and A. Dereux	*Near-field vibrational spectroscopy for nanoscale chemical analysis* C. A. Michaels, S. J. Stranick, and D. B. Chase
1:50 90	*In situ characterization of optical near-field probes in aperture NSOM* A. Drezet, S. Huant, and J. C. Woehl **(CHANGED TO POSTER TuP49)**	*Near-field Raman imaging of defects in molecular crystals with subdiffraction resolution:* P. G. Gucciardi, S. Trusso, C. Vasi, S. Patanè, and M. Allegrini
2:10 92	*Enhanced light confinement in a near-field optical probe with at triangular aperture* D. Molenda, U. C. Fischer, H.-J. Maas, C. Höppener, H. Fuchs, and A. Naber	*Catalytic hydrogenation of benzene on single catalytic sites studied by near-field Raman spectroscopy* Christian Fokas, Renato Zenobi, and Volker Deckert
2:30 94	*Imaging ferroelectric domains by electro-optically modulated near-field microscopy* T. Otto, S. Grafström, F. Schlaphof, H. Chaib, and L.M. Eng	*Photo-initiated energy transfer in nanostructured complexes observed by near-field optical microscopy* Gregory A. Wurtz, Jasmina Hranisavljevic, Jin-Seo Im, and Gary P. Wiederrecht
2:50 96	*Investigation of aperture SNOM levers fabricated by FIB patterning and wet chemical etching* J. Renger, S. Grafström, and L.M. Eng, B. Schmidt and L. Bischoff, and B. Köhler	*Light delivery for heat assisted magnetic recording* W. A. Challener, C. D. Mihalcea, K. R. Mountfield, and K. Sendur
3:10 98	*Scanning near-field optical quantum computer* S. K. Sekatskii, M. Chergui, and G. Dietler	*Near-field super-resolution effects of a ZnO nano thin film* Wei Chih Lin, Hsun Hao Chang, Yu Hsuan Lin, Yuan Hsin Fu, and Din Ping Tsai
3:30	*Coffee break / Technical exhibition*	

* Abstracts of the talks given in Hubble auditorium are located on even pages, abstracts of the talks in Lander auditorium are on odd pages.

Time/ Page	*Hubble auditorium* **Novel concepts in near-field optics** Chaired by Jean-Jacques Greffet	*Lauder auditorium* **Theory and modeling** Chaired by Paul Scott Carney
4:00 100	*Near-field radiation efficiency a bow-tie antenna in the presence of recording media* I. K. Sendur and W. A. Challener	*Local imaging of photonic structures: image contrast from Impedance Mismatch* G. W. Bryant, A. L. Campillo, and J.W. P. Hsu
4:20 102	*Towards single-photon tunneling* I.I. Smolyaninov, C.C. Davis, A.V. Zayats, and A. Gungor	*Optical near fields and the degree of polarization* T. Setala, A. Shevchenko, M. Kaivola, and A. T. Friberg
4:40 104	*Giant optical transmission through a sub-wavelength aperture* Tineke Thio, G.D. Lewen, K.M. Pellerin, R.A. Linke, H.J. Lezec, and T.W. Ebbesen	*3D Electro-magnetic modeling of apertureless SNOM/AFM cantilever probes* L.Vaccaro, H. P. Herzig, and R. Dändliker
5:00 106	*Polarizing effects of near field probes determined by multiple heterodyne detection* P.Tortora, L.Vaccaro, R. Dändliker, and H. P. Herzig	*Comparison of linear and second harmonic images of dielectric dots in near-field optical microscopy* Thierry Laroche and Daniel Van Labeke
5:20 108	*Near-field optics using super-resolution near-field optical structures* D. P. Tsai, W. C. Lin, H. Y. Lin, F. H. Ho, H. H. Chang, Y. H. Fu, and Y. H. Lin	*Three dimensional simulation of optical waves in a subwavelength- sized aperture in a thick metallic screen* Kazuo Tanaka, Mengyun Yan, and Masahiro Tanaka
5:40 110	*Near-field nano-ellipsometer for ultra thin film characterization* Qiwen Zhan and James R. Leger	*Resonance shift effects in apertureless scanning near-field optical microscopy* J. A. Porto, P. Johansson, S. P. Apell, and T. Lopez-Rios
6:00	**Tuesday poster session.** *See page 24. Wilson Commons May room (see map). Dinner will be provided.*	

Buses to hotels. Pick up at Hutchison Hall starting at 6:00pm - 9:30pm and drop off at hotels every 1/2 hours. Last bus leaves at 9:30pm.

Wednesday August 14

	*Pick up at Hotels starting at **7:00am - 9:00am** and drop off at Hutchison Hall*	
8:00 30	*Invited speaker. Hubble auditorium.* **Quantum information science.** Ian Walmsley	
Time/ Page	*Hubble auditorium* **Theory and modeling and Local field enhancement** Chaired by Garnett Bryant	*Lander auditorium* **Nanofabrication and manipulation** Chaired by Tineke Thio
9:00 112*	*Design of near-field optical probes with high field enhancement by finite difference time domain electromagnetic simulation* John T. Krug, II, Erik J. Sánchez, and X. Sunney Xie	*CASSE formation and operating characteristics of high resolution aperture SNOM probes* J. Toquant, A. Bouhelier, and D. W. Pohl
9:20 114	*Near-field Raman spectroscopy using a sharp metal tip* A. Hartschuh, N. Anderson, and L. Novotny	*Enhanced photoisomerization and light induced mass-transport in the near-field of irradiated metallic nano-objects* P. Karageorgiev, B. Stiller, and L. Brehmer
9:40 116	*Detection of an adenine molecule by tip-enhanced Raman NSOM* S. Kawata, Y. Ishida, H. Watanabe, N. Hayazawa, and Y. Inouye	*Fabrication of 25-nm Zn Dot with selective photodissociation of adsorption-phase dietylzinc by optical near field* T. Yatsui, M. Ueda, Y. Yamamoto, T. Kawazoe, M. Kourogi, and M. Ohtsu
10:00	*Coffee break. Do not forget to visit our technical exhibition room.*	
Time/ Page	*Hubble auditorium* **Local field enhancement** Chaired by Satoshi Kawata	*Lander auditorium* **Nanofabrication and manipulation and Nano-optics of single molecules and quantum dots** Chaired by Lori Goldner
10:30 118	*Mapping single molecular fluorescence lifetime near metal probes* E.M.H.P. van Dijk, A.C. Krijgsman, W.H.J. Rensen, M.F. García-Parajó, L. Kuipers, and N.F. van Hulst	*Optical spectroscopy on individual porphyrin wheels* C. R. L. P. N. Jeukens, K. Takazawa, P. C. M. Christianen, J. C. Maan, M. C. Lensen, J. A. A. W. Elemans, A. E. Rowan, and R. J. M. Nolte
10:50 120	*Probing the optical near-field enhancement at a metal tip using a single florescent molecule* B. Hecht, A. Kramer, W. Trabesinger, and U.P. Wild	*Near-field and confocal surface enhanced resonance Raman spectroscopy from room temperature to cryogenic temperatures* A. J. Meixner, T. Vosgröne, and P. Anger
11:10 122	*Near field enhancement of conductive tips in Raman spectroscopy of carbon nanotubes* A. Bek, R. Vogelgesang, and K. Kern	*Near-field imaging of surface plasmon on Au nano-structures fabricated by scanning probe lithography* Jeongyong Kim, Ki-Bong Song, Jun-Ho Kim, Seong Q Lee, and Kang-Ho Park

* Abstracts of the talks given in Hubble auditorium are located on even pages, abstracts of the talks in Lander auditorium are on odd pages.

11:30 124	*Second-harmonic generation at metal tips in apertureless near-field optical microscopy* S. Takahashi and A. V. Zayats	*Near-field optical structuring of ultra thin terpolymer films* S. Trogisch, Ch. Loppacher, S. Grafström, L.M. Eng, F. Braun, T. Pompe, and B. Voit
11:50 126	*Surface plasmon nano optics* J. R. Krenn, H. Ditlbacher, G. Schider, A. Hohenau, A. Leitner, and F. R. Aussenegg	*Fabrication of a temperature-controllable B-doped Si probe for optical near-field photochemical vapor deposition* T-W. Kim, T. Yatsui, M. Kourogi, and M. Ohtsu
12:10 128	*Characterizing the electric field enhancement and fluorescence quenching induced by a sharp gold tip.* M. R. Beversluis, A. Bouhelier, A. Hartschuh, and L. Novotny	*Near-field spectroscopy of II-VI quantum dots* M. Brun, N. Chew, L. Woehl, H. Mariette, and S. Huant CANCELLED
12:30 130	*Phonon-enhanced near-field interaction observed with infrared s-SNOM* R. Hillenbrand, T. Taubner, and F. Keilmann	
12:45	*Conference excursion to Genesse Country Village and Museums. Pick up your lunch boxes at the plaza before entering the bus. You may eat your lunch on the bus. Buses are leaving from Hutchison Hall at **12:45pm**. Buses are coming back to the hotels at **5:05pm**.*	
7:00	**Conference Banquet.** *George Eastman House. The buses will loop between the hotels and the Eastman house from **6:15pm** to **10:15pm** every 1/2 hour. Last bus leaves at **10:15pm**.*	

Thursday August 15

Pick up at Hotels starting at 7:00am - 9:00am and drop off at Hutchison Hall		
8:00 31	*Invited speaker. Hubble auditorium.* **Dynamics of biophysical processes studied with multiphoton microscopy.** Ahmed Heikal	
Time/ Page	*Hubble auditorium* **Nonlinear and ultrafast phenomena** Chaired by Daniel Van Labeke	*Lander auditorium* **Theory and modeling** Chaired by Ole Keller
9:00 132*	*Time resolved motion of a femtosecond pulse inside a microresonator* H. Gersen, D.J.W. Klunder, J. P. Korterik, A. Driessen, N.F. van Hulst, and L. (Kobus) Kuipers	*Understanding local measurement of dichroism and birefringence in thin polymer films* G. W. Bryant and L. S. Goldner
9:20 134	*CARS microscopy: 3D vibrational imaging of living cells* X. Sunney Xie and Ji-Xin Cheng	*Numerical analysis of plasma resonances in noble metal nanostructures* Hiroharu Tamaru, Hitoshi Kuwata, and Kenjiro Miyano
9:40 136	*Near-field second-harmonic generation excited by local field enhancement* A. Bouhelier, M. Beversluis, A. Hartschuh, and L. Novotny	*Manifestation of an electric dipole order induced by optical near fields* A. Shojiguchi, K. Kobayashi, K. Kitahara, S. Sangu, and M. Ohtsu
10:00	*Coffee break.*	
Time/ Page	*Hubble auditorium* **Nonlinear and ultrafast phenomena and Local field enhancement** Chaired by Niek Van Hulst	*Lander auditorium* **Nano-optics of single molecules and quantum dots** Chaired by Alfred Meixner
10:30 138	*Femtosecond coherent near-field spectroscopy of single quantum dots* Tobias Günther, Kerstin Müller, Christoph Lienau, Thomas Elsaesser, Soheyla Eshlaghi, and Andreas Wieck	*The electrodynamics of fluorescing molecules interacting with metallic nano-cavities* J. Enderlein
10:50 140	*Near-field second harmonic microscopy with half-metal-coated tip: application to imaging of ferroelectric domains* H.Y. Liang, I.I. Smolyaninov, C.C. Davis, R. Ramesh, and C.H. Lee	*Near-field autocorrelation spectroscopy: Quantum mechanical level repulsion in interface quantum dots* Francesca Intonti, Valentina Emiliani, Christoph Lienau, Thomas Elsaesser, Vincenzo Savona, Erich Runge, and Roland Zimmermann
11:10 142	*Gradient-field Raman: selection rules in the near field* H. D. Hallen, E. J. Ayars, and C. L. Jahncke	*Vibrational modes of an individual single wall carbon nanotube observed by near-field enhanced Raman spectroscopy* Norihiko Hayazawa, Takaaki Yano, Yasushi Inouye, and Satoshi Kawata

* Abstracts of the talks given in Hubble auditorium are located on even pages, abstracts of the talks in Lander auditorium are on odd pages.

11:30 144	*Investigation of local field enhancement at the end of SNOM tips using photosensitive azobenzene-containing materials* F. H'Dhili, R. Bachelot, G. Lérondel, D. Barchiesi, R. Fikri, A. Rumyantseva, P. Royer, and N. Landraud	*Scanning near-field optical microscopy using semiconductor nanocrystals as a local fluorescence and fluorescence resonance energy transfer source* G. T. Shubeita, S. K. Sekatskii, G. Dietler, I. Potapova, A. Mews, and Th. Basché
11:50 146	*Near-field Raman imaging of organic molecules by an apertureless metallic probe scanning optical microscope* Norihiko Hayazawa, Yasushi Inouye, Zouheir Sekkat, and Satoshi Kawata	*Real-space mapping of exciton and bi-exciton wave functions in GaAs quantum dot by near-field optical imaging spectroscopy* T. Saiki, K. Matsuda, S. Nomura, M. Mihara, and K. Aoyagi
12:10 148	*Plasmon condenser with a microscatter for optical far/near field conversion* T. Yatsui, T. Abe, M. Kourogi, and M. Ohtsu	*Spontaneous emission of an atom placed near nanobodies* V.V. Klimov
12:30 150		*Raman spectroscopy of fullerene- or perylene-filled nanotubes* Débarre A., Jaffiol R., Julien C., Nutarelli D., Richard A., and Tchénio P.
12:50	**Final remarks.** *Hubble auditorium.*	
*Buses to hotels for those not going to Niagara Falls. Pick up every half hour from Hutchison Hall **12:30-2:00pm** and drop off at the hotels*		
1:30	**Excursion to Niagara Falls for those who signed up.** *Lunch box is provided. Buses are leaving from Hutchison hall at **1:00pm. Do not cross the border into Canada. You may not be allowed to enter the US again.** Depart Niagara Falls no later than **6:30pm.** If you're not on the bus we won't wait for you – people have scheduled flights. Arrive to the hotels at approximately **8:00pm***	

POSTER SESSIONS SCHEDULE

Monday

Theory and Modeling

Nano-Optics for Single Molecules and Quantum Dots

Local Field Enhancement

Applications in Material Science

Applications in Biology

Nanofabrication and Manipulation

Tuesday

Novel Concepts in Near-Field Optics

Nonlinear and Ultrafast Phenomena

Applications in Chemistry

Cavity Nano-Optics

Advances in Instrumentation

Industrial Applications

Light in Confined Structures

ABSTRACTS

Effects of Coherence on the Spectra of Optical Fields

Emil Wolf, Department of Physics and Astronomy and the Institute of Optics, University of Rochester, Rochester, NY 14627, USA

It is generally taken for granted that the spectrum of light remains unchanged on propagation in free space. Researches carried out in the last few years, both theoretical and experimental, have revealed that this is not always so. Specifically it was demonstrated that the spectrum of a radiated field depends not only on the source spectrum but also on the spatial coherence properties of the source. We will discuss these developments and we will note their implications for near field optics. We will also describe a very recent discovery which revealed that in fully coherent fields drastic spectral changes take place in the neighborhood of phase singularities.

Coherence and manipulation of spin states in semiconductor nanostructures

Jay A. Gupta and D. D. Awschalom[1]
Department of Physics, University of California, Santa Barbara, CA 93106

The potential of semiconductor quantum dots as media for spin-based storage of quantum information is based on hopes that carrier confinement may reduce decoherence mechanisms through spatial localization and attendant discretization of the electronic energy spectrum. Time-resolved optical experiments have been performed to study carrier spin dynamics in a variety of quantum dot systems, including chemically-synthesized CdSe nanocrystals ranging from 2.2-8 nm in diameter,[2] and CdS_xSe_{1-x} nanocrystal-doped glasses.[3] Nanosecond-scale spin precession lifetimes that persist to room temperature in these quantum dots are limited by inhomogeneous dephasing under an applied transverse magnetic field. Comparisons of transverse and longitudinal spin relaxation in these systems reveal different dynamical timescales, evidenced through studies of temperature and field dependencies.

The manipulation of spin states in nanocrystal-doped glasses is demonstrated with measurements of the AC Stark shift produced when an intense pump pulse is tuned below the semiconductor bandgap. Optically-induced spin splittings are then realized through the pronounced polarization dependence of directly-observed meV-scale shifts. Recent experiments in semiconductor quantum wells indicate that these spin splittings can be described as an effective light-induced magnetic field whose duration is limited only by the laser pulse duration of ~150fs.[4] We have demonstrated that this light-induced field can coherently rotate electron spins up to ~ $\pi/2$ radians, providing opportunities for all-optical tipping pulses in electron spin resonance experiments.

[1] Work supported by the DARPA, ONR, and NSF.

[2] J.A. Gupta, X. Peng, A.P. Alivisatos and D. D. Awschalom, Phys. Rev. B **59**, R10421 (1999).
[3] J.A. Gupta and D.D. Awschalom, Phys. Rev. B **63**, 085303, (2001).
[4] J.A. Gupta, R. Knobel, N. Samarth and D.D. Awschalom, Science **292**, 2458 (2001).

Quantum Information Science

Ian A. Walmsley

University of Oxford, Clarendon Laboratory, Parks Rd. Oxford OX1 3PU, UK

Landauer's deceptively simple statement that information processing is physics has recently led to some remarkable changes in the way we view communications, computing and cryptography. By employing quantum physics instead of classical physics several things that were thought impossible have now proven possible. Quantum communications links, for example, are impossible to eavesdrop. And quantum computers can turn algorithms that are euphemistically labeled "difficult" for a Pentium into calculations that are "simple". The details of what constitutes "difficult" and what "easy" are the subject of complexity theory, but it suffices to know that a problem like finding the factors of a 1024-digit number would take longer than the age of the universe on a computer designed according to the laws of classical physics, and can be done in the blink of an eye on a quantum computer. If we can ever build one.

Quantum information processing offers a qualitatively different way in which to think about manipulating information. But it is also a necessary way to think about information. Moore's law famously indicates that the number of transistors per die increases exponentially with time. The implication is that there will be about one electron per transistor by the year 2016, and that this lone electron will be confined to a region small enough that it will act as a quantum mechanical particle, and not as a classical charged billiard ball. Fortunately, as quantum physics becomes more important in designing computers, we can do well by doing right.

This talk will provide an overview of the sorts of enhancements that quantum physics can provide for technology, and a short survey of applications and potential applications. These include quantum interferometry and metrology, microscopy, communications, cryptography, frequency standards and clock synchronization, as well as computation and information processing. [1]

The rudimentary features of quantum mechanics needed to implement the technologies are interference and entanglement, and one of the major thrusts of the field has been to develop methods for the generation and measurement of these properties in systems that are both easy to control and have appropriate scaling properties. One of the critical issues in this area is how to design systems and control. schemes that are robust with respect to unavoidable environmental noise. The critical practical issues that confront real-world implementation of these concepts are many, and important performance parameters that might limit the utility of quantum-enhanced technologies will also be examined.

References

[1] A number of books at various levels provide a good starting point for exploring the subject. A comprehensive M. Nielsen and I. L Chuang, *Quantum Information and Quantum Computation*, (Cambridge University Press, 2001), and that edited by D. Bouwmeester, A. K. Ekert and A. Zeilinger, *The Physics of Quantum Information*, (Springer, Berlin, 2000) There are also numerous review articles in journals, such as *Fortschritte der Physik*, 48 (9) (2000); Special Focus Issue on Experimental Proposals for Quantum Computation, eds. S. L. Braunstein and H.-K. Lo. A journal is now devoted to this subject area: *Quantum Information & Computation*, Rinton Press, Princeton, NJ.

Dynamics of Biophysical Processes Studied with Multiphoton Microscopy

Ahmed A. Heikal and Watt W. Webb

School of Applied and Engineering Physics, Cornell University, Clark Hall, Ithaca, NY 14853.

Multiphoton (MP) fluorescence microscopy (MPFM) [1] provides several advantages over one photon (1P) fluorescence microscopy for biological studies. The inherent high three-dimensional spatial resolution in MPFM originates from the nonlinear dependence of MP-fluorescence on the illumination intensity. As a result, the excitation volume is limited to the focus of the excitation laser, which minimizes out-of-focus photobleaching and photodamage. Such localized excitation also eliminates the detection pinhole that is required for 1P-confocal microscopy for depth discrimination, and thereby provides simpler fluorescence detection. Since infrared lasers are usually used in MPFM, large penetration depth can be achieved for deep tissue imaging. Finally, light scattering is also minimized because the MP-fluorescence detection wavelength is always to the blue of the excitation wavelength. These unique features make MPFM the method of choice for visualizing individual cells deep within living tissues or organs such as intact brain. Understanding of numerous biological processes on the molecular level can be elucidated using MP-fluorescence spectroscopy, dynamics, and microscopy.

This tutorial will focus on the molecular background of multiphoton excitation, methodology, and its biological applications. Multiphoton excitation will be discussed in terms of molecular symmetry, resonant and non-resonant pathways, intensity-dependence, and the polarization selectivity of the excitation laser. Because the nonlinear properties of fluorescent markers are critical for MP-fluorescence, special attention will be focused on selected fluorophores. Of particular interest are intrinsically fluorescent proteins (IFP), from *Aequorea victoria* jellyfish (green) or Discosoma coral (red), which are noninvasive and site-specific fluorescent markers as well as pH indicators for biological research [2,3]. We will also outline a new design strategy, based on donor-acceptor-donor conjugated configuration, for molecular systems with large MP-excitation cross-section [4,5]. Finally, we will evaluate the potential of quantum dots and nanoparticles as fluorescent markers for biological applications.

The application aspect of this tutorial will focus on the exploitation of endogenous autofluorescence in live cells and tissues for studying energy metabolism by functional imaging of the native reduced nicotinamide adenine dinucleotide (NADH) and flavin adenine dinucleotide (FAD). Two-photon (2P) redox fluorescence microscopy of these biomolecules allows for noninvasive monitoring of the mitochondrial respiratory chain using 2PFM [6,7]. As an example, we will focus on our recent studies of *in vivo* activity of mitochondrial respiratory chain various native nervous tissues [7] and single cardiac cells [6]. Finally, we will review recent advances in multiphoton-excitation techniques and applications. Innovative approaches for excitation volume confinement will be discussed along with related applications.

References

[1] W. Denk, J. H. Strickler and W. W. Webb, *Science* **248**, 73 (1990).
[2] A. A. Heikal, S. T. Hess, G. S. Baird, R. Y. Tsien and W. W. Webb, *Proc. Natl. Acad. Sci. U. S. A.* **97**, 11996 (2000).
[3] A. A. Heikal, S. T. Hess and W. W. Webb, *Chem. Phys.* **274**, 37 (2001).
[4] M. Albota, D. Beljonne, J.-L. Bredas, J. E. Ehrlich, J-Y. Fu, A. A. Heikal, S. F. Hess, T. Kogej, M. D. Levin, S. R. Marder, D. McCord-Maughon, J. W. Perry, H. Rockel, M. Rumi, G. Subramaniam, W. W. Webb, X.-L. Wu and C. Xu, *Science (Washington, D. C.)* **281**, 1653 (1998).
[5] A. A. Heikal, S. Huang, M. Halik, S. R. Marder, W. Wenseleers, J. W. Perry and W. W. Webb *Biophys. J.* **82**, 493a (2002).
[6] S. Huang, A. A. Heikal and W. W. Webb, *Biophys. J.* **82**, 2811 (2002).
[7] K. A. Kasischke, H. D. Vishwasrao, A. A. Heikal and W.W. Webb, *Neuron*, submitted.

Single-molecule near-field optical energy transfer microscopy

B. Hecht
Nano-Optics group, Institut of Physics, University of Basel, CH-4056 Basel, Switzerland.
W. Trabesinger, A. Kramer, and U.P. Wild
Physical Chemistry Laboratory, Swiss Federal Institute of Technology, CH-8093 Zurich, Switzerland.
M. Kreiter
Max Planck Institut für Polymerforschung, D-55128 Mainz, Germany.

The nano-optical interaction between an atomic force microscopy (AFM) tip and a single dipolar emitter is investigated [1]. Changes of the excited state lifetime and the fluorescence rate of a single fluorescent molecule are recorded simultaneously as a function of the tip position relative to the molecule. A sketch of the setup is shown in Fig. 1 (a). It consists of a sample-scanning confocal optical microscope based on an inverted microscope (Zeiss Axiovert 135) in combination with a tip-scanning AFM (Digital Instruments, Bioscope). An actively mode-locked Nd:YAG laser (Coherent Antares), frequency-doubled to 532 nm with 150 ps pulse width and 76 MHz repetition rate serves as a light source. For online acquisition of fluorescence lifetime data during scans, time-correlated single photon counting in combination with an averaging scheme is employed. Specifically, the output of a time-to-amplitude converter is converted into a continuous step function and averaged by a low-pass filter. Details are described elsewhere [2]. AFM measurements are performed in contact mode with commercial cantilevers (Digital Instruments, DNP) with Si_3N_4 tips in the shape of a quadratic pyramid (base length 4 μm, height 3.3 μm).

A sub-diffraction-limited area of decreased fluorescence (b,d) and shortened lifetime (c, e) is observed for both, gold-coated (b, c) and bare (d, e) Si_3N_4 tips. The results are discussed in terms of molecular fluorescence in a system of stratified media. The outlined methodology holds promise for applications in ultra high-resolution near-field optical imaging at the level of single fluorophores.

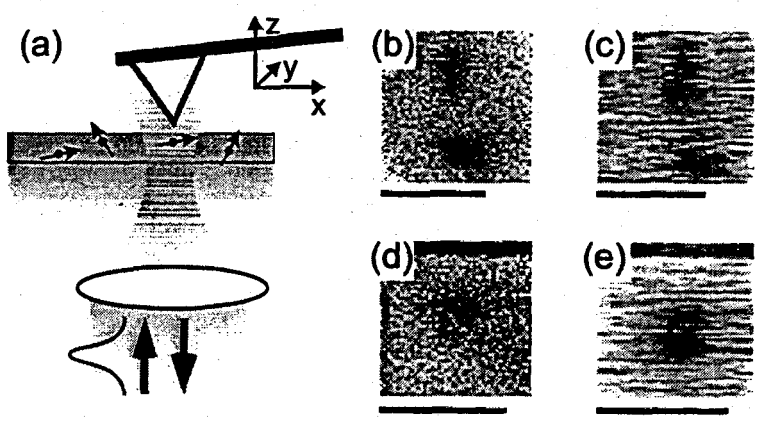

Figure 1: (a) Sketch of the experimental setup. A ps pulsed laser is used to excite the fluorescence of single molecules in a 20 nm thin polymer film. Fluorescence rate and lifetime are recorded simultaneously and continuously as an AFM tip scans over a molecule of interest. (b),(d) Fluorescence rate as a function of the tip position for a gold-coated and a bare Si_3N_4 AFM tip, respectively. (c),(e) Excited-state lifetime as a function of the tip position for a gold-coated and a bare Si_3N_4 AFM tip, respectively. Scale bar =200 nm.

References

[1] W. Trabesinger, A. Kramer, M. Kreiter, B. Hecht, and U.P. Wild, submitted.

[2] W. Trabesinger, C.G. Hübner, B. Hecht, and U.P. Wild, submitted.

In-situ Imaging of Magnetic Domains in Ultrathin Films by Near-Field and Far-Field Magneto-Optical Microscopy

G. Meyer, T. Crecelius, G. Kaindl, and A. Bauer
Freie Universität Berlin, Insitut für Experimentalphysik, Arnimallee 14, 14195 Berlin Germany

We have studied *in-situ* the magnetic-domain structures and magnetization-reversal processes of ultrathin Fe/Cu(100) films in ultrahigh vacuum (UHV) by magneto-optical Kerr effect (MOKE), Kerr microscopy, and scanning near-field magneto optical microscopy (SNOM). The films were a few monolayers thick and were grown at 80 K on a Cu(100) single crystal. With SNOM, we were able to image details of domain structures which could not be resolved by far-field Kerr microscopy (Fig. 1). Since magneto optics is not affected by external magnetic fields SNOM could be used to study locally the magnetization-reversal process. The experiments were performed in a UHV chamber designed for combined MOKE, Kerr microscopy and SNOM measurements at variable temperature (20 K to 450 K) and in external magnetic fields up to 1500 Oe [1]. The chamber is part of a three-chamber UHV system, with the other two chambers being equipped with film-preparation facilities as well as a scanning tunneling microscope (STM).

The SNOM is operated in shared aperture mode. Tip-sample distance is controlled by either detecting shear-forces or by stabilizing the intensity of the reflected optical signal. We found the latter method to be particularly appropriate for scanning crystal surfaces in UHV. Magneto-optical contrast in SNOM images is obtained by means of a Sagnac-Interferometer [2]. In comparison to a conventional crossed-polarizers setup, a Sagnac interferometer has the advantage that it is inherently insensitive to reciprocal effects, e.g. birefringence, which often lead to artifacts in magneto-optical SNOM.

We expect that the combination of near-field and far-field magneto-optical microscopy will enable us to further clarify the domain structures in ultrathin magnetic films, especially at spin-reorientation transitions where micro-domain states play an important role. Recently, we succeeded in imaging such micro-domain states in Fe/Cu(100) films at various external magnetic fields. This will probably lead to a better understanding of the spin-reorientation transition in these films.

Fig. 1: 15 × 15 μm^2 SNOM image of a demagnetized state in a 3 monolayers thick Fe/Cu(100) film. Light and dark areas represent domains of magnetization pointing in opposite directions perpendicular to the surface.

References

[1] G. Meyer, T.Crecelius, G. Kaindl, and A. Bauer, *J. Magn. Magn. Mater.* **240**, 76-78 (2002).
[2] B.L. Petersen, A. Bauer, G. Meyer, T. Crecelius, and G. Kaindl, Appl. Phys. Lett. **73**, 538 (1998).

Optical switching due to whispering gallery modes in dielectric micro-spheres coated by a Kerr material

M. Haraguchi, M. Fukui, Y. Tamaki, T. Okamoto, University of Tokushima, 2-1 Minami-Josanjima, Tokushima 770-8506, Japan.

Micro-size optical resonators, e.g., dielectric micro-spheres, may lead to the realization of new micro-size optical devices with a Kerr nonlinear material. We have found that the whispering gallery modes (WGM) in a dielectric microsphere can be efficiently excited through a near-field coupling and the optical self-switching phenomena can be induced in the nonlinear microsphere, using the Finite-Difference Time-Domain (FDTD) method [1]. For device applications like signal processings, it is important to confirm that the switching phenomena of nonlinear spheres can be controlled by a control light. In this study, we have evaluated optical characteristics of spheres, coated by a film having a Kerr-nonlinearity, on a substrate. Note that the optical response of the spheres is controlled by the signal and the control lights. It may be possible to dominantly control such a response by the control light. We propose a new micro-size nonlinear optical modulator consisting of such a nonlinear sphere.

We employ the configuration in which a 1μm-size sphere is set on a dielectric prism in vacuum, as shown in Fig.1. The refractive indices of the sphere and the prism are 2.52 and 1.51, respectively. The linear refractive index of the Kerr material is also 2.52. The 3rd order nonlinear susceptibility of the Kerr-material $\chi^{(3)}$ is 7×10^{-14} [m^2/V^2]. All the refractive indices and $\chi^{(3)}$ are assumed to be wavelength-independent. The incident angle of the signal light is fixed at 55°. We evaluate reflectance for the signal light. The control light is input from the direction parallel to the surface of the prism, as shown in Fig.~¥ref{fig1}. The signal and control lights are assumed to be a Gaussian beam with beam waists of 1.5μm on the prism surface for the signal light and of 1μm at the side of the sphere for the control light, respectively. The center of the beam spot of the signal light is positioned at the contact point between the prism and the sphere. We employ the TM-polarized and TE-polarized lights.

Reflectance for the signal light is sensitive to the excitation condition of the WGM. When the control light is incident, reflectance for the signal light, which is coupling with the WGM, can be varied because the control light can modify the refractive index of the Kerr materials, leading to the extinction of the WGM. When the wavelength of the incident light is adjusted to the characteristic wavelength of the WGM of the sphere, reflectance for the signal light can be switched by using the control light whose intensity is about two-order smaller than that of the signal light. The on/off ratio is about 10. Our results indicate that a new micro-size nonlinear optical switch or modulator may be realized by using a nonlinear sphere.

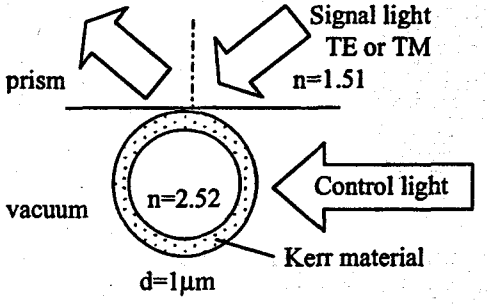

Figure 1: The configuration employed here. The sphere is coated by a Kerr material film with a thickness of 60nm.

References

[1] M. Haraguchi, T. Okamoto and M. Fukui, 3rd Asia-Pacific Wrokshop on Near Field Nano Optics, Melbourne, Dec. 2001, (should be published on the special issue of *IEICE Trans. on Electronics*).

Optical and mid-infrared scattering-type near-field optical microscopy at 10 nm resolution

T. Taubner, R. Hillenbrand, and F. Keilmann,
Max-Planck-Institut für Biochemie, D-82152 Martinsried, Germany, taubner@biochem.mpg.de

We compare two apertureless, scattering-type SNOMs which we operate at different wavelengths, 0.6 μm and 10 μm. By imaging of a common test sample we proove that

+ a spatial resolution of 10 nm is reached at both widely different wavelengths,
+ the image contrast depends on the same mechanism at both wavelengths.

Scattering-type scanning near-field optical microscopy (s-SNOM) uses the optical near-field interaction between an illuminated metal or dielectric probe tip and the sample surface[1-5]. Its spatial resolution is not limited by diffraction but rather by the actual size of the scattering probe tip (< 20 nm). The experiments have readily achieved a wavelength-related resolution of λ/100, a value not possible with aperture-based SNOMs.

Our microscopes use tapping-mode AFM with commercially available, metallized cantilever tips. These act as scattering probes which are illuminated by mid-infrared[3] or visible[4,5] light. We detect the scattered light interferometrically, in the visible by using a heterodyne setup already reported[4,5], while our infrared s-SNOM has recently been extended by a homodyne receiver. The interferometric detection serves to detect phase and amplitude of the scattered light separately and simultaneously, and thus allows to also map near-field phase contrast. We emplo quency, a method to effectively suppress

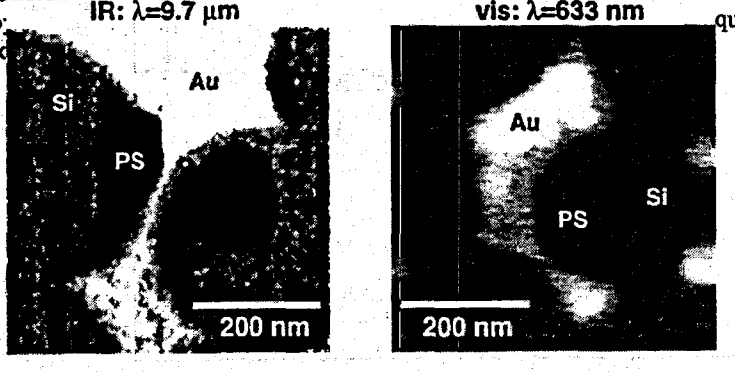

We show examples of imaging (the optical amplitude) of a nanostructured sample in both microscopes. The achieved resolution is ≈10 nm. Common to both the mid-infrared and the visible wavelengths, the 25 nm high Au islands are the brightest objects, while the PS particles appear darker than the Si substrate. The observed brightness agrees with an electrostatic model which predicts a simple analytical relation to the local refractive index of the sample material[4]. This categorizes s-SNOM contrast into the material classes of metals, semiconductors, and polymers enabling a simple material recognition on a 10 nm scale[5].

References

[1] F. Zenhausern, Y. Martin and H. K. Wickramasinghe, *Science*, **269**, 1083 (1995).
[2] A. Lahrech et al., *Optics Letters*, **21**, 1315 (1996).
[3] B. Knoll and F. Keilmann, *Nature*, **399**, 134 (1998).
[4] R. Hillenbrand and F. Keilmann, *Physical Review Letters*, **85**(14), 3029 (2000).
[5] R. Hillenbrand and F. Keilmann, *Applied Physics Letters*, **80**, 25 (2002).

Spontaneous Emission in Nanoscopic Dielectrics

H. Schniepp and V. Sandoghdar
Swiss Federal Institute of Technology (ETH), 8093 Zurich, Switzerland

It is well-known that the fluorescence lifetime of an emitter can be strongly modified when its electromagnetic surrounding is changed by introducing interfaces, mirrors, resonators, etc. There have been also theoretical and experimental reports on the modification of the spontaneous emission of emitters in the near field of a sharp scanning probe tip, or a sample with lateral nanostructures. Here we present a systematic study of the spontaneous emission rate for atoms placed inside subwavelength dielectric particles. By fluorescence lifetime measurements on single nanoparticles we have demonstrated for the first time the change of paradigm from the super-wavelength regime of Mie resonances to the nanoscopic realm of Rayleigh scattering.

As a model system we use polystyrene nanospheres (n=1.59) doped with europium ions emitting at a wavelength of λ_0=615nm. Spheres of various diameters ranging from 100nm to 2000nm were spin coated to produce a very sparse distribution on the surface of a cover glass. In order to perform well-defined control experiments, we have combined atomic force microscopy and fluorescence confocal microscopy to make measurements to select isolated nanospheres. As predicted by the theory [1], the radiative spontaneous decay rate drops as the sphere diameter is decreased (Fig. 1, circles). To provide further evidence for the radiative nature of the effect we reduced the index contrast at the surface of the spheres by covering the sample with a droplet of water (n=1.33, triangles) or immersion oil (n=1.52, squares) and repeating the measurements on the same particles studied in the dry state. Again, we find a very good agreement between the measurements and the theoretical calculations. The comparison between theory and experiment for the different media also allows us to separate radiative and non-radiative parts of the decay process.

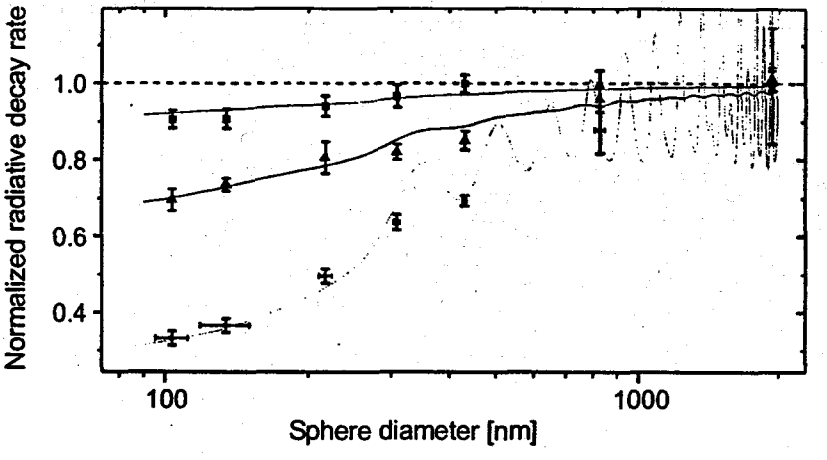

Fig. 1: Symbols display fluorescence decay rates from single Eu^{3+}-doped dielectric spheres normalized to the decay rates in a bulk dielectric. Measurements were done for particles on a glass substrate exposed to air (lower curve), water (middle curve) and immersion oil (upper curve). The lines are results of calculations [1].

In addition, we found that isolated doublets of 100nm spheres show significantly higher decay rates than the isolated single spheres of the same diameter. This underlines the sensitivity of the spontaneous emission process to the electromagnetic boundary conditions at the nanometer scale as well as the necessity of well-controlled experiments with sufficient spatial resolution. In conclusion, our results demonstrate that the fluorescence lifetimes of emitters placed inside a dielectric change substantially and in a systematic way when the medium size is decreased to sub-wavelength dimensions where no longer resonances are supported by the object [2].

References

[1] H. Chew, *Phys. Rev. A.* **38**, 3410 (1988)
[2] H. Schniepp and V. Sandoghdar, submitted

Development of Photothermal Near-field Scanning Optical Microscope

Masanori Fujinami, Kiminori Toya, Hiromi Murakawa, Tsuguo Sawada,
The University of Tokyo, Department of Advanced Materials Science, Hongo, Tokyo 113-0033, Japan.
E-mail: fujinami@k.u-tokyo.ac.jp

Much attention to a near-field scanning optical microscope (NSOM) has been paid in this decade by overcoming the diffraction limit to reach nanometeric size and, fluorescence, photo-luminescence, Raman scattering, and their time-resolved measurements have been combined with NSOM. Photothermal spectroscopy is a highly sensitive and versatile technique. In this study, we have developed a photothermal(PT)-NSOM and investigated the performance. Photothermal spectroscopy relies on absorption of optical radiation by molecule and subsequent non-radiative relaxation. The optical and mechanical effects induced by heat are measured as thermal lens spectroscopy (TLS), photoacoustic spectroscopy, etc. Therefore, the methods based on photothermal effect become applicable to fluorescent and non-fluorescent molecules. The detection limit in TLS is estimated to be in the order of 10^{-8} absorbance and, in addition, a thermal lens microscope enables us to detect single molecule detection, which is comparable to a laser-induced fluorescence microscope. Generation of heat by non-radiative relaxation induces the change in refractive index of matrix. Laser beam with Gaussian intensity profile is usually used as an excitation light, so that refractive index gradient, called as a thermal lens, plays a role as a concave lens for the probe beam with another wavelength. As a result, the intensity of center of the probe beam linearly depends on the size of the concave lens and the quantitative analysis can be done to measure it.

The schematic diagram of PT-NSOM based on an inverted optical microscope is shown in Fig. 1. The molecules were excited by the evanescent wave emitted from the small aperture of the optical fiber probe. In order to measure the thermal lens, two types of methods for incident of the probe beam were investigated. One is coaxial mode to introduce the excitation and the probe beams into the fiber probe. It is known in the near-field light theory that the propagated light cannot be removed completely even if the light is emitted from the aperture with a diameter of less than wavelength. It is, therefore, expected that the transmitted component of the probe beam is deflected by the refractive index gradient induced. Another method is that the probe beam is introduced by the objective lens with high NA (=1.45). The central intensity of the reflected probe beam should be changed by the refractive index gradient and was measured.

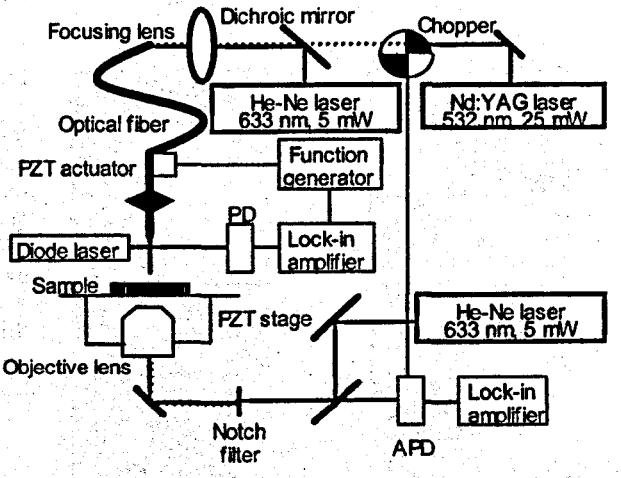

Figure 1: Schematic diagram of photothermal-NSOM

In both of the methods, the photothermal signal for the thin film of sunset yellow FCF on a glass can be obtained, as shown in Fig. 2. Further, we have succeeded in measurement of the photothermal image for a thin Au/glass sample. These results are the first evidence of detection of photothermal signal in NSOM. Fast modulation frequency for excitation laser beam and short time constant in lock-in-amplifier are required in order to obtain the photothermal signal image with high space resolution, so that the improvement of S/N ratio is now in progress.

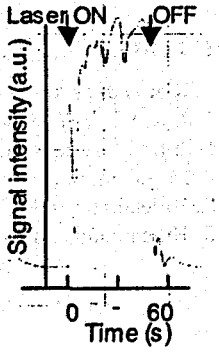

Fig. 2 Photothermal signal of PT-SNOM

Eigenfield patterns of optically resonant nanoparticles mapped by phase-contrast near-field microscopy

R. Hillenbrand, F. Keilmann
Max-Planck-Institut für Biochemie, D-82152 Martinsried, Germany, hillenbr@biochem.mpg.de

In small metal particles light can resonantly excite collective oscillation modes of conduction electrons. This plasmon resonance results in strong scattering and enhanced near-fields that have been subject of several near-field studies [1-4]. By using a scattering-type near-field optical micoscope, mapping both amplitude and phase, we succeeded to resolve the optical field patterns on the surface of single gold particles excited into plasmon resonance [5].

Our microscope uses a commercial cantilevered tip as scattering near-field probe, illuminated by focused light @633 nm. The backscattered light is detected by a heterodyne Mach-Zehnder interferometer in order to simultaneously map both amplitude s and phase φ of the backscattered light. Higher harmonic demodulation of the signal suppresses unavoidable background (i.e. scattering from the sample, cantilever beam and the tip's shaft)[6]. This allows to asses the pure near-field information at 10 nm spatial resolution without height induced artifacts.

We present amplitude and phase images of particles excited dominantly in dipolar or, as in Fig. 1(a), quadrupolar mode. Note the occurrence of field singularities (marked by circles), observed for the first time in a non-propagating near field [5]. Particularly strong, highly confined near-fields were found in narrow gaps between resonant particles (Fig. 1(b)), a promising site for a future observation of single molecules by spatially-resolved. surface-enhanced Raman scattering or nonlinear spectroscopy.

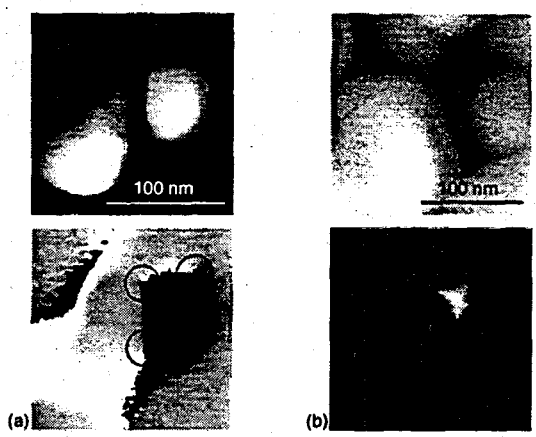

Figure 1:

(a) Near-field images of a gold particle in optical resonance, amplitude (top) and phase (bottom, 360° full scale). The images exhibit a quadrupolar plasmon mode, recognizable by a dark line in the amplitude image accompanied by a phase jump of 180°.

(b) Highly confined optical field in a gap between closely packed gold particles (top: topography, bottom: optical amplitude).

References

[1] T. Klar *et al.*, *Physical Review Letters* **80**, 4249 (1998).
[2] J. R. Krenn *et al.*, *Physical Review B* **60**, 5029 (1999).
[3] J. R. Krenn *et al.*, *Physical Review Letters* **82**, 2590 (1999).
[4] P.-M. Adam, S. Benrezzak, J. L. Bijeon and P. Royer, *Journal of Applied Physics* **88**, 6919 (2000).
[5] R. Hillenbrand and F. Keilmann, *Applied Physics B* **73**, 239-243 (2001).
[6] R. Hillenbrand and F. Keilmann, *Physical Review Letters* **85**, 3029 (2000).

Subsurface Solid Immersion Microscopy for Photonic Nanostructures

Bennett Goldberg, Steven Ippolito, Zhiheng Liu, and M. Selim Ünlü,
Boston University, Boston, MA 02215

Near-field microscopy is limited by the small transmission of sub-wavelength apertures (10^{-3} – 10^{-6} for a<100nm) and by the serial scan process with relatively slow image acquisition rates. These factors restrict the utility of NSOM to experiments where proximity of the probe provides new information or where the source is bright, largely time independent and long lived. As a result, time resolved, pump probe, Raman and non-linear spectroscopies are not widespread with resolution below 100nm.

Over the past decade solid immersion microscopy has emerged to provide tremendous imaging capability to complement the restrictions of optical scanned probe techniques. The technique is based upon using a transparent (at the wavelength of interest) semi-spherical lens where the object space is either at the interface of the lens and the material under study, or embedded within a similar material.

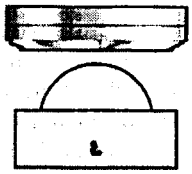

Fig 1. Schematic diagram of numerical aperture increasing lens (NAIL), combining the sample and semi-sphere as super SIL for subsurface solid immersion microscopy.

The solids used are high index materials ($2.0 < n < 3.5$) and with the combination of the reduction of the wavelength by l/n, and an increase in the numerical aperture, diffraction limited resolution increases of greater than 10 ($\sim n^2$) in the lateral direction and greater than 30 ($\sim n^3$) in the longitudinal direction have been demonstrated, together with factors of 10 increase in light gathering ability. [1-4]

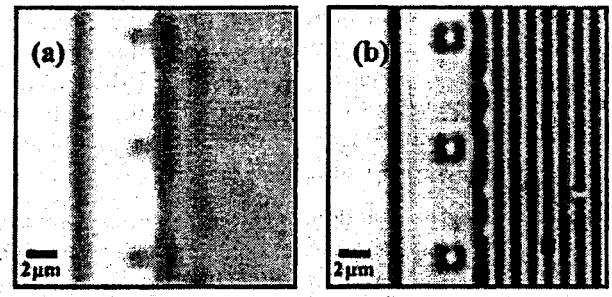

Figure 2. Images taken by Hamamatsu μAMOS-200, IC Failure Analysis System, demonstrate how a NAIL improves resolution well beyond the state-of-the-art in through-the-substrate imaging of Si circuits. (a) Image obtained using the 100X objective having NA=0.5 and (b) image with the 10X objective (NA=0.25) and NAIL increasing the NA to 3.3.

We have recently applied solid immersion techniques to subsurface microscopy, where the wavelength in the medium is defined by the sample under study, and thus the only method to improve the spatial resolution is to increase the collected solid angle, i.e., the *NA* must be increased. This is because the large index *n* in the object space in standard subsurface microscopy of planar samples does not increase the *NA* due of refraction at the planar boundary. Recently, we have implemented a solid immersion microscopy technique for subsurface imaging [4]. A Numerical Aperture Increasing Lens (NAIL) is placed on the surface of a sample as illustrated in Fig. 1 with parameters chosen such that the object space coincides with the aplanatic points of the NAIL's spherical surface. The convex lens surface effectively transforms the combined lens and planar sample into an integrated super-sphere solid immersion lens. Figure 2 shows the direct comparison using imaging through the backside substrate of a silicon SRAM IC. The NAIL subsurface immersion microscopy increases the lateral resolution by a factor of 12 laterally and over 100 longitudinally.

We will present new results on using subsurface solid immersion microscopy to demonstrate the n^3 improvement in longitudinal resolution, as well as new work on quantum dot and photonic bandgap systems. In quantum dot systems, we have implemented backside imaging to provide high-throughput time-resolved spectroscopy of single quantum dots, especially in the density regime where dot-to-dot coupling is important.

References

[1] B. D. Terris, H. J. Mamin, D. Rugar, W. R. Studenmund, G. S. Kino, "Near-field optical data storage using a solid immersion lens," *Applied Physics Letters* 65 (1994): 388. B. D. Terris, H. J. Mamin, D. Rugar, "Near-field optical data storage," *Applied Physics Letters* 68 (1996): 141.

[2] Qiang Wu, G. D. Feke, Robert D. Grober, and L. P. Ghislain, "Realization of numerical aperture 2.0 using a gallium phosphide solid immersion lens," *Appl. Phys. Lett.*, 75, 4064 (1999).

[3] Khaled Karrai, Xaver Lorenz, Lukas Novotny, "Enhanced reflectivity contrast in confocal solid immersion lens microscopy," *Applied Physics Letters* 77 (2000): 3459.

[4] S. B. Ippolito, B. B. Goldberg, M. S. Ünlü, "High spatial resolution subsurface microscopy," *App. Phys.Let* 78 (2001): 4071.

Surface Plasmon Polariton Waveguiding in Random Surface Nanostructures

S. I. Bozhevolnyi, V. S. Volkov,
Institute of Physics, Aalborg University, DK-9220 Aalborg, Denmark
K. Leosson,
Micro Managed Photons A/S, COM, DTU, Bldg. 345v, DK-2800 Kgs. Lyngby, Denmark

Strong (Anderson) localization of light in random media, i.e., capturing light in a random cavity, is one of the most fascinating optical phenomena. Strong localization of light happens due to interference in recurrent multiple scattering in random (non-absorbing) media and is expected when the scattering mean free path l decreases below the light wavelength. The value of l diverges in the limit of both short and long wavelengths [1] implying that the localization effect can be realized only in a limited wavelength interval, similar to the photonic band gap effect (PBG) in periodic media [2]. In fact, there are many similarities between these phenomena: both are related to interference in multiple light scattering, lead to the inhibition of light propagation and exhibit a threshold character with respect to the dielectric contrast. Given the similarities between the phenomenon of strong localization and the PBG effect, we realized that one should be able to employ channels and cavities in (non-absorbing) strongly scattering random media for essentially the same purposes as those in the PBG structures, i.e., for light guiding along line defects. One might suggest that the localization can be realized in a broader wavelength range than the PBG effect, since the former is not as directly governed by the geometrical characteristics of structured media as the latter. Furthermore, the absence of symmetry in random structures facilitates matching the modes propagating in differently oriented channels and thereby may reduce the associated bend loss.

We propose to use channels in strongly scattering non-absorbing random media for guiding electromagnetic waves and demonstrate this concept using near-field microscopy of surface plasmon polaritons (SPP's) propagating along the gold film surface covered with randomly located scatterers [3]. In the wavelength range of $720-790\ nm$, we observe complete inhibition of the SPP propagation inside the random structures composed of individual ($\sim 50-nm$-wide) gold bumps (and their clusters) placed on a $40-nm$-thick gold film with the bump density of $75\ \mu m^{-2}$. We demonstrate well-defined SPP guiding along corrugation free $2-\mu m$-wide channels in random structures and virtually loss-free bending by 20^o (Fig. 1).

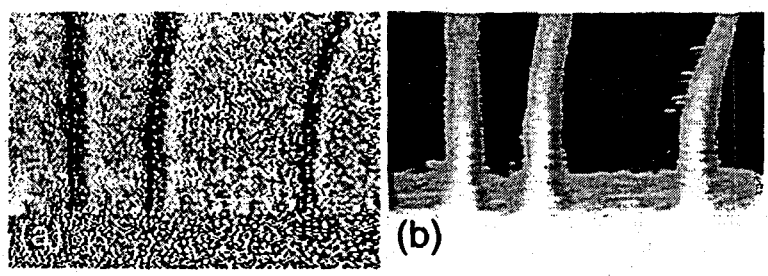

Figure 1: Gray-scale (a) topographical and (b) near-field optical images ($32\times 22\ \mu m^2$) taken at $\lambda = 750\ nm$ showing SPP guiding along straight (left), 10^o- (middle) and 20^o-bent (right) line defects.

References

[1] S. John, in *Scattering and Localization of Classical waves in Random Media*, edited by P. Sheng (World Scientific, Singapore, 1990), p.1.

[2] J. D. Joannopoulos, R. D. Meade, and J. N. Winn, *Photonic Crystals* (Princeton Press, NJ, 1995).

[3] S. I. Bozhevolnyi, V. S. Volkov, and K. Leosson, submitted to *Phys. Rev. Lett.*

Bandwidth enhancement for shear-force feedback by exploiting the nonlinear probe-sample interaction

C.L. Jahncke
St. Lawrence University, Canton, NY 13617.
H.D Hallen,
North Carolina State University, Raleigh, NC 7695-8202.

The combination of a high Q oscillators (200-700) with a relatively low resonant frequency (30-40kHz) as is the case with high Q tuning forks[1] used in near-field optical microscopy limits the feedback bandwidth. As feedback gains are increased, the system oscillates at a frequency that is approximately the width of the resonance peak -- typically 10's of Hertz. The oscillation is asymmetric (figure 1) as a result of the nonlinear interaction between the probe and the sample. When the probe is too far from the surface, it takes longer to find the surface due to the slow recovery time of the high Q oscillator. Alternately, when the probe is close to the surface, the vibration is rapidly quenched. We exploit the nonlinear interaction between the probe and the sample to increase the bandwidth of the feedback loop.

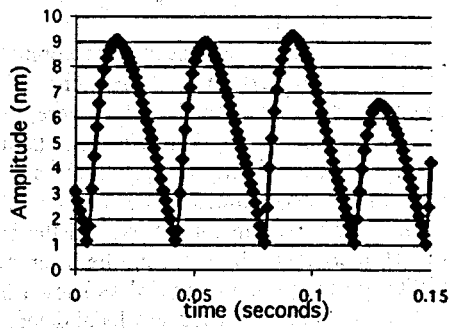

Figure 1: Asymmetric oscillations indicating the nonlinear tip-sample interaction

The nonlinear tip-sample interaction can be modeled as a tapping force producing an accurate representation of resonance curves at different probe sample separations[2]. We use this model to study the system dynamics by alternately adding in and removing the tapping force from the simple driven damped harmonic oscillator equation. We look at the 1/e fall and rise time of the signal respectively. We find that at resonance, the time response of the probe with the tapping off is much slower than the time response of the probe with the tapping on (figure 2a). However, as we move off resonance to either the low frequency or the high frequency side, we see an improvement in the time response. Additionally the time response for the two directions becomes the same on the high frequency side. We perform several experiments to investigate the time response of the feedback system. Figure 2b shows the time for the probe to find the feedback setpoint as an 8msec ramp pulse pulls the probe away from the surface. The gains are carefully optimized in each case to prevent overshoot. This experiment is analogous to the tapping off case for our model and we see similar behavior. Our experiments show that the time response is faster and the time for the in and out motion of probe becomes the same on the high frequency side of the resonance curve resulting in increased bandwidth.

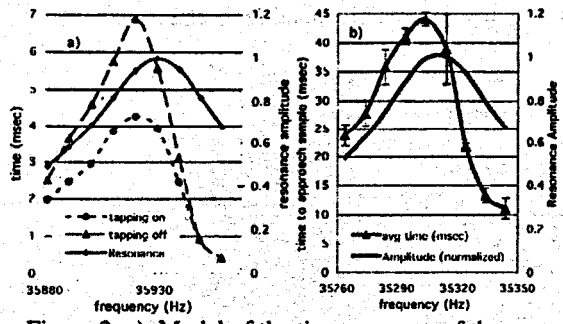

Figure 2: a) Model of the time response of the probe with tapping on and tapping off. b) Time for the probe to find a surface given an 8msec ramp away from the surface. The resonance curve is overlaid in a and b for reference.

References

[1] K. Karrai and R.D. Grober, *Appl. Phys. Lett.* 66, 1842 (1995).
[2] M. J. Gregor, P.G. Blome, J. Schofer and R.G. Ulbrich, *Appl. Phys. Lett.* 68, 307 (1996).

Mapping the Intensity Distribution in a Photonic Crystal Microcavity

P. Kramper
Universität Konstanz, Fachbereich Physik & Optik-Zentrum Konstanz, 78457 Konstanz, Germany,

V. Sandoghdar
Swiss Federal Institute of Technology (ETH), 8093 Zürich, Switzerland.

Photonic crystals have been the subject of intensive studies in the past few years. A point defect in a photonic crystal results in a resonance in the band gap and confinement of light to a region smaller than one wavelength. A linear array of such point defects creates a photonic band gap waveguide and the combination of such waveguides will in turn produce a wealth of optical elements such as beam splitters and interferometers.

In this paper we present a combination of direct laser spectroscopy and scanning probe optical microscopy to perform measurements of sharp resonances in a deep two-dimensional photonic crystal microresonator. Photonic crystals were fabricated by electrochemical preparation of macroporous silicon. The structure in our experiment consists of a triangular crystal of air cylinders with a depth of 100 μm and a lattice constant of 1.5 μm providing a band gap around 4 μm [1]. Two line defects and an isolated point defect were incorporated in the crystal as shown in Fig. 1b).

In a first experiment we excited the spectrally sharp and locally highly confined modes of the point defect microcavity by focusing the beam of a widely tunable continuous-wave optical parametric oscillator (OPO) on the photonic crystal as shown in Fig. 1a). An uncoated tapered fluoride glass monomode fiber (nearfield probe 1) is used as a local detector. By raster scanning the fiber tip against the exit plane, we map the spatial distribution of the light transmitted by the photonic crystal with a resolution of one optical wavelength. Then by repeating these measurements for different laser wavelengths, we recorded two sharp resonances with quality factors of 190 and 640 [2]. Two-dimensional Finite Difference Time Domain calculations were performed for the experimentally investigated microresonator structure. The spectrum reproduces the two resonances and agrees very well with the measured ones.

In order to visualize the modes in the cavity, we have added a second near-field probe at the top side of the photonic crystal. The fiber extracts locally the energy out of the cavity mode. By scanning the fiber across the surface we have mapped the intensity distribution directly to be well beyond one optical wavelength (see fig. 1c). By tuning the OPO to an off-resonant wavelength the signal vanishes as expected. We compare our results with those of the calculations and discuss possible imaging mechanisms.

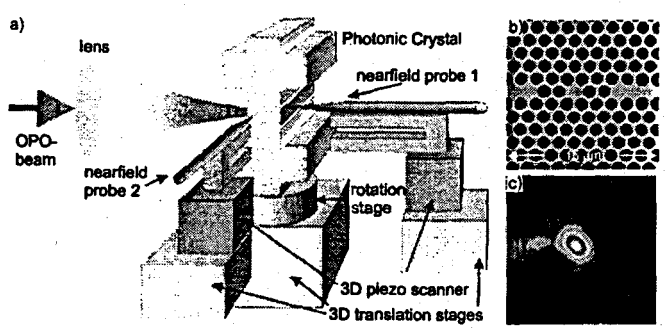

Figure 1: a) Setup for near-field intensity mapping. b) The investigated microresonator structure. c) Intesity distribution as seen by the near-field probe #2 on resonance.

[1] A. Birner, U. Grüning, S. Ottow, A. Schneider, F. Müller, V. Lehmann, H. Föll, and U. Gösele, Phys. Stat. Sol (a), **165**, 111 (1998).
[2] P. Kramper, A. Birner, M. Agio, C.M. Soukoulis, F. Müller, U. Gösele, J. Mlynek and V. Sandoghdar, Phys. Rev. B. **64**, 233102 (2001).
[3] P. Kramper, M. Agio, C. M. Soukoulis, A. Birner, U. Gösele, R. Wehrspohn, and V. Sandoghdar, *in preparation.*

Polymer NFO probe made by a nanomolding method

G. M. Kim[1], E. ten Have[2], F. Segerink[2], B.J. Kim[2,], N. F. van Hulst[2], and J. Brugger[1,2]*

[1] *Ecole Polytechnique Federale de Lausanne (EPFL), CH-1015 Lausanne, Switzerland*
[2] *MESA+ Research Institute, University of Twente, 7500 AE Enschede, The Netherlands*

Many polymers have the ability to conform themselves to surface contours down to few nanometers. We studied the filling of transparent epoxy-type EPON SU-8 into nanoscale apertures made in a thin metal film as a new method for polymer/metal NFO structures. As shown [1], topographically flat structures with a high optical contrast can be obtained. Mold replica processes combining silicon micromachining with the photo-curable SU-8 offer great potential for low-cost nanostructure fabrication. This has led to the successful implementation of plastic probes for atomic force microscopes [2] and to some initial attempts for NFO applications [3]. Besides offering a route for mass-production the transparent pyramidal probes are expected to improve light-transmission thanks to a wider geometry near the aperture.

After a series of initial experiments combining silicon MEMS, mold geometry tuning by oxidation, anti-stiction coating by self-assembled monolayer (SAM), and mechanical release steps, we propose here following new method: The mold is fabricated on silicon wafer by self-terminating etching and defines the pyramidal geometry of the actual probe. The non-uniform SiO_2 growth at regions with high curvature was used to create pits with a well defined radius ranging between 50-250 nm [4]. A SAM of dodecyltrichrorosilane was then formed on the mold surface as anti-stiction coating, and a 150-nm thin layer of opaque Al layer was deposited. A focused ion beam drilled well-defined 50-100 nm apertures in the Al film directly inside the mold. SU-8 was spin-coated on the wafer, which filled the mold and the nano-apertures in the Al layer. A second layer SU-8 was structured by lithography to form the probe shape. The subsequent stage of bonding with optical fiber and releasing of the fabricated probe from the tip mold follows essentially the procedure described earlier [3]. Since the SAM reduces the adhesion force between the surfaces of mold and metal layer, the probe is released together with the apertured metal layer.

The major improvement is the possibility to fabricate NFO apertures directly on wafer scale during the micro-fabrication process and not on free-standing tips. The structures are currently being tested. First results indicate a lateral optical resolution in the 100 nm range.

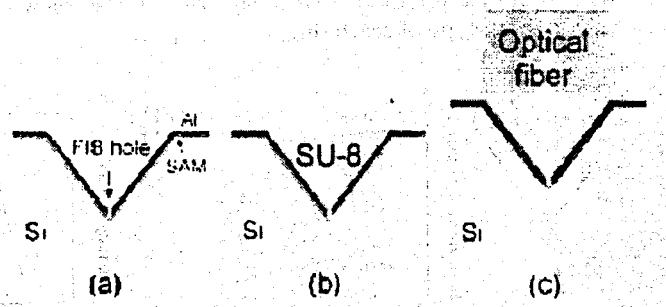

Figure 1: Schematic view of probe fabrication : (a) aperture making on the mold, (b) SU-8 probe structuring, (c) releasing the probe with apertured metal

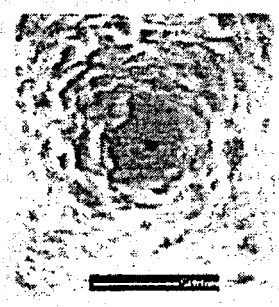

Figure 2: FIB image of aperture made on the mold

References:

[1] B.J. Kim, et.al., J. Microelectronic Engineering 57, 755 (2001)
[2] Genolet, et.al., Rev. Sci. Instrum. 70, 2398 (1999)
[3] B.J. Kim, et.al., J. Microsc. 202, 16 (2001) ; Genolet, et.al., Rev. Sci.Instrum. 72, 3877 (2001)
[4] G.M. Kim, et.al., J. Nanoscience and Nanotechnology 2, 55 (2002)

* present address : *Institute of Industrial Science, Tokyo University, Tokyo 153-8505, Japan*

Ultrafast Spectroscopy in the Spatial Domain: Sub-10 fs Radiative Decay Times of Surface Plasmons in Plasmonic Band Gap Structures

D. S. Kim, S. C. Hohng, and Y. H. Ahn
School of Physics, Seoul National University, Seoul 151-742, Korea
V. Malyarchuk , R. Müller and Ch. Lienau
Max-Born-Institute für Nichtlineare Optik und Kurzzeitspektroskopie, D-12489 Berlin, Germany.
J. W. Park and J. H. Kim
Korea Research Institute of Standards and Science, Yunsung, P. O. Box 102, Taejon 305-600, Korea.
Q. H. Park
Department of Physics, Korea University, Seoul 136-701, Korea.

Plasmonic bandgap structures have been proposed to find applications in novel nano-optic devices, e.g. as spectral filter or near-field light sources [1]. To this end, a microscopic understanding of their unusual optical properties, specifically plasmonic excitations, is needed. In this paper, we propose and demonstrate a novel experimental approach to directly measure the coherence properties of surface plasmons (SP) in plasmonic band gap structures, determining the line-shapes of near and far-field transmission spectra.

We locally photo-excite SP at the air-metal interface of grating, and measure the coherent SP propagation across the metal nanostructure by probing the light intensiy in another grating (Fig 1a). The experiments are performed near the air-metal [1, 0] SP resonance. Shown in Fig. 1b are the near-field scan images of the non-illuminated grating at two different excitation wavelengths. In both cases, light intensity rapidly decreases as we probe deeper into the grating. This is due to the radiative loss of SP in the presence of the periodic array of holes. The measured SP coherence lengths can be shorter than 2 μ and are strongly wavelength-dependent as evident in Fig. 1(b) and 1(c). Since SP velocity is very close to the speed of light, this short coherence length is indicative of ultrashort radiative lifetime of SP in these structures. The short radiative lifetime is consistent with the time delay experienced by femtosecond pulses propagating through the grating, as shown in Fig. 1(d). Our experiments show that the decay of the coherent SP polarization in peridioc nanohole arrays are T_1-dominated, given by the radiative SP decay. We will also show that the origin of this ultrafast radiation is a resonant Rayleigh-type of scattering.

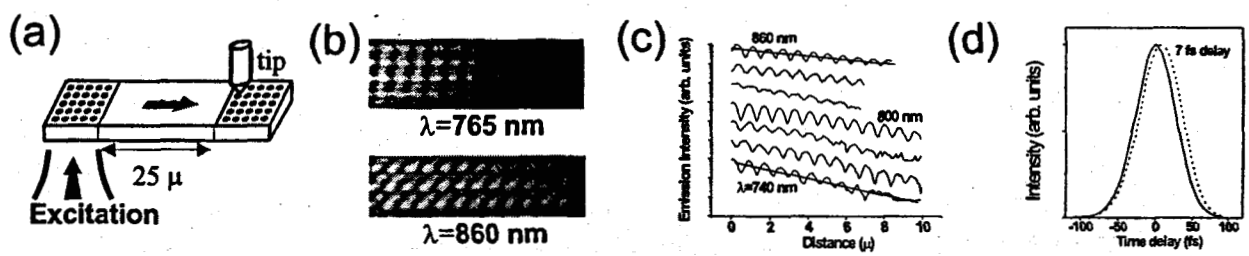

Figure 1: **(a)** Schematics of our experiment **(b)** Near field scan images at excitation wavelengths of 765 nm (top) and 860 nm (bottom). **(c)** Logarithmic plot of cross-sectional scans at various excitation wavelengths, from top to bottom, 860, 840, 800, 780, 760 and 740 nm. **(d)** Transmission through a sapphire substrate (solid lines) a nanohole array evaporated onto the sapphire substrate (dashed lines), showing a 7 femtoseconds time delay.

References

[1] T. W. Ebbesen *et al.*, Nature **391**, 667 (1998).

Fast Optical Dual-Beam Technique to characterize Thermal Axial Elongation of Near-field Probes

A. La Rosa, B. Biehler, A. Sinharay
Department of Physics, Portland State University, Portland, OR 97207

We use purely optical means to monitor in real time the thermal elongation that near-field optical probes undergo upon the application of pulsed light. This new approach overcomes the limited frequency bandwidth encountered in methods based on electronic feedback responses. With the use of two laser beams, one serving as a heat source and the other to monitor the corresponding probe elongation in an interferometric optical set up, we are able to measure for the first time thermal time constants in the microsecond regime. This work is relevant to NSOM applications that use modulated light.

Corresponding author:
Andres H. La Rosa
Assistant Professor
Department of Physics
P.O. Box 751
Portland State University
Portland, Oregon 97207-0751

Ph (503) 725-8397
Fax (503) 725- 9525
andres@pdx.edu

Waveguiding through a two dimensional metallic photonic crystal

Fadi Baida, Daniel Van Labeke, Y. Pagani*
Laboratoire d'Optique P.M. Duffieux
Université de Franche Comté
CNRS, UMR 6603
Institut des Microtechniques de Franche Comté
Route de Gray, 25030 Besançon,France
**Email :daniel.vanlabeke@univ-fcomte.fr*

Most of the experiments on photonic crystals are performed with dielectric structures. Recently Bozhevolnyi et al. have presented very interesting results demonstrating photonic band gap effects in metallic planar photonic crystals [1-4]. The surface plasmon is produced by attenuated total reflection in the Kretschmann configuration on a glass-gold-air structure. The planar photonic crystal is made with gold dots (200nm diameter, height 45 nm). Propagation of the Plasmon through the structure is studied with a near-field microscope in the detection mode (STOM-PSTM).

We present 2D-FDTD [5] simulations of those experiments. The structure is a 2D triangular lattice of infinite metallic rods where various channels are created by suppressing series of rods. The crystal parameters are the same than in the experiments (period 400nm, rod diameter 200nm). The permittivity of gold is described by a Drude model. We study the injection and the propagation of light through linear waveguides of various widths and for different incident wavelengths. We also study the propagation in a 90° bent line defect. We show that the optical properties depend on the direction of injection. The two cases of ΓM and ΓK directions are compared. An example is presented in figures (a-f).

Our simulations succeed to reproduce most of the experimental results: a guiding effect is obtained through linear and bent structures. The quantitative comparison will be discussed.

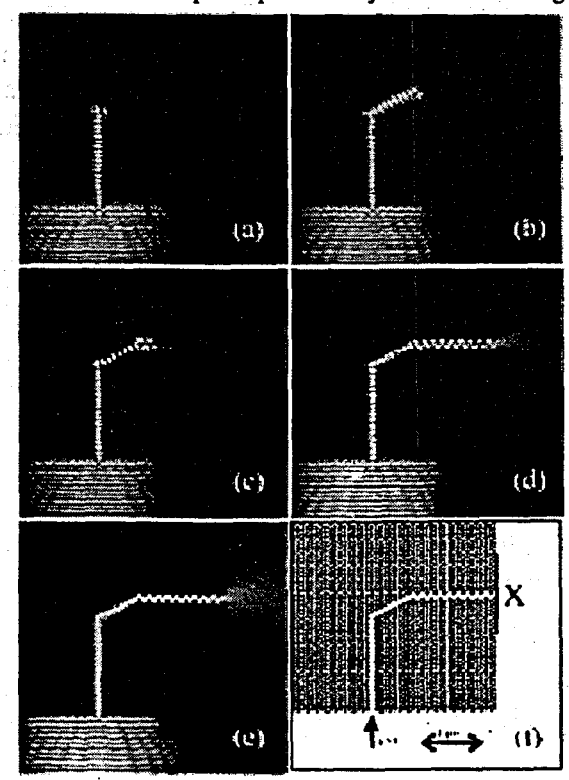

Figure: Propagation through a 90° bent line defect with injection along ΓM direction. (a) λ=727nm, (b) λ=750nm, (c) λ=785nm, (d) λ=815nm and (e) λ=850nm.

References

[1] S. I. Bozhevolnyi, V.S. Volkov, K. Leosson, A. Boltavessa, *Appl. Phys*. Lett. 29 pp1076-1078 (2001)
[2] S. I. Bozhevolnyi, V.S. Volkov, K. Leosson, *Optics. Comm.* 196,41-45 (2001)
[3] S.I. Bozhevolnyi, V.S. Volkov, K. Leosson, J. Erlan, *Opt.Lett.* 10 pp734—736 (2001)
[4] S.I. Bozhevolnyi, J. Erland, K. Leosson, P. Skovgaard, J. Hvan, *Phys.Rev. Lett.* 86,3008-3011 (2001)
[5] G. Parent, D. van Labeke, F. Baida, *J. Microscopy*, 202 pp296-306 (2001)

Scanning probe microscopies using quartz crystal resonator

Yongho Seo, Wonho Jhe,
Center for Near-field Atom-photon Technology and School of Physics,
Seoul National University, Seoul 151-747, Korea.

After the invention of the tuning fork based-NSOM, the quartz crystal tuning fork has been investigated for a force sensor in field of scanning probe microscopy including NSOM. Recently, Seo *et al.*[1] realized a high-frequency dithering probe using a quartz crystal resonator (QCR), which is operated at several-MHz resonance frequency and is known to be one of the highest-frequency dithering piezo-electric devices. However, because of its high stiffness ($\sim 10^4$ N/m for tuning fork and $\sim 10^6$ N/m for QCR), there has been a limitation as a sensitive force sensor. On the other hand, its small dithering amplitude (≤ 0.1 nm) and high Q-value ($10^4 \sim 10^6$) are important advantages for high force sensitivity. We demonstrate various scanning probe microscopies using tuning fork and QCR.

We employed a QCR with a resonance frequency of $f_0 = 2$ MHz as an NSOM shear force sensor. In order to allow the optical fiber to guide the light down to the fiber tip near the sample surface and also to be mechanically connected to the QCR, we perforated the QCR near its center and then inserted the tapered fiber tip into the hole. Figure 1(a) shows NSOM images of a grating with 0.8 μm pitch. The scanned area and scanning time are 10×10 μm^2 and 0.5 s, respectively. Notice it is the fastest NSOM image (scanning speed = 1.3 mm/s).

The tuning fork based electrostatic force microscopy (EFM) and magnetic force microscopy (MFM) were developed. Electrochemically etched Ni tip was attached at a prong of the tuning fork ($f_0 = 32$ kHz). By applying dc field at the tip (10 V), the ferro-electric polarization of PZT thin film can be manipulated within 100 nm line width. Its image was obtain by scanning the same area keeping the gap (10 nm) between the tip and PZT, constantly. Figure 1(b) shows an EFM image of PZT thin film after some characters was written. Its scanned area is 8×8 μm^2.

With the same method, a Co tip was attached to the tuning fork and an MFM image was obtained in lift-mode. MFM image of commercial hard disk is shown in Fig.1(c). Its scanned area is 30×30 μm^2.

Figure 1: NSOM image of an optical grating (left), electrostatic force microscopy image of PZT thin film (center) and magnetic force microscopy image of hard disk (right).

References

[1] Y. Seo, J. H. Park, J. B. Moon, and W. Jhe, *Appl. Phys. Lett.* **77**, 4274 (2000).

Near-Field measurement of short range correlation in optical waves transmitted through Random Media

V. Emiliani, F. Intonti, D. Wiersma and M. Colocci, LENS and INFM, Florence, Italy 50125.
M.Cazayous, University Paul Sabatier, 31062 Toulouse, France
A. Lagendijk, Univ. of Twente, Enschede, The Netherlands
F. Aliev, Univ. of Puerto Rico, San Juan, Puerto Rico 00931

A wave propagating in a random media undergoes multiple scattering from the inhomogeneities which give rise to a complicated, irregular intensity *bulk speckle pattern*. The statistical properties of such pattern are described by the correlation function $C = \langle \delta I \delta I' \rangle$, where δI is the fluctuation of the intensity with respect to its average value. The leading contribution to C is the short-range correlation term and is given, in the weak scattering regime, by the square of the field correlation function: $C_1 = |\langle EE'^* \rangle|^2$. The spatial dependence of C_1, for a monochromatic source is given by $(sink\Delta r/k\Delta r)^2 exp(-\Delta r/l_s)$ [1], where k is the wave vector and l_s the transport mean path. This expression predicts the formation of isotropic speckles with the size of the transport mean path with further intensity modulation on the scale length of the wavelength. While the first property has been experimentally verified for optical waves, the second has been so far observed only for microwave radiations [1].
In this paper, near field images of the speckle pattern formed after diffusion through a disordered medium are presented. The subwavelength spatial oscillations predicted by the theory are resolved and their dependence on the excitation wavelength is verified.
The sample studied is a disordered structure of porous silica glass with connected pores ($100nmsize$). Light from a He-Ne (632 nm) and a diode Laser (780 nm) is transmitted through a pulled coated near field probe. The diffusely transmitted light from the sample is collected in far field and detected with a GaAs photomultiplier. Near field optical maps are recorded by scanning the sample in respect to the near field probe. The wavelength dependence is obtained by changing the excitation beam in consecutive scans so that the *same* sample region is scanned in the two measurements. Fig. 1(a) shows the 2D near filed map of the speckle patterns for excitation wavelength of 780 nm. Fig. 1(b) shows the spatial dependence of C obtained for excitation at 780 nm and 632 nm. In the same figure the experimental curves are compared with the theoretical ones (solid lines). The agreement between experimental results and theoretical prediction, is the first evidence of the short range correlation term for optical waves.

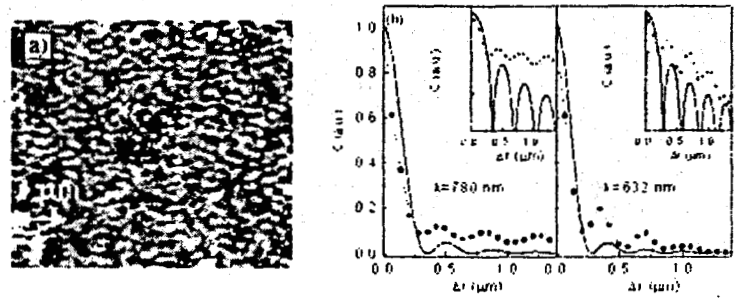

Figure 1: (a)2D map of the transmitted light for 780 nm incident wavelength. (b) Plot of the experimental $C(\Delta r)$) for the wavelengths reported in the figure, compared with the theory.

References

[1] P. Sebbah, B. Hu, A. Z. Genack, R. Pnini, and B. Shapiro, *Physical Review Letters* 88, 123901 (2002) and references therein.

Absorption of evanescent light by Cs atoms of an optically forbidden transition

S. Tojo, M. Hasuo, and T. Fujimoto, Kyoto University, Graduate School of Engineering, Kyoto Japan, 606-8501

Near the critical angle we have observed the reflection spectra of the electric quadrupole transition, that is an optically forbidden transition, of cesium $6^2S_{1/2} \rightarrow 5^2D_{5/2}$ with the hyperfine structure of the ground state resolved. To observe those spectra a highly-sensitive measurement was needed since the oscillator strength of the optically forbidden transition is smaller than that of an electric dipole transition by $\sim 10^{-7}$.

The frequency of the external-cavity diode laser light is scanned over the Cs quadrupole line (685nm) with frequency modulation. The p-polarized laser beam is incident on the prism of Pyrex glass. The incident angle of the laser light is varied over a small interval around the critical angle. This prism serves as one side of the cell which contains a cesium vapor. The reflected laser light and the reference laser light are simultaneously detected by a balance receiver consisting of two photodiodes; this gives the difference between the signal beam intensity and the reference beam intensity. Another part of the laser light goes through the reference cell, the absorption spectrum of which is to be compared with the reflection spectrum.

Figure 1 (the solid line) shows a reflected spectrum of $6^2S_{1/2}(F = 4) \rightarrow 5^2D_{5/2}(F')$ transition. The recorded spectrum is the first derivative of the absorption line owing to the frequency modulation. The incident angle detuning from the critical angle is +2.1 mrad. The temperature is 558K and the atom density is $2.19 \times 10^{22} m^{-3}$.

We calculate the reflection spectrum on the bases of Fresnel's low [1] and compare it with the experimental absorption spectrum in Fig. 1 (the dashed line). Here, the oscillator strength is estimated from the absorption spectrum by the reference cell, i.e., $f = 4.92 \times 10^{-7}$. As shown in Fig. 2, we compare between the experiment and the calculation against the incident angle from under the critical angle (the '-' sign) to over that (the '+' sign). The absorption of the evanescent light is enhanced about a factor 2 from that of the calculation on the assumption of an electric dipole transition.

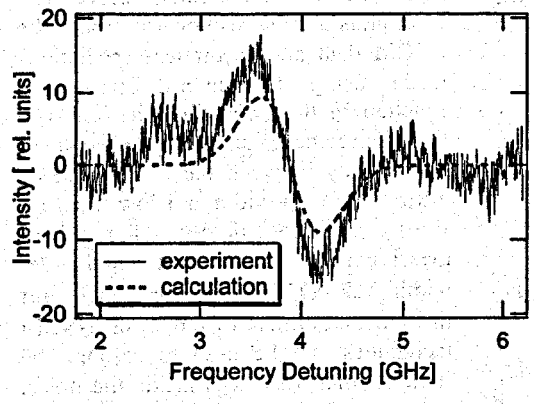

Figure 1: The first derivative of the reflection spectra at +2.1 mrad over the critical angle.

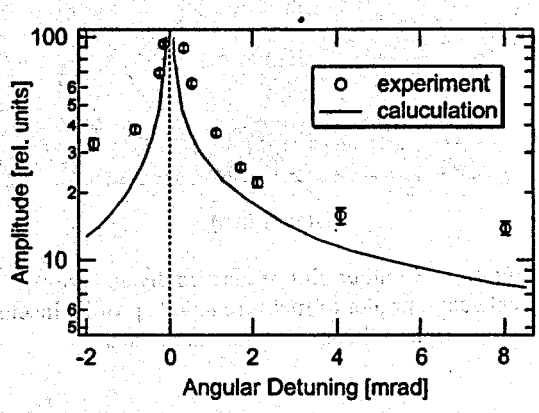

Figure 2: Dependence of signal amplitude on the angular detuning.

References

[1] G. Nienhuis, F. Schuller, and M. Ducloy, *Phys.Rev.A* **38**, 5197 (1988).

Optical Characterization Of Holey Fibers Using NSOM techniques

C.W.J Hillman, W.S. Brocklesby, T.M Monro, W. Belardi and D.J Richardson
Optoelectronics Research Centre, University of Southampton. Southampton. UK. SO17 1BJ.

A holey fiber (HF) is an optical fiber whose optical properties and confinement mechanism are defined by air holes that run the entire length of fiber, rather than a traditional high index core and low index cladding. These fibers can offer many variations on the traditional mode profiles of core/clad fibers. One area of particular interest is the ability to produce tight confinement of the optical mode, and thus high effective nonlinearity when compared to standard fibers.

In order to understand the properties of holey fibers, it is necessary to know the structural profiles and optical mode profiles in some detail. Each different pattern of holes will have individual optical mode properties, which can be calculated using knowledge of the exact physical structure of the fiber. The current work describes how we can use NSOM-based techniques to measure the optical mode structure. This is compared with the calculated mode structure, which relies on very accurate atomic force microscope (AFM) images of the physical structure.

Most characterization of holey fibers relies upon mode measurement by imaging the end of the fiber, and structure measurement using scanning electron microscopy. Both these techniques have drawbacks. Holey fiber modes can be extremely small, making imaging difficult. One of the interesting things about holey fiber modes is that they can have evanescent components in radial directions, where the light extends into the air holes in the fiber. These cannot propagate through a traditional imaging system. These components can be available to a near field measurement. The physical profile needs to be accurate to better than 10nm in order for the mode calculations to be effective – this resolution is much more easily obtained through AFM than SEM techniques.

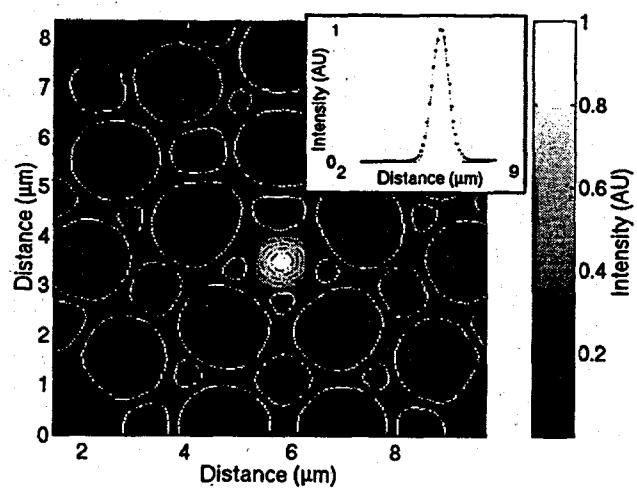

Figure 1 - Contour plot of topography and grey scale/contour plot of measured mode profile. Inset shows comparison of theory and measured data.

To obtain a direct experimental measurement of the near field mode profile[1], we have applied technologies developed for scanning near field optical microscopy (NSOM). The greyscale image in Fig.1 shows the data collected in a NSOM scan with an aluminized tip held 10nm above the fiber surface. The inset plots a cross-section from both the NSOM data and theoretical predictions made using the hybrid orthogonal function method described in Ref. [2]. Good agreement can be seen. The small discrepancy between the modes can be attributed to tip width and low intensity fiber cladding modes. For these measurements the experimental $1/e^2$ width was 0.710μm, as opposed to our theoretical estimate of 0.632μm. NSOM techniques can be used to explore the field at small distances inside the holes, and also to explore the transition from guided mode to free space propagation. These NSOM-based techniques will ultimately prove invaluable tools with which to better characterize the unique and exciting properties of this new class of optical fiber.

References

[1] D.J. Butler, K.A. Nugent, and A. Roberts, *Journal of Applied Physics*, **75(6)**, 2753-2756 (1994)
[2] T.M.Monro, D.J.Richardson, N.G.R.Broderick, and P.J.Bennett, *IEEE Journal of Lightwave Technology*, **17**, 1093-1102 (1999)

Near-field Probe Characterization by Nanoscopic Holes

M. Wellhöfer, O. Hollricher,
WITec GmbH, Hörvelsinger Weg 6, D-89081 Ulm, Germany.
O. Marti,
University of Ulm, Dept. Exp. Physics, Albert-Einstein-Allee 11, D-89069 Ulm, Germany.

Resolution in near-field optical microscopy is a point of intensive discussion. The maximum resolution in a near-field image is determined by aperture size, probe-sample distance and the sample itself. But there are also effects due to nonlinear interaction between the electromagnetic (optical) waves and the surface that often make image interpretation very complicate.

There have been several attempts to determine the aperture size of a near-field tip by far-field methods, but none of these methods can deliver the real shape and size of the effective optical aperture. Our approach is to develop a sample with defined nanoscopic holes in an opaque metal layer.

By scanning the tip across such a hole one obtains a transmission pattern, from which the size and form of the optical aperture can be determined. Important is, that the diameter of the nanoscopic hole is smaller than (or at least equal to) the probe under test. Many problems have their origin in the fact that the size and shape of the used near-field aperture can only be roughly estimated.

We show first results of a calibration test sample. The SNOM measurements are performed in transmission geometry, illumination mode. Deconvolution of the obtained optical near-field images with the sample geometry can give an idea of the shape and size of the effective optical aperture.

Light wave propagation through submicrometer high-dielectric contrast systems

R. Quidant, J. C. Weeber and A. Dereux
Equipe Optique Submicronique, Laboratoire de Physique de l'Université de Bourgogne, Dijon, F-21078.

The miniaturization of optical circuitry has become of crucial interest as the limited speed of electrons within electric connections will soon be restrictive in high-rate information technologies. One alternative to allow the control of light wave propagation at the submicrometer scale is the use of optical confinement provided by high-dielectric contrast materials.

In this study, guiding properties of TiO_2 on glass systems featuring submicrometer transverse sections are investigated using a Photon Scanning Tunneling Microscope (PSTM). For this purpose, an original coupling technique based on a local evenescent light source has been developed. First results show strong confinement of guided light in 200 *nm* wide wires and their ability for defining twisted optical paths within compact volumes [1, 2]. Different geometries are considered: linear wires, splitters with high-opening angles (figure 1.a) and micro-rings. Furthermore, a resonant non-radiative photonic transfer through a periodic alignment of mesoscopic TiO_2 particles is demonstrated (figure 1.b-c). Experiments in agreement with calculations based on the Green dyadic method reveal a strong influence of the particles shape and sizes on the propagation efficiency [3].

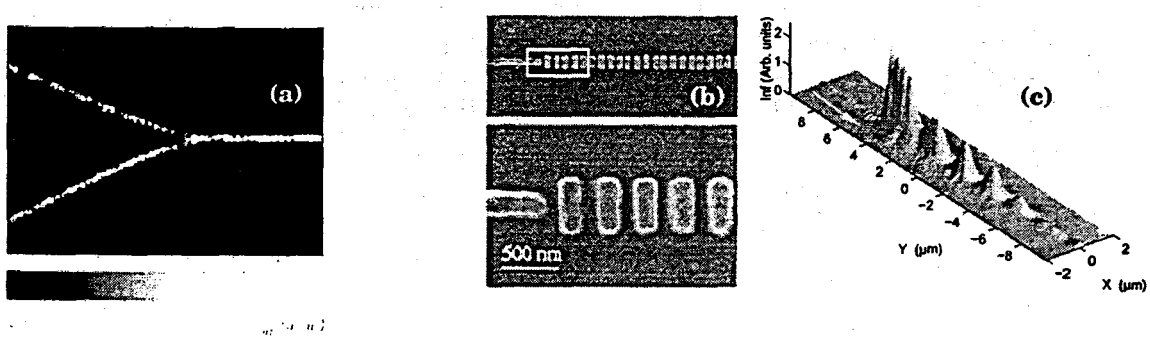

Figure 1: (a) PSTM image of a mode sustained by a 200 *nm* wide and 150 *nm* high waveguide (propagating from the right to the left), splitted by a 45° full opening angle junction; (b) SEM images of a 15 μm long periodic alignment of mesoscopic particles positioned at the end of a micro-guide. (c) 3D PSTM image of the light transfer through the discrete structure when the mode of the input micro-guide is excited.

References

[1] R. Quidant, J. C. Weeber, A. Dereux *et al*, *Phys. Rev. E* **64**, 066607, (2001).

[2] R. Quidant, J. C. Weeber, A. Dereux *et al*, *EuroPhys. Lett.* **57**, 191, (2002).

[3] R. Quidant, J. C. Weeber, A. Dereux *et al*, *Phys. Rev. E* **65**, 036616, (2002).

Characterization and fabrication of fully metal coated Scanning Near-Field Optical Microscopy SiO_2 tips

L. Aeschimann [a, b], T. Akiyama [a], R. Eckert [b], H. Heinzelmann [b], U. Staufer [a], N. F. De Rooij [a]

a) University of Neuchâtel, Institute of Microtechnology, Jaquet-Droz 1, 2000 Neuchâtel, Switzerland.

b) Swiss Center for Electronics and Microtechnology CSEM, Jaquet-Droz 1, 2000 Neuchâtel, Switzerland.

In spite of the considerable progress achieved in fabricating scanning near-field optical microscopy (SNOM) probes, the process to prepare smooth tip surfaces with aperture sizes under 100nm is still expensive and time consuming. Recently, silicon cantilever-based SNOM probes with aluminum-coated quartz tips have been batch fabricated using micro machining technology [1, 2]. The fabrication process of such probes was reconsidered and optimized in view of reproducibility, efficiency and cost. The new probe tips are again made of SiO_2, 12um in height, fabricated at the end of silicon cantilevers. A hole is located underneath the tip base in the cantilever for light insertion from the backside. Different designs of cantilevers have been realized for dynamic and contact mode imaging (Fig. 1).

The tip apex is fully covered with a metal layer in the range of 60nm thickness. Still, far-field measurements showed the typical polarization behavior of conventional SNOM aperture probes. In order to elucidate these observations, several experiments were performed: The light transmittance was measured on several tip arrays where we varied different parameters like metal coating and tip cone opening angle. For each metal we have tested (Al, Ir, Au, Cr), high light transmission was observed (10^{-2}–10^{-4}). The measured transmittance values for the different coatings follow the same tendency as the skin depth. We also found that a smaller cone opening angle of the tip leads to a higher light transmittance through the tip. This fact was verified again for different metal coatings and confirmed by theoretical modeling [3]. Consequently, the fabrication process has been optimized to get sharper tips.
It may be expected that the tip heats up upon light irradiation. This could even lead to melting or enhanced oxidation which could change the optical properties of the tip. We, therefore, analyzed the tip coating with transmission electron microscopy before and after light transmission (Fig. 1). It could be shown that the polycrystalline structure of the metal coating stays intact during illumination.

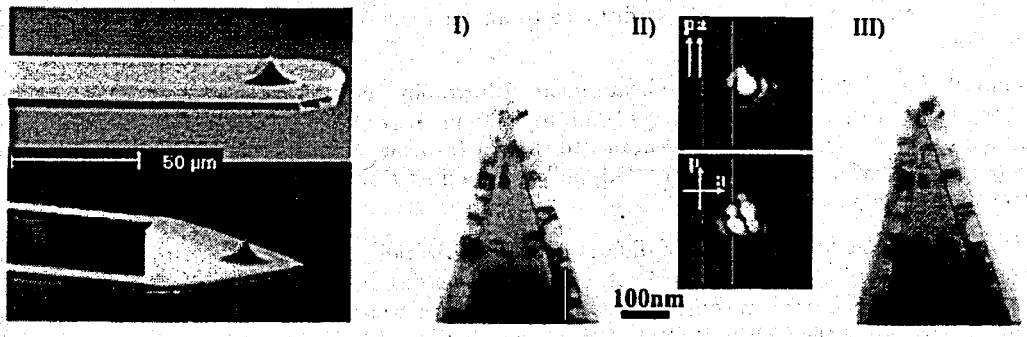

Figure 1: Two different designs of silicon cantilevers with SNOM tips (left). Transmission electron microscope images before I) and after III) illumination of the tip. The typical diffraction patterns II) for parallel and crossed polarization in the far-field of the tip end were observed.

References

[1] G. Schürmann, W. Noell, U. Staufer, N.F. de Rooij, R. Eckert, J.M. Freyland, H. Heinzelmann, *Applied Optics* 40 (28), 5040 (2001).

[2] R. Eckert, J. M. Freyland, H. Gersen, H. Heinzelmann, G. Schürmann, W. Noell, U. Staufer, N. F. de Rooij, *Appl. Phys. Lett.* 77 (23), 3695 (2000).

[2] L. Vaccaro, abstract submitted to the same conference.

3-dimensional field distribution from nanometer single slit studied by NSOM

C. H. Wei, W. S. Fann,

Institute of Atomic and Molecular Sciences, Academia Sinica, and Department of Physics,

National Taiwan University, P.O. Box 23-166, Taipei, Taiwan, Republic of China.

J. Tegenfeldt, R. Austin,

Department of Physics, Princeton University, Princeton

The EM wave field distribution under different conditions has been studied since the 19th century. Fraunhofer studied the field distribution far away from the slit plane. Fresnel studied the field distribution within a tenth of the wavelength. After Bethe's work[1], many theoretical methods were used to attack this problem such as multipole-multipole expansion and finite difference time domain (FDTD) computer simulations. Despite a large number of theoretical investigations, few experiments have been performed to examine the EM wave field distribution from nano-size aperture at optical wavelength region. Recent developments in nano-lithography and near-field scanning optical microscopy (NSOM) allow us to explore optics on this length scales. We use a NSOM to map out the 3D EM wave field distribution from narrow rectangular slits defined in an aluminum film. Our experiment results may provide information to improve the theoretical understanding of light in this condition and may help to study light-matter interaction at the nanometer scale. There are also potential applications in other fields such as spectroscopy of biological molecules [2].

We use a modified NSOM system operating in light collection mode. In this system, we have two operation modes. One is feedback-on mode and the other is feedback-off mode. In feedback-on mode, we use optical shear-force feedback mechanism to maintain constant tip-sample distance and obtain both topographical and optical NSOM images. In feedback-off mode, we modify the bias-voltage of piezo tube, by which we can control the tip-sample distance to an accuracy of 1 nm, and obtain a 3D EM-wave field distribution.

Nanoslits have been prepared by e-beam micro lithography and subsequent reactive ion etching. Slits have been made with widths in the range 50nm to 1000nm. Laser light with 532nm wavelength is incident on the slit with polarization (E field) parallel to the slit (p-polarized wave) or the E-field perpendicular to slit (s-polarized wave). An aluminum coated, pulled glass fiber tip is used to detect the field distribution of the transmitted light.

Field distribution NSOM images of different light polarization, slit width, and tip-sample distances are presented. We find that with the same slit and tip-sample distance, the FWHM of the field distribution of a transmitted p-polarized wave is narrower than that of a transmitted s-polarized wave. However, the maximum intensity of the transmitted s-polarized wave is two or three times the maximum intensity of the transmitted p-polarized wave. The intensity as a function of tip-sample distance is also discussed.

References

[1] H. A. Bethe, "Theory of diffraction by small holes". Phys. Rev. 66, 163 (1944).

[2] J. Tegenfeldt, etc. "Near-field scanner for moving molecules", Phys. Rev. Lett. 86, 1378-1381 (2001).

A compact Sensor-Head for Near-Field Optical Microscopy and Spectroscopy

H. U. Danzebrink, C. Dal Savio, Th. Dziomba, D. Kazantsev, B. Güttler, Physikalisch-Technische Bundesanstalt (PTB), Bundesallee 100, 38116 Braunschweig, Germany.

H.-A. Fuß, Surface Imaging Systems (S.I.S.) GmbH, Kaiserstraße 100, 52134 Herzogenrath, Germany.

A compact sensor head based on a scanning force microscope (SFM) using cantilever probes has been developed [1]. The idea is to replace the microscope objective of a conventional optical microscope by this compact module and turn the optical microscope into a scanning force and near-field optical microscope with subwavelength resolution (see Fig. *1*).

The heart of our instrument is the sensor head which replaces one of the microscope objectives in the turret. Within the sensor head miniaturised mechanical alignment components allow adjustment of both the optical parts relative to each other and the cantilever holder which incorporates the dither piezo for dynamic SFM mode. The optical components consist of a number of specially designed mirror optics. In the whole sensor head no refractive elements like lenses are used. Therefore it is possible to use the head – depending on the material of the near-field probe – in a wide spectral range from ultraviolet to the far infrared. For illumination of the near-field probe aperture – presently a microfabricated silicon cantilever probe – the measurement beam from a compact Nd:YAG laser (λ = 1064 nm) is coupled into the back of the cantilever using our mirror optics. Light transmitted through the small probe aperture interacts with the sample surface and is collected in transmission and reflection.

In order to analyze the optical information the microscope is combined with a Fourier transform spectrometer. To demonstrate the lateral resolution and mechanical stability of the scanning system, we will present images of two kinds of PL-active semiconductor samples at room as well as low temperatures. First, images of structures in a metal layer on an InGaAsP wafer surface, fabricated by e-beam lithography, will be shown. Furthermore, images of self-assembled InAs quantum dots on a GaAs substrate have been obtained. The resulting near-field and far-field optical PL spectra achieved with the same sensor head will be discussed.

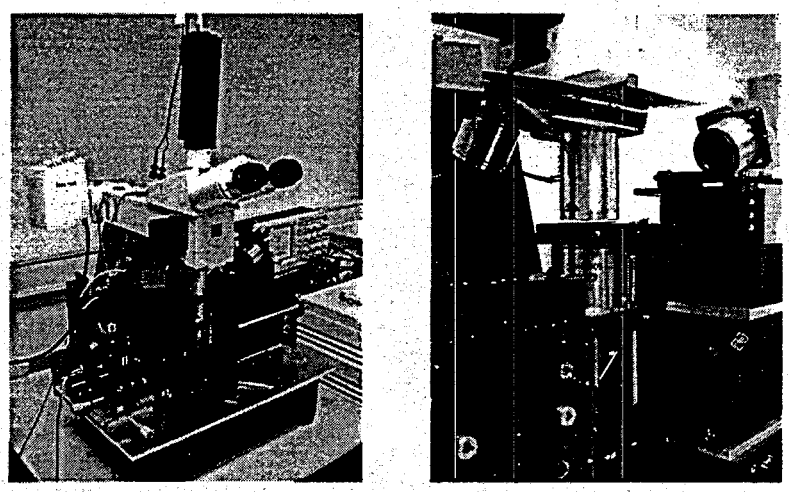

Figure 1: Photographs showing views of the sensor head which is plugged into the microscope's turret.

References

[1] C. Dal Savio, H. Wolff, Th. Dziomba, H.-A. Fuß and H.-U. Danzebrink, A compact sensor-head for simultaneous scanning force and near-field optical microscopy, *Precision Engineering* **26**, 201 (2002).

Mapping evanescent field of integrated waveguide with an apertureless scanning near-field optical microscope

S. Aubert, A. Bruyant, R. Bachelot, G. Lérondel, P. Royer
Université de technologie de Troyes, Laboratoire de nanotechnologie et d'instrumentation optique,
12, rue Marie Curie – BP 2060 – 10010 Troyes cedex - France

V. Minier
Groupement d'électromagnétisme expérimental et d'optoélectronique,
16, chemin du vieux chêne – 38240 Meylan – France

J. Broquin
Institut de Microélectronique, Electromagnétisme et Photonique,
23, rue des martyrs – BP 257 – 38016 – Grenoble - France

Advances in integrated optics require new characterization techniques. Recent works with photon scanning tunneling microscope (PSTM) demonstrated the performance of near-field optical microscopy for waveguide study [1]. In this paper we show feasibility of such experiment with an apertureless scanning near-field optical microscope [2,3,4] (ASNOM).

The evanescent field at the top surface of an integrated waveguide is mapped. The guide has been realized by ion exchange technology (Ag^+/Na^+) [5]. The core, 5 µm wide, is located 2µm beneath the surface. No topography related to waveguide is seen as shown in fig 1A. Preliminary results show unambiguously a mode beating as shown in fig 1B.

The advantages of the ASNOM are discussed notably in terms of resolution and probe features. Additionally process of image formation is analyzed. Especially fringes pattern appearing in the image (fig 1C) reveals the intrinsic interferometric nature of the signal, due to interference between field scattered by the tip and the background field related to guide losses.

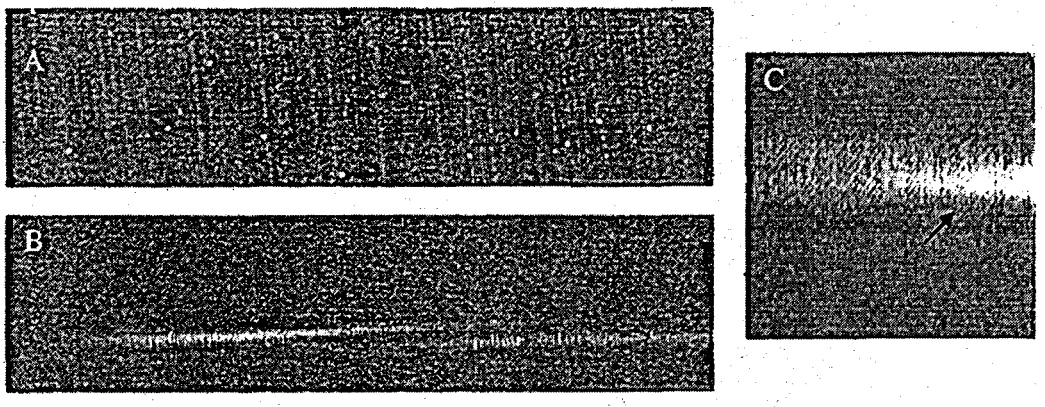

Figure 1: ASNOM image recorded above an Ag^+/Na^+ ion exchange waveguide (20 µm x 85 µm). (A) Simultaneously recorded AFM image. (B) Near-field optical image of the evanescent field. (C) Zoomed view (10 µm x 10 µm) of the near-field image showing 45° tilted fringes

References

[1] M. L. M. Balistreri, J. P. Korterik, L. Kuipers and N. F. van Hulst, *Appl. Phys. Lett.* **79**, 910 (2001).
[2] F. Zenhausern, M. P. O'Boyle and H. K. Wickramasinghe, *Appl. Phys. Lett.* **65**, 1623 (1994)
[3] Y. Inouye and S. Kawata, *opt. Lett.* **19**, 159 (1994)
[4] R. Bachelot, P. Gleyzes and A. C. Boccara, *Opt. Lett.* **20**, 1924 (1995)
[5] J. Broquin, *Proceedings of the SPIE* **4277**, 105 (2001)

Subwavelength-sized aperture fabrication in aluminum by a self-terminated corrosion process in the evanescent field

D. Haefliger and A. Stemmer,
Nanotechnology Group, Swiss Federal Institute of Technology Zurich,
Tannenstrasse 3, 8092 Zurich, Switzerland

Broad application of aperture scanning near-field optical microscopy (SNOM) experiences some difficulties in producing inexpensive probes of high reproducible quality. Here a simple method to fabricate apertures of high quality for scanning near-field optical microscope probes based on aluminum-coated silicon nitride cantilevers is presented [1]. The process takes advantage of a reliable, one-step, low-power, laser-thermal oxidation process of aluminum in water [2]. The fabrication process circumvents the need of expensive vacuum equipment such as focussed ion beam and reactive ion etching devices, and avoids complex lithography processes including the use of resist layers and etchants.

The crucial step of our aperture fabrication method consists of direct exposure of an aluminum-coated probe tip to an optical evanescent field that is created at a glass-water interface by total internal reflection of a laser beam. The aluminum forms a thin passivating oxide layer (Al_2O_3-$2H_2O$) when immersed into neutral water at room temperature. By heating the aluminum close to 373 K due to absorption of the laser radiation (λ = 488nm), this passivation then is inhibited and corrosion of the metal occurs [2]. Due to the irradiance decaying exponentially with increasing distance from the interface, the evanescent field acts as heat source of limited spatial extent. The aluminum is removed from the probe tip at the front-most part up to a point where the radiation intensity falls below a certain threshold required for corrosion. The extent of the evanescent field thus defines the height of the tip, which is uncovered from the aluminum coating. The self-terminating process yields apertures with protruding silicon nitride tips of highly reproducible height (Fig. 1). Control of the tip height is achieved by varying the power and angle of incidence of the laser beam, as both define the intensity profile of the evanescent field. The diameter of the aperture depends on the geometry of the silicon nitride substrate, which is defined by the cantilever fabrication process. A remarkably flat aperture rim is observed. We expect this method to be applicable to probes made of polymers, as the process temperature does not exceed 373 K.

The suitability of the aperture probes for SNOM imaging is verified on a high-contrast topography-free test sample [3]. Near-field optical resolution in transmission mode of 85 nm is achieved.

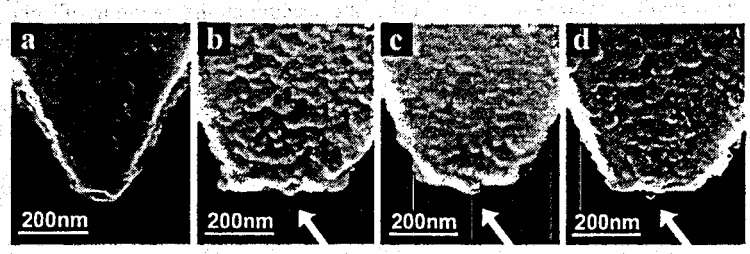

Figure 1: Lateral view of SNOM probe tips. a) Unprocessed probe. Probes in b) and c) are fabricated at a laser incidence of 63° exposed 10 sec. and 15 sec. to the evanescent field (peak intensity: 2.5 mW/μm^2). The protruding silicon nitride tips both measure 20 nm, providing evidence for the self-terminating property of the process. d) A lower angle of incidence of 62° produces an evanescent field of higher penetration depth resulting in a longer protrusion of 30 nm height (aperture diameter is 38 nm).

References

[1] D. Haefliger and A. Stemmer, *Appl. Phys. Lett.*, in press
[2] D. Haefliger and A. Stemmer, *Appl. Phys. A* **74**, 115 (2002).
[3] T. Kalkbrenner, M. Graf, C. Durkan, J. Mlynek, and V. Sandoghdar, *Appl. Phys. Lett.* **76**, 1206 (2000)

Study of the influence of the optical impedance matching onto Near-Field Optical Microscopy Imaging in Polarisation mode

A. Gademann, I. V. Shvets, Trinity College Dublin, Physics Department, Dublin 2, Ireland.
C. Durkan, University of Cambridge, Department of Engineering, Trumpington Street, Cambridge CB2 1PZ, United Kingdom.

Here we report results of dependency of near field optical images on polarisation of light and optical impedance matching between the probe and the sample.

Our instrument is a reflection mode Scanning Near-Field Optical Microscope (SNOM) operated with a 635nm diode laser. The feedback system is based on shear-force measurement method proposed by Kantor et al [1] and uses a piezoelectric tuning fork with one arm fixed to the base as a sensing element. The detection part is based on an elliptical mirror, the sample and tip are located in one of the focal points and the photo multiplier tube is in the second one, as proposed by C. Durkan [2]. The controller records two images simultaneously, one topographic image and one optical image. This makes it easier to separate real optical information from topography contrast.

The sample used was an array of metal lines (Cr, Au) on glass with a width of 1000 nm and separation in the submicrometer range. The sample effectively forms an optical electromagnetic transmission line and we can therefore monitor the optical coupling from the SNOM probe into individual transmission lines. Transmission lines can support three types of electromagnetic modes: Transverse Electric and Magnetic (TEM) at any frequency, and also Transverse Electric (TE) and Transverse Magnetic (TM) modes above the cut-off frequency. The cut off frequency is determined by the separation between the lines. Due to the cut-off frequency the sample could only support TEM modes, at the wavelength used in the experiment: 635 nm. In this study we investigated what effect light with a polarisation perpendicular and parallel to the line has on the recorded image. The effect was explained by optical coupling from a waveguide into a transmission line dependent on the impedance mismatch [3,4].

The work presented here shows influence of the line spacing on the coupling of light from SNOM probe to the transmission line. This is done by using samples with different size line spacing and therefore having a range of values of optical impedance.

Results on both types of samples will be shown and analysed. This study shows that the theory used for describing microwave structures can be adapted to optical frequencies. This should improve understanding of the near-field regime and can be of importance for development of unconventional probes for Scanning Near-Field Optical Microscopy.

References

[1] R. Kantor, M. Lesnak, N. Berdunov and I.V. Shvets, *Appl. Surf. Sci.* **144-145**, 510 (1999).

[2] C. Durkan and I. V. Shvets, *Ultramicroscopy* **61**, 227 (1995)

[3] C. Durkan and I.V. Shvets, *J. Appl. Phys.* **83**, 1837 (1998)

[4] C. Durkan and I.V. Shvets, *J. Appl. Phys.* **83**, 1171 (1998)

Highly efficient near-field probes

Shu-Guo Tang, Tom D. Milster, Optical Data Storage Center/ Optical Sciences Center, University of Arizona, Tucson, Arizona, 85721, USA

Both solid immersion lenses (SIL) and aperture probes are currently being developed as near-field techniques to be used in optical data storage systems [1], [2]. SIL systems, while offering substantially improved spot size, do not have the resolution observed from aperture probes. However, aperture probes suffer from low throughput, limiting the optical efficiency. This paper presents a new technique that combines a SIL and a dielectric aperture probe. The combination aperture can achieve higher performance (in terms of spot size and efficiency) for optical data storage and microscopy than those observed when the SIL or the aperture probe is used alone.

The basic geometry of the combination aperture is a conical dielectric probe attached to the bottom of a SIL with refractive index 1.843. As shown in Fig. 1(a), light from an objective lens of 0.5 NA is focused through the small aperture probe and propagates to the recording layers. The entrance diameter and the exit diameter of the probe are 320 nm and 200 nm, respectively. The probe height is 400 nm. Details of the probe design can be found in Reference [3]. We use a 488 nm wavelength Argon laser as the light source, and thus the effective NA (NA_{EFF}) of the APSIL is 2.4.

Our prior experiment demonstrates that the APSIL exhibits a resolution of 200 nm full-width $1/e^2$ spot size, 50% optical efficiency in reflection and high-density recording capability [4]. Figure 1(b) shows three series of marks written with spacing of approximately 1 um along the vertical groove wall of the recording medium by the systems of combination aperture, far field and SIL, respectively, when using a 1mw at 1ms pulse. ~ 300 nm diameter marks can be recorded from the combination aperture system, which are smaller than those from the systems of far-field and SIL. In fact, our recent experiment result shows as small as 100 nm diameter marks can be recorded in an optimal writing condition of the polarization and the focus position. In addition, the modulation transfer function (MTF) of the combination aperture system is obtained experimentally. The cut-off frequency is well beyond 4 μm^{-1}.

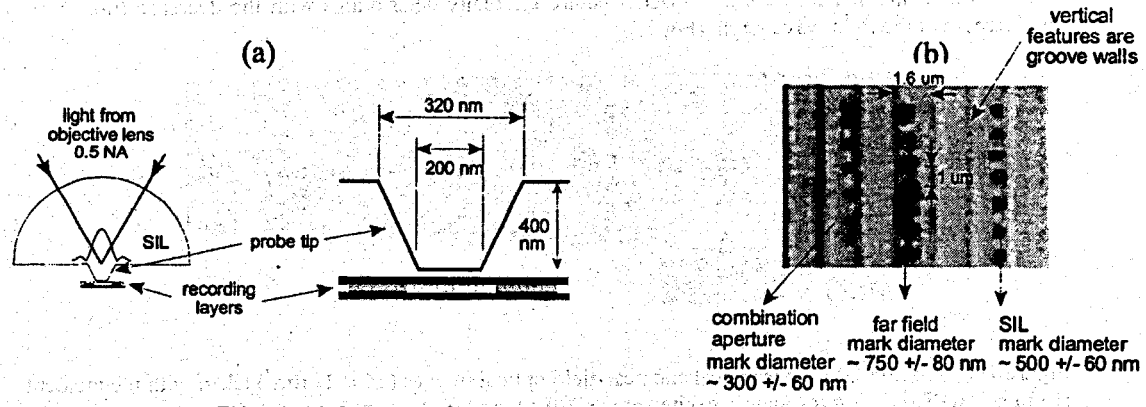

Figure1: (a) Geometry of a combination aperture. (b) Data mark recording from the systems of combination aperture, far-field and Sil.

References

[1] S. M. Mansfield and G. S. Kino. Solid Immersion Microscope. *Appl. Phys. Lett.*, **57** (1990) 2615.

[2] R. Wolfe E. M. Gyorgy P. L. Finn M. H. Kryder E. Betzig, J. K. Trautman and C-H. Chang. Near-Field magneto-optics and high-density data storage. *Appl. Phys. Lett.*, **61** (1992) 142.

[3] K. Hirota, Y. Zhang, T. D. Milster, and J. K. Erwin. *Jpn. J. Appl. Phys.* Design of a near-field probe using a 3-dimensional finite difference time domain method. *Jpn. J. Appl. Phys.*, **39** (2000) 973.

[4] S-G. Tang, T.D. Milster, J. K. Erwin, and W. L. Bletscher. *Opt. Lett.*, **26** (2001) 1987.

Experimental Studies of Surface Plasmon Polariton Band Gap Effect

V. S. Volkov, S. I. Bozhevolnyi,
Institute of Physics, Aalborg University, DK-9220 Aalborg, Denmark.

Surface plasmon polaritons (SPPs) represent quasi-two-dimensional waves, which can exist at a metal-dielectric interface. The SPP fields decay exponentially into both media and exhibit an extremely high sensitivity to interface properties. Given the variety of photonic band gap (PBG) structures (composed of regions with periodic modulation of refractive index) developed for light control, one may suggest to employ periodically located surface scatterers for the SPP control and manipulation. The SPP band gap (SPPBG) effect [1] and the SPP guiding [2] along line defects in a periodically corrugated gold film surface have been recently demonstrated by use of near-field optical microscopy. Here we report the results of our further investigations of the SPPBG effect.

Using near-field optical microscopy, we investigate the reflection of SPPs propagating at corrugated gold-film surfaces with areas of surface scatterers arranged in triangular lattices of different periods (520 nm, 480 nm, 440 nm, and 410 nm) and their guiding along straight 20-μm-long line defects. The obtained results reveal the dependence of the manifestation of the SPPBG effect (SPP reflection and guiding) on the parameters of the surface structures (period, fill factor and the lattice orientation). We found that the SPPBG effect is stronger along GK direction for all investigated periodic structures. Our results demonstrate that the SPPBG effect becomes less pronounced with the decreasing of the fill factor and disappears for the fill factor less than *0.2*. We show also that the center of the SPPBG shifts towards shorter wavelengths with the decrease in the lattice period. Typical results demonstrating the SPPBG effect for a 520-nm-period triangular lattice of gold scatterers are shown in Fig.1. Pronounced SPP reflection by the periodic surface structure together with the efficient SPP guiding along line defects along GK direction is seen on the near-field optical image taken at λ=740 nm (Fig.1b). It is also seen that the SPP guiding along defects and attenuation inside the SPPBG structure gradually deteriorates with the decrease (not shown) and increase of the light wavelength (Fig.1c).

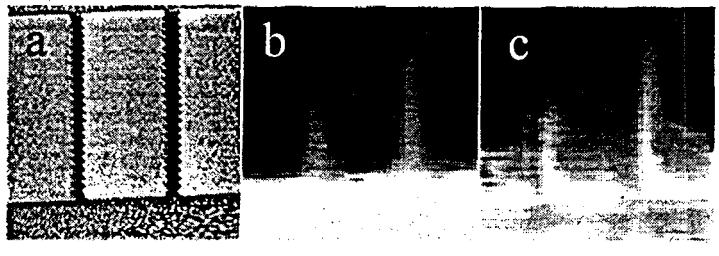

Figure 1: Gray-scale (a) topographical and near-field optical images (24×24 μm^2) taken with the incident (from below) SPP being resonantly excited at (b) 740 nm and (c) 842 nm.

References

[1] S. I. Bozhevolnyi, J. Erland, K. Leosson, P. M. W. Skovgaard, and J. M. Hvam, *Phys. Rev. Lett.* **86**, 3008 (2001).

[2] S. I. Bozhevolnyi, V. S. Volkov, K. Leosson, and J. Erland, *Opt. Lett.* **26**, 734 (2001).

Quantitative fluorescence microscopy on single molecules at the cell membrane performed with a near-field scanning optical microscope.

Bärbel I. de Bakker, M.F. García-Parajó, N.F. van Hulst, Applied Optics group &MESA+ Research Institute, University of Twente, P.O. Box 217, 7500AE Enschede, The Netherlands.

F. de Lange, A. Cambi, B.Joosten, C.G. Figdor, Tumor Immunology Laboratory, University Hospital Nijmegen, The Netherlands.

The statement 'scientific life is complex' holds in general but applies especially to biological processes. The recent trend in Biology to turn from macro- to nano-science e.d. from bulk to single molecule studies will help in unraveling these complex and highly diverse mechanisms. We use near-field scanning optical microscopy (NSOM) to reveal the assembly and functioning of individual bio-molecules.

The molecules of our interest are trans-membrane proteins, LFA-1 and DCSIGN, which are present on the surface of T- and Dendritic-cells. These cells defend our body against bacteria and viruses. Activation of the trans-membrane proteins at the cell membrane ensures well-directed traveling of the cells from the blood stream to the place of infection and signaling to other cells to eliminate the invaders. It is thought that LFA-1 and DCSIGN mediate the process of cell- traveling and -signaling by changing their distribution and assembly on the membrane. The questions to address are: how are LFA-1 / DC-SIGN –proteins distributed on the cell membrane? And, what is their packing density both in activated and non-activated state? For visualization, the proteins are fluorescently labeled in two ways: fusion to the green fluorescent protein or by external Cy5-antibody labeling.

Our setup is a combined near-field- and confocal- scanning optical microscope with a large scan range (40 x 40 x 26 μm in x,y,z). The confocal part of the setup is used to get a general view of the cell under study. Then the near-field probe is positioned to the place of interest. The high spatial resolution provided by NSOM allows studying the stoichiometry of single proteins present at the membrane. The advantages of NSOM over confocal microscopy are the higher spatial resolution and the small excitation volume, which reduces the cell background [1]. Besides single molecule sensitivity the setup allows multi-color excitation and –detection, useful to simultaneously co-localize different molecules. In addition, polarization sensitive detection provides information about the three-dimensional orientation of individual molecules.

Here we will present our most recent results of quantitative fluorescence microscopy obtained with NSOM. We will discuss the distribution of individual proteins at the cell membrane and a quantitative analysis of the individual components within clusters of proteins.

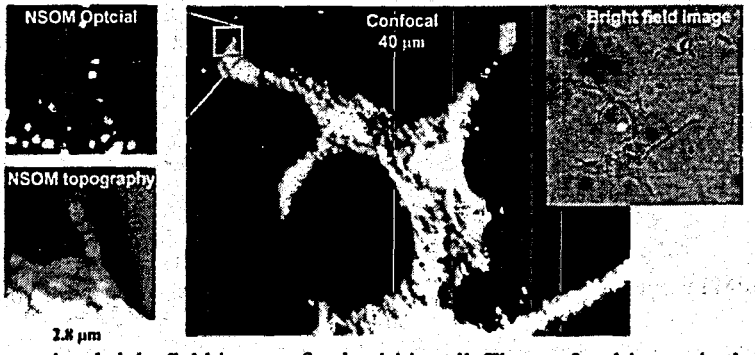

Figure: The right image is a bright field image of a dendritic cell. The confocal image in the middle shows Cy5-labeled proteins at the cell membrane. A zoom in with NSOM provides both a topographical and an optical image as shown in the two images on the left side. The optical NSOM image shows fluorescent spots with a FWHM of 75nm.

References

[1] F. de Lange, A. Cambi, R. Huijbens, B.I. de Bakker and C. Figdor, *J. Cell Sci.* **114**, 4153-4160 (2001).

Novel Near-field Aperture on the AgO_x Thin Film

Fu-Han Ho, Hsun-Hao Chang, Yu-Hsaun Lin, Din-Ping Tsai
Department of Physics, National Taiwan University, Taipei 10617, Taiwan

For near-field scanning optical microscopy (NSOM), "aperture" is needed as a collector or an emitter to probe into the near-field zone with spatial resolution beyond the diffraction limit. A new and better way to have some kind of the aperture is then always requested by the further applications of the NSOM. In this paper, AgO_x thin-film with 15nm thickness was studied for its capability of generating an effective aperture. We investigate the optical properties and structure changes of the AgO_x film. An optical static tester that is an optical microscope with a reflection-mode pump-probe system and CCD [1] was used for our experiments. For the AgO_x films with one interface in air, we found two kinds of structures produced by different input energies. The local changes of the film by focused laser beam were imaged directly by CCD and SEM. Figure 1(a) showed a crystalline dot can be found at the film when the laser energy in the range of tens milliwatts (mW), and the pulse duration around hundreds nanoseconds (ns). After the increasing of the pulse duration above thousands of nanoseconds (ns), a ring (or hole) can be produced as shown in Fig.1 (b). The sizes of both structures were not clear on the images of the CCD due to strong scattering, however, the SEM micrograph showed the sizes of both structures could be less than 100 nm individually. Results demonstrated the sizes of them could be controlled by the input laser powers and pulse duration. The reflectance of both structures can be extremely high at proper laser power, but they behaved differently. Similar results were found on the AgO_x films sandwiched by protection layers.

Productions of the dots or rings (or holes) shown in the Fig. 1 may be considered as a nanoscatters or nanoapertures at the nanometer thin film. Applications of these "apertures" on the near-field optical recording has attracted manifold attention recently [2,3]. Our experiments have successfully demonstrated that AgO_x thin-films can work as a masking or active layer in a near-field optical disk [4]. The carrier-to-noise ratio (CNR) of the 100 nm mark size can be more than 20dB. We have also found the properties of photonic switch and amplifier on making an artificial structure of Ag dots on AgO_x nanometer thin film. Results showed the switching time of these structures were in the range of the microseconds. The unique local optical interactions and thermal properties of the AgO_x thin films may have great potential for various applications on submicron photonic devices.

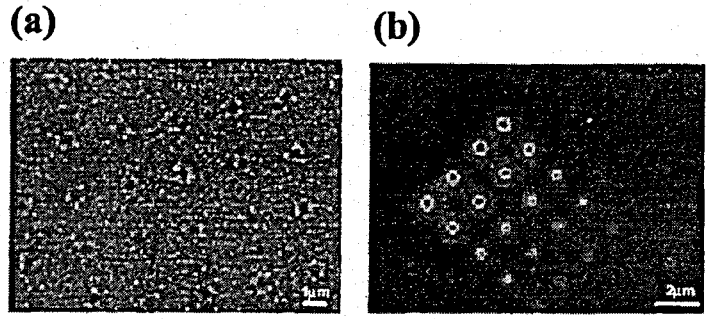

Figure 1: SEM micrographs of (a) crystalline dots formed on the AgO thin-film, (b) rings (or holes) structures.

References

[1] M.Mansuripur, J.K. Erwin, W.Bletscher, P. K. Khulbe, K. Sadeghi, X. Xun, A. Gupta, and S. B. Mendes, Appl. Opt. **38**, 7095 (1999).
[2] D. P. Tsai and W. C. Lin, Appl. Phys. Lett. **77**, 1413 (2000).
[3] W. C. Liu, C.-Y. Wen, K.-H. Chen, W. C. Lin and D. P. Tsai, Appl. Phys. Lett. **78**, 685 (2001).
[4] H. Fuji, J. Tominaga, L. Men and T. Nakano, Jpn. J. Appl. Phys. **39**, 980 (2000).

Unraveling the fluorescence emission of the red fluorescent protein DsRed using NSOM

M. Koopman, E.M.H.P. van Dijk, M.F. Garcia-Parajo and N.F. van Hulst

Applied Optics group, MESA+ Research Institute & Faculty of Applied Physics, University of Twente, P.O. Box 217, 7500 AE Enschede, The Netherlands

The green fluorescent protein from the *Aquerea victoria* (*av*GFP) and its mutants have become invaluable markers for monitoring protein localisation and gene expression *in vivo*. The main advantage of all these naturally fluorescent proteins is that they provide visible strong fluorescence that can be genetically encoded into many other proteins. Recently, a new red fluorescent protein (DsRed) from the coral *Discosoma* was cloned [1]. DsRed has an emission maximum at 583 nm, exhibits bright red fluorescence and is highly resistant against photobleaching. In combination with other GFP mutants, DsRed appears to be excellent candidate for multicolour labelling and fluorescence resonance energy transfer (FRET) applications. However it has become clear that the protein forms closely packed tetramers and there is indication for incomplete protein maturation with unknown proportion of immature green species [2,3].

We have applied a single molecule sensitive near-field scanning optical microscopy (NSOM) to elucidate the nature of the fluorescence emission in the DsRed. The NSOM is well suited for this study, because the evanescent excitation enables us to minimize the background from the thick aqueous gel in which the proteins are rigidly embedded. Therefore we are able to collect the fluorescence emission of individual DsRed molecules in time using excitation powers lower than 500 W/cm^2, which minimises the risk of premature bleaching. The time trajectories clearly show different discrete levels, an indication of the tetrameric nature of DsRed. In addition, we have excellent control of the excitation/ detection polarization so we can determine the relative emission dipole and thus orientation of all subunits. We use this information to reveal the type of interaction between different components of the tetrameric unit. Our results indicate that energy transfer between identical monomers occurs efficiently with red emission arising equally likely from any of the chromophoric units. Photo-dissociation of one of the chromophores weakly quenches the emission of adjacent ones. Dual colour excitation (at 488 nm and 568 nm) single molecule microscopy has been performed to reveal the number and distribution of red vs. green species within each tetramer. We find that 86% of the DsRed contain at least one green species with a red-to-green ratio of 1.2-1.5 [4]. Based on our findings, oligomer suppression would not only be advantageous for protein fusion applications but would also enhance the fluorescence properties of individual monomers.

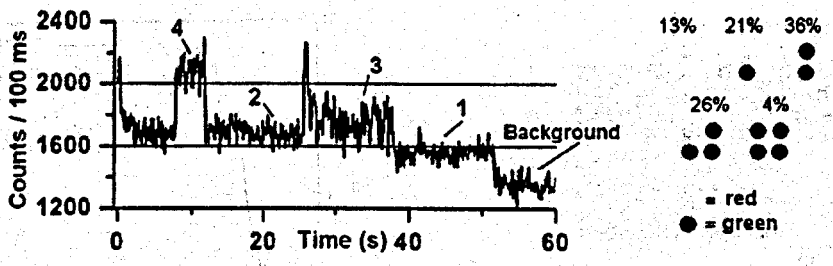

Figure 1: Fluorescence time trajectory and distribution of red versus green species in the DsRed tetramer

References

[1] M.V. Matz, A.F. Fradkov et al., *Nat. Biotechnol.* **17**, 969 (1999).
[2] G.S. Baird, D.A. Zacharias and R.Y. Tsien, *Proc. Natl. Acad. Sci.* **97**, 11984 (2000)
[3] B. Lounis, J. Deich et al., *J. Phys. Chem. B*, **105**, 5048 (2001)
[4] M.F. Garcia-Parajo, M. Koopman et al., *Proc. Natl. Acad. Sci.* **98**, 14392 (2001)

Nanometer-sized Metal Clad Optical Waveguides

T. Onuki, T. Tani, T. Tokizaki,
National Institute of Advanced Industrial Science and Technology, Tsukuba, Ibaraki 305-8568, Japan.
Y. Watanabe, K. Nishio, T. Tsuchiya,
Tokyo University of Science, Noda, Chiba 278-8510, Japan.

The cross sectional size of a conventional waveguide is restricted by the diffraction limit. To overcome the limit, the utilization of metals as the core or the clad has been proposed [1]. In the waveguide with metal, light field couples with the surface plasmon on the interface between the metal and a dielectric material. The coupled mode (surface plasmon polariton: SPP) can propagate in the waveguide, even though the core size is much smaller than the wavelength. We have realized a structure of nano-waveguides using anodic oxidation with a scanning near-field optical microscope (SNOM) [2], and also confirmed the SPP propagation in the waveguide using the same SNOM.

A nanometer-scale core is fabricated by anodic oxidation using a SNOM probe tip on a composite metal film, which consists of a 30-nm-thick titanium (Ti) film on a 30-nm-thick silver (Ag) film. When the positive bias voltage (V_b) is applied to the sample against the tip under the tip approaching, the metal film is locally oxidized under the tip. The thickness of the oxide can be controlled by changing V_b. Fig.1(a) is the AFM image of the oxide (TiO_2) structure as a waveguide core, which was fabricated by moving the tip with the speed of 10 nm/sec and V_b of 30 V. The length, the thickness and the width are 6 μm, 70 nm and 350 nm, respectively. Since the bottom of the core contacts the Ag layer, the SPP is excited on the interface between the TiO_2 core and the Ag clad layer. In order to observe the SPP propagation, we fabricate a dot-like structure at the left end of the waveguide with a higher bias voltage. At the dot structure the Ag layer may be oxidized, and the signal light converted from the SPP is scattered from the hole in the Ag layer.

The waveguide is observed by transmission mode SNOM. Figure 2(b) shows the SNOM image using light with the wavelength of 532 nm and the polarization parallel to the waveguide, and Fig.3 shows the intensity profile along the waveguide. The transmission change ($\Delta T/T_o$) increases along the waveguide toward the dot structure. This behavior is understood by the SPP propagation: The SPP is excited by the near-field on the aperture of the SNOM tip, and is propagated in the waveguide. At the dot structure, the SPP is scattered and converted to the signal light. When the probe tip is closer to the dot structure, we expect stronger signal because of lower propagation loss. Subtracting the background signal that is directly incident from the tip aperture to the detector, we can fit the behavior by an exponential curve (dashed line) and estimate the propagation length of the SPP of 2 μm. We have already measured the propagation length of 6 μm at the wavelength of 830 nm [2]. The wavelength dependence is understood by a numerical simulation taking account of the dispersion of the SPP.

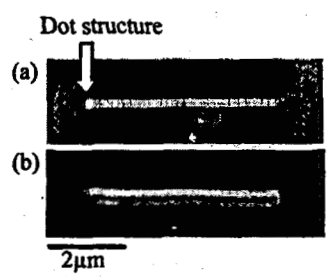

Fig.1 (a) AFM image and (b) SNOM image of the nano-waveguide.

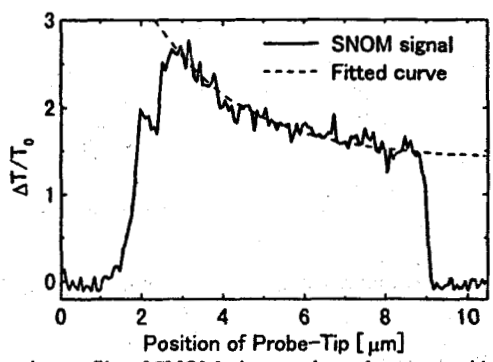

Fig.2 Intensity profile of SNOM image along the waveguide.

References

[1] J. Takahara, S. Yamaguchi, H. Taki, A. Morimoto and T. Kobayashi, Opt. Letters., 22, 321 (1997).
[2] T. Onuki, Y. Watanabe, T. Tsuchiya, T. Tani and T. Tokizaki, submitted to Appl. Phys. Lett.

Watching Single Molecule DNA Synthesis with Zero-mode Waveguides

M. Levene, J. Korlach, S. Turner, H. Craighead and W. W. Webb
Applied and Engineering Physicss, Cornell University, Ithaca, NY 14853.

The ability to observe the synthesis of a single molecule of double-stranded DNA from a single-stranded template constitutes a rapid and robust technique for DNA sequencing as well as providing a platform for basic research into the kinetics of the underlying enzymology. An effective system requires the development of fluorescent nucleotide analogs that are compatible with DNA polymerase and an optical system capable of observing individual nucleotide incorporation events in the presence of micromolar ligand concentrations. Such high concentrations of nucleotides are required to maintain the proper functioning and processivity of the polymerase, allowing for read lengths of up to a megabase. Typical far-field observation volumes are 1000 times larger than required for adequate background rejection, and conventional near-field approaches may suffer from low optical efficiency and non-trivial extensions to a highly parallel system. We have developed a simple system to achieve sub-wavelength observation volumes using zero-mode waveguides comprised of small holes in a metal film. In this case, the core of the waveguide contains the solution under study, and the surrounding metal film forms the cladding. Metal-clad waveguides with lateral dimensions far below the threshold for optical propagation of a single mode permit only evanescent light penetration a few tens of nanometers into the guide. For 50nm diameter circular waveguides, the entire volume of illumination near the entrance pupil of the guide is on the order of tens of zeptoliters (10^{-21} l), 10,000 times smaller than that of a typical high numerical aperture objective. Such small volumes enable single molecule observation even of micromolar solutions of fluorescent species present in the core of the waveguide. The typical setup for using zero-mode waveguides is shown in figure 1. Using these waveguides and suitable fluorescent nucleotide analogs, we observed DNA polymerase activity appropriate for single molecule sequencing. This work was supported by DOE grant DE-FG02-99ER62809, NSF grant DBI-0080792 and NCRR-NIH grant P41-RR04224.

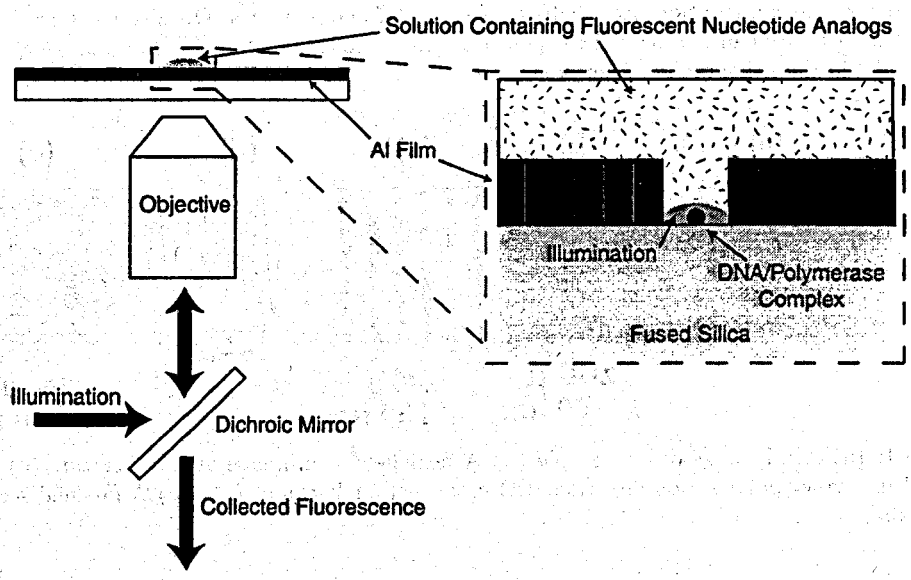

Figure 1: Optical system for single molecule DNA sequencing.

Plasmonic Band Gap Structures as Spatial Sine Wave Generators

S. C. Hohng, Y. C. Yoon, and D. S. Kim
School of Physics, Seoul National University, Seoul 151-742, Korea
V. Malyarchuk and Ch. Lienau
Max-Born-Institute für Nichtlineare Optik und Kurzzeitspektroskopie, D-12489 Berlin, Germany.
J. W. Park and J. H. Kim
Korea Research Institute of Standards and Science, Yunsung, P. O. Box 102, Taejon 305-600, Korea.
Q. H. Park
Department of Physics, Korea University, Seoul 136-701, Korea.

Recently, Ebbesen et al [1] showed that metal films punctured with periodic hole arrays permit a dramatically enhanced transmission of light near surface plasmon (SP) resonances. In this contribution, we demonstrate that the Ebbesen structure, under certain conditions, can be used as a spatial sine-wave generator in the far-field regime. The complicated near-field pattern becomes drastically simplified in the far-field, because only the zero-th and the first diffraction order of the grating contribute.

We employ a near-field scanning optical microscope in the transmission geometry to study a gold film grown on a sapphire substrate, punctured with a periodic array of holes with 200 nm diameter and 770 nm period. Fig. 1(a) shows a topography of our sample taken with a metal-coated tip with a sub-100 nm resolution. We excite the sample near the air-metal [1, 0] SP resonance. A complicated near-field image is shown in Fig. 1(b), arising from a coherent superposition of plasmons assiocated with many different diffraction orders of the grating. As we increase the tip-to-sample distance z, the complicated pattern quickly becomes sinusoidal within a distance of 1-2 wavelengths as shown in Fig. 1(c). The orientation of the stripes is perpendicular to the polarization direction, and the cross-sectional scan shown in Fig. 1 (d) displays a nearly perfect sinusoidal behavior. This spatially sinusoidal pattern can persist up to z=15 μ when the spot size is 30 μ. The far-field pattern, at normal incidence, becomes homogeneous when we increase the excitation wavelength (Fig. 1(e)).

As we deviate from normal incidence, the sinusoidal pattern can persist to longer wavelengths, which suggests possible contributions from half-wavelength diffraction modes. Our results show that the plasmonic band gap structure can be an efficient, polarization-controlled, spatial sine-function generator that can be very useful in the lithography of periodic patterns.

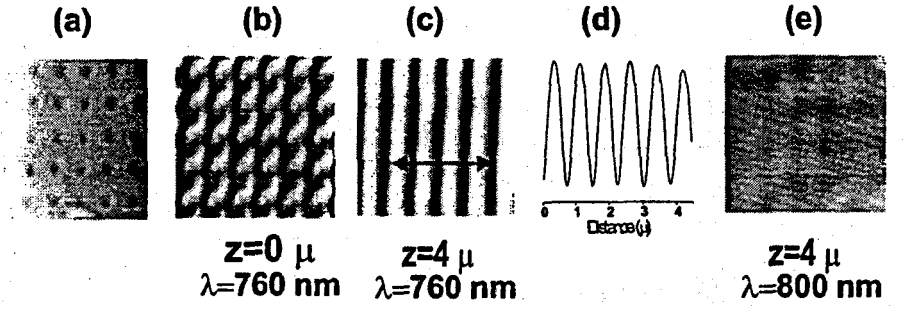

Figure 1: (a) AFM image of our sample (b) A near field scan image at $\lambda = 760nm$. (c) A far field scan at z=4 μ. arrow=polarization direction. (d) cross sectional scan of (c). (e) A far-field scan at z=4 μ and $\lambda = 800nm$

References

[1] T. W. Ebbesen *et al.*, Nature **391**, 667 (1998).

Surface-Enhanced Raman Spectroscopy of Single Biomolecules

Thomas Huser, Chad E. Talley, Christopher W. Hollars
Dep. of Chemistry and Materials Science, Lawrence Livermore National Laboratory, Livermore, CA 94550

Stephen M. Lane
Dep. of Physics and Advanced Technologies, Lawrence Livermore National Laboratory, Livermore, CA 94550

Surface-enhanced Raman spectroscopy (SERS) using single metal nanoparticles adsorbed onto a solid support provides a unique tool for investigating biological systems. Biological molecules such as amino acids, nucleic acids, DNA and proteins are attached to the metal nanoparticles using thiol chemistry to confine the molecules to the surface in a well-defined orientation. By carefully selecting the molecular orientation with respect to the nanoparticle surface, specific interactions, such as protein conformational changes and protein-protein association, can be monitored through their Raman spectra. Additionally, dynamics on the millisecond timescale are characterized using a single channel photodetector to monitor distinct Raman frequencies that correspond to specific molecular orientations or binding events. Results from these studies at the single molecule level will be reported and progress of their application to single cells will be discussed.

Surface Plasmon Propagation in Structured Metal Films

Jan Seidel, Stefan Grafström, and Lukas M. Eng
Institut für Angewandte Photophysik, Technische Universität Dresden, D-01062 Dresden, Germany
jseidel@iapp.de, www.iapp.de

Propagation of optical-frequency surface plasmons at metal / dielectric interfaces as well as their interaction with defined surface structures are of interest for applications in integrated optics. Investigations concerning the propagation of such surface excitations and their physical characteristics when interacting with well-defined surface structures are presented. Near-field optical methods are needed to directly reveal the properties of these travelling surface waves, such as the optical transmission across barriers of defined width (see figure) or the coupling to free-space electromagnetic waves. These characteristics can be immediately determined using an attenuated-total-reflection (ATR) excitation set up together with fiber probes for near-field optical detection. We show results for various structures written into a silver film with a focused ion beam (FIB). Additionally the influence of different types of near-field probes (metallic versus non-metallic) on both surface plasmon imaging and scattering is discussed.

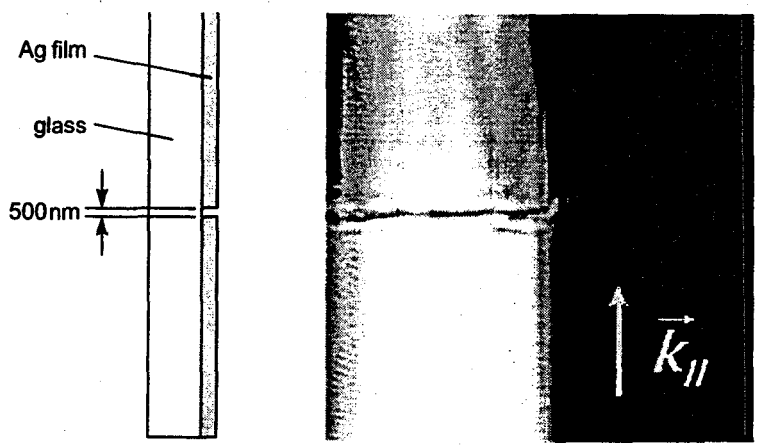

Figure: A groove measuring 500 nm in width in a thin silver film (60 nm thickness) showing reflection (interference pattern) and transmission (about 75% of the incident intensity) of the surface plasmon, which was excited at 633 nm. The propagation direction is given by the surface plasmon wave vector $k_{//}$.

References

[1] S. I. Bozhevolnyi and F. A. Pudin, *Two-dimensional micro-optics of surface plasmons*, Phys. Rev. Lett. **78**, 2829 (1997).

[2] P. Dawson, F. de Fornel, and J.-P. Goudonnet, *Imaging of surface plasmon propagation and edge interaction using a photon scanning tunneling microscope*, Phys. Rev. Lett. **72**, 2927 (1994).

[3] V. N. Konopsky, K. E. Kouyanov, and N. N. Novikova, *Investigations of the interference of surface plasmons on rough silver surface by scanning plasmon near-field microscope*, Ultramicroscopy **88**, 127 (2001).

[4] J.-C. Weeber, J. R. Krenn, A. Dereux, B. Lamprecht, Y. Lacroute, J. P. Goudonnet, *Near-field observation of surface plasmon polariton propagation on thin metal stripes*, Phys. Rev. B **64**, 045411 (2001).

[5] A. Bouhelier, Th. Huser, J. M. Freyland, H.-J. Güntherodt, and D. W. Pohl, *Plasmon transmissivity and reflectivity of narrow grooves in a silver film*, J. Microsc. **194**, 571 (1999).

The observation of PC12 with Nonoptically Probing Near-Field Microscopy

Y. Kawata, M. Murakami, and C. Egami
Shizuoka University, Department of Mechanical Engineering,
Johoku, Hamamatsu 432-8561, Japan
E-mail: kawata@eng.shizuoka.ac.jp
T. Tsuboi and S. Terakawa
Hamamatsu University School of Medicine, Photon Medical Research Center
Handa, Hamamatsu, 431-3192, Japan

We have developed the nonoptically probing near-field microscope by using organic films as a detection system of light distribution. In the system, the optical fields near specimens are converted to the topographical change of a photosensitive film, and then the topography of the film is detected with an atomic force microscope (AFM). Urethane-urea copolymer films are used for the conversion material from the optical fields to the topographical change. Since the developed technique does not require the scanning of a probe tip, it is possible to observe of living or moving biological specimens or very fast phenomena. We have succeeded in imaging of biological specimens with the resolution of subwavelength resolution [1,2].

We observed rat pheochromocytoma cells (PC12) as specimens. PC12 cells were cultured on an urethane-urea copolymer film. The growing process of neurites, after nerve growth factor (NGF) was given, was imaged with the developed technique. We also tried to observe exocytotic response, depolarizing stimulation was given by applying a solution with high concentration of KCl. Figure 1 shows a typical image of differentiated (NGF-treated) PC12 cells. We also observed many granules (< 350 nm in diameter) which were emitted terminal.

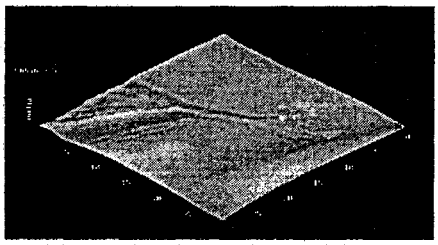

図 1: Differentiated PC12 cell

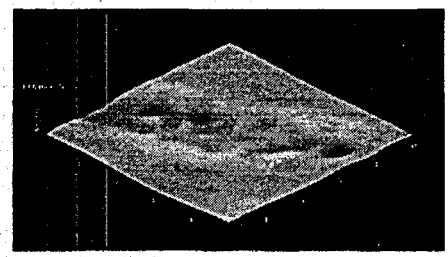

図 2: Observation of a neurite

References

[1] Y. Kawata, C. Egami, et al. *Opt. Commun.* **161**, 62 (1999).

[2] Y. Kawata, M. Murakami, et al. *Appl. Phys. Lett.* **78**, 2247 (2001).

[3] Y. Kawata, S. Kunieda, and T. Kaneko, *Opt. Lett.* **27** 297 (2002).

A Light Source for Nano-Optical Devices
:Electric Current Excitation of 2-Dimensional Optical Wave in Nano Metal-Gap

J. Takahara[1], A. Eda[1], K. Nakamura[2], M. Yokoyama[2] and Tetsuro Kobayashi[1]
[1]Osaka University, Graduate School of Engineering Science, Toyonaka, Osaka, 560-8531, JAPAN.
[2]Osaka University, Graduate School of Engineering, Suita, Osaka, 565-0871, JAPAN.
E-Mail: takahara@ee.es.osaka-u.ac.jp

We have proposed "low-dimensional optical waveguides" theoretically in order to guide nano-sized optical beam ($<<\lambda_0$)[1]. Low-dimensional optical wave is the key concept for realizing nano-optical devices. The drawback of low-dimensional optical waveguide is a difficulty to excite suitable mode for the formation of nano-sized optical beam. This is because wavenumber k and mode profile of low-dimensional optical wave are different from 3-dimensional (3D) optical wave, i.e. propagating light wave in free space.

The purpose of this study is to propose the excitation method for low-dimensional optical wave. In this paper, we propose a new kind of light source for nano-optical devices, i.e. a source of low-dimensional optical wave, and report the experimental results. We have reported that 2-dimensional (2D) optical wave can be guided along microstructures embedded in nano metal-gap [2]. Metal-gap structures are thought to be 2D optical waveguides or the waveguides of a coupled mode of surface plasmon polariton (SPP). Here, we propose a metal-gap structure including luminescent materials as a source of 2D optical wave. Besides, we report the experimental results of novel light emission from the 2D optical wave source.

The metal-gap structure including luminescent materials is shown in Fig 1, where 100nm-thick organic heterostructure is sandwiched by Au and Mg/Ag layers. The luminescent materials of α-NPD and Alq_3 are known as organic LED materials. Broad-spectrum light emission (λ_0=450-700nm) with the peak position of λ_0=509nm was observed by applying voltage to metal (~20V). The polarization of the light emission was measured at λ_0=490 and 550nm as shown in Fig. 2. TM polarization, i.e. electric field was perpendicular to the interface, was observed at λ_0=550nm although the emission at λ_0=490 nm was not polarized.

Propagation mode analysis shows that Fano mode (TM) is the dominant propagation mode at λ_0=550nm although propagation modes of 3D optical wave are prohibited due to cut-off. Therefore, such polarization is attributed to the direct excitation of 2D optical wave by electric current. These structures are applicable to a low-dimensional optical wave source in nano-optical devices in the future.

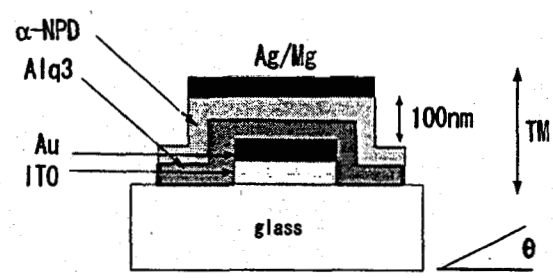

Figure 1: Cross sectional view of metal-gap structure

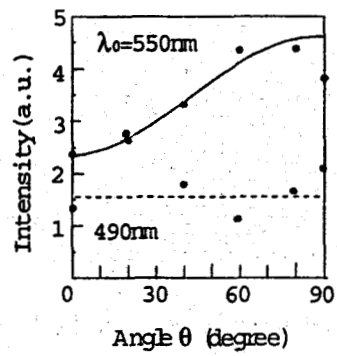

Figure 2 : Polarization of the emission

References

[1] J. Takahara, *et. al.*, Opt. Lett. 22, 475-477 (1997).
[2] J. Takahara *et. al.* ,Technical Digest of NFO-6, MoP77, p. 144 (2000).

Fluorescence Apertureless Near-field Optical Microscope for Biological Imaging

J. M. Gerton, L. A. Wade, G. A. Lessard, and S. R. Quake,
California Institute of Technology, Applied Physics Department, Pasadena, CA 91125.

An apertureless near-field optical microscope has been developed with resolution better than 30 nm. The apparatus combines an epifluorescence microscope and an atomic force microscope (AFM) to obtain optical contrast with resolution limited by the sharpness of the AFM probe. The microscope is being developed to probe single fluorescent molecules which are convenient and ubiquitous labels in biological systems such as DNA and proteins. Single molecule targets will also serve as optical point-sources for the unequivocal measurement of the microscope resolution. In order to optimize the sensitivity of the microscope toward the single molecule level, 20 nm diameter fluorescent particles of organic dye have been used as targets in a variety of studies. Optical images of these particles are broadened to 40 – 50 nm FWHM, yielding a resolution no worse than 30 nm. Significantly, AFM images of these particles are broadened by the same amount due to tip-shape artifacts which result from probing an object that is macroscopic on the scale of the AFM probe.

In previous work [1], we showed that optical contrast is provided by a modulation of the fluorescence rate when a metal-coated AFM probe is brought into the near-field of an illuminated fluorescent sample. A two-dimensional optical image is generated by rastering the AFM probe, in tapping mode, over a surface on which the sample resides, while simultaneously collecting fluorescence and probe-tip location data. The physics of the optical contrast mechanism is being investigated by comparison of the optical modulation amplitude under different illumination conditions. In particular, both evanescent and non-evanescent fields of varying polarization will be used. The results of these studies should help to distinguish two possible sources of the optical contrast: non-radiative coupling of the fluorescent sample to the AFM probe, and perturbation of the illumination-laser field by the AFM probe. Such insight should aid in optimizing the sensitivity of the microscope, so that it may be used at the single-molecule level and applied to a wide range of problems in biology and other fields, such as proteomics and molecular-scale electronics.

References

[1] J. T. Yang, G. A. Lessard, S. R. Quake *Applied Physics Letters* **76**, 378 (2000).

NEAR-FIELD OPTICS AND QUANTUM OPTICS: AN ASSIGNATION ARRANGED BY FOUR KIND OF PHOTONS

Ole Keller
Institute of Physics, Aalborg University
Pontoppidanstræde 103, DK-9220 Aalborg Øst, Denmark
e-mail: okeller@physics.auc.dk

In quantum optics information on the electrodynamics of atoms, molecules, mesoscopic particles, $\cdots$, usually is obtained through correlation measurements performed far from these objects. In the far field the statistical response of the detector in principle gives an unambiguous fingerprint of the quantum statistics of the source particle, possibly blurred by the vacuum fluctuations in the field. The "only" role of the photon is to transfer the information between source and detector (with the vacuum speed of light) [1].

Photons emitted from an atom statistically are born not only inside the atom but also in the entire near-field zone of the atom. In near-field optics we normally study optical interactions on semiclassical ground, i.e. without quantizing the electromagnetic field.

In the present communication I shall describe recent theoretical efforts to understand quantum optical correlations in the near-field zone of a source particle. In this zone the space-time birth domain statistics of the photon is mixed with the quantum mechanical statistics of the source particle. The four kind of photons (scalar, longitudinal, two transverse) appearing in a manifestly invariant relativistic description [2] all participate in the correlation.

It appears that information on the spatial localizability of photons [3]-[7], and on single-photon tunneling might be obtained from near-field correlation studies. Also a novel view on polychromatic photon wave mechanics [3, 5, 7], and on the position operator problem for photons seems to emerge in the horizon.

References

[1] L. Mandel and E. Wolf, *Optical Coherence and Quantum Optics* (Cambridge Univ.Press, Cambridge, 1995).

[2] S. Weinberg, *The Quantum Theory of Fields: Foundations (Vol. 1)* (Cambridge Univ. Press, Cambridge, 1996).

[3] I. Bialynicki-Birula, in *Progress in Optics XXXVI*, edited by E. Wolf (North-Holland, Amsterdam, 1997), p. 345.

[4] I. Bialynicki-Birula, Phys.Rev.Lett. **80**, 5247 (1998).

[5] O. Keller, "Emergence of a polychromatic photon in a pure spin transition: exponential localization (to be published).

[6] O. Keller, SINGLE MOLECULES **3**, 5 (2002).

[7] O. Keller, Phys.Rev.A **62**, 022111 (2000).

Spontaneous coherent emission of light

R. Carminati, K. Joulain, J.P. Mulet and J.J. Greffet[a]
Laboratoire EM2C, Ecole Centrale Paris,
CNRS, 92295 Chatenay-Malabry Cedex, France
[a] *also with University of Rochester,*
The Institute of Optics, Rochester, NY 14627, USA

It is usually taken for granted that light spontaneously emitted by a thermal source such as a light bulb is spatially incoherent. In other words, it is generally assumed that fields produced by different points of a thermal source cannot interfere. By contrast, different points of a radio antenna emit waves that interfere constructively in particular directions producing well-defined angular lobes. The intensity emitted by a thermal source is the sum of the intensities emitted by different points so that it cannot be directional. Thus, the difference in directionality of light emitted by a laser and a thermal source is a direct consequence of the difference of spatial coherence of the fields in the plane of the source. Since the currents generating the thermally emitted fields are due to uncorrelated random thermal motion, it seems that a thermal source cannot be spatially coherent or directional. However, it has been shown recently by Carminati et al. (1999)[1] and Shchegrov et al. (2000) [2] that the field generated by a plane interface at temperature T may have a large coherence length and can be quasi monochromatic *in the near-field.* In other words, a thermal source is partially coherent in the near-field.

This paves the way for the construction of a thermal source that could radiate light within narrow angular lobes as an antenna instead of having the usual quasi lambertian angular behaviour. In this paper, we will report experimental measurements demonstrating that it is indeed possible to build an infrared antenna by ruling a grating on a polar material such as a semiconductor[3]. Such an antenna radiates infrared light in a narrow solid angle when it is heated as shown in Figure 1. This is a signature of the spatial coherence of the source. We will discuss the physical origin of the spatial coherence of the thermal source. We will in particular show that this effect is due to the excitation of a surface phonon-polariton, a mixed vibration which is half a photon and half a phonon.

Another remarkable property of this source is that the emissivity is enhanced by a factor of 20 compared to the emissivity of a flat surface. No enhancement is observed for s-polarized light. Finally, we will show that the emission spectrum depends on the observation direction. This behaviour was first predicted by E. Wolf.[4] as a consequence of spatial correlations of random sources. This behaviour is trivial for coherent sources like an antenna but has been observed so far only for secondary partially coherent sources.

All the above properties are fundamentally related to the surface-phonon polariton and can be summarized by its dispersion relation. We will report measurements of the reflectivity spectra that allowed us to measure the dispersion relation[3]. Using this dispersion relation, we will discuss possible applications to the design of efficient photovoltaic cells, infrared sources in the far field and in the near field and enhanced radiative heat transfer at short distances.

References

[1] Remi Carminati, J.J. Greffet, " Near-field effects in spatial coherence of thermal sources" *Phys.Rev.Lett.* **82**, 1660 (1999).

[2] A.V. Shchegrov, K. Joulain, R. Carminati and J.J. Greffet, *Phys.Rev.Lett.* **85**, 1548 (2000).

[3] Jean-Jacques Greffet, R.Carminati, K. Joulain, J.P. Mulet, S.Mainguy, Y. Chen, *Nature* **416**, 61 (2002).

[4] E.Wolf, D.F.James, *Rep.Prog.Phys.* **59**, 771 (1996).

Principle of apertureless near-field optical microscopy: Tip vibration and global illumination

R. Fikri, D. Barchiesi, P. Royer
Université de Technologie de Troyes, Nanotechnology and Optical Instrumentation Laboratory (LNIO)
12 rue Marie Curie - BP 2060 - FR-10010 Troyes cedex

Apertureless scanning near-field optical microscopy (ASNOM) involves an interaction of a thin metallic tip near the sample with the incident light.Therefore the perturbation of the probe on the detected near-field is no more negligible [1]. Modulation of the probe position relative to the sample is used to separate the tiny near-field signal from the background. The modulated signal is measured using lock-in detection and multiple of the modulation frequency are available. A theoretical study of the tip modulation has been recently performed [2] (and Refs. therein) but the experimental field used in that paper is nonphysical and is not modified by the presence of the probe.

Here, we study numerically two-dimensional ASNOM by taking into account the real vibration and scanning of the tip. Finite element calculations of the detected signal was performed to investigate f, 2f and 3f detection, and Total Internal Reflection illumination (TIR) condition as well as External Reflection illumination (ER).

We demonstrate that the perturbation of the probe on the far field detected signal differs strongly in both cases. Moreover, the modulation of the probe position cannot be considered separately from the near-field diffracted by the sample, especially if it is made of resonant particles. The finite element approach with excitation or forcing function term enables a physical description of the detected intensity level [3]. Moreover, adaptative mesh enables error and computer memory control.

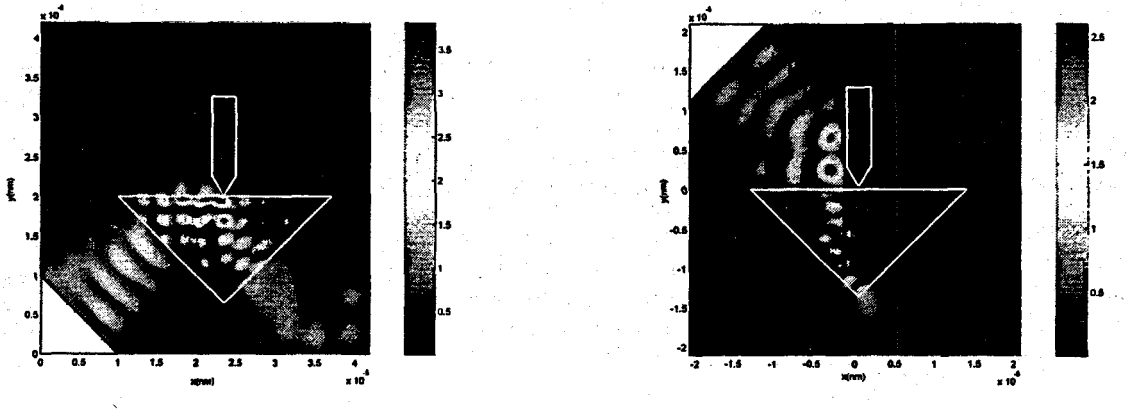

Figure 1: Intensity in ASNOM with TIR and ER illumination.

References

[1] A. Madrazo, M. Nieto-Vesperinas, *J. Opt. Soc. Am. A* **14**, 618 (1997).

[2] J. N. Walford, J. A. Porto, R. Carminati, J. J. Greffet, P. M. Adam, S. Hudlet, J. L. Bijeon, A. Stashkevitch, P. Royer, *J. Appl. Phys.* **68**, 5159 (2001).

[3] J. Jin, *The Finite Element Method in Electromagnetics* (John Wiley and Sons, New York, 1993).

A Novel Scanning Near-Field Microwave Microscope

Steven M. Anlage, Atif Imtiaz, Sheng-Chiang Lee and Alexandre Tselev
Center for Superconductivity Research, Physics Department,
University of Maryland,
College Park, MD 20742-4111 USA.

The new frontiers of physics in condensed matter and materials science is on nano-meter length scales. Classical techniques of probing the electrical properties of materials are limited in resolution to the wavelength of the incident electromagnetic wave. We report here a novel near-field microscope that is capable of operation at radio and microwave frequencies [1-4]. The spatial resolution is comparable to NSOM in the scanning capacitance mode of the microscope [5]. Our objective is to image materials contrast at microwave frequencies on nm length scales. To demonstrate the capabilities of this microscope, we have imaged $La_{0.67}Ca_{0.33}MnO_3$ colossal magneto-resistive (CMR) thin films. These materials are known to phase segregate into antiferromagnetic insulating and ferromagnetic metallic regions on the scale of 10's of nm. We will present evidence of sheet resistance material contrast on short length scales in CMR films using the near-field microwave microscope with STM-feedback distance control. We will discuss the data on these films in the light of a transmission line model of the microscope that we have developed. The microscope is an attractive platform for measuring local losses and local nonlinear properties of a rich variety of correlated-electron materials.

References

[1] D. E. Steinhauer, C. P. Vlahacos, S. K. Dutta, B. J. Feenstra, F. C. Wellstood, and Steven M. Anlage, "Quantitative Imaging of Sheet Resistance with a Scanning Near-Field Microwave Microscope," Appl. Phys. Lett. 72, 861-863 (1998)

[2] D. E. Steinhauer, C. P. Vlahacos, C. Canedy, A. Stanishevsky, J. Melngailis, R. Ramesh, F. C. Wellstood, and Steven M. Anlage, "Imaging of Microwave Permittivity, Tunability, and Damage Recovery in (Ba,Sr)TiO_3 Thin Films," Appl. Phys. Lett. 75, 3180-3182 (1999).

[3] Sheng-Chiang Lee, C. P. Vlahacos, B. J. Feenstra, Andrew Schwartz, D. E. Steinhauer, F. C. Wellstood, and Steven M. Anlage, "Magnetic Permeability Imaging of Metals with a Scanning Near-Field Microwave Microscope," Appl. Phys. Lett. 77, 4404-4406 (2000).

[4] David E. Steinhauer and Steven M. Anlage, "Microwave Frequency Ferroelectric Domain Imaging of Deuterated Triglycine Sulfate Crystals," J. Appl. Phys. 89, 2314-2321 (2001)

[5] Atif Imtiaz and Steven M. Anlage, cond-mat/0203540.

Dissipative shear force on nanoscale probes induced by electromagnetic field fluctuations

Jorge R. Zurita-Sánchez[1], *Jean-Jacques Greffet* [2,3] *and Lukas Novotny*[1]

[1] *University of Rochester, The Institute of Optics, Rochester, NY 14627.*

[2] *Laboratoire d'Energétique Moléculaire et Macroscopique, Combustion, Ecole Centrale Paris, France.*

[3] *Currently on sabbatical at University of Rochester, The Institute of Optics, Rochester, NY 14627.*

Most near-field microscopes use shear force scheme to control the tip sample distance. Causes for this effect are not clearly understood. Recent experiments using oscillating nanoscale probes in ultra-high vacuum environments show that the probes experience a dissipative force that substantially increases as the probe approaches to a planar surface [1, 2, 3]. This shows that there is a mechanism that is not related to chemical binding nor friction due to adsorbed molecules. Possible mechanisms have been suggested in Refs. [1, 2, 3, 4]. (*e.g.* electromagnetic field fluctuations, electron tunneling). Here, we explore the possibility of the electromagnetic coupling between two interfaces. To model the tip-surface interaction we consider two dielectric half-spaces with complex dielectric constants separated by a constant vacuum gap. We calculate the dissipative force per unit area acting on one of the half-spaces which is harmonically oscillating parallel to the surface of the fixed half-space. We focus on the dissipation originated from the electromagnetic field fluctuations which depends on the vacuum gap and the temperature. We derive a theoretical expression for the shear force and evaluate it numerically using experimental data for the dielectric constant. We compare with experimental data measured by other groups.

References

[1] K. Karrai and I. Tiemann, *Phys. Rev. B* **62**, 13174 (2000).

[2] B.C. Stipe, H.J. Martin, T.D. Stowe, T.W. Kenny, and D. Rugar, *Phys. Rev. Lett.* **87**, 96801 (2001).

[3] I. Dorofeyev, H. Fuchs, G. Wenning, and B. Gotsmann *Phys. Rev. Lett.* **83**, 2402 (1999).

[4] J.B. Pendry, *J. Phys. Condens. Matter* **9**, 10301 (1997).

Mesoscopic Structures and Dynamics of MEH-PPV Thin Films by Picosecond Scanning Near-field Optical Microscopy

N. Tamai, Y. Nabetani
Department of Chemistry, School of Science, Kwansei Gakuin University
2-1 Gakuen, Sanda, 669-1337, Japan

Y. Ma, J. Shen
Key Lab. of Supramolecular Structure and Materials, College of Chemistry,
Jilin University, 119-Jie Fang Road, Changchun, P. R. China

Recently, much attention has been paid for the application of conjugated polymers such as poly-*p*-phenylene vinylene (PPV) and its derivatives for organic LEDs. In most of these studies, a spin coating technique has been widely used to prepare thin films. However, luminescence properties of PPV derivatives are strongly dependent on the spin coating conditions [1]. For the application of PPV derivatives to LEDs, analyses of mesoscopic structures, defects, and luminescence properties in small domains of spin coating thin films are indispensable. In the present study, we have examined the mesoscopic structure and dynamics of the conductive polymer, poly[2-methoxy, 5-(2'-ethyl-hexyloxy-p-phenylene vinylene)] (MEH-PPV) on glass and ITO substrates by picosecond time-resolved fluorescence SNOM [2].

Dilute (0.022 wt%) chloroform and xylene solutions are used for spin coating on various substrates. Humidity in the sample preparation condition is adjusted by using saturated inorganic solution of $CaCl_2$ and NH_4Cl. From the topographic and fluorescence images, it was found that the ring-shaped assemblies (wheels) with a diameter of sub μm to a few μm are formed only from chloroform solution on substrates. This wheel is characteristic for high humidity conditions, and no wheel structure is observed from xylene solution. This result suggests that the small water droplets induced by solvent evaporation play an important role for the formation of wheel structure [3].

Fluorescence dynamics and fluorescence spectra in sub-wavelength small domains of the wheel structure prepared from chloroform and the rock-like structure from xylene have been examined and compared. In the wheel structure, luminescence decay of the single-chain exciton was found to be faster in the circumference of the wheel than in the surroundings or the inside of the wheel. The luminescence spectrum in the circumference is red-shifted as compared with the surroundings. These results are interpreted in terms of exciton migration among the polymers and trapping by the aggregate of MEH-PPV. On the other hand, luminescence decays of the thin film prepared from xylene solution were almost independent of the observed position. Morphology-related intrapolymer interaction and excited-state dynamics in sub-wavelength domains will be discussed on the basis of these results.

References

[1] I. D. W. Samuel, G. Rumbles, C. J. Collison, R. H. Friend, S. C. Moratti, and A. B. Holmes, *Synt. Met.al*, **84**, 497 (1997); Y. Shi, J. Liu, and Y. Y. Yang, *J. Appl. Phys.*, **87**, 4254 (2000).

[2] Y. Nabetani, M. Yamasaki, A. Miura, and N. Tamai, *Thin Solid Film*, **393**, 329 (2001).

[3] O. Karthaus, N. Maruyama, X. Cieren, M. Shimomura, H. Hasegawa, and T. Hashimoto, Langmuir, 25, 6071 (2000).

Characterization and modification of the plasmon resonances in a single gold nanoparticle

T. Kalkbrenner
Universität Konstanz, Fachbereich Physik & Optik-Zentrum Konstanz, 78457 Konstanz, Germany,
&
V. Sandoghdar
Swiss Federal Institute of Technology (ETH), 8093 Zürich, Switzerland

The optical properties of metallic nanoparticles have gained increasing interest in the past years. In this paper we present the first demonstration of optical tomography on a single gold nanoparticle, allowing us to identify its optical axes. We then show how the plasmon resonances of the gold particle can be modified when it is placed in front of a flat substrate. Finally, we discuss our results on optical near-field imaging of a sample by recording the changes in the plasmon resonance width and center frequency.

The starting point of our work is the procedure that we had reported previously for mounting an individual gold nanoparticle at the end of a tapered fiber tip [1]. We then use shear force control to position the particle against a desired surface. By illuminating the system with white light, we record the plasmon resonance in the scattered signal (fig. 1b). In addition, however, we also rotate the polarization of the incident light as well as the tip itself to separate the contributions from different axes of the gold particle, which in general is not perfectly spherical (see fig. 1a). This tomography measurement allows us to detremine the orientation of the long and short axes of an ellipsoid nanoparticle. After this thorough characterization of the system, the dipolar plasmon mode of one of the particle's principal axes is excited by tuning the polarization to the appropriate angle. By approaching the particle to a surface and recording a spectrum of the scattered light at each distance, we have observed modification of the linewidth as well as the line center of the plasmon resonance. Fig. 1 c) shows the change in position and width of the plasmon while an 80 nm-particle is approached to a glass substrate.

Furthermore, we have performed a novel form of SNOM by monitoring the modifications of the plasmon resonances as the particle is scanned across a sample. By plotting the changes in the position and width of the line at each scan pixel, we have obtained optical images of the sample.

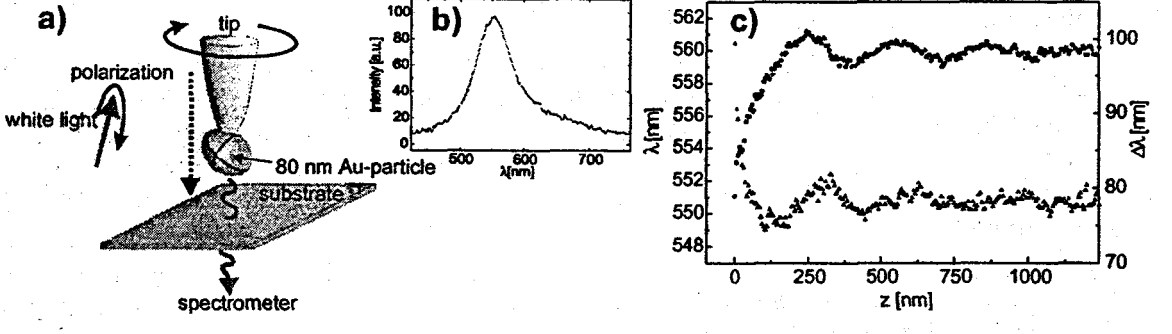

Figure 1: a) Schematics of the experiment. b) Plasmon resonance of a single gold nanoparticle at the end of a tapered fiber tip. c) Changes in the lineshift (circles) and linewidth (triangles) of the plasmon resonance while approaching the particle to a glass surface.

Having demonstrated that one can characterize and manipulate the plasmon resonances of a single metallic nanoparticle in front of a substrate, in future we plan to apply our know-how to perform well-controlled investigations of Surface Enhanced Raman Scattering (SERS) [2] at the single molecule level.

References

[1] T. Kalkbrenner, M. Ramstein, J. Mlynek, and V. Sandogdar, *J. of Microsc.* **202**, 72 (2001).
[2] R.M. Stöckle, Y.D. Suh, V. Deckert, and R. Zenobi, *Chem. Phys. Lett.* **318**, 131 (2000).

Fourier Polarimetry of Mesostructure in Thin Polymer Films

Lori S. Goldner, Michael J. Fasolka, Jeeseong Hwang, Kathryn Beers, Garnett W. Bryant
National Institute of Standards and Technology, Gaithersburg, MD 20899.
Augustine M Urbas, Peter DeRege, Timothy Swager, Edwin L. Thomas
Dept of Materials Science and Engineering, Massachusetts Institute of Technology, Cambridge, MA 02319

Recent advances in near-field techniques permit measurements of local birefringence and dichroism only in specific limits – for example, when the dichroism of the tip is sufficiently small and the fast and dichroic axis of the sample are aligned [Refs 1-2]. We overcome these difficulties and extend NSOM polarimetry to a more general case, demonstrating how to take into account substantial tip dichroism and birefringence without loss of accuracy, and how to approach the more general case of films with separate dichroic and fast axes. We demonstrate the adaptation of Fourier polarimetry to NSOM and perform, for the first time, complete measurements of the local dichroism, alignment of the dichroic axis, birefringence, alignment of the fast axis, and topography. We show that the limit of accuracy of these measurements depends on (1) changes in the tip dichroism during a scan and (2) the noise floor of the experiment. In a separate paper in this volume we discuss near-field modeling of our results.

To demonstrate these techniques, we use two self-assembled thin-film polymer systems. Polymer self-assembly presents an attractive means of creating the micro- and nano-patterned spatial arrays required for many opto-electronic and coatings technologies. The ordering processes studied here are microphase separation, exhibited by block copolymers (BCs), and crystallization, common in many polymer species.

Below are the first optical images of BC microphase domain morphology. Optical, topographic, and dichroism measurements within a single grain of a 100 nm thick polystyrene-b-polyisoprene (PS-b-PI) photonic BC [Ref. 3] are shown (a-d). OsO_4 stains the PI domains. Domains, grains, and defects in these materials are characterized using both birefringence and dichroism measurements. Images e-h are optical, topographic, and birefringence measurements of a 100nm-thick isotactic PS spherulite. The radial arrangement of crystallite lamella, defect structures located near the crystal nucleus, and possible chain alignment in the "depletion zone" at the spherulite periphery are evident. We will discuss this data as well as dichroism data, and show how in all cases the acquisition of dichroism data, with a separate optical axis, is imperative to correct interpretation of birefringence data.

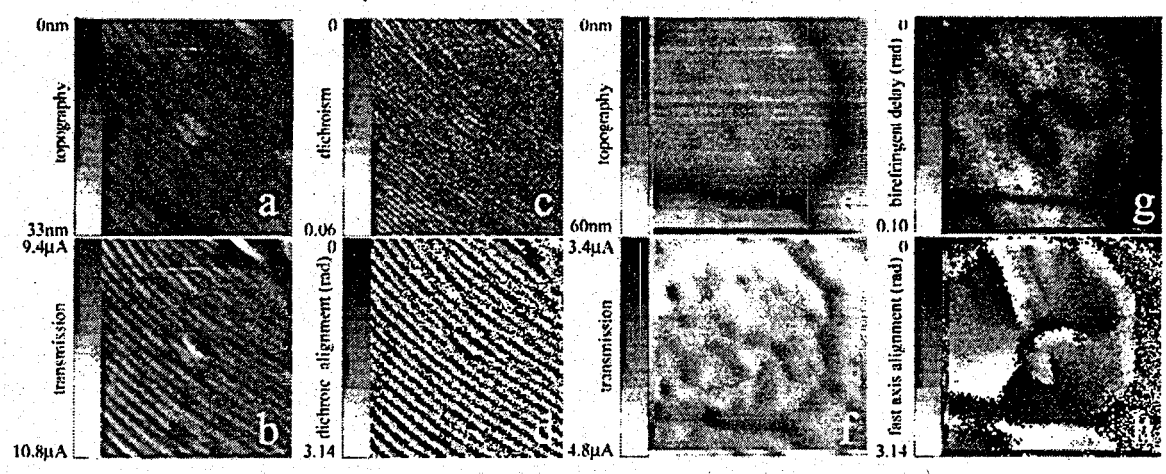

Figure 1: a-d, images of BC film including dichroism and dichroic axis maps; e-h images of PS spherulites showing birefringence and fast axis maps. Transmission in units of PMT current. All images 4μm square.

References

[1] AL Campillo and JWP Hsu, *J. Appl. Phys.* **91**, 647 (2002) and references therein.
[2] PK Wei and WS Fann, *J. Microscopy* **202**, 148 (2000).
[3] A Urbas et al, *Adv. Mater.* **12**, 82 (2000).

Realization of evanescent and propagating Bessel beams: the role of the E_z component of the electric field on confinement

T. Grosjean, D. Courjon,
Laboratoire d'Optique P.M. Duffieux,
Université de Franche-Comté, France

In the previous NFO meeting, we have proposed to use confined evanescent light beams as "virtual" or "immaterial" tips. Unfortunately, this technique was handicapped by the need of using perfectly radially-polarized light beams. In this communication, we propose first a simple, stable and cheap method allowing the generation of beams of any polarization and more especially of purely radially-polarized light beams. Second, we demonstrate both theoretically and experimentally that for very opened systems (far and near–field imaging systems such as confocal and near–field microscopes) the polarization is a limiting factor of resolution and light confinement. Finally, we will present the very first experimental results dealing with virtual tips.

Anisotropy and periodicity in the electron density distribution and the well width fluctuations in a quantum well

Y. Yayon, M. Rappaport, V. Umansky and I. Bar-Joseph

Department of Condensed Matter Physics, The Weizmann Institute of Science, Rehovot 76100, Israel

The two-dimensional electron system (2DES) formed in MBE grown modulation-doped quantum well (QW) is a major platform for studying the physics of interacting electrons. Irregularities in the crystal structure are always present in this system and introduce a disorder potential even in the highest quality samples. It was therefore natural that with the evolution of scanning-probe experimental techniques a considerable effort was directed to resolving spatial inhomogeneities in the system properties. Near-field spectroscopy has proven to be particularly useful in that context. The high spatial resolution that can be obtained, typically 100-200 nm, and the wealth of information contained in the optical spectrum made it a favorable technique for studying the local properties of semiconductor QWs.

In this work we use near-field photoluminescence (PL) spectroscopy to study *spatial correlations* in the electron distribution and in the fluctuations of the QW width. The PL spectrum of 2DES at low electron densities consists of two sharp peeks, the neutral (X) and the negatively charged (X^-) exciton. Our ability to extract the electron distribution derives from the fact that the local *X^- PL intensity* is directly proportional to the local electron density [1]. In addition, using the fact that the *X PL energy* depends quadratically on the local QW width we can extract the well width fluctuations. Hence, by scanning the sample with our near-field scanning optical microscope (NSOM) at low temperatures and measuring the spectrum at each point, we obtain simultaneously a two-dimensional image of the electron density distribution and of the well width fluctuations.

To unveil possible order in these seemingly random images we have studied their two-dimensional autocorrelation function. Examining the behavior of electron density autocorrelation function (Fig. 1b) we can observe the existence of periodic narrow stripes of higher electron density along the $1\bar{1}0$ crystal direction. By deconvolving the tip response function we find that their width is smaller than 150 nm and their period is 1.3 μm. We conclude that the electron distribution in the plane of the QW is anisotropic and periodic. This surprising finding should affect our understanding of various electron behaviors and in particular, the recent finding of anisotropy in transport at high Landau levels [2]. We also find a pronounced symmetry in the well width image (Fig. 2b). It is seen that the narrow regions of the QW (high exciton energy) are arranged in a periodic cubic lattice structure, which is rotated approximately by 45 degrees relative to $1\bar{1}0$. This symmetry was observed in several QW samples. It is important to emphasize, however, that the fluctuations in electron density *are not correlated* with those of the QW width.

To find the source of this ordered behavior we conducted atomic force microscopy measurements of the sample surface and compared it to the near-field measurement. We conclude that elongated structural mounds, which are intrinsic to MBE growth, are responsible for the creation of those electron density and well width textures.

References

[1] Y. Yayon *et al.*, *Phys. Rev. B* **64**, R 081308 (2001).

[2] M.P. Lilly *et al.*, *Phys. Rev. Lett.* **82**, 394 (1999).

Detection of Local Density of States using near-field emission measurements. Application to local spectroscopy.

R. Carminati, K. Joulain, J.P. Mulet and J.J. Greffet[a]
Laboratoire EM2C, Ecole Centrale Paris,
CNRS, 92295 Chatenay-Malabry Cedex, France
[a] *also with University of Rochester,*
The Institute of Optics, Rochester, NY 14627, USA

It is well-known that the measurements made in STM yield the local density of electronic states. It has been shown by Carminati and Saenz[1] that a unified scattering formalism allows to express within the same framework the signal obtained in STM and in SNOM. This result suggests that the SNOM can measure the local density of *electromagnetic* states. Recent results have reported measurements of the electromagnetic LDOS using PSTM measurements[?] which has then been compared to numerical simulations of the LDOS. In this paper, we show that an apertureless microscope used to detect the spontaneous emission by the sample yields the electromagnetic LDOS. The signal is generally dependent on the tip as it is in STM. Within the assumption that the tip can be approximated by a point-like scatterer, it appears that the signal is within a good approximation proportional to the electromagnetic LDOS.

The starting point of our discussion is the general form of the flux established in ref.[1] and ref.[4]. We apply this general expression of the signal to the particular case of an apertureless set-up. In order to obtain the emission signal of the sample, we use the fluctuation-dissipation theorem. This allows to express the field spontaneously emitted by the sample using the Green's function of the system. The relationship between the signal and the LDOS follows directly from this analysis.

In order to discuss possible applications, we consider the case of an ionic crystal. In the near-field, the emission is completely dominated by the contribution of surface waves called surface-phonon polaritons as it has been shown in ref.[3]. A unique feature of the spectrum of the emitted near-field is that it has very large and narrow peaks at some particular frequencies. In other words, the electromagnetic LDOS has a few pronounced peaks. From the measurements of this density of states, we will show that it is possible to recover the complete dielectric constant of the material using a Kramers-Kronig analysis. This paves the way to a local spectroscopic technique to characterize materials with ionic structure.

References

[1] R. Carminati, J.J. Saenz, *Phys.Rev.Lett.* **84**, 5156 (2000).

[2] C.Chicanne et al. *Phys.Rev.Lett.* **88**, 097402 (2002).

[3] A.V. Shchegrov, K. Joulain, R. Carminati and J.J. Greffet, *Phys.Rev.Lett.* **85**, 1548 (2000).

[4] J.A. Porto, R. Carminati and J.J. Greffet, *J.Appl.Phys.* **88**, 4845 (2000).

Optical Microscopic Studies of Nanoscale Dynamics in Polymer-Dispersed Liquid Crystal Films

D. A. Higgins, X. Liao, J. E. Hall, E. Mei, Department of Chemistry, Kansas State University, Manhattan, KS, 66506.

Near-field scanning optical microscopy (NSOM) is used to study local electric-field-induced molecular reorientation dynamics in native and dye-doped polymer-dispersed liquid crystal (PDLC) thin films.[1,2] PDLC films were prepared by spin casting an aqueous emulsion containing nematic liquid crystal and poly(vinyl alcohol) (PVA) onto indium-tin-oxide coated glass substrates. Dye-doped versions were prepared by dissolving fluorescent BODIPY dyes into the liquid crystalline phase. Initial characterization by topographic, birefringence, and fluorescence NSOM imaging shows the films are comprised of micrometer-sized liquid crystal droplets encapsulated in a thin PVA film. Although dominated by far-field contrast, static optical images of the droplets can be used to obtain information on the local liquid crystal and dye organization in droplets of different sizes and shapes. Fig. 1 shows representative images. In order to study local liquid crystal and dye reorientation dynamics, an electric field was applied to the sample using the aluminum-coated NSOM probe. Field-induced reorientation of the liquid crystal and dye molecules within the droplets were then detected optically. Dramatic spatial variations in the dynamics are observed in frequency-dependent imaging experiments, and in frequency- and time-domain single-point measurements. These spatial variations are interpreted to reflect spatial variations in the local viscoelastic properties of the liquid crystalline phase, based on previously published models. Unlike the static imaging results, the dynamics data show high-resolution features. It is therefore concluded the reorientation processes dominating the optical contrast occur in the near-field regime. The results are shown to arise from the confinement of field-induced reorientation dynamics to the upper regions of individual liquid crystal droplets, nearest the NSOM probe. Studies of the dye-doped PDLCs show dramatic field-dependent changes in the dye order parameter. In addition, the field-dependence of the order parameter is observed to vary spatially within individual droplets for dyes that are weakly aligned by the liquid crystal. These results are interpreted to reflect spatial variations in the extent of dye interactions with the applied electric field and with the surrounding liquid crystal host.

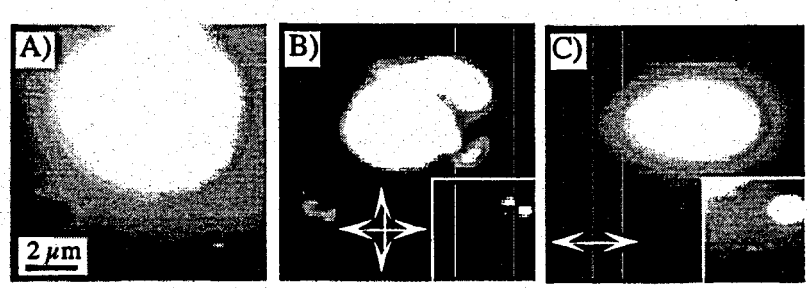

Figure 1: Simultaneously-recorded (A) topography, (B) birefringence, and (C) fluorescence images of dye-doped PDLC droplets.

References

[1] D. A. Higgins, X. Liao, J. E. Hall, E. Mei, *J. Phys. Chem. B* ***105***, 5874 (2001).

[2] E. Mei, D. A. Higgins, *J. Chem. Phys.* **112**, 7839 (2000).

A new generation of near-field probes fabricated by focused ion beams

Erik J. Sánchez, John T. Krug, II, X. Sunney Xie
Harvard University, Department of Chemistry and Chemical Biology
Cambridge, MA 02138.

We present the design and fabrication of NSOM probes with high field enhancement to reproducibly achieve sub 20 nm optical/topographic imaging resolution. This work is an extension of our initial work on tip enhanced nonlinear optical microscopy (TENOM). (See Ref. 1.) These probes are fabricated using a high-resolution focused ion bean (FIB) system. The fabrication is guided by 3-D finite difference time domain (FDTD) simulations to optimize the geometry of the NSOM probe for intensity enhancement factors as high as ~8000. (See Ref. 2.) We have imaged thylakoid membrane layers containing PSII and PSI protein assemblies with FIB milled probes, and were able to observe distinctly different local emission spectra. This portends a spectroscopic mapping of photosynthetic membranes. In addition to utilizing the FIB for milling the probe, we have used ion and electron beam assisted deposition (IBAD/EBAD) of SiOx on the nanometer scale. Such deposition is typically carried out in the semiconductor industry for nanometric repair. We have analyzed the chemical composition of the deposited materials, and deposited SiOx layers at the ends of our probes. These "spacer layers" serve to minimize fluorescence quenching of the sample by the probe. This new generation of apertureless NSOM probes, combined with the dielectric spacers, will allow the imaging of isolated or aggregated chromaphoric proteins with high spatial resolution and high sensitivity. The probe and spacer layer fabrication methodology will be of general interest for nano-optics.

References

[1] E. J. Sánchez, L. Novotny, and X.S. Xie, *Physical Review Letters* **82**, 4014-4017 (1999).
[2] J. T. Krug, II, E. J. Sánchez, and X. S. Xie, *Journal of Chemical Physics*, In press.

Crystallization Study of Organic Light Emitting Devices by Polarization Modulation Near-Field Optical Microcopy

Pei-Kuen Wei[1], Shen-Yu Hsu[1], Hsieh-Li Chou[1], WunShain Fann[2]

[1] Institute of Applied Science and Engineering Research, Academia Sinica.
[2] Institute of Atomic and Molecular Sciences, Academia Sinica
128, Section 2, Academia Road, Taipei, Taiwan 11529, R. O. C.

We present a new setup of collection-mode polarization modulated near-field optical microcopy for actually measuring the mesoscale crystallization of thin films. Previous polarization modulation NSOMs (PM-NSOM) were operated in transmission mode.[1] Two major problems should be solved for the polarization signals. First, the birefringence in the fiber is a severe problem for PM-NSOM, it will destroy polarization state of the incident light. Second, there is a large depolarization effect when light passing through the probe tip. In comparison to transmission mode near-field optical microcopy, our new collection mode microscopy provides no axial polarization, free of fiber birefringence and flexibility for tuning wavelength. The Jones matrix calculation verifies that sample's crystallization can be obtained by simply subtracting the polarization vector from tip's anisotropy. We've used this setup to measure the crystallization of organic light emitting devices (OLEDs). The OLEDs, especially the hole-transport-layer (naphthaphenylene benzidine (NPB)), are easily subject to crystallization.[2] The crystallization is related to the dichroic ratio when a rotated linearly polarized light passing through it. Figure 1 shows the mesoscale crystalline domains and dichroic ratios of NPB films before and after annealing. The performances of OLEDs (L-V and I-V curves) vs. the crystallization for different annealed samples are also measured. Detail comparisons will be presented in the conference.

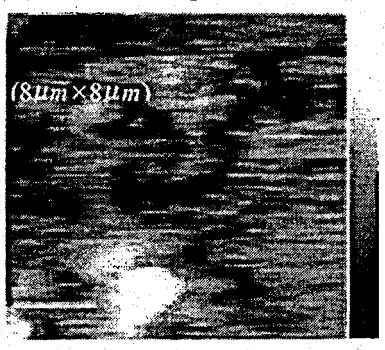

Dichroic image of NPB film: before heating

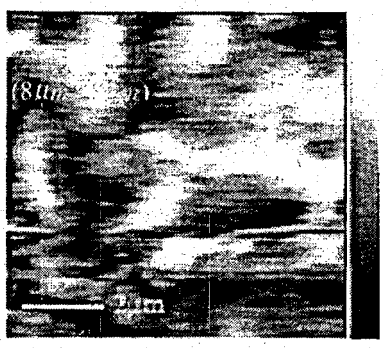

Dichroic image of NPB film: after thermal annealing

[1] P. K. Wei and W. S. Fann, *J. of Microscopy.* **202,** 148 (2001)

[2] Z. Q. Gao, W. Y. Lai, T. C. Wong, C. S. Lee, I. Bello, and S. T. Lee, *Appl. Phys. Lett.* **74,** 3269 (1999)

Three-dimensional imaging in near-field optics

P Scott Carney
University of Illinois at Urbana-Champaign, Department of Electrical and Computer Engineering, Urbana, IL 61801
John C Schotland, Vadim A Markel
Optical Radiology Laboratory, Department of Radiology, Washington University in Saint Louis.

We report on recent advances in three-dimensional structure calculation for near-field optics. We have reported semi-analytic solutions for the linearized inverse problem in the literature [1, 2, 3]. The algorithms that result from our analysis are computationally efficient regularized and stable.

In this talk we will address inclusion of polarization effects, boundary conditions and sampling which have not been addressed in our publications. We will also discuss experimental progress in the power extinction[2] and frustrated total internal reflection modalities [1].

References

[1] P. Scott Carney and John C. Schotland, "Three-dimensional total internal reflection microscopy," Opt. Lett. **26**, 1072-1074 (2001).

[2] P. Scott Carney, Vadim A. Markel and John C. Schotland, "Near-field tomography without phase retrieval," Phys. Rev. Lett. **86** 5874-5877 (2001).

[3] P. Scott Carney and John C. Schotland, "Inverse scattering for near-field microscopy," Appl. Phys. Lett. **77**, 2798-2800 (2000).

Clustering of Photoluminescence in InGaN Films Grown by MOCVD and MBE

J.O. White, M.S. Jeong, J.Y. Kim, K. Samiee, Y.W. Kim, J.M. Myoung, K. Kim,
University of Illinois, Frederick Seitz Laboratory and Elect. and Computer Engineering Department., Urbana, IL 61801.

E.K. Suh, M.G. Cheong, C.S. Kim, C.-H. Hong, H.J. Lee,
Semiconductor Physics Research Center, Chonbuk National University, Chonju 561-756, Korea.

We have grown 0.3 μm thick InGaN films by MBE, and 1-2 nm thick InGaN quantum wells by MOCVD. In both types of sample, high photoluminescence efficiency is often accompanied by a high spatial intensity variation. The intensity is not random on all length scales, but is concentrated in micron-sized regions.

The origin of the spatial variation is investigated by near-field scanning optical microscopy, spectroscopy, and cross-sectional transmission electron microscopy. We find that the variation is not due to fluctuations of indium content because there is no corresponding shift in wavelength. The combination of high-resolution optical and electron microscopy provides evidence that the spatial variation results from an underlying variation in dislocation density.

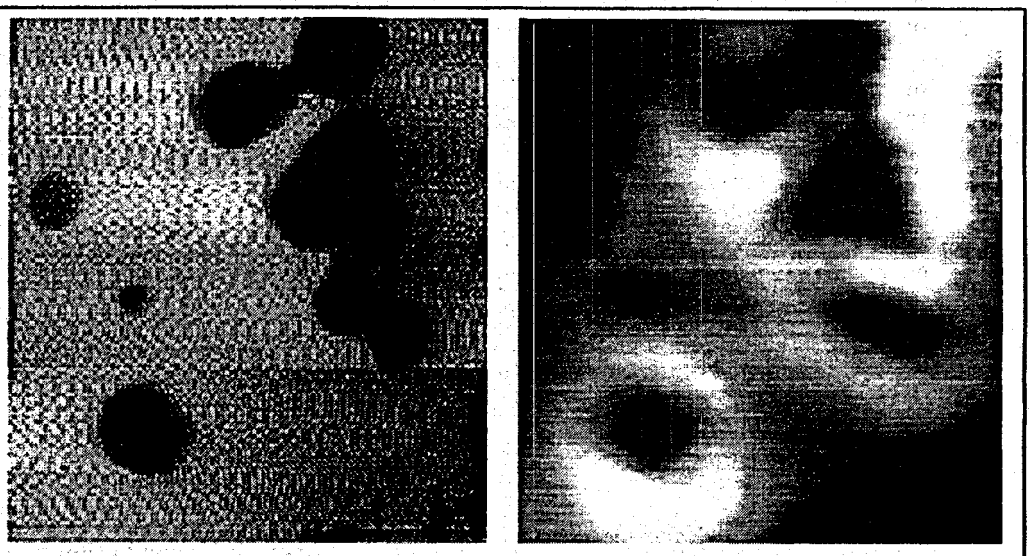

Fig. 1 10×10 μm^2 topographic (l) and photoluminescence (r) images of a multiple quantum well sample of InGaN/GaN. Note that the photoluminescence is strongest in the vicinity of the pits, and decreases with distance away from the pits. Transmission electron microscopy reveals that the pits act as a getter, removing dislocations from the surrounding region, thus enhancing the luminescence.

The clustering is quantified by calculating the image entropy and space bandwidth product of the near-field images. We find that the image entropy decreases as the indium content increases, reflecting the organization of photoluminescence into micron-sized clusters.

SNOM Imaging of Photonic Nanopatterns, Metal Islands and Molecular Aggregates

U. C. Fischer, J. Heimel, H J. Maas, A. Naber, H. Fuchs, University of Muenster, 48149 Muenster, Germany.

J. C. Weeber, A. Dereux, University of Burgundy, 21004 Dijon, France.

In Scanning Near-Field Optical Microscopy (SNOM), a nanoscopic source of light is scanned at a small distance accross the surface of the object. The emission of the source, modulated by the object, serves as a signal for SNOM. The SNOM image as obtained with a point dipole as a source is defined as a photonic nanopattern. This photonic nanopattern can be calculated numerically on the basis of the Greens Dyadic method. The photonic nanopattern depends on the orientation of the dipole, its distance to the object, on the local properties of the object and on the detection scheme of the SNOM. With the tetrahedral tip (T-tip) as a source, images of metal test objects can be interpreted as photonic nanopatterns with a dipole inclined at an angle of 45° and a distance of 10 - 20 nm to the surface of the object Ref. [1]. The nanopatterns of small metal objects have a completely different appearance exhibiting finer details than those of dielectric objects with a real and positive dielectric function, indicating, that the excitation of surface plasmons of a wavelength in the order of 40 - 60 nm determine the shape of the observed photonic nanopatterns. Details smaller than half this wavelength are also resolved in SNOM images of metal grains Ref. [2, 3] or aggregates of dye molecules on a gold substrate. Numerical calculations indeed give a hint, that a metallic substrate may lead to higher resolved details in the photonic nanopatterns of objects adsorbed on the metal substrate. We expect that the contrast in the SNOM signal of dye molecules adsorbed on a metal film depends mainly on the real part of the polarisability of the molecules Ref. [4, 5] which, for the selected dye aggregates, show characteristic features in a bandwidth of only 10 nm. This property and the high resolution in the SNOM images is the basis of our attempt to SNOM imaging of dye molecules at molecular resolution.

References

[1] H. J. Maas, A. Naber, U. C. Fischer, H. Fuchs. *J. Opt. Soc. Am*,in print.

[2] J. Koglin, U. C. Fischer, H. Fuchs. *Phys. Rev. B* **55**,7977 (1997).

[3] J. Heimel, U. C. Fischer, H. Fuchs. *J. Microscopy* **201**,53 (2001).

[4] U. C. Fischer, J. Heimel. *Jpn. J. Appl. Phys.* **40**,4391 (2001).

[5] U. C. Fischer, E. Bortchagovsky, J. Heimel, R.T. Hanke, submitted.

Near-field Vibrational Spectroscopy for Nanoscale Chemical Analysis

C. A. Michaels, S. J. Stranick,
National Institute of Standards and Technology, Gaithersburg, MD 20899.
D. B. Chase,
DuPont Central Research and Development, Wilmington, DE 19880

The ability to measure chemical bond changes on the nanometer scale is of critical importance for the characterization of surfaces relevant to catalysis, materials and biological problems. Our goal has been to develop a technique for the in-situ, non-destructive, nanoscale chemical imaging of surfaces. The strategy for realizing this goal involves coupling the high spatial resolution of near-field scanning optical microscopy (NSOM) [1,2] with the chemical specificity of vibrational spectroscopy [3]. The combination of the sub-diffraction spatial resolution attainable in the near-field with the high chemical specificity of infrared absorption and/or Raman spectroscopy promises a powerful new analytical capability that overcomes critical measurement limitations of both far-field Raman and infrared microscopes (low spatial resolution) and scanned probe microscopes (lack of chemical specificity).

Initial applications of this technique have been focused on measuring lateral variations in chemical composition for thin organic films such as polystyrene (PS)/polyethylacrylate (PEA) polymer blends, a model system for the study of degradation and corrosion of organic coatings. Figure 1(a) shows the far-field IR absorbance spectra of PS (solid line) and PEA (dashed line) in the CH stretching region along with the spectrum of the broadband IR laser (gray) tuned to the center wavelength (λ = 3.36 μm) used to acquire this data. Figure 1(b) shows an 8 x 8 μm near-field spectral image frame of the PS/PEA film acquired at 2980 cm^{-1} with a ~ 300 nm diameter aperture probe. The broadband nature of the light source allows for the analysis of the relative importance of scattering/near-field coupling effects and absorption as sources of near-field image contrast based on their respective variation with wavelength. Scattering/near-field coupling effects dominate the image contrast for this sample although analysis of the spatial and spectral variations in near-field transmission contrast over many image frames suggest the that minority phase (bright features) composition is PS rich, in agreement with the results of a selective etching/AFM analysis of a similar sample.

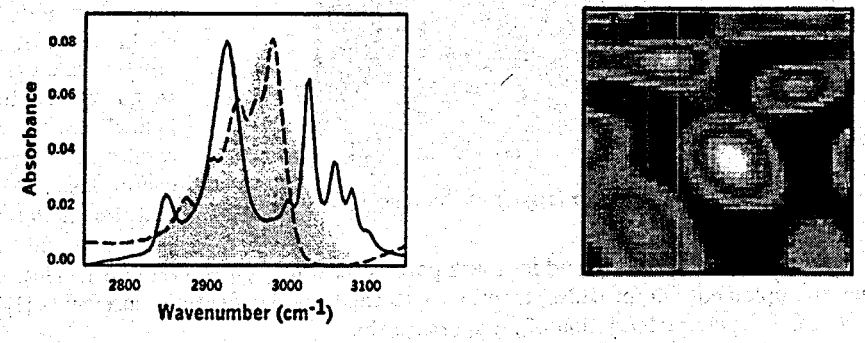

Figure 1. (a) Far-field absorbance spectra of PS (solid line) and PEA (dashed line) along with laser spectrum (gray) used to acquire near-field IR transmission images of a thin PS/PEA blend film. (b) 8 x 8 μm near-field transmission image of PS/PEA blend film acquired at 2980 cm^{-1}.

References

[1] D.W. Pohl, W. Denk, and M. Lanz, *Appl. Phys. Lett.* 44, 651 (1984).
[2] A. Lewis, M. Isaacson, A. Harootunian, and A. Muray, *Ultramicroscopy* 13, 227 (1984).
[3] Y.T. Chabal, *et al.*, Vibrations at Surfaces, Elsevier, Amsterdam, 1990.

In Situ Characterization of Optical Near-field Probes in Aperture NSOM

A. Drezet, S. Huant, and J. C. Woehl,
Laboratoire de Spectrométrie Physique, Université Joseph Fourier Grenoble et CNRS,
38402 Saint Martin d'Hères, France.

The optical resolution of an aperture near-field scanning optical microscope (NSOM) is linked to two critical parameters: the aperture diameter and the feedback distance. Accessing these parameters experimentally is difficult, however, and often depends on the quality and applicability of external calibration curves. Information about the aperture diameter of the fiber tip is normally deduced from its optical transmission or from the angle dependence of its far field emission [1]. Less frequently, it is obtained through direct observation under an electron microscope. The tip-sample distance for a certain feedback setpoint can be evaluated by defining a reference point for zero distance (like a tunneling current between the tip's metal coating and a specially prepared sample surface) and by using the known behavior of the piezo scanner [2]. However, it is unclear how a calibration curve obtained under such specific conditions changes for near-field imaging of other surfaces. There is also no guarantee that the optical aperture remains unchanged during the measurements, e.g. by inadvertent contact with the sample surface.

We present a method that allows the characterization of the near-field tip and of the feedback distance *in situ*, i.e. under the actual experimental conditions and on a tip by tip basis. It uses the unique spectroscopic properties of nanometric test objects: fluorescent nanospheres. Due to the isotropic distribution of randomly oriented molecular transition dipole moments inside the sphere, such an object acts as a volume detector of the average square of the electric field intensity emanating from the fiber tip. Fluorescence images of rather large nanospheres do not present enough features for such an analysis. Nanospheres that are small compared to the optical aperture, however, allow a detailed analysis in terms of aperture diameter and feedback distance. We will illustrate this behavior with experimental results for various feedback conditions. A simple but realistic model of the optical probe will be presented which allows a determination of fiber tip and feedback parameters during a NSOM experiment. Our method is universal, easy to implement and provides, together with the usual far-field measurements [1] a complete, i.e., far-field *and* near-field characterization of an aperture tip.

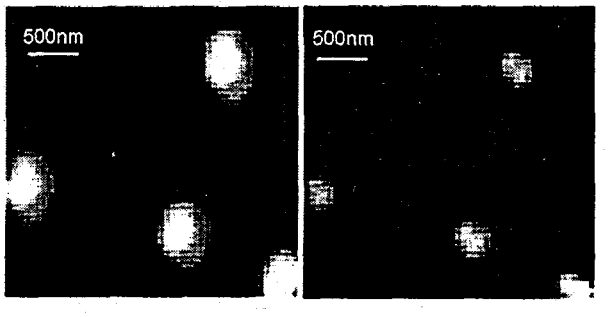

Topography (left) and fluorescence image (right) of fluorescent nanospheres.

References

[1] C. Obermüller and K. Karrai, *Appl. Phys. Lett.* **67**, 3408 (1995); A. Drezet, J. C. Woehl, and S. Huant, *Europhys. Lett.* **54**, 736 (2001)

[2] K. Karrai and I. Tiemann, *Phys. Rev. B* **62**, 13174 (2000).

Near-Field Raman imaging of defects in molecular crystals with sub-diffraction resolution.

P. G. Gucciardi, S. Trusso, C. Vasi, CNR - Istituto per i Processi Chimico-Fisici, sez. di Messina, Via La Farina 237, I-98123 Messina, Italy.

S. Patanè, I.N.F.M., Dipartimento di Fisica della Materia e Tecnologie Fisiche Avanzate, Università di Messina, Salita Sperone 31, I-98166 Messina, Italy.

M. Allegrini, I.N.F.M., Dipartimento di Fisica, Università di Pisa, Via Buonarroti 2, I-56127 Pisa, Italy.

In this paper we report on the development of an aperture Near-Field Optical Microscope (SNOM) for fast Raman imaging of organic materials. The apparatus, using pulled, metallized optical fiber probes, works in reflection mode and is optimized for what concerns both the light collection and detection schemes. A single-grating, short focal lenght monochromator is preferred since it provides a high luminosity, in spite of the low spectral resolution (tens of cm^{-1}). A photomultiplier, working in photon counting mode, permits to achieve higher detection efficiencies with respect to conventional (non-intensified) CCD cameras. Thus, spectral analysis as well as fast and detailed Raman imaging (128×128 points) can be performed with integration times of 100 ms per point, without the need of any field enhancement effect. Simultaneous acquisition of the topography, elastic scattering and Raman scattering maps, allows for unambiguous identification of different species chemical. The comparative analysis of the three images permits to identify and eleminate the eventual occurrence of fictitious contributions in the Raman map (artifacts).

The results we report on concern two high Raman-efficiency molecular samples: a 7,7',8,8'-tetracyanoquinodimethane (TCNQ) crystal showing surface defects, and a TCNQ thin film characterized by the presence of sub-micrometer sized organometallic copper-salt complexes [1]. In the first case (fig. 1a) the effects of the surface deformation are studied, while in the second sample (fig. 1b) we are able to chemically image the formation of salt complexes, based on the different Raman activity of the two species. Sub-diffraction resolution is achieved in both studies. A comparative analysis with independent MicroRaman maps, supports the SNOM results assessing the superior spatial resolution of the Near-Field technique.

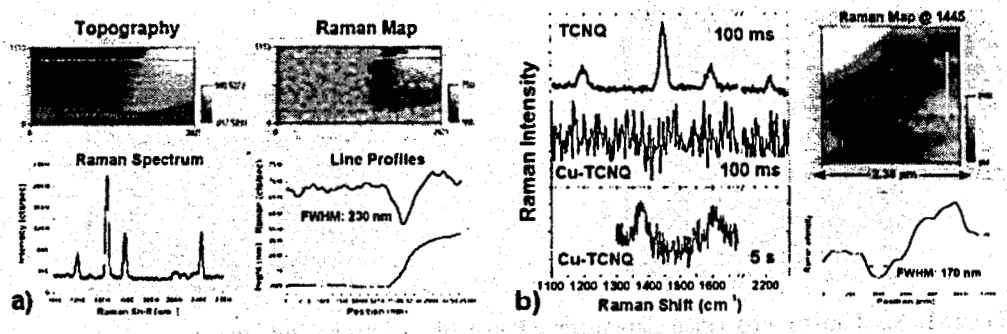

Figure 1: (a) SNOM analysis of a surface defect in a TCNQ crystal. The Raman activity at 1445 cm^{-1} in the surroundings (~ 230 nm) of the defect is depleted probably because of stress relaxation effects. (b) Integration times as short as 100 ms can be used to discriminate local Cu-TCNQ complexes in a TCNQ thin film with sub-200 nm resolution.

References

[1] P. G. Gucciardi, S. Trusso, C. Vasi, S. Patanè, M. Allegrini, *Phys. Chem. Chem. Phys* **2002, in press.**

Enhanced Light Confinement in a Near-Field Optical Probe with a Triangular Aperture

D. Molenda, U. C. Fischer, H.-J. Maas, C. Höppener, H. Fuchs, and A. Naber
Physics Institute, Wilhelm-Klemm-Str. 10, D-48149 Münster, Germany

For most applications, the resolution capability of conventional near-field optical aperture probes on the basis of metal-coated tapered glass fibers is limited to ~80-100 nm [1]. One reason for this is the low transmission efficiency of aperture fiber probes which is a result of a relatively small full taper angle of 20°-40° [1]. A second reason for the limited resolution capability is the unfavourable distribution of the light electric field in close vicinity to the aperture. In a circular aperture, the incoming field is strongly enhanced at opposing metallic edges, thus producing at least two well-separated near-field optical light sources of equal brightness. Apparently, a substantial improvement of optical resolution would result if it were possible to enhance the field at one edge clearly more than at the others. This can, however, only be accomplished by reducing the symmetry of the aperture.

We introduce here a new concept for an aperture probe which exhibits considerably improved properties regarding transmission as well as light confinement [2]. A fundamental feature of this probe is an aperture with a shape of an equilateral triangle. By means of a new optical characterization method [3], we are able to show, that a triangular aperture (TA) has a clearly predominant field enhancement at only one of its three edges when it is illuminated with light of suitable polarization. Thus, compared to a circular aperture of equivalent size, the optical resolution capability is approximately doubled without a corresponding loss of brightness.

We have developed a simple method which allows us to fabricate TA Probes with a small aperture size and a full taper angle of ~90°. The glass body has a shape of a tetrahedron and an ultra-sharp tip with a radius of curvature of only a few nanometers. After rotational evaporation of the glass body with ~100 nm aluminum, an aperture at the very end of the coated tip is created by controlled squeezing against a smooth substrate. The ultra-sharp corner enables us to form routinely even small apertures with high accuracy. From the geometry of the glass tip, the apertures are expected to have a shape of an equilateral triangle. It is demonstrated, that a TA probe is particularly suited to fluorescence measurements in a resolution range clearly < 40 nm.

Figure 1: SEM images of a Triangular-Aperture Probe. Size of images: 1.4 μm.

References

[1] B. Hecht, B. Sick, U. P. Wild, V. Deckert, R. Zenobi, O. J. F. Martin, and D. W. Pohl, *J. Appl. Phys.* **81**, 2492 (1997).
[2] A. Naber, D. Molenda, U. C. Fischer, H.-J. Maas, C. Höppener, N. Lu, and H. Fuchs, submitted.
[3] C. Höppener, D. Molenda, H. Fuchs, and A. Naber, *Appl. Phys. Lett.* **80**, 1331 (2002).

Catalytic Hydrogenation of Benzene on Single Catalytic Sites studied by Near-Field Raman Spectroscopy

Christian Fokas and Renato Zenobi, Department of Chemistry, Swiss Federal Institute of Technology, ETH-Hönggerberg, HCI, CH-8093 Zürich, Switzerland.

Volker Deckert, Institut für Angewandte Photophysik, TU Dresden, D-01062 Dresden, Germany.

Heterogeneous catalysis is of great industrial importance, but for many widely used catalytic processes, fundamental understanding is incomplete. One difficulty is that catalytic processes often take place at elevated pressure and temperature that prevent their study with the tools of ultrahigh vacuum surface science. A second problem is that reactions take place at nanometer sized catalytic metal grains finely dispersed on an inert support material. Methods with excellent spatial resolution and yielding a high degree of molecular information are thus required. In this presentation, we show how scanning near-field optical microscopy (SNOM) coupled with surface-enhanced Raman spectroscopy (SERS), a vibrational spectroscopy method, can be used to analyze chemical transformations at single catalytic sites [1].

The reaction we have chosen for study is the hydrogenation of benzene to cyclohexane taking place on a palladium catalyst, $C_6H_6 + 3H_2 \rightarrow C_6H_{12}$. A comprehensive set of Raman spectra was recorded for normal and deuterated benzene, cyclohexane, but also possible intermediates such as cyclohexene, 1,3-cyclohexadiene, and 1,4-cyclohexadiene, both for bulk liquids as well as for surface adsorbed compounds. This is important for unambiguous assignemnt of the reactands, intermediates, and products on the catalyst. The catalyst surface itself was produced by photolithographic etching, followed by metal deposition into the etched pitches [2]. This results in isolated, individually addressable metal grains on its surface. The grains consisted of silver (for enhancement of the Raman scattering) covered with a very thin layer of palladium (for catalytic activity). Near-field Raman spectroscopy was done with a spatial resolution in the 50 - 100 nm range, using a modified near-field instrument (Aurora, Veeco/Thermomicroscopes) and high optical throughput, etched aperture probes. It was possible to operate the entire set-up under reactive conditions.

The Raman spectra revealed the presence of surface bound molecular species that were chemically distinct from either the reactants or the products. A surprise was the discovery that even pure silver grains show some catalytic activity for benzene hydrogenation. A possible chemisorbed surface species formed by a Diels-Alder reaction was observed when 1,3-cyclohexadiene was adsorbed on the catalyst. Furthermore, this compound produced a fluorescent species on the nonreactive part of the support surface, whose spatial distribution was also imaged by SNOM. Finally, SNOM / Raman line scans over a single catalytic site reveal the spatial distribution of the SERS enhancement as well as the association of reactive intermediates with the catalytic sites.

References

[1] C. Fokas and V. Deckert, *Appl. Spectrosc.* **56**, 192 (2002)
[2] M. Schildenberger et al., *Catal. Lett.* **56**, 1 (1998)

Imaging ferroelectric domains by electro-optically modulated near-field microscopy

T. Otto, S. Grafström, F. Schlaphof, H. Chaib, and L.M. Eng,
University of Technology Dresden, Institute of Applied Photophysics, 01062 Dresden, Germany
otto@iapp.de , www.iapp.de

We report on a novel method for imaging domains in a ferroelectric crystal by means of electro-optical near-field microscopy, which makes use of the symmetry breaking induced by the electro-optic effect (see Fig. 1a). The sample is illuminated locally through a glass fiber tip while the transmitted power is collected with a microscope objective. The spatial contrast is due to the birefringence associated with the ferroelectric polarization. We exploit the electro-optic effect for modulating this birefringence by applying an alternating electric field between the tip (made conductive by a thin chromium layer) and the sample back electrode. This makes phase-sensitive detection applicable, providing a very high sensitivity. At the same time, the electro-optic modulation breaks the symmetry between antiparallel domains, thereby making such domains optically distinguishable. We show that the three-dimensional optical indicatrix orientation of a ferroelectric system may be obtained from one single image scan (see Fig. 1b). The resolution achieved at domain boundaries in $BaTiO_3$ was estimated to be about 250 nm. Note that this result applies for a tip having no additional aperture beside the fiber core. Therefore, the high resolution is determined by the small volume underneath the tip which is affected by the modulated electric field rather than the optical spot size. A simple theoretical model based on Fresnel's law together with the optical and electro-optical constants taken from the literature [2] is in good agreement with the experiment.

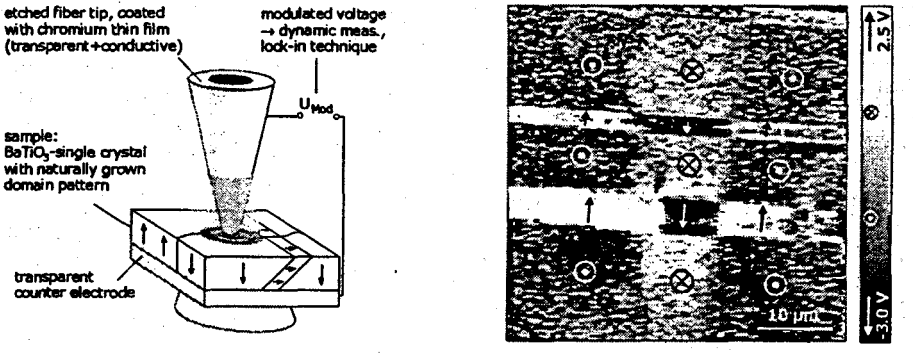

Figure 1:

(a) Principle of EO-SNOM. The optical properties are modulated by an alternating external electric field which leads to a modulation of the transmitted light intensity that is detected with its amplitude and phase.

(b) EO-SNOM image on a $BaTiO_3$ single crystal taken with a chromium-coated fiber tip (aperture equals approx. fiber core of d = 5µm). In addition to a- and c-domains, one can also clearly distinguish antiparallel a- and c-domains.

References

[1] T. Otto, Diploma Thesis, TU Dresden (2001).
[2] M. Zgonik, P. Bernasconi, M. Duelli, R. Schlesser and P. Günter, *Phys. Rev. B* **50**, 5941 (1994).

Photo-initiated Energy Transfer in Nanostructured Complexes Observed by Near-Field Optical Microscopy

Gregory A. Wurtz, Jasmina Hranisavljevic, Jin-Seo Im and Gary P. Wiederrecht,

Chemistry Division, Argonne National Laboratory, Argonne, Illinois 60439-4831.

Metallic particles of nanometric size manifest a variety of remarkable behaviors. Depending on whether these particles form semicontinuous films or well defined arrays they can show strong localization of electromagnetic modes or support controlled propagation of the light below the diffraction limit [1, 2]. Complex systems made from metallic nanoparticles are extensively used in spectroscopic techniques where they trigger non-linear effects as in surface enhanced Raman spectroscopy (SERS) leading to signal enhancement from adsorbed species of many orders on magnitude (10^4 is typical). Although little has been done to characterize the near-fields originally responsible for effects like SERS, it is clear that the ability to characterize optical fields produced by nanostructured objects is of primarily importance to comprehend, control, manipulate and eventually design devices or efficiently implement experiments based upon near-field interactions.

We report the characterization of the field distribution around metallic nanometer-sized particles using scanning near-field optical microscopy (SNOM). Special attention has been paid to the optical interaction between the particle and the J-aggregate from cyanine dyes adsorbed on the particle's surface. Comparing results obtained on bare particles and J-aggregate coated particles we show that the near-field contrast is sensitive to optically induced energy transfer occurring between the particle and the J-aggregates. For bare silver particles a large field enhancement is observed at a wavelength of 404 nm in TM polarization. Both distribution and intensity of the scattering pattern are interpreted to be the result of the contribution of the particle plasmon resonance to the diffracted field [3]. Near-field images reveal that this enhanced field is efficiently absorbed by the J-aggregates upon optical excitation of the particle's plasmon band. We will discuss our near-field observations on the bases of far-field time resolved measurements that suggest that a charge transfer follows optical absorption from the particle [4].

This work was supported by the Division of Chemical Sciences, Office of Basic Energy Sciences, U. S. Department of Energy under contract W-31-109-Eng-38.

References

[1] V. P. Drachev, W. D.Bragg, V. A. Podolskiy, V. P. Safonov, W-T. Kim,, Z. C. Ying, R. L. Armstrong and V. M. Shalaev, Journal of the Optical Society of America B **18**, 1896 (2001).

[2] M. Quinten, A. Leitner, J. R. Krenn, and F. R. Aussenegg, Optics Letters **23**, 1331 (1998).

[3] G. A. Wurtz, N. M. Dimitrijevic and G. P. Wiederrecht, Japanese Journal of Applied Physics **41**, L1331 (2002).

[4] J. Hranisavljevic, N. M. Dimitrijevic, G. A. Wurtz and G. P. Wiederrecht, Journal of the American Chemical Society, in press (2002).

Investigation of aperture SNOM levers fabricated by FIB patterning and wet chemical etching

J. Renger, S. Grafström, and L.M. Eng
Institut für Angewandte Photophysik, TU Dresden, D-01062 Dresden, Germany
renger@iapp.de, www.iapp.de

B. Schmidt and L. Bischoff, Forschungszentrum Rossendorf, D-01314 Dresden, Germany

B. Köhler, Fraunhofer Institut für Zerstörungsfreie Prüfverfahren - EADQ, D-01326 Dresden, Germany

Aperture probes for near-field optical microscopy are currently limited in tip geometry due to the etching process involved in the production of fiber tips [1] or the principal crystallographic planes when dealing with Silicon-based SNOM tips integrated into a microfabricated cantilever [2]. Also, the reproducibility in tip production is still small. Therefore, a novel concept for the micofabrication of aperture SNOM probes with user-defined shapes and aperture sizes has been proposed by Schmidt, Bischoff and Eng [3]. These tips are directly incorporated into a cantilever the properties of which may be varied in a broad range. We believe that these SNOM-levers will offer novel applications in biology and material science.

To produce such cantilevers with an integrated optical tip, focused ion beam (FIB) 3D-patterning was used to define both the tip and cantilever as a monolithic structure in the silicon substrate. By varying the ion dose of implanted Gallium (Ga) ions we are able to construct levers with various force constants at small cantilever lengths of < 20 μm (see Fig. 1a). A point-like FIB irradiation of Silicon leading to hole erosion by sputtering, allows us to produce tips having a truncated Gaussian shape of high aspect ratio (see Fig. 1b). Various forms are possible, including open and closed tips. This method allows to achieve hollow tips of less than 100 nm in diameter. The cantilever and tip structure predefined by Ga^+-FIB implantation and sputtering is subsequently etched in $KOH:H_2O$ solution to remove the surrounding, non-irradiated Silicon. Ga-doped areas are more resistant against the etchant during the wet anisotropic etching process [4] so that the SNOM lever finally is formed as a free-standing structure.

We present investigations of the mechanical and optical properties of the levers and the tips, respectively. The micromechanical cantilever structures with lateral dimensions of a few microns and a thickness of only some tens of nanometers were tested interferometrically to deduce their lowest mechanical resonance frequency which was found to be in the range of 0.5 to 5 MHz, depending on their lateral dimensions and the cross sectional shape. The corresponding spring constants range from 0.01 to ~1 N/m therefore offering the incorporation in many applications. For studying the optical properties the light transmission through as-constructed apertures within a flat extended support was investigated for different apertures and cone sizes.

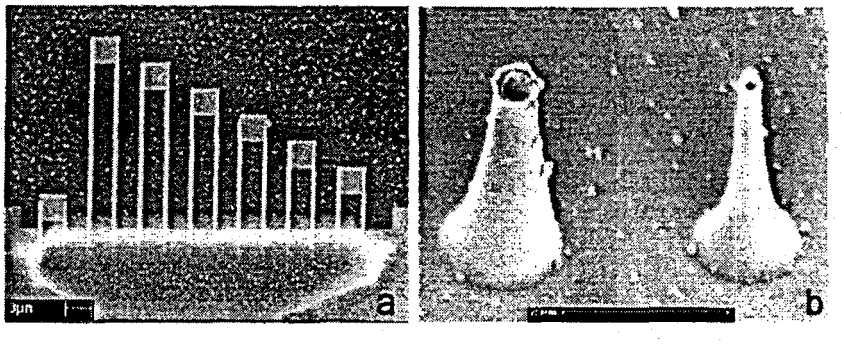

Fig. 1: (a) FIB microfabricated cantilevers of different sizes, and (b) hollow aperture tips of different shapes.

References

[1] R. Stöckle, C. Fokas, V. Deckert, B Sick, B. Hecht, and U.P. Wild, *Appl. Phys. Lett.* **75**, 160 (1999)
[2] Witec GmbH, Ulm (Germany), http://www.witec.de/snom.html
[3] Patentanmeldung 100 57 656.7 (21.11.2000)
[4] B. Schmidt, L. Bischoff, and J. Teichert, *Sensors and Actuators* **A 61**, 369 (1997)

Light Delivery for Heat Assisted Magnetic Recording

W. A. Challener, C. D. Mihalcea, K. R. Mountfield and K. Sendur
Seagate Technology, Pittsburgh, PA 15203

Storage densities of magnetic hard disc drives have exceeded 100 Gbpsi in the laboratory, corresponding to bit cell dimensions of 170 nm by 37 nm. The dimensions of the magnetic grains in each bit cell have also been reduced to maintain a sufficient signal-to-noise ratio. As grain size is reduced, the magnetic anisotropy of the grains must be correspondingly increased to maintain thermal stability of the magnetic state of the grain. The large anisotropies of these grains at the highest storage densities require recording fields near the limits available with conventional recording technology. To reach much higher densities one proposal[1] is to preheat the bit cell to reduce the anisotropy of the grains during recording.

Optical power densities for recording conventional magneto-optic media are on the order of 10 $mW/\mu m^2$. Heat assisted magnetic recording with a focused optical spot in the far field has been demonstrated at these optical power densities.[1,2] We are investigating techniques to deliver optical power with high efficiency to bit cells in the media with dimensions less than 50 nm.

Surface plasmon enhanced optical transmission through sub-wavelength holes[3] may be one method to obtain the required power densities. In one experiment a collimated laser beam at 660 nm was incident upon a 50 nm gold film through a glass substrate (Kretschmann configuration) in which there was a 10 x 10 array of holes in the gold film. The diameter of each hole was 50 nm and the angle of incidence was varied to excite the surface plasmon in the gold film. At resonance the intensity of the transmitted light was about twenty-five times larger than would be expected by the total cross sectional area of the hole array.

This work was performed under the support of the U.S. Department of Commerce, National Institute of Standards and Technology, Advanced Technology Program, Cooperative Agreement Number 70NANB1H3056.

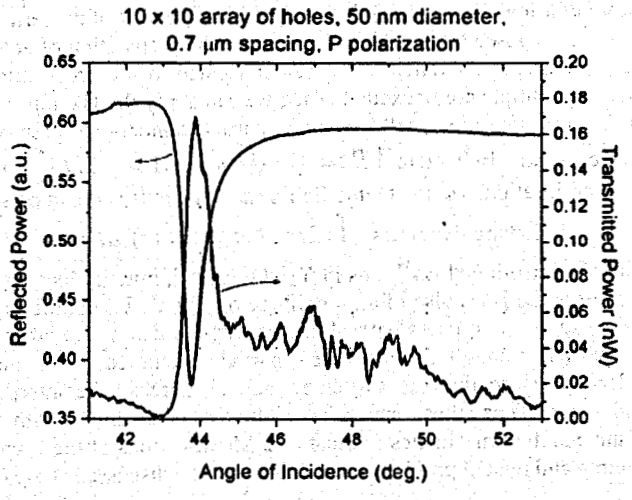

Figure 1: Optical power transmitted through an array of 50 nm holes in a gold film with a 50 nm thickness vs. angle of incidence at 660 nm wavelength .

References

[1] T. Rausch, J. Bain and T. Schlesinger, *Data Storage*, 16 (June, 2001).
[2] M. Alex, A. Tselikov, T. McDaniel, N. Deeman T. Valet and D. Chen, *IEEE Trans. Magn.* 37, 1244 (2001).
[3] H. F. Ghaemi, T. Thio, D. E. Grupp, T. W. Ebbesen and H. J. Lezec, *Phys. Rev. B* 58, 6779 (1998).

Scanning Near-field Optical Quantum Computer

S. K. Sekatskii, M. Chergui, G. Dietler, Institut de Physique de la Matière Condensée Université de Lausanne, BSP, CH 1015 Lausanne – Dorigny, Switzerland

An idea to use the Fluorescence Resonance Energy Transfer (FRET) between a single fluorescence center of the SNOM tip and the sample for the drastic improvement of the spatial resolution and other characteristics of Near-field Optical Microscopy has been introduced a few years ago [1], and recently the first FRET SNOM images were demonstrated [2]. Here we show that similar approach, when applied at liquid helium temperatures with the rare-earth dopant ions in crystals as the fluorescence centers, can be used for quantum computing, preparation of non local multiparticle entangled states and other experiments in the field of the quantum mecanics foundation [3].

It was earlier demonstrated that the transverse relaxation time T_2 (decoherence time) is close to the radiation decay time and lies in a micro- or even millisecond region for a number of rare-earth ions in crystalline matrices at liquid helium temperature. For example, the value T_2 = 2.6 ms was reported for the $^7F_0 - {}^5D_0$ transition of Eu^{3+} ion in Y_2SiO_5 crystal [4]. Under these circumstances FRET, which is usually completely incoherent and irreversible process, becomes a coherent and reversible one. (Indeed, coherent interactions have been already observed for doublet and quartet Nd^{3+} ions in CaF_2 crystal [5]). Electronic excitation flows between donor and acceptor back and forth with a period of $T_{FRET} = \pi\hbar^3 / \alpha\kappa d_D d_A$. Here $d_{D,A}$ are donor's and acceptor's dipole moments, r – distance between them and factors α, κ take into account relative orientation of the interacting dipoles and overlapping of their spectra. We show that for a typical case the characteristic Förster distance (at such a distance the FRET rate is the same as the donor's radiation decay rate) is equal to ~20 nm. Thus the parameters involved (time scale of a few microseconds and distance scale of a few nanometers) fall well within the reach of modern AFM/SNOM technology. Let us illustrate how the proposed approach can be used for the preparation of non local multiparticle entangled states [3]. First, one prepares excited donor center located in the probe microscope's tip apex; acceptor centers located in the sample are unexcited. Then we can apply the HV pulse onto the tip carrying piezo in such a manner that after its end we will have two - particle donor – acceptor system in any desired quantum state, including e. g. the Bell state $|B\rangle = (1/\sqrt{2})(|D^*A\rangle + |DA^*\rangle)$. Here asterisk denotes the electronic excitation location. To create this Bell's state, the pulse should be such that the donor – acceptor distance $r(t)$ has the following dynamics : $\int (2\alpha\kappa d_A d_D / \hbar^3(t))dt = \pi/2$; we name it $\pi/2$ – pulse. For example, for the aforementioned Eu^{3+} ions in Y_2SiO_5 crystal, initially located at the distance of 2 μm from each other, one needs the HV pulse of an amplitude of 199 V and duration of 20 μs to implement such a $\pi/2$ – pulse. Repeating this process with already entangled donor and other acceptors we will be able to prepare three – particle entangled states, four – particle entangled states, and so on. These states can be extremely nonlocal because there is sufficient time to increase the interparticle distance up to a few millimeters and more. Thus, these states have obvious connections with the experiments aiming the verification of the quantum mechanics foundations. Modifications of the proposed scheme can be used for quantum computing and related problems, which also will be discussed at the Conference.

References

[1] S. K. Sekatskii and V. S. Letokhov, *Appl. Phys. B.: Laser. Opt.* **63**, 525 (1996).
[2] S. A. Vickery and R. S. Dunn, *Biophys. J.* **76**, 1812 (1999); *J. Microsc.* **202**, 408 (2001); G. T. Shubeita, S. K. Sekatskii, G. Dietler and V. S. Letokhov, *Appl. Phys. Lett.* **80**, (2002).
[3] S. K. Sekatskii, M. Chergui and G. Dietler, *Phys. Rev. Lett.*, submitted.
[4] R. W. Equall, Y. Sun, R. L. Cone and R. M. Macfarlane, *Phys. Rev. Lett.* **72**, 2179 (1994).
[5] T. T. Basiev, V. V. Fedorov, A. Ya. Karasik, K. K. Pukhov, *J. Luminesc.* **81**, 189 (1999).

Near-field super-resolution effects of a ZnO nano thin film

Wei Chih Lin, Hsun Hao Chang, Yu Hsuan Lin, Yuan Hsin Fu, Din Ping Tsai
Department of Physics, National Taiwan University
Taipei, Taiwan 10617

Super-resolution near-field structure (super-RENS) was first reported by Tominaga et al. in 1998. They have successfully shown that a multi-layered structure of polycarbonate/SiN (170 nm)/Sb (15 nm)/SiN (20 nm)/$Ge_2Sb_2Te_5$ (15 nm)/SiN (20 nm) on a digital versatile disk (DVD) gives the estimated recorded marks of 90 nm at a constant linear velocity of 2.0 m/s. The carrier-to-noise ratio (CNR) can be more than 10 dB. Super-RENS is considered a more feasible way of the near-field optical recording with simple recording head design, less mechanic damage, and high recording speed.

We investigate the possibility of a new type near-field super-resolution optical structure, polycarbonate/ ZnS-SiO_2 /ZnO_x/ZnS-SiO_2 /$Ge_2Sb_2Te_5$/ZnS-SiO_2 . Figure 1(a) shows the structure of the new type super-RENS that we investigated. The active layer is a 15 nm ZnO_x thin film. The active layer of ZnO_x and recording layer of $Ge_2Sb_2Te_5$ are both the as-deposited thin films sputtered by a RF-reactive ion-sputter. The carrier-to-noise ratio (CNR) is obtained by using DVD optical disk tester from Pulstec Inc. (DDU-1000, wave length = 637 nm, NA = 0.6). Figure 1(b) shows the preliminary result of CNR values of various recorded mark size for the phase-change DVD disk consists of polycarbonate/ZnS-SiO_2/ZnS-SiO_2/$Ge_2Sb_2Te_5$/ZnS-SiO_2 and ZnO_x type super-RENS. The write power, erase power, bottom power, and the readout power are 5.8 mW, 0 mW, 0 mW, and 3 mW, respectively. The NA of objective is 0.6, and the wavelength of laser is 637 nm, the results of CNR clearly show the multi-layered thin film structure is feasible for the super-resolution beyond the diffraction limit.

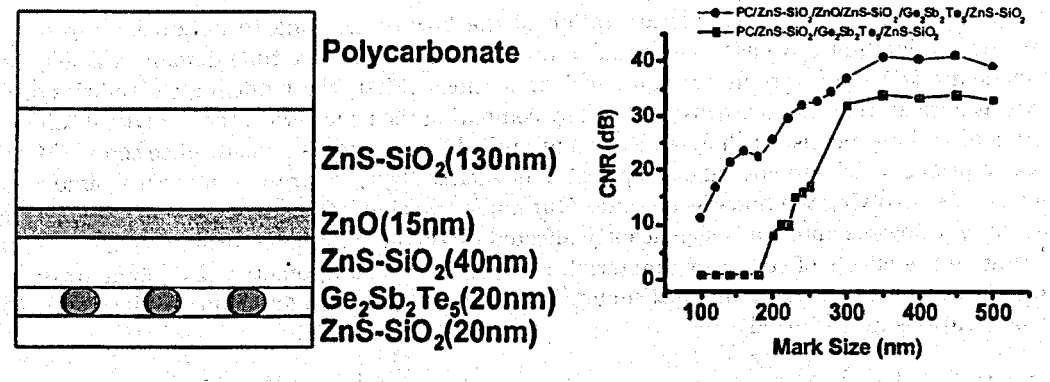

(a) (b)

Fig. 1(a) is the scheme of the structure of a new type super-RENS, polycarbonate / ZnS-SiO_2/ ZnO_x/ ZnS-SiO_2/$Ge_2Sb_2Te_5$ /ZnS-SiO_2. Fig 1(b) is the CNR values of various recorded mark size for the phase-change DVD disk and ZnOx super-RENS.

References

[1] J. Tominaga, T. Nakano, N. Atoda, Appl. Phys. Lett. **73**, 2078 (1998).
[2] D. P. Tsai and W. C. Lin, Appl. Phys. Lett. **77**, 1413 (2000).
[3] W. C. Liu, C.-Y. Wen, K.-H. Chen, W. C. Lin and D. P. Tsai, Appl. Phys. Lett. **78**, 685 (2001).
[4] Toshio Fukaya, Dorothea Buchel, Shunichiro Shinbori, Junji Tominaga,and Nobufumi Atoda, Din Ping Tsai and Wei Chi Lin, J. Appl. Phys. **89**, 6139(2001).
[5] W. C. Liu, D. P. Tsai, Phys. Rev. B (in press).

Near-field radiation efficiency of a bow-tie antenna in the presence of recording media

I. K. Sendur, W. A. Challener, Seagate Research, Pittsburgh, PA 15203-2116.

Conventional magnetic recording techniques will likely reach physical limits to storage density which are due to the super-paramagnetic effect. Some recent studies have investigated heat assisted magnetic recording (HAMR) to overcome this limit. The HAMR technique uses a focused optical beam from a laser to reduce the coercivity of the medium. For future storage densities, intense optical spots well below the diffraction limit are required in a HAMR system.

Recent advances in near-field optics suggest spatial resolution significantly better than the diffraction limit. We have investigated the bow-tie antenna as a near-field optical transducer which combines spatial resolution well-below the diffraction limit with transmission efficiencies approaching unity. Efficiency of this antenna was illustrated in the microwave region via laboratory experiments, and the possible application of this antenna at optical frequencies was discussed. Although the concept of using this antenna seems very promising, the underlying physics at optical frequencies is different and more complicated than the microwave region due to surface plasmon effects in metallic films. A verification of this performance at optical frequencies and a better understanding of the underlying physics is very desirable.

In a recent study, Oesterschulze et al. [1] proposed a high transmission probe based on a bow-tie antenna. They presented numerical simulations of various geometries involving hollow pyramidal silicon dioxide tips that are partly covered with aluminum resulting in a tilted bow-tie antenna. These simulations at optical frequencies illustrated improved transmission efficiencies for the new probe design compared to the conventional aperture tips.

In this study we investigate the possible utilization of the bow-tie antenna to obtain intense optical spots below the diffraction limit. We use commercially available finite-difference time-domain (FDTD) electromagnetic modeling (EM) software in our numerical simulations. First, the modeling capabilities of the FDTD software at optical frequencies are investigated by comparing the results with the analytical solutions of Mie scattering of various metals. Such a verification at optical frequencies is crucial, since some EM software makes assumptions which are not valid at optical frequencies. Next, we present numerical simulations for various geometries involving the bow-tie antenna. Our numerical simulations suggest that the near-field radiation pattern of a bow-tie antenna is significantly affected by the presence of recording media. Furthermore, we investigate the effects of composing material, frequency, antenna geometry, and configuration on the near-field radiation pattern using numerical simulations. Optical spot sizes and transmission efficiencies for various configurations are reported.

Acknowledgments

This work was performed under the support of the U.S. Department of Commerce, National Institute of Standards and Technology, Advanced Technology Program, Cooperative Agreement Number 70NANB1H3056.

References

[1] E. Oesterschulze, G. Georgiev, M. Muller-Wiegand, A. Vollkopf, and O. Rudow, *Journal of Microscopy* **202** 39 (2001).

Local Imaging of Photonic Structures: Image Contrast from Impedance Mismatch

G. W. Bryant,
National Institute of Standards and Technology, Gaithersburg, MD 20899-8423.
A. L. Campillo,
Department of Physics, University of Virginia, Charlottesville, VA 22903.
J.W. P. Hsu,
Bell Laboratories, Lucent Technologies, Murray Hill, NJ 07974.

Image contrast remains an ubiquitous issue for near-field optical microscopy. Local imaging of even the simplest photonic structures can produce surprising results that must be analyzed carefully to correctly identify the contrast mechanisms.

Photonic structures made from square arrays of air holes in SiN membranes are locally imaged by near-field scanning optical microscopy (NSOM) in illumination mode[1]. Holes with diameters smaller than and larger than the wavelength of light are investigated. Counterintuitively, holes appear dark and the film is bright in transmission images for both hole sizes. The contrast is opposite to the expectation based on film reflectivity. As shown in Fig. 1, finite-element calculations[1] of the NSOM transmission images of a single hole in a SiN film agree well with the experimental images. Surprisingly, the image contrast is determined almost entirely by how light is emitted by the tip. The film appears brighter than a hole in the NSOM image because more light is emitted from the tip when the film is imaged. Simulations of a tip above a thin uniform film show that the core flux, transmitted flux and reflected flux all have the same dependence on film index. The drastic increase in core flux when the tip is over a film results from the reduction in tip/air impedance mismatch when light in the tip core is forward focused out of the core by the high index film in front of the tip aperture.

This is an example in which contrast is a direct consequence of strong tip/sample coupling that modifies tip emission and is not a consequence of subsequent scattering of the tip field by the sample. These results lead to the remarkable conclusion that substantial increases in tip throughput can be achieved simply by blocking the tip aperture.

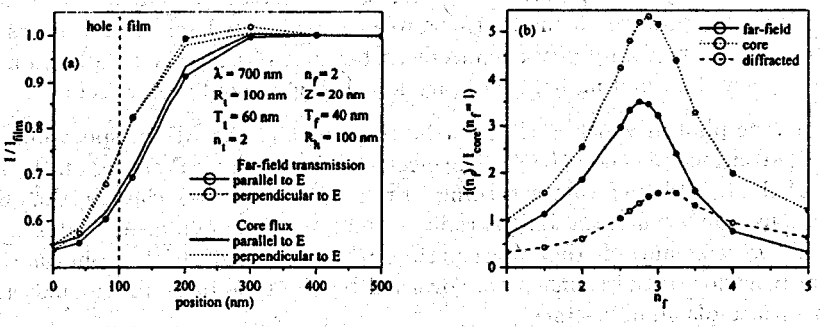

Figure 1: (a) The calculated NSOM transmission scan of a thin SiN film with a 100 nm radius hole and the calculated flux emitted from the core. Scans are parallel and perpendicular to the tip polarization. (b) Calculated dependence of the flux emitted by the tip core, transmitted to the far-field, and diffracted back around the tip on the index of a 40 nm uniform film placed 20 nm in front of the tip aperture.

References

[1] A. L. Campillo, J. W. P. Hsu and G. W. Bryant, *Optics Letters* **27**, 415 (2002).

Towards single-photon tunnelling

I.I. Smolyaninov, C.C. Davis,
University of Maryland, ECE Department, College Park, MD 20742.
A.V. Zayats,
Queen's University of Belfast, Belfast, BT7 1NN, UK.
A. Gungor,
Fatih University, Istanbul, Turkey.

Current progress in nanotechnology is based on such novel quantum electronic devices as single-electron transistors, quantum dots, quantum wires, etc. At the same time, there is a strong tendency to replace "slow" electronic devices with "fast" photonic ones. This drive is especially evident in the areas of computing and communication. Here we report strong evidence of a single-photon tunneling effect, a direct analogue of single-electron tunneling.

Classical realization of light tunneling is based on a glass surface illuminated in the total internal reflection geometry, e.g., using a prism. In this case, all incident light is reflected and only an evanescent field (exponentially decaying from the surface) exists over a smooth surface. If for example a tapered glass fiber is placed sufficiently close to the glass-air interface, the evanescent field is transformed into propagating waves in the fiber. Thus, optical tunneling through an air gap (which can be considered as a tunnel barrier) occurs.

If a nanometer-scale object exhibiting well defined localized electromagnetic modes is placed in the tunnel gap, tunneling from the sample into the fiber tip is facilitated at the frequency of tunneling photons which is in resonance with some localized optical mode of such object. Similar to single-electron tunneling, which is observed in systems in which tunneling electrons significantly modify the energy spectrum of local density of states (LDOS), tunneling photons can significantly modify the LDOS spectrum of a system exhibiting third-order nonlinear effects through local changes of the dielectric constant. As a consequence of the refractive index change, the polarizability and, therefore, the LDOS of the system are modified. Excitation of localized electromagnetic modes (in simple case, localized surface plasmons) may lead to very large local electromagnetic field intensity enhancement because of the very small volume of these modes, thus requiring a very low illuminating light intensity for observing nonlinear effects.

In this scenario, the photon which is close to the resonance of the LDOS spectrum tunnels through a barrier via a localized surface plasmon (LSP). The electric field of this LSP acting on the nonlinear material results in a shift of the LDOS spectrum according to the refractive index change, thus blocking tunneling of subsequent photons. Only when the LSP is radiated and after the nonlinear material is relaxed into its initial state, the LDOS resonance at this wavelength is recovered, and another photon can tunnel. Therefore, the temporal behavior of the tunneling is governed by the time of nonlinear material thermalization and the localized surface plasmon lifetime.

The measurements of light tunneling through individual subwavelength pinholes in a thick gold film covered with a layer of polydiacetylene provide strong evidence of single-photon tunneling. While the dependencies obtained for larger pinholes were linear, transmission of some small pinholes exhibited saturation and even staircase-like behavior. The experimental data has been fitted assuming the intensity dependent LDOS resonances analogous to the model described above. The fitting curves obtained with one and two intensity dependent local plasmon resonances show good agreement with the experiment. Single-photon tunneling effect may find many applications in the emerging fields of quantum communication and information processing and can be used for light manipulation in active elements of photonic circuits.

Optical Near Fields and the Degree of Polarization

T. Setälä, A. Shevchenko, M. Kaivola,
Optics and Molecular Materials, Helsinki University of Technology,
P. O. Box 2200, FIN-02015 HUT, Finland
A. T. Friberg,
Department of Microelectronic and Information Technology, Royal Institute of Technology,
Electrum 229, SE-164 40 Kista, Sweden

The degree of polarization is an important quantity for characterizing electromagnetic fields, as it describes the correlations that prevail between the orthogonal components of the electric field. Conventionally, the state of polarization of a fluctuating electromagnetic field is considered in terms of the 2×2 coherence matrix or the related four Stokes parameters. The two-dimensional formalism applies to fields having planar wavefronts, such as well-collimated and uniform optical beams or radiated wide-angle far fields, which can locally be considered as planar. However, the two-dimensional techniques are inadequate to describe the partial polarization of arbitrary fields and optical near fields, in particular.

For arbitrary electromagnetic fields, the 3×3 coherence matrix contains all information required to describe the partial polarization of the field [1]. Analogously to the 2D case, we expand the coherence matrix in terms of proper basis matrices, which we choose to be the Gell-Mann matrices or the eight generators of the SU(3) symmetry group. By doing so, the nine expansion coefficients are seen to have physical interpretations similar to those of the four Stokes parameters in the 2D formalism, and therefore, we may interpret the coefficients as the generalized Stokes parameters. Using this analogy with the 2D case, we are led to a formula for the degree of polarization, P_3, of three-dimensional fields [2, 3, 4],

$$P_3^2 = \frac{3}{2}\left[\frac{\mathrm{tr}\,(\Phi_3^2)}{\mathrm{tr}^2\,(\Phi_3)} - \frac{1}{3}\right] = \frac{1}{3}\frac{\sum_{j=1}^{8}\Lambda_j^2}{\Lambda_0^2}. \tag{1}$$

Here Φ_3 is the 3×3 coherence matrix, tr stands for the trace operation, and Λ_j $(j = 0...8)$ are the nine generalized Stokes parameters. From the first form of Eq. (1) we immediately see that the degree of polarization is invariant under unitary transformations, and thus, it is independent of the orientation of the orthogonal coordinate system. It can also be shown that the value Eq. (1) gives for the degree of polarization is bounded to the interval $0 \leq P_3 \leq 1$. More importantly, physical insight into the 3D degree of polarization can be gained by expressing P_3 explicitly in terms of the degrees of correlation, $|\mu_{ij}|$ $(i, j = x, y, z)$, between the orthogonal electric field components. It can be shown that [4],

$$P_3^2 \geq \frac{|\mu_{xy}|^2\phi_{xx}\phi_{yy} + |\mu_{xz}|^2\phi_{xx}\phi_{zz} + |\mu_{yz}|^2\phi_{yy}\phi_{zz}}{\phi_{xx}\phi_{yy} + \phi_{xx}\phi_{zz} + \phi_{yy}\phi_{zz}}, \tag{2}$$

where ϕ_{ii} $(i = x, y, z)$ stand for the diagonal elements of the coherence matrix, i.e., the intensities of the field components. Equation (2) states that the square of the degree of polarization is always greater than or equal to the average of the squared correlations weighted by the corresponding intensities. The equality holds for such an orientation for which the diagonal elements are the same. In that case, the square of the degree of polarization reduces to the pure average of the squared correlations. We emphasize that the dimensionality (2D vs. 3D) is a crucial issue as regards the quantitative value and the interpretation of the degree of polarization.

References

[1] C. Brosseau, *Fundamentals of Polarized Light: A Statistical Optics Approach*, Wiley, New York, 1998.

[2] J. C. Samson, *Geophys. J. R. astr. Soc.* **34**, 403 (1973); R. Barakat, *Opt. Acta* **30**, 1171 (1983).

[3] T. Setälä, M. Kaivola, and A. T. Friberg, *Phys. Rev. Lett.* **88**, 123902 (2002).

[4] T. Setälä, A. Shevchenko, M. Kaivola, and A. T. Friberg, *Phys. Rev. E*, submitted.

Giant Optical Transmission through a Sub-Wavelength Aperture

Tineke Thio, G.D. Lewen, K.M. Pellerin, R.A. Linke, NEC Research Institute, Princeton NJ 0854.

H.J. Lezec and T.W. Ebbesen, ISIS, Université Louis Pasteur, 67000 Strasbourg, France.

The transmission of light through an aperture in a metal film is very small when the aperture diameter d is smaller than the optical wavelength λ; deep in the sub-wavelength regime ($d<<\lambda$) the transmission T, normalised to the aperture area, is expected to scale as $T/f\sim(d/\lambda)^4$. The low throughput makes it difficult to use apertured probes for high-resolution applications which also require high intensities.

However, when the aperture is placed in a metal film which has periodic surface corrugations, the optical transmission can be enhanced by up to several orders of magnitude, and can be as large as $T/f=3$, that is, three times more light is transmitted than is directly impinging on the aperture, despite the fact that the aperture diameter is well in the subwavelength regime. [1]

The astonishingly high transmission efficiency is a consequence of a resonant interaction between the incident light and surface plasmon polaritons at the corrugated surface. The interaction is allowed by the periodic surface corrugation, and the resonant wavelengths are determined by the lattice constant of the corrugation, as well as the dielectric constant of the adjacent medium. The resonant wavelength is thus tunable.

Conversely, the single hole acts as a probe of the surface plasmon modes at the metal surface. The information we have gleaned about the surface plasmon modes have enabled us to optimise the surface corrugation geometry for maximum transmission enhancement through the central aperture. The structure with the highest transmission enhancement is a set of ring grooves around the central aperture, where the groove width is half the radial periodicity, and the groove depth is a few times the skin depth of the metal. Furthermore, we find that the light coupling into the hole is optimised when the shape of the aperture entrance matches that of the surrounding corrugation. The resolution of the device is determined by the exit diameter.

This phenomenon holds an immense potential for applications which require both high resolution and high throughput. This includes high-speed applications suh as high-density optical data storage, and NSOM of low-efficiency processes such as Raman scattering or non-linear optical effects.

References

[1] T. Thio, K.M. Pellerin, R.A Linke, H.J. Lezec and T.W. Ebbesen, *Optics Letters* **26**, 1972 (2001).

More information at http://www.neci.nj.nec.com/homepages/thio/

3D Electro-magnetic modeling of apertureless SNOM/AFM cantilever probes

L.Vaccaro, H. P. Herzig, R. Dändliker,
Institute of Microtechnology, University of Neuchâtel, Neuchâtel, Switzerland.

In spite of the significant progress observed in the fabrication of near-field probes, the procedure to obtain a smooth tip surface with a clear sub-100 nm aperture is expensive and time consuming. Recently, apertureless silicon cantilever-based probes for near-field scanning optical microscopy have been batch fabricated using micromachining technology [1]. The probes comprise a 25 μm quartz conical near-field tip on a silicon cantilever. Transmission electron microscopy reveals a 60 nm thick polycrystalline aluminum layer, that completely covers the quartz tip. Far-field measurements show the typical polarization properties of conventional SNOM aperture probes. An optical transmission of 10^{-5} has been measured in the far field and an excellent resolution is obtained in the near-field [2].

Numerical simulations have been performed to demonstrate that when the light is focused on the rear part of the cantilever a region of high intensity is localized at the tip apex. The study has been carried out using of a program that solves the Maxwell equations in integral form (MAFIA4, CST GmbH, Germany).

Three-dimensional modeling confirms the non-zero optical transmission. More specifically two non-degenerate hybrid modes, EH and HE, are propagating into the structure[1]. As displayed in the figure, the energy distribution plotted at different distances in the x-y plane above the apex shows a strong confinement of the field for EH modes. Its width will be discussed as a function of different geometrical parameters, such as cone angle, tip diameter etc. For the HE modes two very sharp peaks appear on the side of the tip apex. And, already at very short distance, they merge into the two giant lobes that are emerging from the side of the cone. These results correspond to the different behavior of s- and p-polarization in scattering of evanescent waves from subwavelength structures [3].

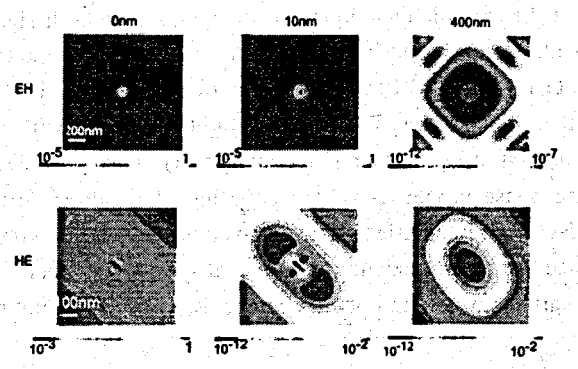

Figure 1: Field intensity plotted at different distances from the tip apex

The far field energy pattern calculated at 400 nm above the apex is in very good agreement with the experimental data for both modes (cf. [2]).

References

[1] G. Schürmann, W. Noell, U. Staufer, N. F. de Rooij, R. Eckert, J. M. Freyland, H. Heinzelmann, *Appl. Opt.*, **40**, 5040 (2001).

[2] R.Eckert, J.M. Freyland, H. Gersen, H. Heinzelmann, G. Schürmann, W. Noell, U. Staufer, N.F. de Rooij, *Appl. Phys. Lett.* **77**, 3695 (2000).

[3] O.J.F. Martin, C. Girard, A. Dereux , *J. Opt. Soc. Am. A* **13**, 1801 (1996).

[1] The first letter indicated which field is prevalent in the z-component.

Polarizing effects of near field probes determined by multiple heterodyne detection

P.Tortora, L.Vaccaro, R. Dändliker, H. P. Herzig,
Institute of Microtechnology, University of Neuchâtel, Neuchâtel, Switzerland.

Photon scanning tunneling microscopy [PSTM] has been recently used in many fields of optics to determine the evolution of electromagnetic waves in the near-field zone, revealing to be a reliable and sub-wavelength resolving technique. Many of the experiments involving PSTM have showed unexpected as well as unusual optical effects. In particular, PSTM has been recently used to study the propagation of the different modes within optical waveguides [1]. After exciting in the same waveguide TE and TM modes, an unexpected beat pattern was detected in the evanescent field at the waveguide-air interface. The same result has been reached employing a PSTM set-up integrated with a heterodyne technique [2], that allows simultaneous amplitude and phase measurement of the local optical field with subwavelength resolution. Here, phase mapping shows the appearance of phase singularities across the waveguide in correspondence with the beating locations. As reported by [3] we believe that the observed results are induced by the near field detection, with the fiber probe generally used in PSTM In fact, the polarization effects in the near field conversion by SNOM probes are not well understood [4]. In this framework it appears important to introduce the notion of vectorial optical transfer functions.

A new set-up will be presented, aiming the measurement of the vectorial near-field probe optical transfer function. It consists, basically, of a four beat signal heterodyne technique. In this new set-up both signal and reference beams contain TE and TM components of equivalent intensity. Every component of the two beams is modulated at a different frequency (ω_1.. ω_4) by means of four acousto-optic modulators. The tip of the fiber probe interacts in free space with the signal beam. The coupled light interferes with the reference signal producing four beat signals modulated at ω_i- ω_j (for i=1,2 and j=3,4). This provides a labeling that allows to distinguish amplitude and phase properties of the coupling, depending on the orientation between the E vector and the tip axis. By appropriate orientation of E-vector with respect to the tip axis we can determine the Jones matrix (and hence the transfer function) of the total system "tip-fiber".

We aim to exploit this method to determine the polarization state in optical near fields, information not yet experimentally accessible [5]..

References

[1] M. Balistreri, A. Driessen, J.P. Korterik, L. Kuipers, and N.F. van Hulst, *Opt. Lett.* **25**, 637 (2000).
[2] M. Balistreri, J.P. Korterik, L. Kuipers, and N.F. van Hulst, *Phys. Rev. Lett.* **28**, 294 (2000).
[3] B. Vohnsen, S. I. Bozhevolnyi, *Phys. Rev. Lett.* **87**, 259401 (2001).
[4] A.Nesci, R. Dändliker,M. Salt, H.P. Herzig accepted for publication in *Opt. Commun.* (2002).
[5] G. Lévêque, G. Colas des Francs, and C. Girard, *Phys. Rev. E* **65**, 036701 (2002).

Comparison of linear and second harmonic images of dielectric dots in near-field optical microscopy

*Thierry Laroche, Daniel Van Labeke**
Laboratoire d' Optique P.M. Duffieux
Université de Franche Comté
CNRS, UMR 6603
Institut des Microtechniques de Franche Comté
Route de Gray, 25030 Besançon,France
**Email :daniel.vanlabeke@univ-fcomte.fr*

Several groups have succeeded to performe near-field optical microscopy with non-linear processes. Their results are so encouraging that non-linear near-field microscopy could be a new tool to probe surfaces with a high lateral resolution.

In this paper we use a perturbative approximation of the Rayleigh method to compare the linear and non-linear (second harmonic) Scanning Near Field Optical Microscopy images. The sample is a two-dimensional grating of KDP dots. They are illuminated by external reflection and a SNOM image is obtained by a tip used in the collection mode. For the calculation, a plane wave expansion at the two frequencies, ω and 2ω are used in vacuum and in the sample. Then the boundary conditions are matched for the fields at ω which leads to the transmitted field. The second harmonics polarisation is thus deduced and we can calculate the near-field at 2ω.

Figures below show the images of the same square dot (10nm height, 200nm width) obtained with a near-field detection at ω and 2ω respectively. The images are very different.

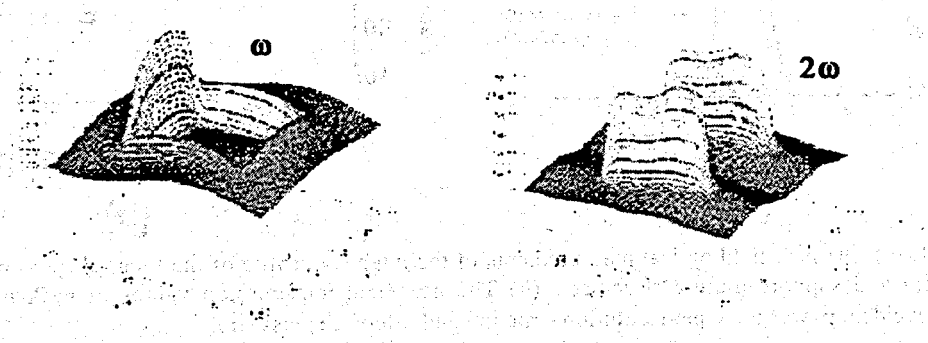

Figure: Near-field images of a KDP dot (10nm height, 200nm width) obtained in near-field microscopy at ω and 2ω. External illumination at 1064nm, SNOM in collection mode.

We will also discuss the influence of the various parameters on image formation and compare our results with other theoretical studies and experimental works.

References

[1] S.I. Bozhevolnyi, B. Vohnsen, K. Pedersen, *Opt. Comm.* 150 pp 49—55 (1998)
[2] Y. Shen, J. Swiatkiewicz, J. Winiartz, P. Markowicz, *Appl. Phys. Lett.* 77 pp2946-2948 (2000).
[3] A.V. Zayats, V. Sandoghdar, Opt. Comm. 178 pp245-249 (2000).
[4] D. Van Labeke, D. Barchiesi, *J.Opt. Soc. Am.* A9 pp 732-739 (1992)

Near-field optics using super-resolution near-field optical structures

D. P. Tsai, W. C. Lin, H. Y. Lin, F. H. Ho, H. H. Chang, Y. H. Fu, Y. H. Lin
Department of Physics, National Taiwan University, Taipei 106, Taiwan

Super-resolution near-field optical structure was first applied in the near-field recording by Tominaga et al.[1-2]. An active layer of Sb or AgO_x thin film was prepared along with a dielectric spacing layer to perform similar function of a fiber probe. However, the detailed mechanism of the active layer is still the key issue of the study and application of the super-resolution near-field optical structures[3-8]. In this paper, the near-field optics of the surface plasmons enhanced super-resolution near-field optical structures, substrate/ ZnS-SiO_2 (170 nm)/ AgO_x (15 nm)/ ZnS-SiO_2 (40 nm) or substrate/ ZnS-SiO_2 (170 nm)/ ZnO (15 nm)/ ZnS-SiO_2 (40 nm) have been studied theoretically and experimentally. Nonlinear near-field optical effects and enhencement of the near-field intensity were found. Fig. 1(a) is the near-field optical measurements of the intensity profile of the focused spot on a glass slip and a cover glass slip coated the super-resolution strucutre. A strong peak enhancement of the transmission intensity is clear shown. Fig. 1(b) displays the near-field transmission values of peak intensity at various incident power for a focused laser spot on both super-resolution structure and reference glass slip. The excited localized surface plasmons were proposed as the fundamental working mechanism of the super-resolution near-field optical structutres. Applications of the ultrahigh density near-field optical recording, nanolithography, and nanoscopy using various super-resolution near-field optical structutres demonstrate the novelty of this technique.

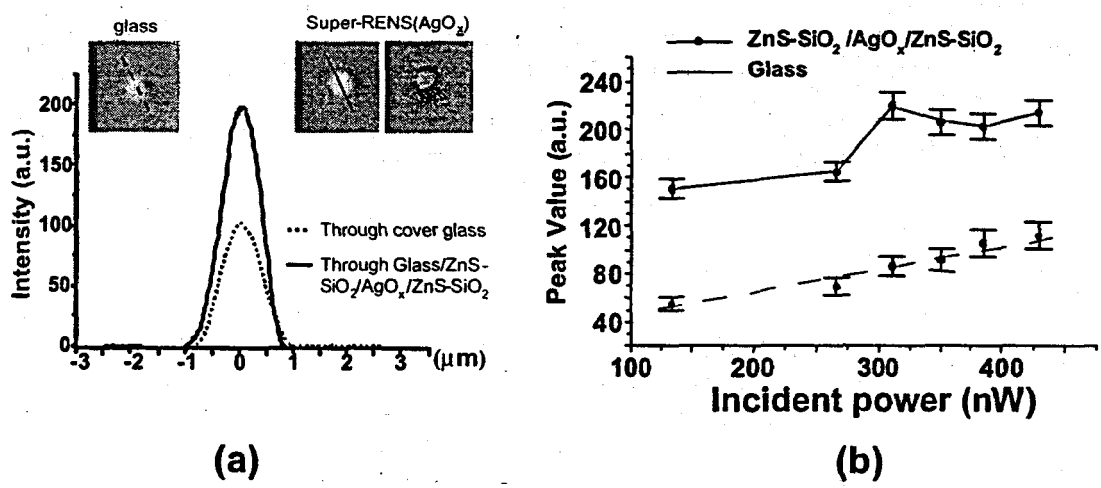

Figure 1. (a) The near-field optical measurements of the intensity profile of the focused spot on reference glass slip and super-resolution strucutre. (b) The near-field transmission values of peak intensity at various incident power for super-resolution structure and reference glass slip.

References

[1] J. Tominaga, T. Nakano, N. Atoda, Appl. Phys. Lett. **73**, 2078 (1998). H. Fuji, J. Tominaga, L. Men, T. Nakano, H.Katayama, and N. Atoda, Jpn. J . Appl. Phys., Part 1 **39**, 980 (2000).
[2] J. Tominaga, et al., Jpn . J. Appl. Phys., Part1 **40** 1831 (2001).
[3] D. P. Tsai, W. C. Lin, Appl. Phys. Lett. **77**, 1413 (2000).
[4] D. P. Tsai, et al., Jpn. J. Appl. Phys. **39**, part 1, No. 2B, 982 (2000).
[5] W. C. Liu, C. Y. Wen, K. H. Chen, W. C. Lin, D. P. Tsai, Appl. Phys. Lett. **78**, 685 (2001).
[6] T. Fukaya, D. Buechel, S. Shinbori, J. Tominaga, N. Atoda, D. P. Tsai, W. C. Lin, J. of Appl. Phys. **89**, 6139 (2001).
[7] F. H. Ho, W. Y. Lin, H. H. Chang, Y. H. Lin, W. C. Liu, D. P. Tsai, Jpn. J. Appl. Phys. **40**, pt. 1 no. 6A, 134 (2001).
[8] W. C. Liu, D. P. Tsai, Phys. Rev. B (in press, 2002).

Three Dimensional Simulation of Optical Waves in a Subwavelength- sized Aperture in a Thick Metallic Screen

Kazuo Tanaka, Mengyun Yan, and Masahiro Tanaka,
Department of Electronics and Computer Engineering of Gifu University, Yanagido 1-1, Gifu City Japan 501-1193

The interaction between an object and optical near-field in a subwavelength-sized aperture in the metallic screen is one of the fundamental physical processes in the near-field optics (NFO) [1]. So, the investigation of electromagnetic near-fields in a small aperture in a metallic screen is very important subject of NFO. Furthermore, three-dimensional (3D) analysis of electromagnetic fields in an aperture in a metallic screen is one of the fundamental problems in electromagnetic theory and has been treated in many papers such as famous Bethe's paper [2, 3] so far. However, most of the papers treated the case where the screen is the perfect conductor that is infinitely thin or that has finite thickness. In this paper, diffraction of optical waves by a subwavelength-sized aperture in a thick metallic (dielectric of complex permittivity) screen is simulated by the 3D volume integral equation. We consider the scattering problem as follows: A small square-shaped aperture whose area is given by $a_x \times a_y$ is made in the thick metallic screen (slab) with thickness w. The size of metallic screen is infinite and its relative complex-valued permittivity is given by ε_1. The optical plane wave is assumed to be incident from the region below the metallic screen shown. We solve the problem by using the volume integral (Lippman-Shwinger) equation. Since the size of the metallic screen has infinite size, the original form of the volume integral equation cannot be used. We derive the new form of the integral equation by which we can treat the problem as that the screen has a finite size. Descretizing the integral equation by the conventional method, we employed the Generalized Minimum Residual Method (GMRES) with fast Fourier transformation (FFT) in order to solve the system of the simultaneous linear equations. We can treat the problem that has about a million unknowns by this technique with conventional PC. Numerical results were confirmed by using the reciprocity relation. The parameter of the problem is given by as follows: the wavelength is $\lambda = 488nm$ incident angle is $\theta_i = \varphi_i = 0.0$ (vertical incidence), incident electric vector $\mathbf{E_i(x)}$ is parallel to the x-axis, aperture size is about $a_x \times a_y \approx 0.190.19$ wavelength (about 9393 nm). and complex permittivity of the metallic screen is given by ε_1=-7.38- j7.18 (silver). We show examples of distributions of total electric near-fields on the aperture are given in Fig. 1 for various shapes of the aperture.

Figure 1: Total electric near-field distributions on the (a) square-shaped, (b) circular-shaped and (c) triangular-shaped aperture in a metallic screen of silver ($\varepsilon_1 = -7.38 - j7.18$). Three areas of apertures are nearly same. The thickness of the metallic screen is $w \approx 0.3$ wavelength (about 147 nm). Electric vector of the incident wave is horizontal direction (λ=488nm).

References

[1] E. Betzig and R. J. Chichester, *Science* **252**, 1422 (1993)

[2] H. A. Bethe, *Phys. Rev* **252**, 163 (1944)

[3] C. J. Bouwkamp, *Rep. Prog. Phys* **1**, 35 (1954)

Near-field nano-ellipsometer for ultrathin film characterization

Qiwen Zhan and James R. Leger
Department of Electrical and Computer Engineering, University of Minnesota
200 Union Street SE, Minneapolis, MN 55455

Abstract

We describe a near-field ellipsometer for accurate characterization of ultrathin dielectric films. Optical tunneling through dielectric films mimics the absorption in metallic films, enabling accurate measurement of the index of refraction of dielectric film in the ultrathin regime. The possibility of achieving a refractive index resolution of 0.001 for films as thin as 1 nm is shown by regression modeling. A solid-immersion nano-ellipsometer that incorporates this near-field ellipsometric technique with a solid-immersion lens is constructed. Experimental results are included to demonstrate the viability of this technique. Such a nano-ellipsometer can accurately characterize thin films ranging in thickness from sub-nanometer to microns with transversal resolution on the order of 100 nm.

Resonance shift effects in apertureless scanning near-field optical microscopy

J.A. Porto [1], *P. Johansson* [2], *S.P. Apell* [1], *and T. López-Rios* [3]
[1] *Department of Applied Physics, Chalmers University of Technology and Göteborg University, S-41296 Göteborg, Sweden*
[2] *Department of Natural Sciences, University of Örebro, S-701 82 Örebro, Sweden*
[3] *Laboratoire d'Etudes des Propriétés Electroniques des Solides, (LEPES/CNRS), BP 166, 38042 Grenoble Cedex 9, France*

Scanning near-field optical microscopy (SNOM) [1] has attracted considerable attention as a technique to obtain optical images of objects with subwavelength resolution. One of the most promising techniques is apertureless SNOM, where light is focused at the tip of a scanning probe microscope (SPM) and the field enhancement near the tip is used to obtain subwavelength resolution. In this work we consider a metallic apertureless tip and a metallic surface and study the effects associated with the shift in energy of the resonances of the tip-surface system as the tip approaches the surface.

The tip is modeled with a finite-size sphere, whose radius corresponds approximately to the radius of curvature of the real tip. The main features of the theory employed are: (i) retardation effects are included, (ii) higher multipoles of the sphere are taken into account, and (iii) the multiple scattering between the sphere and the surface is considered [2].

A main result is that the maximum of the signal (far-field scattered intensity) as a function of the tip-surface distance may appear at much larger distances than the maximum of the local-field enhancement, contrary to what is sometimes assumed. In some cases, the maximum of the signal appears at tip-surface distances of 10 nm while the maximum local-field enhancement is at a tip-surface distance of approximately 1 nm (see Fig. 1). Different multipoles are responsible for each maximum: the maximum of the signal is associated with lower multipoles while the maximum of local-field enhancement is associated with much higher multipoles. This behavior is associated with the shift in energy of the resonances of the coupled system tip-surface as the tip approaches the surface.

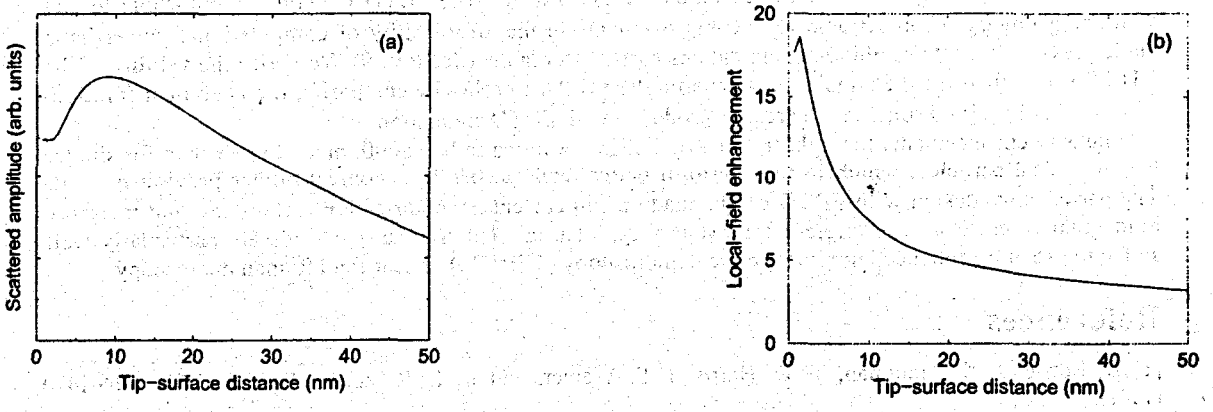

Figure 1: Scattered far-field amplitude (a) and local-field enhancement (b) as a function of the tip-surface distance for a gold tip and a gold surface for a photon energy of 2.4 eV.

References

[1] M. A. Paesler and P. Moyer, *Near-Field Optics: Theory, Instrumentation, and Applications* (Wiley, 1996).

[2] P. Johansson, S.P. Apell, and D.R. Penn, *Phys. Rev. B* **64**, 054411 (2001).

Design of near-field optical probes with high field enhancement by finite difference time domain electromagnetic simulation

John T. Krug, II, Erik J. Sánchez, and X. Sunney Xie
Harvard University Department of Chemistry and Chemical Biology, Cambridge, MA 02138

Aperture near-field scanning optical microscopy (NSOM) provides a means for generating sub-diffraction limited optical images. (See Ref's. 1-3.) This technique typically utilizes aluminum coated, tapered optical fibers as imaging probes. The finite skin depth of metals at optical frequencies, however, places a fundamental limit on the spatial resolution obtainable with these probes (~30 nm). This fundamental limitation is aggravated by several practical problems with the aperture approach, including probe heating, low power throughput, and difficulty in probe preparation.

Shortly after the development of the mature aperture NSOM technique, a number of groups began work on means of generating near-field images with apertureless probes. (See Ref's. 4-6.) Early apertureless NSOM experiments utilized the probe as an elastic scattering center, and the signal was detected at the excitation frequency in the far field. The complex dependence of the far-field signal on the topographic features of the sample renders interpretation of image contrast extremely difficult. Unlike these approaches, our new approach uses the apertureless probe to provide a highly localized excitation source for a particular molecular transition. (See Ref. 7.) The spectroscopic response of the sample, such as fluorescence, Raman or nonlinear response, provides an optical signal at a frequency different from that of the excitation, and is detected in the far field. This approach generates images that are relatively simple to interpret at resolutions better than ~20 nm, though it requires very large field enhancements that can only be achieved with well-tailored probe geometries.

We report the three dimensional electromagnetic simulation of gold nanoparticles with specific geometries as a means to the rational design of apertureless NSOM probes. (See Ref. 8.) Analytical solutions for field enhancement by spheroidal particles are used to provide physical insight for probe design. These solutions indicate that probes need to be not only sharp, but also finite in length in order to generate the highest field enhancement. Finite difference time domain (FDTD) simulations of gold particles illuminated by near infrared radiation are performed. The FDTD method is applicable to any arbitrary geometry of object, and recent improvements in the affordability of computational power have made previously cost-prohibitive computations easily affordable. (See Ref. 9) We verify the validity of the 3-D FDTD method for the simulation of apertureless NSOM probes by comparing the analytical solutions of scattering by a gold sphere to the results produced with FDTD simulation.

Intensity enhancements for right trigonal pyramids are found to be ~8000, much higher than for similar length conical particles, which in turn perform better than quasi-infinite conical probes previously used. The particles we design with FDTD can be made using current nanofabrication techniques, and therefore hold great promise as apertureless NSOM probes. These right trigonal pyramids are particularly well suited to use in tip enhanced nonlinear optical microscopy (TENOM) or near-field Raman microscopy.

References

[1] E. Betzig, J. K. Trautman, T. D. Harris, J. S. Weiner, and R. L. Kostelak, *Science* **251**, 1468-1470 (1991).
[2] D. W. Pohl, W. Denk, and M. Lanz, *Applied Physics Letters* **44**, 651-653 (1984).
[3] A. Lewis, M. Issacson, A. Harootunian, and A. Murray, *Ultramicroscopy* **13** (1984).
[4] S. Kawata and Y. Inouye, *Ultramicroscopy* **57**, 313 (1995).
[5] W. Denk and D. W. Pohl, *Journal of Vacuum Science and Technology, B* **9**, 510-13 (1991).
[6] F. Zenhausern, Y. Martin, and H. K. Wickramasinghe, *Science* **269**, 1083-5 (1995).
[7] E. J. Sanchez, L. Novotny, and X. S. Xie, *Physical Review Letters* **82**, 4014-4017 (1999).
[8] J. T. Krug, II, E. J. Sanchez, and X.S. Xie, *Journal of Chemical Physics*, In press.
[9] K.S. Kunz and R.J. Luebbers, *The Finite Difference Time Domain Method for Electromagnetics* (CRC press, Boca Raton, Florida, 1993).

CASSE Formation and Operating Characteristics of high resolution Aperture SNOM Probes

J. Toquant, A. Bouhelier, and D. W. Pohl}*
Institute of Physics, University of Basel,
Klingelbergstrasse 82, CH-4056 Basel, Switzerland

Controlled all solid state electrolysis (CASSE) allows to open and close apertures at the apex of silver-coated SNOM probes with high precision and reproducibility[1,2]. We integrated this technique into a standard SNOM, the probe being mounted in imaging position. A small part of the sample stage is reserved for the solid electrolyte. Control of light transmission during formation provides a measure for the aperture size. The opening process is stopped at a predetermined level of transmissivity (Fig.1 lhs.).

Immediately after formation, the probe is ready for imaging: The sample stage just has to be transferred from the electrolyte position to the sample position. This minimizes corrosion effects of the metal coating and avoids risky manipulations after aperture formation. The SNOM images obtained so far provide resolution in the 40 nm range with good contrast and reproducibility.

Deteriorations of the aperture after extended usage usually can be repaired by returning to the electrolytic formation position. Inversion of the electrolytic process results in deposition of silver at the tip apex and subsequent closure of the aperture (Fig.1 rhs.). It turned out that the deposition process is less well controllable than that of removal. However, there is no need to stop it at a well defined aperture size. Instead, after complete closure, the aperture can be re-opened by the readily controllable removal process. The repair capability greatly facilitates SNOM imaging studies since aperture deterioration no longer implies complete interruption and time-consuming re-mounting procedures.

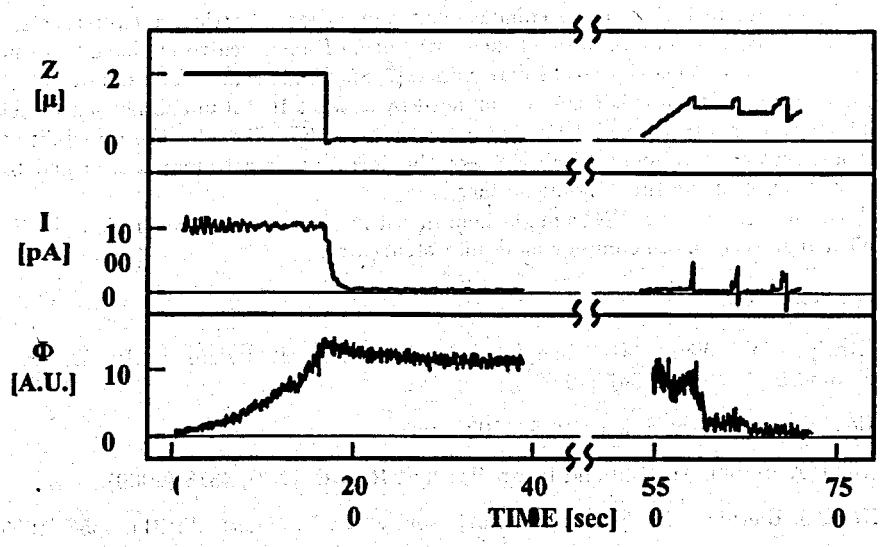

Fig.1: 'z-piezo' extension, current through electrolyte (I) and light flux through aperture probe (Φ) during aperture formation (left: opening, right: closing)

[1] D. Mulin, D. Courjon, J-P. Malugani, B. Gauthier-Manuel, Appl. Phys. Lett., **71**, 437 (1997).
[2] A. Bouhelier, J. Toquant, H. Tamaru, H.-J. Guntherodt, D.W. Pohl and G. Schider, Appl. Phys. Lett., **79**, 683 (2001).

* Present address: University of Rochester, The Institute of Optics, Wilmot Building, Rochester, NY 14627.

Near-field Raman spectroscopy using a sharp metal tip

A. Hartschuh, N. Anderson, L. Novotny,
University of Rochester, The Institute of Optics, Rochester, NY 14627.

Combined with near-field techniques, Raman spectroscopy is a promising tool for identifying and analyzing the molecular composition of complex materials, providing spatially resolved chemical maps with nanoscale resolution. Basic drawback of Raman methods is the comparatively low scattering cross-section precluding the detection of single scatterers. However, this drawback can be overcome using surface enhanced raman scattering (SERS). SERS has been shown to provide enormous enhancement factors of up to 10^{15} allowing for Raman spectroscopy even on the single molecule level [1, 2].

Despite all the activity in SERS, questions concerning the basic mechanisms still remain. It is accepted that the largest contribution stems from enhanced electric fields at metal surfaces amounting up to 10^{11} - 10^{12} [3]. But, in order to explain the reported factors of 10^{15}, additional mechanisms, e.g. chemisorption and charge transfer induced resonance Raman, have to be involved. The electric field enhancement factor critically depends on the details of the surface structure, e.g. metal particle size and shape, as well as on the respective polarization direction of the incident light field. Whereas single spherical particles produce rather weak signals, dimer configurations with light fields polarized along the long dimer axis appear to be important [2, 3, 4].

By placing a laser illuminated tip over a particle film, we mimic these configurations and limit SERS to the area close to the tip position. A focused Hermite-Gaussian (1,0) beam is used to produce a longitudinal electric field along the tip axis, which is required for field-enhancement [5, 6]. While raster scanning the sample, the topography and Raman signals are recorded simultaneously.

In order to evaluate the resulting enhancement factors for a particular tip-particle configuration, the exact number, position and orientation of the contributing Raman scatterers have to be known. In the case of dye molecules, this can usually not be determined [7, 8]. Single-wall carbon nanotubes (SWNTs) render a characteristic Raman signal which can be enhanced by at least 10^{12} if in contact with fractal silver colloidal clusters [9]. Furthermore, the well defined size and shape of SWNTs offer the possibility to simultaneously localize single scatterers topographically, detect the corresponding Raman signal and to characterize the topographic features of the surrounding surface.
The results of our studies on SWNTs might help in optimizing metal tip controlled SERS, thus allowing for the chemical analysis of more complex molecular structures.

References

[1] K. Kneipp, Y. Wang, H. Kneipp, L.T. Perelman, I. Itzkan, R.R. Dasari and M.S. Feld, Phys. Rev. Lett. **78**(9), 1667 (1997).

[2] S. Nie and S.R. Emory, Science **275**, 1102 (1997).

[3] H. Xu, J. Aizpurua, M. Käll and P. Apell, Phys. Rev. E **62**(3), 4318 (2000).

[4] H. Xu, E.J. Bjernfeld, M. Käll and L. Börjesson, Phys. Rev. Lett. **83**(21), 4357 (1999).

[5] E.J. Sanchez, L. Novotny and X.S. Xie, Phys. Rev. Lett. **82**, 4014 (1999).

[6] L. Novotny, M.R. Beversluis, K.S. Youngworth and T.G. Brown, Phys. Rev. Lett. **86**(23), 5251 (2001).

[7] R.M. Stöckle, Y.D. Suh, V. Deckert and R. Zenobi, Chem. Phys. Lett. **318**, 131 (2000).

[8] N. Hayazawa, Y. Inouye, Z. Sekkat and S. Kawata, Chem. Phys. Lett. **335**, 369 (2001).

[9] K. Kneipp, H. Kneipp, P. Corio, S.D.M. Brown, K. Shafer, J. Motz, L.T. Perelman, E.B. Hanlon, A. Marucci, G. Dresselhaus and M.S. Dresselhaus, Phys. Rev. Lett. **84**(15), 3470 (2000).

Enhanced photoisomerization and light induced mass-transport in the near-field of irradiated metallic nano-objects

*P. Karageorgiev *, B. Stiller, L. Brehmer*
Physics of Condensed Matter, Institute of Physics, University of Potsdam
P.O. Box 60 15 53, 14415 Potsdam, Germany.

Photoexcitation of chemical reaction with resolution below the diffraction limit can be achieved in the far-field using a two-photon reaction activated by diffraction-limited laser-spot, or in the near-field using a sub-wavelength aperture. We present an alternative method based on interaction of light with a conductive nano-object.

The illumination of metallic nano-particle causes a strongly localized electromagnetic field close to the particle (i.e. near-field). Depending on the light wavelength and on the material and shape of the particle, the intensity of the near-field can be 10^5 higher than the irradiating intensity. The photoexcitation of organic molecules by such an extremely enhanced near-field have been experimentally observed through surface-enhanced Raman scattering, luminescence and second harmonic generation. As the photoexcitation is the first step of any photochemical reaction, one might expect that the subsequent interstate crossing of suitable molecules in the vicinity of illuminated metallic nano-object would be also enhanced. In other words, the enhanced near-field could be used to achieve a strongly localized photochemical reaction.

To check out this assumption we used azobenzene-containing polymers which can undergo reversible isomerization under illumination of specific spectral band. During photoisomerization an electron density redistribution takes place causing a change in both the magnitude and direction of the molecular dipole moment. Since in the sample the azogroups were noncentrosymmetrically oriented along the normal to the substrate, the changing normal component of the dipole moment caused a change of a surface potential which was detected by Scanning Kelvin Microscope (SKM).

It was found, that a strongly localized change of the surface potential occurred when a conductive SKM tip was scanned a fixed distance from the surface (noncontact mode) while simultaneously irradiating the sample with light of low intensity at definite wavelength. The magnitude of the photoinduced change of the surface potential had a significant maximum at ca. 11 nm tip-surface distance. No alterations in topography were observed.

We rank the experiment described above to the first example of artificially enhanced photo-isomerization in the vicinity of illuminated metallic nano-object.

The further development of this method is excitation of photoprocess taking place solely in the near-field of the illuminated object. Light-induced mass-transport effect (molecular migration) which occurs in some azobenzene-containing systems under the influence of light intensity gradient was used for this purpose. Since at uniform illumination of a surface with deposited nano-particles the light intensity gradient exists only near to the particles, one might expect that azo-molecules will migrate solely in the vicinity of the particles.

It was found, that after illumination, a knolls arise around gold nano-particles deposited on the surface of azobenzene-containing film. The angular distribution of the matter in the circular knolls depends on the polarization of the light, as well as on the distance between the particles. Presumably the coupling of the plasmons in nearby particles influences the knolls shape.

* Corresponding author. E-mail: ppkara@rz.uni-potsdam.de

Detection of an Adenine Molecule by Tip-Enhanced Raman NSOM

S. Kawata[1,2,3,4] Y. Ishida[1], H. Watanabe[1,5], N. Hayazawa[1,3], and Y. Inouye[2,4,6]
1) Osaka University, Department of Applied Physics, Suita, Osaka 565-0871, Japan
2) Handai FRC, Suita, Osaka 565-0871, Japan
3) RIKEN, Wako, Saitama, 351-0198, Japan
4) CREST, Japan Science and Technology Corporation, Japan
5) Fuji Photo Film Co., Minami-ashigara, Kanagawa 250-0193, Japan
6) Osaka University, School of Frontier Bioscience, Suita, Osaka 565-0871, Japan

When a laser beam is focused at a metallic probe tip located in the near field of sample molecule, plasmon polariton is excited at the probe tip to generate confined strong photon field, resulting in the giant amplification of photon scattering [1,2]. If the molecule is Raman active, the spectral shift is detected due to the molecular vibration [3-5]. In this presentation, we show our experimental result of Raman spectrum of a DNA-base Adenine molecule, detected by the metallic probe tip. The probe is a Silicon Nitride AFM cantilever, coated with 30nm-thick silver film. The excitation light source is a frequency-doubled Nd:YVO4 laser. The light beam is focused by a high NA objective lens (NA~1.4) through an annular aperture (NA>1) to form an evanescent spot in the sample film [6]. The probe scans in this evanescent spot to form an image of the molecular distribution as a spectral map. A cooled CCD images a spectrum dispersed by the grating spectrometer with a notch filter at every position of the sample.

Figure 1 (a) shows the detected Raman spectrum of Adenine nanocrystal. Height of the nanocrystal is 7 nm and width is 30 nm. A quite few number of spectral lines are observed, as marked by arrows, when the probe tip is near enough to the sample (AFM operation is made in contact mode). These lines except the one at 924 cm^{-1} are assigned as the vibrational modes, inherent to Adenine molecule, according to the molecular orbital calculation. For examples, two majors lines, one at 739 cm^{-1} and the other 1328 cm^{-1} are the ring breathing mode and combination of C-N stretching mode and C-C stretching mode. Figure 2 shows the structural formula.

The line 924 cm^{-1} is assigned as a line of glass substrate. This was proved from the experimental result shown in Fig. 1 (b), which is the same as Fig. 1 (a) except that measurement was made when the tip is far from the sample. This result indicates not only that the lines except 924 cm^{-1} are all due to the Raman scattering by Adenine molecule located near the probe tip, but also that the Raman spectrum is detected only when the probe is in the near field of the molecule of interest, otherwise the photon field is not enhanced to scatters Raman-shifted photons.

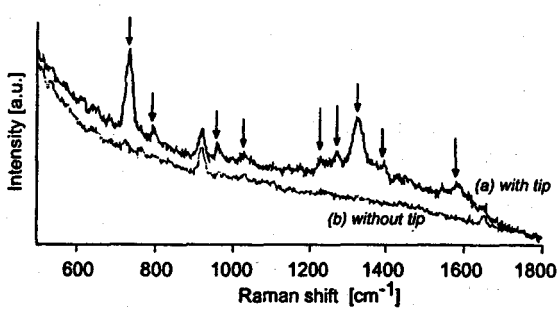

Figure 1: Raman spectra of adenine molecules obtained (a) with a tip and (b) without tip.

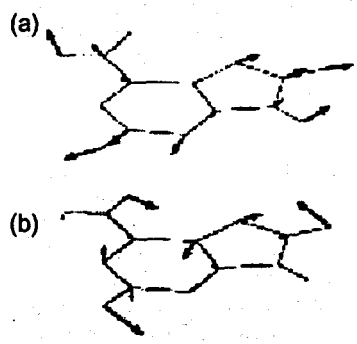

Figure 2: Vibrational modes of adenine at (a) 739 cm^{-1} and (b) 1328 cm^{-1}

References

[1] Y. Inouye and S. Kawata, *Opt. Lett.* **19**, 159 (1994).
[2] S. Kawata ed., Near-field Optics and Surface Plasmon Polariton, (Springer-Verlag, Berlin Heidelberg, 2001).
[3] Y. Inouye, N. Hayazawa, K. Hayashi, Z. Sekkat and S. Kawata, *Proc. SPIE* **3791**, 40 (1999).
[4] N. Hayazawa, Y. Inouye, Z. Sekkat, and S. Kawata, *Opt. Commun.* **183**, 333 (2000).
[5] N. Hayazawa, Y. Inouye, Z. Sekkat, and S. Kawata, *Chem. Phys. Lett.* **335**, 369 (2001).
[6] N. Hayazawa, Y. Inouye and S. Kawata, *Journal of Microscopy* **194**, 472 (1999).

Fabrication of 25-nm Zn Dot with Selective Photodissociation of Adsorption-phase Dietylzinc by Optical Near Field

T. Yatsui,[a] M. Ueda,[b] Y. Yamamoto,[b] T. Kawazoe,[a] M. Kourogi,[a,b] and M. Ohtsu[a,b]
a) ERATO, Japan Science and Technology Corporation, Machida, Tokyo, 194-0004, Japan.
b) Interdisciplinary Graduate School of Science and Engineering, Tokyo Institute of Technology, Yokohama, Kanagawa, 226-8502, Japan.

For realizing nanometer-scale photonic devices and their integration, it is required that nanometer-scale structures are fabricated with nanometric precision. To meet this requirement, we have realized fabrication of 60-nm scale Zn dots with photodissociated gas-phase diethylzinc (DEZn) by optical near field [1]. However, the migration of dissociated Zn limits the lateral size. To overcome this difficulty, we report here successful fabrication of nanometer-scale Zn dot by two-step process; nanometer-scale nucleation and selective deposition on prenucleated Zn with photodissociation of adsorption-phase DEZn by optical near field.

The fiber probe used for photodissociation by optical near field was a sharpened UV fiber probe with an apex diameter of 30 nm. For selective photodissociation of adsorption-phase DEZn, we used He-Cd laser (325 nm) as a light source, because gas-phase DEZn is absorbed hardly at $\lambda > 300$ nm and the absorption spectrum of adsorption-phase DEZn is red-shifted with respect to that of gas-phase [2]. Furthermore, since the extent of molecular adsorption on Zn is larger than that on a substrate [3], the selective growth of adsorption-phase DEZn on prenucleated Zn is expected. As a comparison, the second harmonic of Ar^+ laser ($\lambda = 244$ nm) was used as a light source that resonates the absorption band of gas-phase DEZn. The separation between fiber probe and sapphire substrate was kept within several nanometers by shear-force feedback technique. During deposition, the partial pressure of DEZn was 10 mTorr.

Figures 1(a) and 1(b) show the topographical images of deposited Zn using $\lambda = 325$ and 244 nm, respectively. In Fig. 1(c), the solid and dashed curves are the respective cross sectional profiles through the Zn dots deposited at $\lambda = 325$ and 244 nm. The dashed curve has tails both sides of the peak. These tails correspond to the Zn deposited by photodissociation of gas-phase DEZn. However, the solid curve has no tails and its full width and half maximum and height are 25 and 16 nm, respectively; thus it is clear that the 325 nm propagating light leaked from the probe did not dissociate the gas-phase DEZn. These results indicate that the nanometer-scale nucleation was occurred by optical near field for a 325 nm light. Furthermore, the deposition is grown by molecules adsorbed on prenucleated Zn. Since high-quality ZnO is fabricated by oxidizing Zn, such a nanometric precision of the deposition mechanism could be used to fabricate size- and position-controlled nanometer-scale opto-electronic devices.

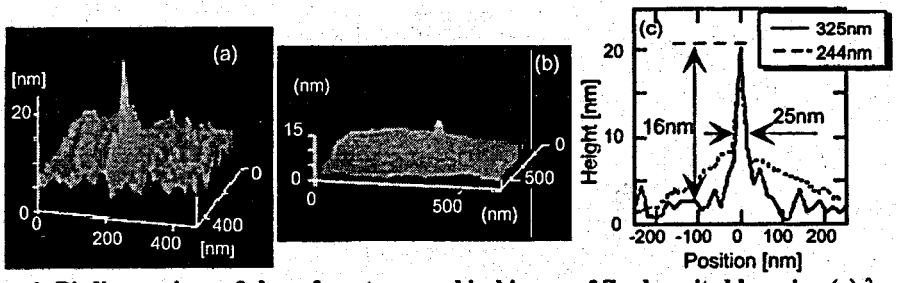

Figure 1: Bird's eye views of shear-force topographical image of Zn deposited by using (a) $\lambda = 325$ nm and (b) $\lambda = 244$ nm. (c) Cross sectional profiles through the deposited Zn dots in (a) and (b).

References

[1] Y. Yamamoto, M. Kourogi, M. Ohtsu, V. V. Polonski, and G. H. Lee, *Appl. Phys. Lett.* 76, 2173 (2000).
[2] Y. Fujita, S. Fujii, and T. Iuchi, *J. Vac. Sci. Technol.* B7, 273 (1989).
[3] D. J. Ehrlich, R. M. Osgood, Jr., And T. F. Deutsch, *J. Vac. Sci. Technol.* 21, 23 (1982).

Mapping single molecular fluorescence lifetime near metal probes

E.M.H.P. van Dijk, A.C. Krijgsman, W.H.J. Rensen, M.F. García-Parajó, L. Kuipers & N.F. van Hulst
Applied Optics group, MESA+ Research Institute, Faculty of Applied Physics, University of Twente, P.O.Box 217, 7500AE Enschede, the Netherlands

Sharp metal probes are being used by a number of groups in an effort to break the diffraction limit [1-3]. The experiments involve bringing a sharp metal probe close to the sample of interest. Excitation light impinging at the end of the probe can induce a very localized enhancement of the field. Different mechanisms for enhancement have been reported. In one case, light with a polarization parallel to the probe axis induces charge oscillations that accumulate at the probe apex (lighting rod effect)[1]. This effect is highly dependent on the geometry of the probe and the polarization of the excitation light. An alternative route to enhancement is probably based on localized collective electron oscillations, e.g. plasmons [2]. Where the enhancement is highly depended on the material of the probe and the excitation wavelength used.

The enhanced localized field can in principle be mapped with single fluorescent molecules. They are used as local nano-reporters of the field strength near the probe. Since the molecules are randomly orientated in the sample they allow the mapping of the field components in all directions [4]. In a conventional single molecule experiment the number of emitted fluorescent photons is assumed to be proportional to the intensity of the field. However, this assumption does not hold when a metal object is brought in the vicinity of the fluorescent molecule. Due to the electromagnetic interaction of the emitting dipole with the metal, the spontaneous emission rate can be enhanced or inhibited, depending on the exact geometry of the metal and the distance to the molecule. This interaction will lead to an enhancement or quenching of the fluorescence, an effect that is not exclusively related to the local field around the probe. The only way to separate field enhancement effects from fluorescence emission modification is to measure the lifetime of the excited state [5].

In this contribution we will present simultaneous measurements of the fluorescence intensity and excited state lifetime as a function of the x, y and z position (fig.1) of the probe with respect to single molecules. Dielectric and metal probes were illuminated at various excitation wavelengths. Direct correlation of the fluorescence intensity and decay rate for individual molecules in real time allow us to distinguish between the different physical phenomena that occur when a metal is brought near a single molecule.

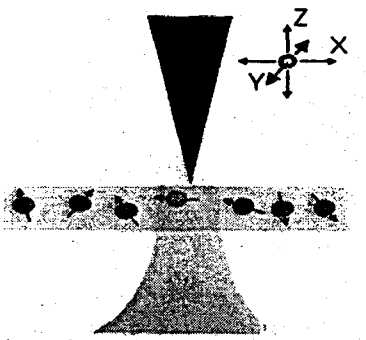

Figure 1: schematic representation of the experiment.

References

[1] E.J. Sánchez, L. Novotny and X.S. Xie, *Phys. Rev. Lett.* **82**, 4014 (1999).
[2] A. Kramer, W. Trabesinger, B. Hecht, U.P. Wild, *Appl. Phys. Lett.* **80**, 1652 (2002)
[3] A.V. Zayats, V. Sandoghdar, *J. Microscopy* **202**, 94 (2001)
[4] J.A. Veerman, M.F. García-Parajó, L Kuipers, N.F. van Hulst, *J. Microscopy* **194**,477 (1999)
[5] R.Vallée, N. Tomczak, H.Gersen, E.M.H.P. van Dijk, M.F. García-Parajó G.J. Vancso, N.F. van Hulst, *Chem. Phys. Lett.* **348**, 161 (2001)

Optical Spectroscopy on Individual Porphyrin Wheels

C. R. L. P. N. Jeukens, K. Takazawa, P. C. M. Christianen, J. C. Maan
High Field Magnet Laboratory, Research Institute for Materials, University of Nijmegen, Toernooiveld 1, 6525 ED Nijmegen, The Netherlands

M. C. Lensen, J. A. A. W. Elemans, A. E. Rowan, R. J. M. Nolte,
Organic Chemistry, University of Nijmegen, Toernooiveld 1, 6525 ED Nijmegen, The Netherlands

We report local spectroscopic studies of micron sized, ring-shaped molecular assemblies of which the constituent molecules (hexakis porphyrinato benzene, see Fig. 1a) are strongly ordered. The absorption and emission spectra of these ordered porphyrin wheels show a polarization, which is directed along the tangent of the ring, enabling the determination of the internal molecular arrangement. Control of the size and internal molecular order of such porphyrin wheels is of considerable interest to understand and mimic energy transport of natural light harvesting antenna systems and to develop future nanoscale applications.

The ring-shaped assemblies are studied using two techniques: 1) SNOM, providing high spatially resolved (~ 100 nm), polarized emission images; and 2) confocal microscopy, providing polarization dependent emission and absorption spectra of an individual ring.

By dropcasting a chloroform solution of the porphyrin molecules on a substrate, the molecules self-assemble into ring-shaped architectures that have a diameter in the range 0.1-10 μm. From polarization measurements we find that the substrate has a large influence on the internal degree of order. Using a hydrophilic substrate leads to a high degree of order (see Fig. 1b) within the wheel without the need of additional treatments such as annealing. Moreover, the lack of any emission intensity in the central part of the wheel clearly shows that no porphyrin molecules are present within the ring, indicating a ring formation mechanism due to the deposition of the molecules around gas-bubbles arising from the evaporation of the solvent. Analysis of the polarization dependent absorption and emission spectra of individual rings shows that the optical dipoles of the molecules are aligned tangentially to the ring (see Fig. 1c). From this fact we deduce the ordering of the molecules in the ring. Finally, we observe that the absorption as well as the emission spectra are ring-size dependent. The large rings (~ 10 μm) show no polarization in emission, while the absorption spectrum shows a small red-shift with respect to the molecular solution, i.e. there is no macroscopic ordering, although there is some interaction between the porphyrine molecules. In contrast, the smaller rings (< 4 μm) show a strongly polarized emission, and a broad, strongly red-shifted absorption spectrum, i.e. a high degree of macroscopic order as a result of a strong interaction between the molecules.

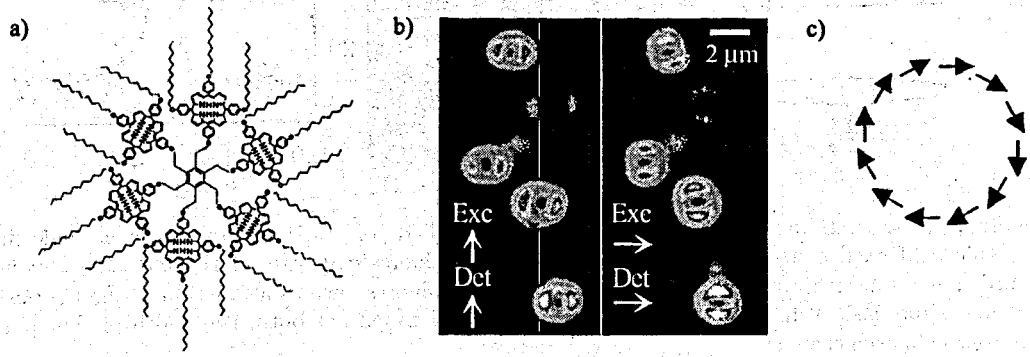

Figure 1: a) Molecular structure of hexakis porphyrinato benzene, b) Fluorescence images of the porphyrin wheels after vertically (left) and horizontally (right) polarized excitation and detection and c) Alignment of the optical dipoles of the molecules in the ring.

References

[1] H. A. M. Biemans, A.E. Rowan, A. Verhoeven, P. Vanoppen, L. Latterini, J. Foekema, A. P. H. J. Schenning, E. W. Meijer, F. C. de Schryver, and R. J. M. Nolte, *J. Am. Chem. Soc.* **120**, 11 054 (1998).

Probing the optical near-field enhancement at a metal tip using a single fluorescent molecule

B. Hecht
Nano-Optics group. Institut of Physics. University of Basel, CH-4056 Basel. Switzerland.
A. Kramer, W. Trabesinger and U.P. Wild
Physical Chemistry Laboratory. Swiss Federal Institute of Technology. CH-8093 Zurich, Switzerland.

The optical near-field in the vicinity of a metal tips of gold and Pt/Ir is mapped using a single-molecule as an optical probe [1]. The setup consists of a sample-scanning confocal optical microscope on top of which a scanning probe microscope is mounted [2]. Linearly polarized light from a tunable dye laser (λ=578.5 nm) is focused to a nearly diffraction-limited spot on the sample by a microscope objective. The sample fluorescence is focused onto a single photon counting avalanche photo diode. A holographic notch filter and a subsequent cut-off filter block the Rayleigh-scattered light. Sample scanning is accomplished by a piezo bimorph scanner, tip scanning by a piezo tube. Shear force interaction between tip and sample is used for the gapwidth control. The shear force detection relies on a quartz tuning fork as sensing element [3]. During an experiment a single molecule is continuously illuminated while the metal tip scans over it. The fluorescence rate of the molecule is recorded as a function of the tip position.
We observe an enhancement of the fluorescence signal by a factor of 5.7±0.3 as compared to the fluorescence in absence of the tip. This is clearly larger than the fourfold enhancement that can arise from constructive interference if the tip acts as a simple mirror. Considering the tip apex as a nanoparticle of nonregular shape, we suggest that, in the case of gold tips, the enhancement is due to resonant plasmon excitation. Consistently, no enhancement has been observed using Pt/Ir tips.

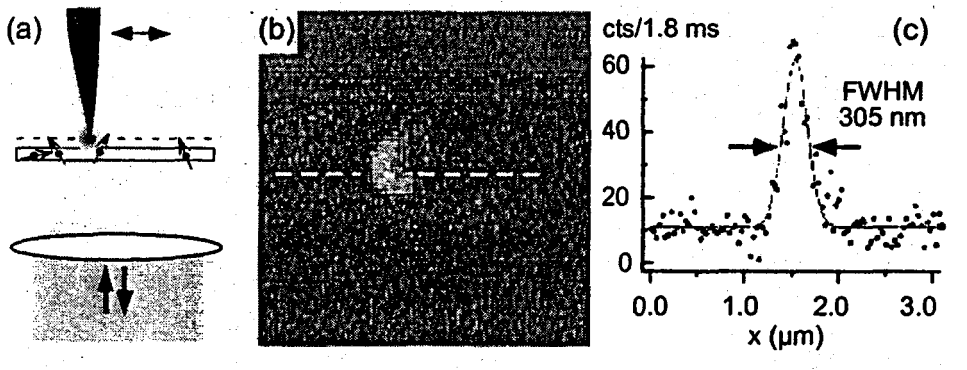

Figure 1: (a) Sketch of the experimental setup. An etched gold tip is scanned over a single fluorescent molecule held fixed in the focus of a laser beam. The fluorescence rate of the molecule is continuously recorded as a function of the tip position. (b) Molecular fluorescence as a function of the tip position. (c) Cut along the dashed line in (b). A Gaussian fit is used to extract both, the width of the spot and the intensity enhancement factor.

References

[1] A. Kramer, W. Trabesinger, B. Hecht, and U.P. Wild, *Appl. Phys. Lett.* **80**, 1652 (2002).

[2] A. Kramer, J.-M. Segura, A. Hunkeler, A. Renn, and B. Hecht, submitted.

[3] K. Karrai, R.D. Grober, *Appl. Phys. Lett.* **66** 1842 (1995).

Near-Field and Confocal Surface Enhanced Resonance Raman Spectroscopy from Room Temperature to Cryogenic Temperatures

A. J. Meixner, T. Vosgröne and P. Anger,
Physikalische Chemie, Universität Siegen,
57068 Siegen, Germany

Since the pioneering work of Kneipp [1], Nie [2], Brus [3], and Käll [4] surface enhanced Raman spectroscopy (SERS) at the single molecule level has attracted considerable attention. In SERS the Raman scattering cross section of molecules adsorbed on silver or gold nano-particles is enhanced by so many orders of magnitude that fingerprint vibrational spectra can be recorded at the single-molecule level under ambient conditions. In order to record Raman spectra with high spatial resolution the enhancement of the electromagnetic field by a silver coated AFM cantilever opposite to a silver film coated with dye has been used. Recently Zenobi et al.[5] have reported Raman signals with a spatial resolution on the order of 50 nm and al Kawata et al.[6] have observed local fluctuations in the SERRS spectra of a R6G-coated silver film on a 30 nm scale at the junction between a silver tip and a silver film.

We investigate surface enhanced Raman spectra of rhodamine dyes dispersed on isolated silver nano-particles or nano-clusters. For excitation we have used an aperture probe or a diffraction limited confocal laser spot. Spectra in the rang from 200 cm^{-1} to 4000 cm^{-1} at room temperature down to 9 Kelvin have been recorded. Many of the lines can be associated with the structure of the adsorbed molecule. Frequency shifts of distinct modes are due to changes of the force constants of the respective chemical bonds in the structure of the adsorbed molecule. The appearance or disappearance of lines is the result of a distorted molecular structure such that the selection rules valid for the free molecule no longer apply. These effects may also occur suddenly from one spectrum to the next an are caused by changing chemical interactions between the dye molecule and the local irregular micro environment on the Ag-particle. They may also provide evidence for the effects leading to chemical enhancement [7] of the Raman scattering cross section.

References

1. K. Kneipp, Y. Wang, H. Kneipp, et al. Phys. Rev. Lett. **78**, 1667 (1997).
2. S.M. Nie and S.R. Emory, Science **275**, 1102 (1997).
3. H.X. Xu, J. Aizpurua, M. Kall, et al. Phys. Rev. E **62**, 4318 (2001).
4. A.M. Michaels, J. Jiang, and L. Brus, J. Phys. Chem. B **104**, 11965 (2000).
5. R. M Stöckle, Y.D. Sur, V. Deckert, R. Zenobi, Chem. Phys. Lett 318, 131 (2000).
6. N. Hayazawa, Y. Inouye, Z. Sekkat, S. Kawata, Chem. Phys. Lett. 335, 369 (2001).
7. A. Otto, Phys. Stat. Sol. (a) **188**, 1455 (2001), and references there in.

Near Field Enhancement of Conductive Tips in Raman Spectroscopy of Carbon Nanotubes

A. Bek, R. Vogelgesang, and K. Kern
Max-Planck Institute for Solid State Research, 70569 Stuttgart, Germany.

Optical spectroscopy at the single molecule level has attracted considerable attention in recent years. Whereas fluorescence and luminescence spectroscopy of single molecules has generated a wealth of new results, Raman spectroscopy has not yet attracted as much attention due mainly to the many orders of magnitude lower cross-sections for the scattering process.

In view of the nanoscopic target sample size, especially when compared to the typical wavelengths of optical radiation, taking advantage of near-field optical effects holds great promise. Indeed, a few experimental investigations of single molecule Raman spectroscopy have been reported, which utilized highly localized near field enhancement effects of laser light in the nm-sized volume near the tip apex of an *aperture-less* scanning near-field optical microscope (such as conductive scanning tunneling microscope (STM) tips or atomic force microscope (AFM) tips with a conductive coating) to help overcome the limitations of minute cross-sections.[1, 2, 3, 4]

A prerequisite for the optimal application of this scheme is the detailed understanding of the interactions between the incident exciting radiation and the sample, as well as other material in the neighborhood, namely, sample holder/substrate and the field enhancing tip.

We investigate the Raman spectra of carbon nano tubes – a relatively robust and strong scatterer – located in the vicinity of field enhancing conductive tips. To minimize the influence of the sample holder/substrate matter we use free standing nano tubes attached to commercial AFM tips, which also allow to handle the specimens with comparative ease. In addition, they may be used as a regular AFM probe to map simultaneously the surface topology of the field enhancing tip. We report on the Raman scattering intensity in variation of the relative location of the carbon nano tube and the field enhancing tip as well as direction and polarization of the incident radiation. The experimental results are compared with theoretical predictions.

References

[1] R. Stockle, Y. Suh, V. Deckert, and R. Zenobi, Chem. Phys. Lett. **318**(1-3), 131 (2000).

[2] N. Hayazawa, Y. Inouye, Z. Sekkat, and S. Kawata, Optics Communications **183**, 1 (2000).

[3] M. S. Anderson, Appl. Phys. Lett. **76**, 3130 (2000).

[4] B. Pettinger, G. Picardi, R. Schuster, and G. Ertl, Electrochemistry (Japanese Electrochemical Society) **68**(12), 942 (2000).

Near-field imaging of surface plasmon on Au nano-structures fabricated by scanning probe lithography

Jeongyong Kim,[1] Ki-Bong Song, Jun-Ho Kim, Seong Q Lee and Kang-Ho Park
Basic Research Laboratory, Electronics and Telecommunications Research Institute, Kajeong-dong 161, Yusong, Taejon 305-600, Korea

Recently it is reported that metal films with periodic hole arrays has unusually high transmission due to surface plasmon (SP) modes excited by photon impinging with specific energy,[1] while details of spatial distributions of SP modes on the films are to be known. Near field scanning optical microscopy (NSOM) can provide a direct view of the field distribution of SP modes due to its high spatial resolution.[2]

We use a NSOM to image spatial modes of SP on metallic nano-structures, fabricated by scanning probe lithography technique, which has advantages of low cost and simplicity. A few nanometer high oxide layers are fabricated on Si or Ti films using nano-oxidation technique with an atomic force microscope (AFM) and consequently the film is covered with thin layer of Au by thermal evaporation. In result, periodic nano-metal-grating structures are formed. The line width can be made smaller than 50 nm and arbitrary metallic grating patterns with varying period or shape can be fabricated. Figure 1(a) shows an AFM image of a line grating produced by nano-oxidation and Au deposition. The period of the line corrugation is chosen to be 318 nm, the half of the laser wavelength (635 nm), to optimize the coupling with SP modes. Various patterns of metal nano-structures and gratings are fabricated and the result of NSOM imaging will be presented.

As a preliminary experiment, we fabricated the isolated metal mounds on an Au thin (~ 30 nm) film and imaged the field distribution with NSOM.[3] The series of mounds are produced by applying 20 μs, 20 V electric pulses to W_2C-coated probes in AFM non-contact mode. The size of the mounds is about 20 nm in height and 50 - 100 nm in width. Figure 1(b) displays a NSOM transmission images. Strong enhancement of light transmission on the metal mounds is observed as bright spots. The width of spots is measured to be as small as 80 nm confirming the high spatial resolution of NSOM. The peak intensity on the mounds is about 10 times higher than the background intensity, strongly suggesting that the excitation of SP modes plays a role in observed enhancement of light transmission.

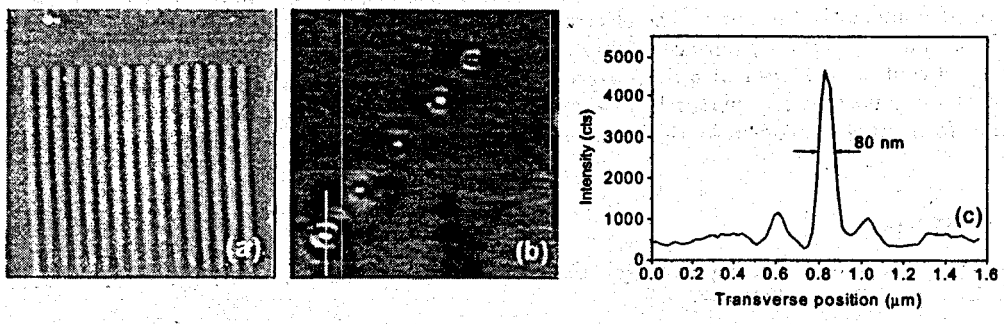

Figure 1: (a) AFM image of a line grating. Image size is 6 x 6 □. (b) NSOM transmission image of metallic mounds fabricated by SPL. Image size is 5 x 5 □. (c) Cross section along the white line in (b)

References

[1] T. W. Ebbesen, H. J. Lezec, H. F. Ghaemi, T. Thio and P. A. Wolff, *Nature* **391**, 667 (1998).
[2] C. Sonnichsen, A. C. Duch, G. Steininger, M. Koch, and G. von Plessen, *Appl. Phys. Lett.* **76**, 140 (2000).
[3] J. Kim, K. B. Song, and K.-H. Park, *Jap. J. Appl. Phys. I*, **41**, 1903 (2002).

[1]Current address: Department of Physics, University of Incheon, Dowha-dong 177, Nam-ku, Incheon 402-749, Korea

Second-harmonic Generation at Metal Tips in Apertureless Scanning Near-field Optical Microscopy

S. Takahashi, A. V. Zayats,
School of Mathematics and Physics, The Queen's University of Belfast, BT7 1NN, United Kingdom.

Apertureless scanning near-field optical microscopy (SNOM) has recently attracted much attention due to its potentiality of high spatial resolution. Among variety of apertureless approaches, an application of second harmonic generation (SHG) at a metal tip apex is a promising technique for light confinement on the nanoscale [1, 2, 3].

Second-harmonic generation is known to be a surface sensitive spectroscopic technique, and its intensity is proportional to the fourth power of the local electric field of the excitation light. SHG at metal surfaces exhibiting nanoscale defect structure can be strongly enhanced due to localised surface plasmons and/or lightning-rod effects at surface defects. In analogy to this, sharp metal tips of the apertureless SNOM can be regarded as good candidates for achieving nanoscopic sources of second-harmonic light. If the field enhancement effects are induced at or by a probe tip, the strongly confined source of the SH light can be realised in the tip-surface junction [1, 3].

Here we present the investigations of the second-harmonic generation at sharp metal tips in the near-field proximity to a surface. Polarisation and distance dependencies of second-harmonic generation have been investigated and compared to respective dependencies for scattered fundamental light. The experimental data for different tip materials are compared in order to elucidate the mechanisms of the electromagnetic field enhancement and light confinement in terms of the contribution of localised surface plasmons at the tip apex and the influence of the tip interaction with a surface.

Second-harmonic generation and excitation light scattering at the tip apex under two illumination conditions has been studied such as direct illumination in the far-field and evanescent wave illumination in the near-field proximity to a surface. The experimental data reveal the polarisation characteristics of linear and SHG scattering depending on the topographic features of the tip. Under the direct far-field illumination, the scattering centre of fundamental and SH light can be different from one another, while in the near-field they are predominantly the same. The electromagnetic interaction between a tip and a surface results in much less influence of the tip surface quality on the near-field SHG in contrast to the far-field SHG. The polarisation contrast achieved with SHG exceeds the contrast of linear scattering. Such polarisation characteristics are important for apertureless near-field optical imaging of ferroelectric and magnetic materials as well as for nonlinear magneto-optical studies and applications on the nanoscale.

References

[1] A. V. Zayats and V. Sandoghdar, *Opt. Commun.* **178**, 245 (2000); A. V. Zayats and V. Sandoghdar, *J. Microsc.* **202**, 94 (2001).

[2] A. V. Zayats, T. Kalkbrenner, V. Sandoghdar and J. Mlynek, *Phys. Rev. B* **61**, 4545 (2000).

[3] S. Takahashi and A. V. Zayats, to be published.

Near-field Optical Structuring of Ultrathin Terpolymer Films

S. Trogisch, Ch. Loppacher, S. Grafström, and L.M. Eng
University of Technology Dresden, Institute of Applied Photophysics, D-01062 Dresden
trogisch@iapp.de, www.iapp.de

F. Braun, T. Pompe, and B. Voit, Institute of Polymer Research Dresden e.V., D-01069 Dresden

We report on the near-field structuring of novel terpolymers [1]. Two different types of terpolymers were used, each containing siloxane groups for covalent bonding to the substrate, spacer groups, and photoreactive groups. The photoreactive part was either a diazosulfonate group, which decomposes under UV irradiation, or an amine group protected by a photolabile part. The two polymers behave like a negative or positive resist, permitting further functionalization of nonirradiated and irradiated areas, respectively. Therefore, these polymers are promising materials for nanotechnological applications, such as surface metallization or initiation of supramolecular chemistry on the nanometer scale.

Films were spin-coated onto glass slides or silicon substrates with a nominal thickness between 5 and 100 nm. Similar film thicknesses were measured with ellipsometry and a scanning-force-microscopy scratching method. The chemical composition on any stage of the polymer modification process was monitored by x-ray photoelectron spectroscopy (XPS) providing quantitative analysis for larger sample areas. The local chemical composition, however, could be inspected with μ-Raman spectroscopy as well as scanning probe techniques, such as Kelvin force microscopy revealing the sample surface potential, near-field optical extinction spectroscopy [2] measuring the local optical absorption, or even tip-enhanced Raman spectroscopy [3].

The presented results show a reduction of the local optical absorption as a function of the UV power absorbed within the diazo-terpolymer film. Furthermore, we show that only nonirradiated film parts provide functional sites for metal salt complexation and development of metallic structures [4]. Note that such processes like as-deposited polymer films have not yet been reported in the literature.

UV structuring by confocal and near-field optical microscopy was successful for the amino-terpolymer. The latter was achieved with tapered optical multimode fibers (ca. 100 nm aperture) providing enough optical transmission in order to remove the protection group of the amine-functionalized polymer. Uncovered amine groups were then marked with Fluorescein Isothiocyanate (FITC) and subsequently imaged in a confocal fluorescence microscope (see Fig. 1). We believe that this kind of optical structuring is applicable down to 50 nm.

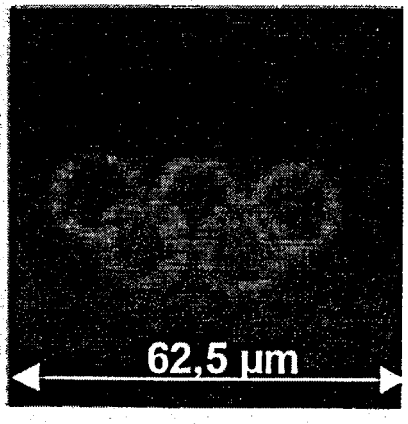

Fig. 1:
Near-field optical structuring of a ultra-thin amino-terpolymer film using a tapered multimode fiber for illumination. UV illumination of the protection group allows the Fluorescein Isothiocyanate (FITC) dye to adsorb to the amine groups, as proven with confocal fluorescence microscopy.

References

[1] F. Braun et al., submitted to *Macromol. Chem. Phys.*
[2] J. Seidel et al., *Appl. Phys. Lett.* **79**, 2291 (2001)
[3] R. M. Stöckle et al., *Chem. Phys. Lett.* **318**, 131 (2000)
[4] Ch. Loppacher et al., *Macromolecules* **35**, 1936 (2002)

Surface Plasmon Nano–Optics

J. R. Krenn, H. Ditlbacher, G. Schider, A. Hohenau, A. Leitner, F. R. Aussenegg
Karl–Franzens–University Graz, Universitätsplatz 5, A-8010 Graz, Austria
www.uni-graz.at/expwww/nanooptics

Within the last decade near–field optical microscopy has contributed significantly to the insight in optical effects based on surface plasmons (SPs). These mixed photon–plasmon excitations at metal surfaces are especially appealing due to their nanoscale sized optical fields [1], strong field enhancement and their temporal response on a sub-10 fs time scale [2]. Therefore SPs seem suitable for realizing ultrafast miniaturized optical elements with spatial dimensions well below the diffraction limit.

Of central importance for such elements is guiding and routing of light signals. We demonstrate experimentally by direct imaging with near–field optical microscopy that a gold nanowire with a width of only 200 nm can serve as a SP waveguide over a distance of a few μm, at a wavelength of 800 nm.

Furthermore we report the experimental realization of SP 'mirrors' and 'beamsplitters', which we use to build a SP interferometer. As an example, Fig.1a shows a 'mirror' constituted by a two–dimensional photonic crystal built up from gold nanostructures. This 'mirror' reflects a (locally excited) SP practically without loss in intensity and directionality. To image the SP field distribution we recorded the fluorescence signal of a thin molecule layer close to the sample surface with conventional microscopy (Fig.1b). This technique [3] allows the fast (real–time) and reliable imaging of SPs in metal nano– and microstructures. It thus constitutes, albeit not allowing superresolution, a tool complementary to near–field optical microscopy for the investigation of SP effects.

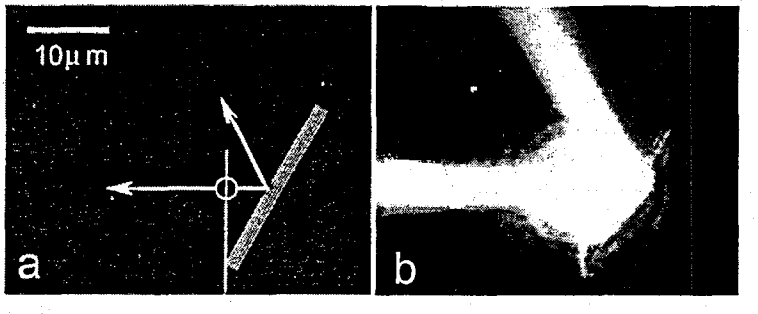

Figure 1: (a) Scanning electron microscope image of a SP 'mirror': two SPs are locally launched by focussing a laser beam on a vertically aligned gold nanowire (focus position marked by circle); the SP directions are indicated by the arrows. (b) Corresponding fluorescence image, the SP propagating to the right is reflected by the 'mirror'; light wavelength 800 nm.

References

[1] J.R.Krenn et al., *Phys.Rev.Lett.* **82**, 2590 (1999).

[2] B.Lamprecht, J.R.Krenn, A.Leitner, F.R.Aussenegg, *Phys.Rev.Lett.* **83**, 4421 (1999).

[3] H. Ditlbacher et al., *Appl.Phys.Lett.* **80**, 404 (2002).

Fabrication of a temperature-controllable B-doped Si probe for optical near-field photochemical vapor deposition

T-W. Kim, T. Yatsui, M. Kourogi, M. Ohtsu*, Japan science and Technology Coporation, 687-1 Tsuruma, Machida, Tokyo, Japan 194-0004*

** Also at: Interdisciplinary Graduate School of Science and Engineering, Tokyo Institute of Technology, 4259, Nagatsuta, Midori-ku, Yokohama, Kanagawa, Japan 226-8502*

Recently, optical near-field photochemical vapor deposition (NFO-PCVD) attracts much attention as a useful technique to realize nanopotonic near field optical devices. NFO-PCVD method has been successfully used in the fabrication of such nanometric matter as Al, Zn, and ZnO [1]. Because the aperture size directly affects the throughput of optical near field and the resultant size of nanometric matter deposited, it is required to maintain the same aperture size of the fiber probe throughout the integration of near field optical devices. Material deposition occurred at the aperture of fiber probe, caused by the dissociation of adsorbed metal-organic molecules, is thought as one of the reasons to change the aperture size and/or the throughput of optical near field during the process of NFO-PCVD. From this viewpoint, control of the adsorption of metal-organic molecules onto the probe aperture becomes important.

We have developed a temperature-controllable B-doped Si probe in order to prevent the deposition of the adsorbed source molecules onto the aperture of fiber probe. The idea is based on the facts that increasing substrate temperature above 80 °C reduces the adsorption of Diethylzinc molecules on the substrate surface [2] and heavily B-doped Si layer plays as a good current-induced heater [3]. The probes are fabricated using anisotropic etching of n-type silicon on insulator (SOI) and thermal diffusion of boron. Figure 1 illustrates the schematic diagram of cross-sectional view and the scanning electronic microscopy (SEM) image of the fabricated B-doped Si probe. The fabricated B-doped Si probe has the aperture size of about 80 nm and the height of 1.8 □m. By inducing electric power of 1 Watt, temperature of B-doped Si probe can be raised above 80 °C. In this paper, we describe the fabrication method of a temperature-controllable B-doped Si probe and discuss the applicability of the probe for NFO-PCVD.

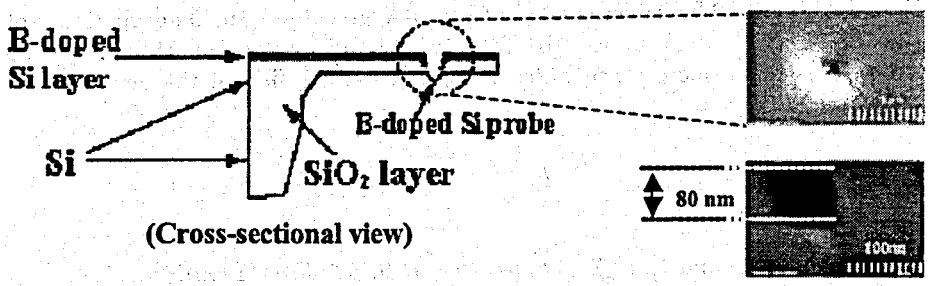

Figure1: schematic diagram of cross-sectional view and SEM image of the fabricated B-doped Si probe (top view).

References

[1] Y. Yamamoto, et al, Appl. Phys. Lett. **76**, 2173 (2000). [2] R. Krchnavek, et al, J. Vac. Sci. Tech. **5**, 20 (1987). [3] H. Yu asa, et al, T. IEE Japan, **117-E**, 275 (1997)

Characterizing the electric field enhancement and fluorescence quenching induced by a sharp gold tip.

M. R. Beversluis, A. Bouhelier, A. Hartschuh, and L. Novotny
University of Rochester, The Institute of Optics, Rochester, NY 14627.

Enhanced electric fields produced at the apex of a sharp gold tip can be used to locally induce two-photon excitation fluorescence of molecules, such as PIC J-Aggregates [1]. Although the underlying mechanism of the enhancement is mostly understood, details regarding the dependence of fluorescence quenching and the magnitude of the field enhancement on the tip size and shape are still being characterized [2, 3].

It has been suggested that the strong longitudinal field produced in highly focused higher order laser mode can drive the field enhancement at a sharp gold tip [4]. Using this technique, we have recorded fluorescence images with sub-20 nm resolution, as shown in Fig. 1(a). In Fig. 1(b), the fluorescence appears at the edges of the aggregates (see arrow) suggesting that the fluorescence is quenched due to the proximity of the metallic tip. The competition between the field enhancement and the fluorescence quenching at a sharp gold tip can be understood by measuring the fluorescence rate dependence on the distance between the tip and sample.

Furthermore, the near-field contrast also depends on the background signal arising due to nonlinear interactions between the gold and the ultrafast excitation pulses, giving rise to second-harmonic and white-light continuum generation. We have found that this component can be altered by changing tip shapes.

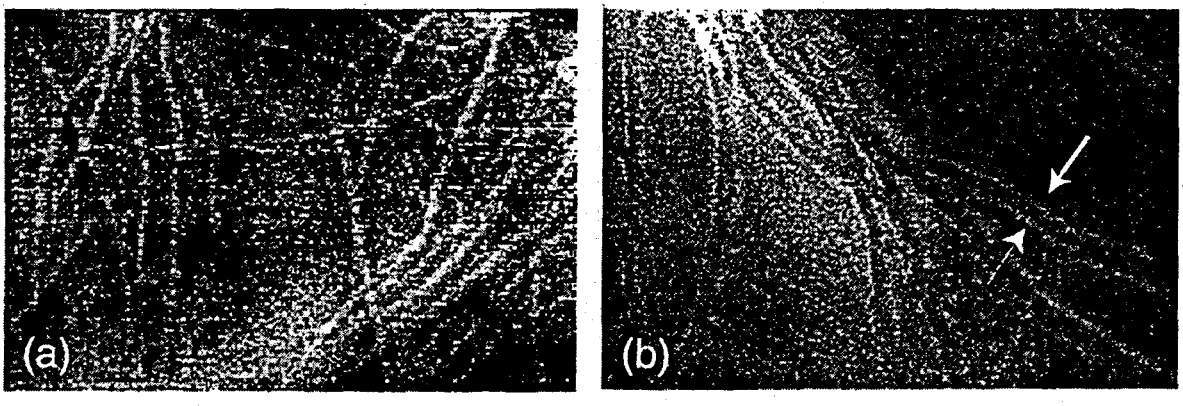

Figure 1: (a) Near-field image (2 by 3 micron area) of PIC J-Aggregates with 20 nm spatial resolution, showing both near-field and far-field fluorescence. (b) Taken with a different tip, another image of J-Aggregates (1 by 1.5 micron area) shows fluorescence which appears to either side of the aggregates, suggesting a quenching mechanism.

References

[1] E. J. Sánchez, L. Novotny and X. S. Xie, *Phys. Rev. Lett.* **82**, 4014 (1999).

[2] H. F. Hamman, M. Kuno, A. Gallagher, and D. J. Nesbitt, *J. Chem. Phys.* **14**, 8596 (2001).

[3] T. J. Yang, Guillaume A. Lessard, and Stephen R. Quake, *Appl. Phys. Lett.* **76**, 378 (2000).

[4] L. Novotny, E. J. Sánchez, and X. S. Xie, *Ultramicroscopy* **71**, 21 (1998).

Near-Field Spectroscopy of single II-VI Quantum Dots

M. Brun, N. Chevalier, J. C. Woehl, H. Mariette and S. Huant
Laboratoire de Spectrométrie Physique, Université Joseph Fourier Grenoble et CNRS
P.O. Box 87, 38402 Saint Martin d'Heres cedex, France.

We have carried out a near-field optical spectroscopy of a *single CdTe/ZnTe* quantum dot using our low-temperature (4.2 K) Near-Field Scanning Optical Microscope - NSOM - described at NFO-6 [1].

The CdTe/ZnTe system has two interesting properties with respect to the extensively studied InAs/GaAs system, which make it a good candidate for NSOM studies. First, there is so far no trace of a so-called "wetting layer" (a very thin supporting quantum well that connects the dots) in photoluminescence (PL) spectra. The absence of such a layer minimizes inter-dot carrier diffusion and, therefore, helps in maintaining the high spatial resolution of NSOM. Second, the valence band-offset is extremely small in such a way that the hole ground state is not the quantum-confined state in the dot, but rather the acceptor state in the barriers. As a consequence, we expect part of the photo-excited holes to be trapped by these acceptors to give rise to a steady-state population of excess electrons in the dots. This favors the formation of *negative excitons*. Therefore, a rich phenomenology is revealed in NSOM studies of such dots.

After having demonstrated the ability of our microscope to actually resolve a single dot in the CdTe/ZnTe system using a "standard" tapered tip, we will describe in detail the spectroscopic properties of the dot as a function of the excitation power.

While the PL spectrum at low excitation power reveals only one single sharp peak due to the radiative recombination of excitons (X) in the single dot, several additional sharp peaks are observed with increasing excitation density. The dominant features are ascribed to exciton complexes and charged exciton complexes such as negatively-charged excitons (X^-), neutral (2X and 3X) and negative ($2X^-$ and $3X^-$) biexcitons and triexcitons [2]. Exciton charging arises due to efficient hole trapping by residual acceptors in the barrier material. A novel spectral feature appearing close to the X^- peak is assigned to X^{2-} negative excitons, i.e., excitons having trapped *two* additional electrons. This feature is found to ***shift to the red with increasing power***: this is thought to be due to a spin-screening effect of the multi-charged zero-dimensional exciton complex.

Finally, we will describe preliminary studies of another very promising II-VI quantum dot system, namely CdSe nanocristals (nanoX) [3]. These nanoX can be produced in different sizes (from 1 nm to 10 nm in diameter), which determine their emission properties. They have a very large PL efficiency at room temperature. Using their typical "blinking effect" [4], we will show that our NSOM is able to discriminate single nanoX dispersed on a thin PMMA film, or inside the film, from clusters of nanoX. Having isolated a single nanocristal under the optical tip, we are currently measuring its near-field PL at room temperature and we will present our fist data at the conference.

References

[1] M. Brun *et al.*, *J. Microscopy* **202**, 202 (2001).

[2] M. Brun *et al.*, *Solid State Commun.* **121**, 407 (2002).

[3] The work on CdSe nanoX is made in collaboration with P. Reiss, J. Bleuse and F. Chandezon from CEA Grenoble.

[4] K. T. Shimisu *et al.*, *Phys. Rev. B* **63**, 205316 (2001).

Phonon-enhanced near-field interaction observed with infrared s-SNOM

R. Hillenbrand, T. Taubner, and F. Keilmann
Max-Planck-Institut für Biochemie, D-82152 Martinsried, Germany, keilmann@biochem.mpg.de

We demonstrate in theory and experiment that the optical near-field interaction can be strongly enhanced by lattice vibrations or phonons. This effect is analoguous to the well-known plasmon enhancement due to metallic conductivity. In contrast however, phonon enhancement is stronger and yields a higher Q resonance compared to plasmon enhancement, because phonons have much longer collisional lifetime compared to metal electrons.

Our experiment consists of imaging a partly gold-covered SiC surface in our scanning near-field optical microscope[1,2], at various illumination wavelengths in the mid-infrared. This instrument has recently been equipped to measure scattering amplitude and phase separately and simultaneously. We observe strong scattering signals in a narrow spectral region near 11 μm. The graph plots the scattering *amplitude* enhancement η, relative to a gold surface, taken from a large series of images[3].

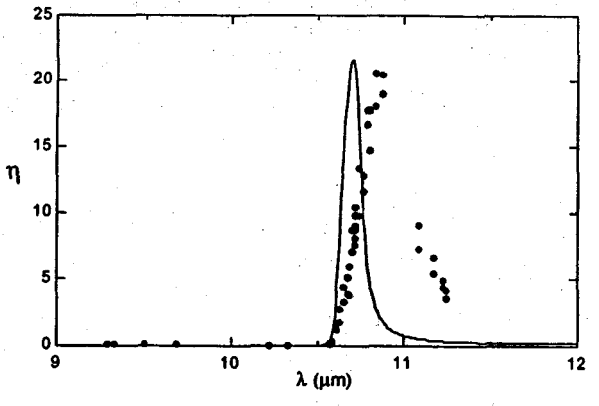

Theoretically, we calculate the near-field microscopic *amplitude* contrast η of SiC relative to gold, by employing our model of dipole/mirror dipole interaction outlined earlier [1,2]. This modelling uses the complex dielectric functions of both materials. Taking account of the 2nd harmonic signal demodulation (needed in the experiment to suppress background scattering [2]), we obtain a resonant response (which we plot scaled down to 60%) expressing the phonon-enhanced near-field interaction.

This near-field study of SiC demonstrates a resonant light-matter interaction of unprecedented dynamic range and spectral sharpness. It adds a new, phonon-related mechanism of field enhancement with forseeable use in near-field microscopy as well as in sensor and photonic applications.

References

[1] B. Knoll and F. Keilmann, *Nature*, **399**, 134 (1998).
[2] B. Knoll and F. Keilmann, *Applied Physics Letters*, **77**, 3980 (2000).
[3] R. Hillenbrand, T. Taubner, and F. Keilmann, *Nature*, in press.

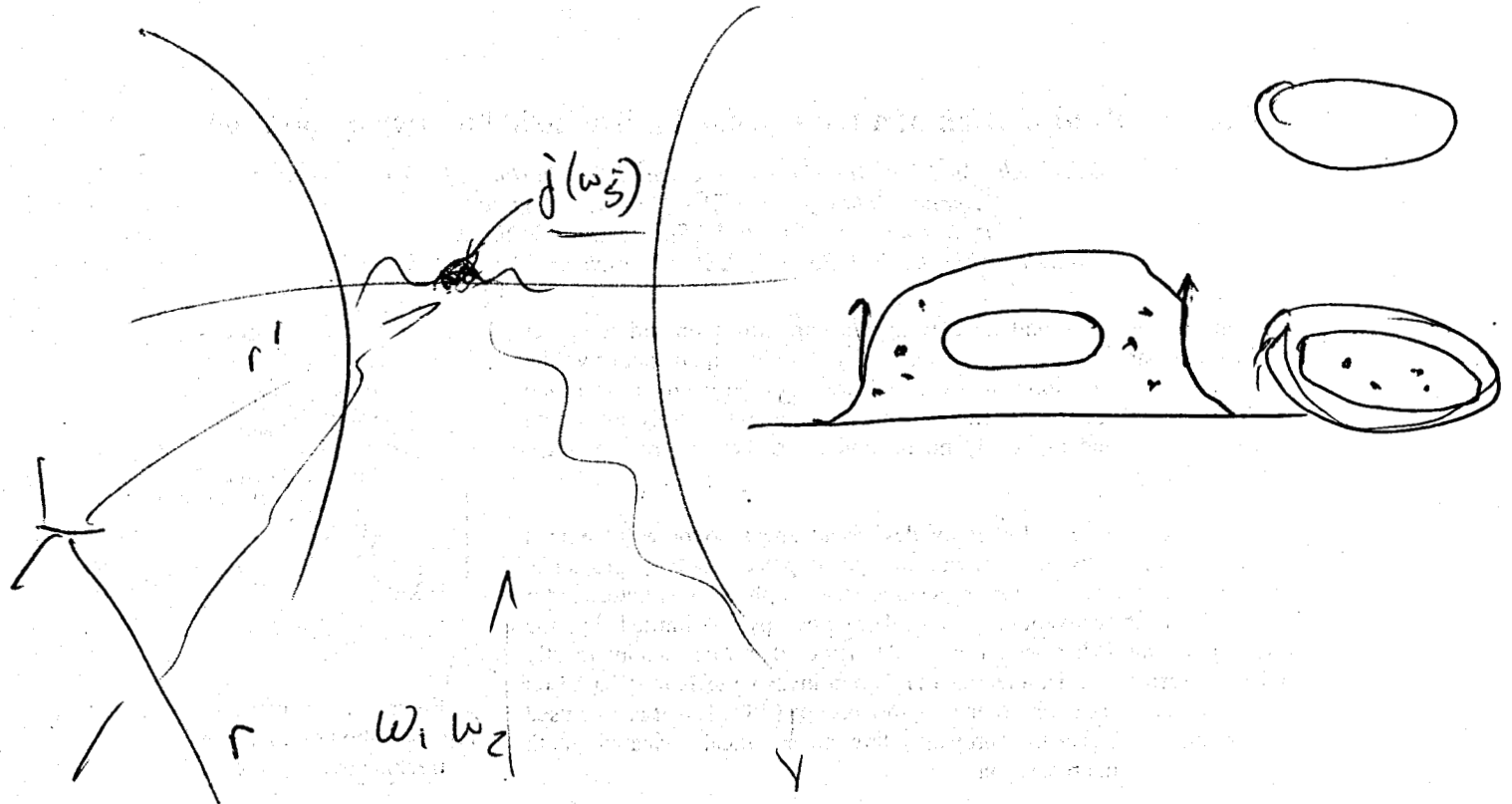

$$\vec{E}(\vec{r}, \omega_3) = \int \overleftrightarrow{G}(\vec{r}, \vec{r}', \omega_3)\, \vec{j}(\vec{r}', \omega_3)\, dV'$$

$$\overleftrightarrow{G}\vec{p} + \overleftrightarrow{G}\overleftrightarrow{Q} + \dots$$

Time resolved motion of a femtosecond pulse inside a microresonator

H. Gersen[1], D.J.W. Klunder[2], J. P. Korterik[1], A. Driessen[2], N.F. van Hulst[1], L. (Kobus) Kuipers[1]
[1)] Applied Optics group, MESA+ Research Institute
[2)] Lightwave Devices Group, MESA+ Research Institute,
University of Twente, P.O. Box 217, 7500 AE Enschede, The Netherlands

Demands on speed and capacity for telecommunication and computer applications are increasing exponentially, while simultaneously the dimensions of the components have to decrease to the micro- or even the nanometer scale. In the optical domain, development of truly integrated optical devices, and especially microcavities, are key in order to meet these challenges.

As the development of photonic devices advances, so too will the need to monitor the transient behavior of optical pulses as they propagate through such devices. However, peeking inside a photonic structure is far from trivial as conventional optical microscopy is limited by the diffraction limit. What occurs inside the device therefore remains mostly hidden. Recently we demonstrated [1] a non-invasive technique based on an optical photon scanning tunneling microscope (PSTM) that can be used to "visualize" pulses as they propagate through an optical device with both temporal and spatial resolution.

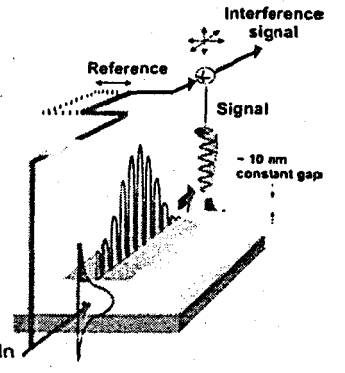

Figure 1 : Schematic representation of the pulse tracking experiment.

Figure 1 schematically depicts how we extended a heterodyne detection phase-sensitive PSTM, which allows the measurement of both the amplitude and phase of propagating light [2], to perform local time-resolved measurements. At a reference time given by the position of an optical delay the position of a pulse is pinpointed. With this technique we have recently been able to observed time-resolved "ballistic" motion of ultrashort optical wave packets within a cylindrical microresonator. Figure 2 shows a measurement at a fixed reference time in which a 120 femtosecond pulse has just passed a ring-resonator. It is clearly visible that part of the pulse is coupled to two different modes in the resonator. By repeating this measurement for different reference times the motion of the pulse in the cavity is followed in time. Our most recent results will be presented at the meeting.

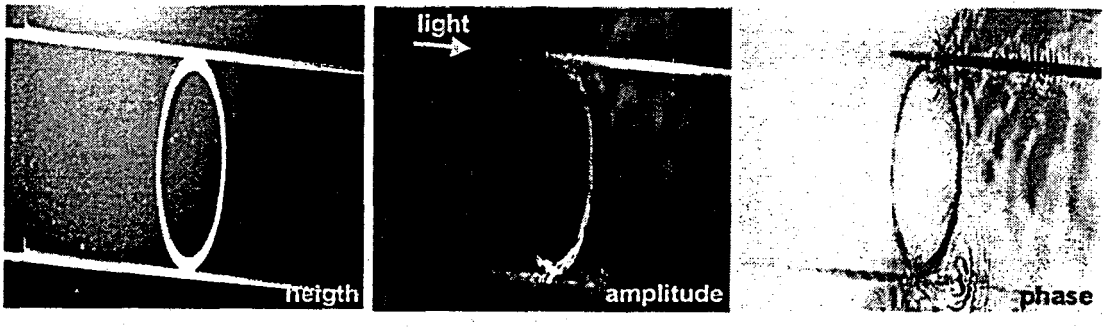

Figure 2 : Visualization of the time resolved motion of a femtosecond pulse (120 fs, λ = 1300 nm) through a cylindrical ring-resonator (radius 25 μm) measured by PSTM. From left to right the simultaneously measured topography of the structure (~250 x 70 μm) and the optical amplitude and phase of the pulses. The optical amplitude clearly shows that part of the pulse which passes the resonator is coupled into the resonator. Two different modes can be distinguished.

References

[1] M.L.M. Balistreri, H. Gersen, J.P. Korterik et al., *Science* **294** (5544), 1080 (2001)
[2] M.L.M. Balistreri, J.P. Korterik, L. Kuipers et al., *Phys. Rev. Lett.* **85**, 294 (2000)

Understanding Local Measurement of Dichroism and Birefringence in Thin Polymer Films

G. W. Bryant, L. S. Goldner,
National Institute of Standards and Technology, Gaithersburg, MD 20899-8423.

Fourier polarimetry has been adapted to near-field scanning optical microscopy (NSOM) and complete measurements of local dichroism, alignment of the dichroic axis, birefringence, independent alignment of the fast axis, and topography have been performed for the first time. The experimental methods and applications to block copolymer thin films are discussed in another presentation. In this presentation, we show how the measured local dichroism and local birefringence is related to local sample properties.

Simulations are performed to determine the contrast mechanisms that contribute to the measured local dichroism and local birefringence in block copolymer thin films. The block copolymer thin films are modeled as thin films with alternating parallel stripes of different polymers. A metal-coated optical-fiber NSOM tip in illumination mode is modeled. A finite-element time-domain approach is used to obtain transmitted fields. Simulations are performed for linear polarization of the probe field parallel and perpendicular to the stripes. Differences in transmission for the two polarizations give the local dichroism. Differences in the field phase for the two polarizations give the local birefringence.

Three contrast mechanisms are simulated: index contrast between polymer stripes, absorption contrast between polymer stripes, and topographic contrast between stripes. Recently it was shown[1] that a large-index film near an NSOM tip can significantly reduce the tip/air impedance mismatch, leading to a higher flux from the tip when the probe is over the film. In this case, the image contrast follows the emitted flux from the tip. However, for block copolymer thin films, scattering in the film, rather than modification of the tip output, is the dominant contrast mechanism. For example, when index variation is the contrast mechanism, the calculated dichroism and polarization dependence of the tip output show the opposite variation for scans across the alternating stripes. For typical copolymer films, the index contrast is a few percent. The calculated dichroism is also a few percent. This is significantly smaller than the observed dichroism, indicating that larger scattering effects, due to absorption and topography, are important. We find that absorption can provide larger dichroism. Near an interface between regions of low and high absorption, the polarization dependence of the transmitted flux depends on how the tip field overlaps the two regions. For tip polarization parallel to the interface, there is a rapid variation in transmitted flux as the tip scans the interface. The transmitted flux changes more slowly for tip polarization perpendicular to the interface. This determines the dichroism, which is nearly zero at an interface, of opposite sign on the two sides of the interface and nearly zero far from the interface. Topographic contrast can also produce large dichroism in films with parallel stripes. Again, the dichroism changes sign near an interface and is zero far from an interface. The dominant effect is the polarization dependence of diffraction by the topographic grating. The effects of topographic and absorption contrast are distinguishable because transmission and reflectivity dichroism have the same sign for absorption contrast and the opposite sign for topographic contrast.

These results are discussed in detail and the understanding we obtain is used to analyze the contrast in the local dichroism and local birefringence measurements of block copolymer thin films.

References

[1] A. L. Campillo, J. W. P. Hsu and G. W. Bryant, *Optics Letters* **27**, 415 (2002).

CARS Microscopy: 3D Vibrational Imaging of Living Cells

X. Sunney Xie, Ji-Xin Cheng
Department of Chemistry and Chemical Biology, Harvard University, Cambridge, MA 02138, USA

Coherent anti-Stokes Raman scattering (CARS) microscopy allows 3D imaging with inherent chemical selectivity based on vibrational spectra of molecules. (See Ref. 1.) To overcome the major drawback of this technique, the presence of a large non-resonant background arising from the electronic contributions, we demonstrated polarization CARS (P-CARS) microscopy. P-CARS effectively suppresses the non-resonant background by taking advantage of the polarization difference between the resonant signal and the non-resonant background. (See Ref. 2.) With P-CARS microscopy, we are able to image the protein distribution in living cells with high contrast. (Figure 1a&b.)

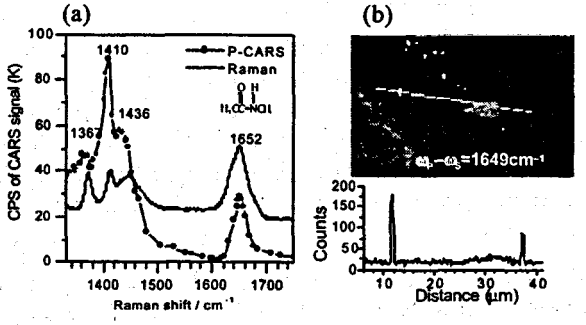

Figure 1. (a) Spontaneous Raman and polarization CARS spectra of N-methylacetamide (insert). The P-CARS amide I band at 1652 cm^{-1} shows a high signal to background ratio. (b) P-CARS image of an epithelial cell based on the contrast of the amide I band. The non-resonant background from water is effectively suppressed with the intensity profile across the line shown below.

Our theoretical study of CARS microscopy based on a Green's function formulation shows that the CARS far-field radiation pattern depends on sample size and shape. (See Ref. 3.) Epi-detection allows high-sensitivity imaging of small cellular organelles such as mitochondria by avoiding the large forward signal from water, while forward-detection can be used for visualizing large features such as nuclear membrane. (See Ref.'s 4-5.)

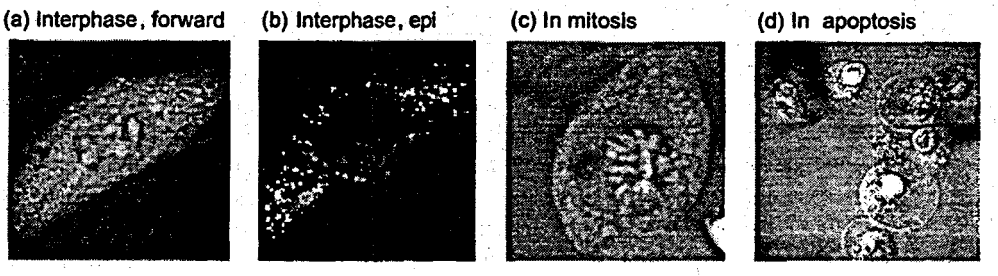

Figure 2. Laser-scanning CARS images of NIH3T3 fibroblasts cells (a) Forward-detected image of a cell in interphase, tuned to 2870 cm^{-1} (lipid C-H stretching). (b) Simultaneously epi-detected image of the same cell as in (a); (c) Forward-detected image of a cell in metaphase, tuned to 1090 cm^{-1} (DNA backbone vibration). (d) Forward-detected image of cells in apoptosis, tuned to 2870 cm^{-1}.

To achieve high speed imaging of living cells and tissues, we developed a laser-scanning CARS microscope that raster scans the collinearly overlapped pump and Stokes beams (See Ref. 6.). With this new microscope, both forward- and epi-detected images can be simultaneously recorded with high vibrational contrast and high spatial resolution. We carried out vibrational characterization of apoptosis in NIH3T3 fibroblast cells at a rate of several seconds per frame. (See Ref. 6.) Figure 2 shows CARS images of NIH3T3 fibroblastcells in interphase, mitosis and apoptosis. These advances show that CARS microscopy is becoming a powerful tool for biological imaging.

References:

1. Zumbusch, Holtom, Xie, Phys. Rev. Lett. 82, 4142-4145 (1999).
2. Cheng, Book, Xie, Opt. Lett. 26 (17), 1341-1343 (2001).
3. Cheng, Volkmer, Xie, J. Opt. Soc. Am. B, in press.
4. Cheng, Volkmer, Book, Xie, J. Phys. Chem. B 105 (7), 1277-80 (2001).
5. Volkmer, Cheng, Xie, Phys. Rev. Lett. 87, 023901 (2001).
6. Cheng, Jia, Zheng, Xie, Biophysical J. in press.

Numerical Analysis of Plasma Resonances in Noble Metal Nanostructures

Hiroharu Tamaru, Hitoshi Kuwata, Kenjiro Miyano,
Research Center for Advanced Science and Technology, The University of Tokyo, Tokyo 153-8904, Japan.

Finite Difference Time Domain (FDTD) method [1] has become a powerful tool for investigation of the optical interactions with materials in the near-field region due to its wide application allowing arbitrary morphology to be taken into account.

Despite its vast usefulness, the method is known to have some difficulties with calculations in some situations; One is the handling of good but not perfect conductors in which the imaginary part of the dielectric function is large, and another is the case of plasma resonance where the real part of the dielectric functions becomes small. Both of these are very much relevant to one of the most interesting aspects of the near-field optical interactions that involves noble metal nanostructures such as the case where Ag nanoparticles interact with each other and with light to exhibit the strong field enhancements and scattering cross sections.

In this work, FDTD calculations of the resonances of some 100 nm sized Ag and Au particles will be discussed. The dispersion relation of these metals are approximated by the Drude dispersion. Full visible range spectra for the near-zone or far-zone fields are calculated by means of Fourier transformation of the impulse response from the system. The resonance frequencies obtained are used as the criteria for the correctness of the calculation, since they are revealed to be one of the most sensitive quantities that are calculated by this method. Mie's theory of light scattering is employed as the exact analytical references for the calculation of spheres.

Different formulations of the FDTD method results in different degree of correctness in the calculation of this resonance. In either case, the time step Δt is shown to be the most sensitive parameter in the calculations. Specificly, the error in resonance frequency $\delta\omega$ tends to scale almost linearly with respect to Δt in some formulations. As an example with a Ag sphere of 100 nm in diameter, even when the Yee cell size is chosen to be as small as 1/80 of the resonance wavelength, the time step had to be decreased to 1/10 of that of the Courrant's condition to obtain the resonance frequency within a few percent of that of the analytical result.

With these cares taken into account, bi-sphere configurations have been studied in detail. The coupled system interact strongly when the sphere spacings are within a few nanometers; the odd and even coupled modes become active according to the excitation polarization. These results have been shown to well account for the actual experiments performed for individual bi-spheres identified by scanning electron microscope [2].

Other morphologies of interests are nanorods [3]. The effect of the depolarization factor arising from its morphology to its resonance frequency and its local field enhancement should be an ideal system to study the relation between the sphere case and the metal tip case as in the probes of the scattering type SNOM.

References

[1] K. S. Yee, *IEEE Trans. Antennas Propagat.* **AP-14**, 302 (1966).

[2] H. Tamaru, H. Kuwata, H. T. Miyazaki and K. Miyano, *Appl. Phys. Lett.* **80**, 1826 (2002).

[3] S.-S. Chang *et al.*, Langmuir **15**, 701 (1999).

Near-field second-harmonic generation excited by local field enhancement

A. Bouhelier, M. Beversluis, A. Hartschuh, and L. Novotny,
University of Rochester, The Institute of Optics, Rochester, NY 14627.

The field near a sharp metal tip can be strongly enhanced if irradiated with an optical field polarized along the tip axis [1, 2]. Illumination from side of the tip is widely used but give rise to a strong background and large illumination area [3, 4]. Tightly focused higher-order beams provide an alternative to side illumination. A strong longitudinal field is created at the focus which can give rise to field enhancement [5]. We demonstrate that the enhanced field produces local second-harmonic (SH) generation at the tip surface thereby creating a highly confined photon source. A theoretical model for the excitation and emission of SH radiation at the tip is developed and it is found that this source can be represented by a single on-axis oscillating dipole. The model is experimentally verified by imaging the spatial field distribution of strongly focused laser modes as seen in Fig. 1. Whereas the SH generated at a tip is mostly sensitive to the field oriented along its long axis, The SH excited by a small gold particle is sensitive to the total field strength, *i.e.* the transverse contribution plus the longitudinal one.

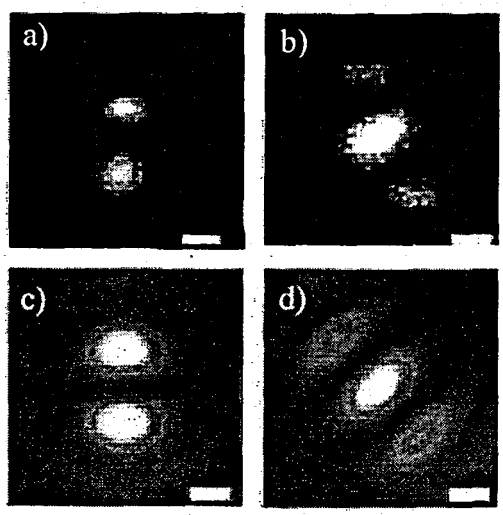

Figure 1: Tip-induced SH image of the focal fields of a strongly converging Gaussian HG_{00} beam (a), and a Hermite-Gaussian HG_{10} beam (b). The lobes are oriented in direction of the incident polarization. (c) and (d) show the calculated longitudinal field distributions ($E^2_{o,z}$) just above the glass surface suggesting that SH generation at the metal tip is induced by the longitudinal field. Scale bars: 250nm.

References

[1] L. Novotny, R. X. Brian, and X. Sunney Xie, *Phy. Rev. Lett.* **79**, 645 (1997).

[2] O. J. F. Martin, and C. Girard, *Appl. Phys. Lett.* **70**, 705 (1997).

[3] F. Zenhausern, M. P. O'Boyle, and H. K. Wickramasinghe, *Appl. Phys. Lett.* **65**, 1623 (1994).

[4] P. Gleyzez, A. C. Boccara, and R. Bachelot, *Ultramicroscopy* **57**, 318 (1995).

[5] L. Novotny, E. J. Sànchez, and X. Sunney Xie, *Ultramicroscopy* **71**, 21 (1998).

Manifestation of an electric dipole order induced by optical near fields

A. Shojiguchi, K. Kobayashi [A], K. Kitahara, S. Sangu [A], M. Ohtsu [A, B],
International Christian University, 10-2-3, Mitaka, Tokyo 181-8585, Japan,
A) ERATO/JST, 687-1 Tsuruma, Machida, Tokyo 194-0004, Japan,
B) Tokyo Institute of Technology, 4259 Nagatuta, Midori-ku, Yokohama, Kanagawa 226-8502, Japan.

Owing to the recent progress in fine processing technology it becomes possible to investigate the interaction via optical near fields among materials in nano meter scale [1]. Since one of the remarkable characters of optical near fields is non-propagating property, it is more suitable to use localized functions as a basis set than to use plane waves to describe optical near fields. We present a phenomenological model of a near field photon-matter system using such a localized function to describe optical near fields. We suppose quantum dots chain as a matter system and model it as one-dimensional N two-level system (in other words, excitons) with a periodic boundary condition. A localized photon is described as a harmonic oscillator localized in each site, and only allowed to hop to the nearest neighbor sites. As a result of the interaction, quantum dots emit and absorb localized photons. A Hamiltonian of the system consists of three parts as follows:

$$H = (H_a + H_b) + H_{int}$$

Here H_a describes localized photons, H_b describes excitons, and H_{int} represents the localized photon-exciton interaction. Each Hamiltonian can be expressed as

$$H_a = \varepsilon \sum_{n=1}^{N} a_n^{+} a_n + V \sum_{n=1}^{N} (a_{n+1}^{+} a_n + a_n^{+} a_{n+1}),$$

$$H_b = E \sum_{n=1}^{N} b_n^{+} b_n,$$

$$H_{int} = U \sum_{n=1}^{N} (a_n^{+} b_n + b_n^{+} a_n),$$

where n indicates the site number, and a_n (a_n^{+}) and b_n (b_n^{+}) represent annihilation (creation) operators of a localized photon and an exciton, respectively.

We investigate dynamical properties of the system driven by the Hamiltonian. As shown in Fig. 1, we predict a coherent oscillation of dipoles of the whole system started from an initial condition, and show that we can classify each dipole oscillation of the system into four groups depending on the parameters of the Hamiltonian.

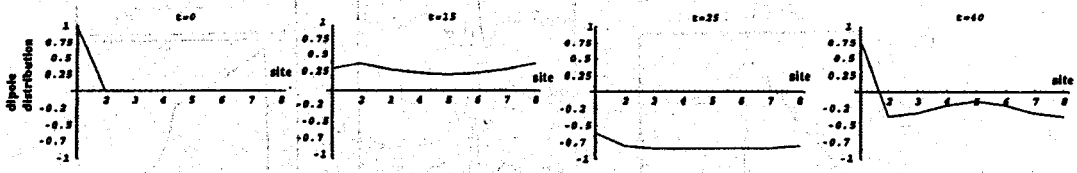

Figure 1: Time evolution of the dipole moment distribution. The vertical and horizontal axes represent the dipole moment and the site number of quantum dots.

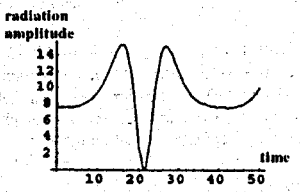

Figure 2: Time evolution of the radiation amplitude. The super-radiatiant state has the value of 20 as the radiation amplitude.

Moreover radiation probability of each state is examined in Fig. 2. It indicates that the state with the coherent oscillation is close to the Dicke's superradiant state. We will discuss the ordering mechanism in detail.

Reference

[1] M. Ohtsu, K. Kobayashi, H. Ito, and G. H. Lee, *Proc. IEEE* **88**, 1499(2000).

Femtosecond coherent near-field spectroscopy of single quantum dots

Tobias Günther, Kerstin Müller, Christoph Lienau, Thomas Elsaesser
Max-Born-Institut für Nichtlineare Optik und Kurzzeitspektroskopie D-12489 Berlin, Germany

Soheyla Eshlaghi, Andreas Wieck
Lehrstuhl für Angewandte Festkörperphysik, Universität Bochum, D-44870 Bochum

Quantum dots currently attract much interest as model systems for artificial solid state atoms and as probes of wavefunction localization in disordered media. The potential of using their optical excitations as bits for semiconductor-based implementations of quantum information processing is under intense investigation. Such implementations rely on the ability to probe and control optical nonlinearities in single and coupled quantum dots on ultrafast time scales, a research field that remains to be explored.

In this paper, we describe and demonstrate a novel technique, combining near-field optics and femtosecond pump-probe spectroscopy to analyze the nonlinear optical response of single quantum dots on ultrafast time scales [1]. We investigate single natural quantum dots (QD) formed at interface fluctuations of a 5 nm (100)GaAs quantum well. Differential reflectivity (ΔR) spectra are resolved with < 200 nm and 100 fs in a near-field pump-probe setup at 12 K at time delays Δt between pump and probe laser.

For $\Delta t>0$, the ΔR spectra show ultrasharp (50 μeV) Lorentzian resonances from single QDs (Fig. (d)). The slow decay of ΔR with time constants of 30 – 100 ps reflects the QD population lifetime (a). The early time ΔR dynamics are unexpected, when modeling the QD as an artifical atom. We find a long persistence of ΔR at negative Δt (b) and pronounced spectral oscillations around the excitionic QD resonance (c). These are clear signatures of the perturbed free induction decay of the coherent QD polarization: Coulomb scattering with photoexcited carriers leads to additional damping of the QD polarization (e). The now established ability to dynamically probe the QD polarization opens new ways for measuring and controlling polarization interactions on femtosecond time scales. Possible applications for quantum information processing will be discussed.

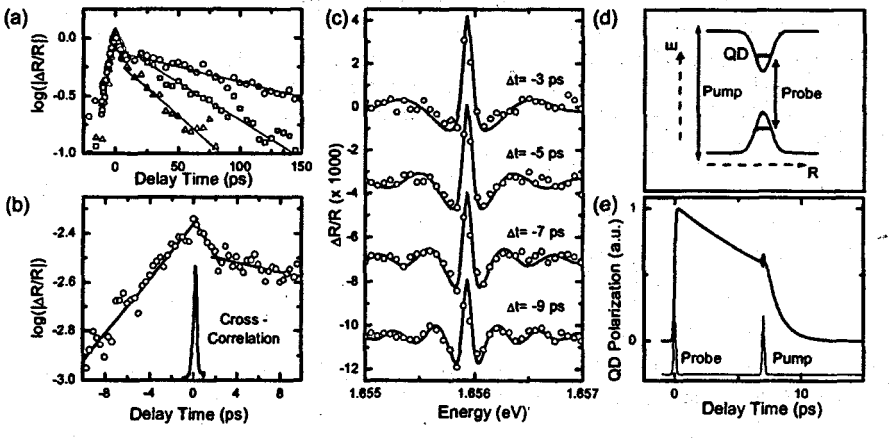

Figure 1: (a) Time evolution of ΔR for three different dot resonances. The slow decay reflects the QD lifetime of 30 to 100 ps. (b) At negative delay times, $\Delta t<0$, a pronounced ΔR signal persists for up to -10 ps, reflecting the perturbed free induction decay of the coherent QD polarization. (c) Near-field $\Delta R/R$-spectra at different $\Delta t<0$ show pronounced spectral oscillations around the excitonic resonance: Coulomb scattering with photoexcited carriers leads to additional damping of the QD polarization. (d) Schematic energy diagram. (e) QD polarization dynamics.

References

[1] T. Günther et al., Phys. Rev. Lett., in press (2002).

The electrodynamics of fluorescing molecules interacting with metallic nano-cavities

J. Enderlein, Institute for Biological Information Processing 1, Forschungszentrum Jülich D-52425 Jülich, Germany

It is well known that the fluorescence emission properties of molecules can be dramatically changed by the presence of metals within wavelength distance [1,2]. Due to the electromagnetic interaction of the emitting dye with the metal, the spontaneous emission rate can be enhanced or inhibited, depending on the exact dye-metal geometry [3]. When considering fluorescence near metals, three effects have to be taken into account: (i) the changed intensity of the exciting electric field, due to the interaction of the incident light with the metal; (ii) the altered lifetime of the excited state of the molecule due to its electromagnetic interaction with the metal; (iii) the partial absorption of emitted energy by the metal.

The photophysical properties of fluorescing molecules near metallic layers have been extensively studied both experimentally [2] and theoretically [4], showing the well known effects of fluorescence lifetime modification, fluorescence quenching, and enhanced photostability. Although it was shown that under favorite conditions (proper fluorophore/metal distance) fluorescence quenching by the metal is compensated by locally enhanced field intensity and enhanced photostability, no dramatic change in total fluorescence yield is observed.

The situation changes dramatically when considering the fluorescence of molecules near nanoscopic metallic particles or within metallic nanocavities. The paper presents a quantitative treatment of fluorescence emission of single molecules in a nanometrically structured metallic environment within the framework of classical electrodynamics, which has proven to be extremely successful in treating similar problems in the past, see e.g. [4]. In particular, the fluorescence excitation and emission of fluorescing molecules within closed metallic nanocavities are studied [5]. It is found that under favorite geometrical conditions, the fluorescence properties of the molecules are significantly enhanced, increasing their detectable fluorescence brightness and photostability by one to two orders of magnitude. These effects become even more pronounced when considering multi-photon excitation of fluorescence. Furthermore, significant changes in absorption and emission spectra are predicted. Besides the pure fundamental interest in the interaction between molecular dipole emitters and metallic nanocavities, the found results have far reaching consequences for many practical applications, such as devising new lasing materials, or fluorescent labels with unusual properties.

[1] E. M. Purcell, *Phys. Rev.*, **69**, 681 (1947).
[2] K. H. Drexhage, *Progress in Optics* **XII**, 165 (1974).
[3] D. Kleppner, *Phys. Rev. Lett.*, **47**, 233 (1981).
[4] R. R. Chance, A. Prock, and R. Silbey, *Advances in chemical physics*, **37**, 1 (1978).
[5] J. Enderlein, *Appl. Phys. Lett.* (2002) in press.

Near-field second harmonic microscopy with half-metal-coated tip: application to imaging of ferroelectric domains

H.Y. Liang, I.I. Smolyaninov, C.C. Davis, R. Ramesh, C.H. Lee
University of Maryland, ECE Dept., College Park, MD 20742

Optical second harmonic generation (SHG) is a sensitive technique for characterization and investigation of the symmetry properties of different samples [1] It is known to be affected by crystal structure, magnetic and ferroelectric order, mechanical strain, etc. Recently we have introduced a near-field optical SHG microscopy technique for imaging of ferroelectric thin films with a bare tapered fiber tip, externally illuminated with femtosecond laser pulses. Our results indicated resolution of the order of 80nm and sensitivity to local crystal symmetry. [2]

In our new experiment, we used weakly focused light from a Ti:sapphire laser regenerative amplifier (working at 810 nm, repetition rate 100kHz, 100 fs puse duration and ~5μJ pulse energy) to illuminate the ferroelectric sample, with an incident angle around 50°. A half-metal-coated tip was used to replace the uncoated tip we used in our previous work [2]. The tip was drawn by a standard heating and pulling procedure from a single mode fiber, then coated with a layer of gold, about 100nm thick, on one side The other side was transparent. The light collection efficiency of this tip is comparable to that of the uncoated tip when properly mounted, and it has the potential of working as one electrode of ferroelectric memory cell. The tip was scanned over the sample surface with a constant tip-surface distance of a few nanometers using shear force feedback control. Therefore, surface topography images were obtained while simultaneously recording the SH near-field distribution.

One concern with this kind of a tip is whether it itself generates SH light. To check this, we studied the distance dependence of SH signal. At a tip-sample distance of several wavelengths, the SH signal dropped down to almost zero, which indicated that the SH was from the sample instead of the tip. At the same time, we noticed a strong enhancement of SH intensity in the near field region. Within ~ 1μm tip-sample distance range, the SH dropped sharply from ~400 counts/second in the near-field of the sample to ~80 counts/second far from the sample. This obvious near-field behavior gives this kind of a tip a potential to obtain higher quality near-field SH images.

In order to apply this tip to the study of ferroelectric domain switching dynamics, we need to relate the SH signal with different remnant polarization of the ferroelectric domains. Similar to our previous work with uncoated tips [3], we performed the study of polarization behavior of near-field SHG using a poled BaTiO3 single crystal. Phase-matched SHG is prohibited in BaTiO3 because of its strong dispersion. As a result, the measured signal originates from the surface, resembling the case of a thin film. For each poling direction of the crystal, we have got different symmetry of the SH signal, and different intensity of SHG. In contrast to our previous work with uncoated tips, near-field SHG detected with half-coated tip is much stronger in the case of S- polarized excitation light. Large differences between SH signal for different crystal poling directions enable us to recover the local poling direction in thin ferroelectric films.

This work was supported in part by the University of Maryland NSF-MRSEC.

Reference:

1. Y. R. Shen *The Principles of Nonlinear Optics* Wiley, New York (1984)
2. I. I. Smolyaninov, H. Y. Liang, C. H. Lee, C. C. Davis, S. Aggarwal & R. Ramesh Opt. Lett. **25**, 835 (2000)
3. I. I. Smolyaninov, H. Y. Liang, C. H. Lee, C. C. Davis, V. Nagarajan, R. Ramesh, Journal of Microscopy **202**, 250 (2000)

Near-field autocorrelation spectroscopy: Quantum mechanical level repulsion in interface quantum dots

Francesca Intonti, Valentina Emiliani, Christoph Lienau, Thomas Elsaesser
Max-Born-Institut für Nichtlineare Optik und Kurzzeitspektroskopie D-12489 Berlin, Germany

Vincenzo Savona, Erich Runge, Roland Zimmermann
Institut für Physik, Humboldt Universität, D-10117 Berlin, Germany

Localized states play a key role for the optical and transport properties of disordered quantum systems, e.g., thin quantum wells (QW). Here, exciton localization within a spatially fluctuating, interface-roughness induced disorder potential gives rise to inhomogeneous broadening of far-field spectra. In experiments with high spatial and spectral resolution the spectra break up into narrow emission spikes (Fig (b)) from excitons localized in single quantum dots (QD). So far, it has been difficult to infer from such spectra precise information about the underlying disorder potential or the nature of the excitonic QD wavefunctions.

In this paper we demonstrate that near-field autocorrelation spectroscopy is a particular sensitive probe of both the underlying disorder potential and the localization length of the excitonic wavefunction. The technique is based on a statistical analysis of the two-energy autocorrelation function of a large ensemble of near-field PL spectra. We discuss near-field autocorrelation spectra $R_c(\Delta E)$ of thin (311)A and (100) GaAs QW and compare these data to a two-dimensional quantum theory of the exciton motion. On a (311)A QW (Fig. (c)), we find clear experimental evidence that the non-negligible spatial overlap of excitonic wavefunctions gives rise to a level-repulsion of the excitonic eigenenergies[1]. This quantum-mechanical hallmark of Anderson localization manifests itself in a prounced dip in $R_c(\Delta E)$ at energies between 1 and 3 meV (Fig (c), inset). Here, a single disorder correlation length of 17 nm reproduces the experimental data well. The system displays weak localization and the wavefunctions extend over several minima of the disorder potential, clearly evidenced by an analysis of the energy-dependent exciton localization length and by the level repulsion dip. Autocorrelation spectra on (100) QWs are markedly different and show characteristic features of strong localization, where several exciton eigenstates are localized within a single potential mimimum and these minima have similar shape and size. Applications of these new technique to other types of nanostructures are discussed.

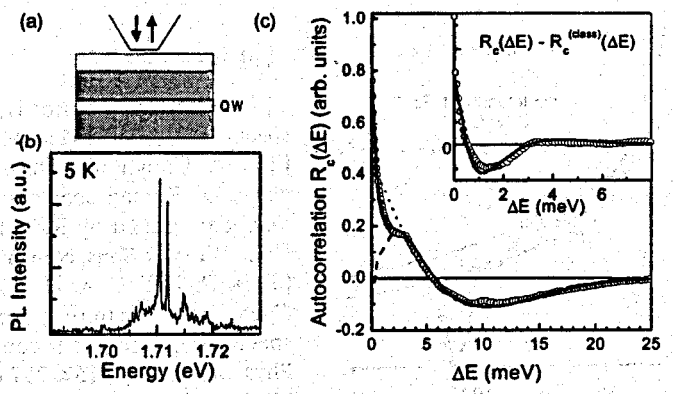

Figure 1: (a) Schematic of the experiment. A 3 nm (311A) GaAs QW is excited and the QW PL is collected through the near-field probe (b) Representative near-field PL spectra. (c) Autocorrelation function $R_c(\Delta E)$ for experiment (circles) and model calculation (solid line). Inset: Difference between $R_c(\Delta E)$ and classical autocorrelation $R_c^{(class)}(\Delta E)$, highlighting the level repulsion effect.

References

[1] F. Intonti et al., Phys. Rev. Lett. 87, 076801 (2001).

Gradient-Field Raman: Selection Rules in the Near Field

H. D. Hallen, E. J. Ayars** and C. L. Jahncke****

** Physics Department, North Carolina State University, Raleigh, NC 27695-8202*
*** Physics Department, Walla Walla College, College Place, WA 99324*
**** Physics Department, St. Lawrence University, Canton, NY 13617*

The metal aperture at the apex of a near-field scanning optical microscope (NSOM) probe locally concentrates the electric field. As these evanescent fields decay on a nanometer length-scale, strong field gradients are produced. These gradients have profound effects on the Raman spectra of samples within them, leading to a "Gradient-Field Raman" (GFR) effect. It leads to new selection rules for surface enhanced Raman spectroscopy (SERS), for example see [1,2] and references within, and also to differences between far-field and near-field Raman spectroscopy measured with a near-field optical microscope. [3,4] We describe how a strong gradient of the electric field can alter the Raman spectra, and investigate its implications on selection rules. Heuristically, the field gradient causes the Coulomb force on a polarized bond to vary during the vibration, providing a new coupling mechanism between the field and the vibration. These selection rules differ markedly from the usual Raman selection rules, and allow Raman-like observation of strong IR (not normally Raman) vibrations.

In NSOM, a sharpened optical fiber is coated with aluminum to form an aperture. The probe is positioned near the surface under lateral force feedback. The NSOM is used in illumination mode, with 514 nm Ar ion laser light coupled into the fiber probe. Reflected light is collimated with a 0.50 NA lens, passed through a holographic filter, focused into a Czerny-Turner spectrometer, and finally collected onto a cooled (-45 C) CCD camera. New peaks not observed in the far-field spectra observed as the probe approaches the surface. Using difference spectra to highlight the changes, we find the distance dependence for the B1 peak of KTP. This vibration is the strong IR absorption mode at 712 cm^{-1} [5] but is not Raman-allowed in the geometry of our far-field experiment. The probe-sample distance dependence of the peaks is shown in Fig. 1, along with the best-fit Raman and GFR models. The GFR describes the data quite well except for the derivative-like variation near 90 nm, which we attribute to coupling with plasmons on the Al probe coating. [6]

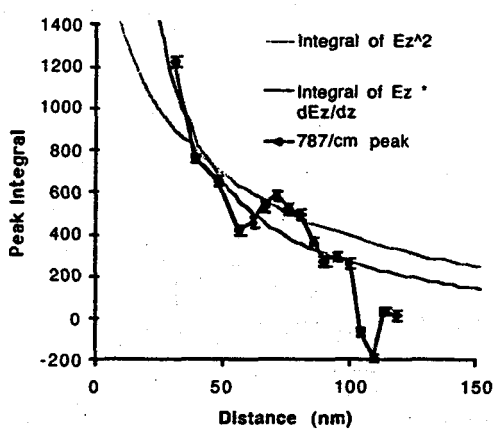

Figure 1. The probe-sample distance-dependence of the NSOM-Raman difference spectra is compared to the standard Raman and GFR models.

References

1] Martin Moskovits, "Surface-enhanced spectroscopy," Rev. Mod. Phys. **57**, 783 (1985).
[2] J. A. Creighton, "The selection rules for surface-enhanced Raman spectroscopy," in *Spectroscopy of Surfaces*, Edited by R. J. H. Clark and R. E. Hester (John Wiley & Sons, New York, 1988) 37.
[3] H. D. Hallen, A. H. La Rosa and C. L. Jahncke, "Near-field scanning optical microscopy and spectroscopy for semiconductor characterization," Phys. Stat. Sol. (a) **152**, 257 (1995).
[4] E. J. Ayars, H. D. Hallen and C. L. Jahncke, "Electric field gradient effects in Raman spectroscopy," Phys. Rev. Lett. **85**, 4180 (2000).
[5] J. C. Jacco, Materials Research Bulletin **21**, 1189 (1986).
[6] H. D. Hallen and E. J. Ayars, (in preparation)

Vibrational Modes of an Individual Single Wall Carbon Nanotube Observed by Near-field Enhanced Raman Spectroscopy

Norihiko Hayazawa[1),2)], Takaaki Yano[1)], Yasushi Inouye[2),3),4)], and Satoshi Kawata[1),2),3),5)]

1)Department of Applied Physics, Osaka University, Suita, Osaka 565-0871, Japan

2)CREST, Japan Corporation of Science and Technology, Japan

3)Handai FRC, Suita, Osaka 565-0871, Japan

4)School of Frontier Bioscience, Osaka University, Suita, Osaka 565-0871, Japan

5)RIKEN, Wako, Saitama, 351-0198, Japan

Local vibrational modes of an individual Single Wall Carbon Nanotube (SWNT) were observed by near-field enhanced Raman spectroscopy. We demonstrated the near-field enhanced Raman spectroscopy with the use of a metallized cantilever tip and a highly p-polarized light illumination onto the tip[1,2]. P-polarized light field excites surface plasmon polaritons localized at the very tip apex which result in the enhanced elctric field well localized at the tip. This localized enhanced electric field is utilized for the near-field Raman excitation, allowing for the observation of the local vibrational modes of single wall carbon nanotubes.

Due to the strong coupling between electron and phonons in the resonance Raman effect, the unique 1D electric density of states (EDOS) of SWNTs play an important role in the unusual resonant Raman spectra of SWNTs associated with the bandgap (E_g) that is equal to the energy difference (E_{ii}) between the two van Hove singularities [3]. Thus, Raman spectroscopy has been realized to be one of the powerful tools to investigate the properties of SWNTs because Raman spectroscopy can allow for the in-situ direct observation of molecular vibration modes. The very large EDOS at the van Hove singularities with the illumination of the corresponding laser energy result in the high intensities of resonant Raman effect of SWNTs. According to the calculation [4] of E_{ii}, at the excitation wavelength of 532 nm (2.33 eV) for the diameter range d_t from 1.22 to 1.51 nm, only the small resonance of E_{33}^S can be expected.

Figure 1a shows the near-field enhanced Raman spectrum of a SWNT. Remarkable tangential G-band peaks of SWNT which is split into 2 peaks at 1593 cm^{-1} and 1569 cm^{-1} and small D-band peak at 1331 cm^{-1} are observed due to the localized enhanced electric field at the tip apex. The observed G-bands are well fitted by the Lorentzian line shape and are lacking in the Breit-Wigner-Fano (BWF) line shape [3] that is observed in the resonant Raman spectra of metallic nanotubes. These G-band features follow the facts that only the semiconducting nanotube is in resonance. On the other hand, in Fig.1b, the far-field Raman spectrum of a SWNT including some impurities (amorphous carbon) without a probe exhibits no distinguishable peak because of no enhancement by the probe. The laser power and the exposure time of each spectrum are 1.65 mW and 1 minute, respectively.

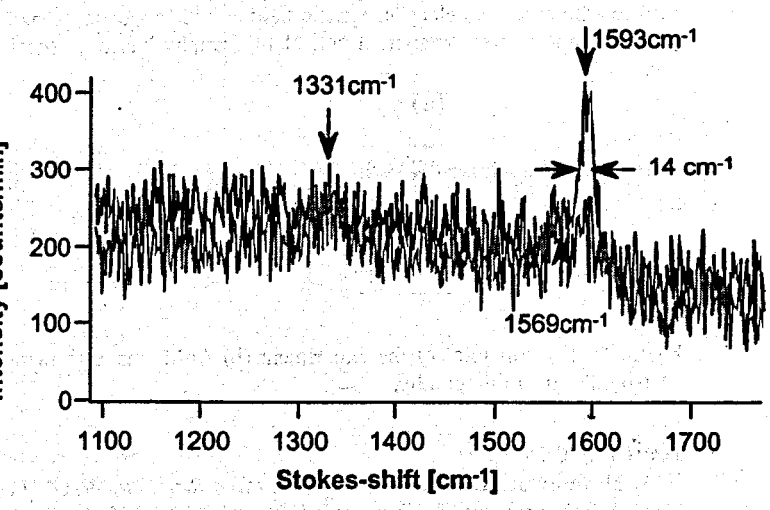

Figure1 a,Near-field and b,far-field Raman spectra of an individual SWNT.

References

[1] N. Hayazawa, Y. Inouye, Z. Sekkat, & S. Kawata, Chem.Phys.Lett. **335**, 369 (2001).

[2] N. Hayazawa, Y. Inouye, Z. Sekkat, & S. Kawata, Opt.Commun. **183**, 333 (2000).

[3] M. S. Dresselhaus and P. C. Eklund, Advances in Physics, 49, 705 (2000).

[4] H. Kataura et al., Synthetic Met. **103**, 2555 (1999).

Investigation of local field enhancement at the end of SNOM tips using photosensitive azobenzene-containing materials

F. H'Dhili, R. Bachelot, G. Lérondel, D. Barchiesi, R. Fikri, A. Rumyantseva and P. Royer
Laboratoire de Nanotechnologie et d'Instrumentation Optique, Université de Technologie de Troyes, 12 rue Marie Curie - BP 2060 - 10010 Troyes Cedex, France

N. Landraud
Laboratoire de Physique de la Matière Condensée, UMR 7643-CNRS, Ecole Polytechnique, 91128 Palaiseau Cedex, France

Recent theoretical works have shown that strong Field Enhancement (FE) can be obtained at the extremity of a metallic apertureless SNOM tip under laser illumination (for example see Refs [1-3]). FE occurs in the tip near-field, within an area of tens of nanometers of diameter. This effect is very promising for the SNOM community because the tip apex could act as a sub-wavelength size optical source.

We introduce a method to experimentally investigate the FE. The method is based on the use of photosensitive samples [4,5]. The experiment is schematically depicted in Fig. 1a. A metallic apertureless SNOM probe is approached at a few nanometers distance from a photosensitive sample (azobenzene-containing material [6]). The probe-sample junction is then illuminated by a laser beam. The photosensitivity of the sample permits us to make a "snapshot" of the spatial distribution of optical intensity in the vicinity of the probe. This distribution is coded by surface topography, which is characterized, after exposure and *in situ*, by Atomic Force Microscopy using the same probe.

The obtained results validate the concept of optical nanosource at the extremity of an apertureless metallic SNOM tip. We study the influence of various parameters, including the probe geometry, the probe material and the polarization state of the incident field. The experimental data are found to be in agreement with numerical calculations of the tip near-field. Additionally we discuss the nature of the local interaction between the enhanced electromagnetic field and the azobenzene molecules. Finally we present preliminary results of apertureless near-field optical lithography based on local field enhancement (see example Fig. 1b).

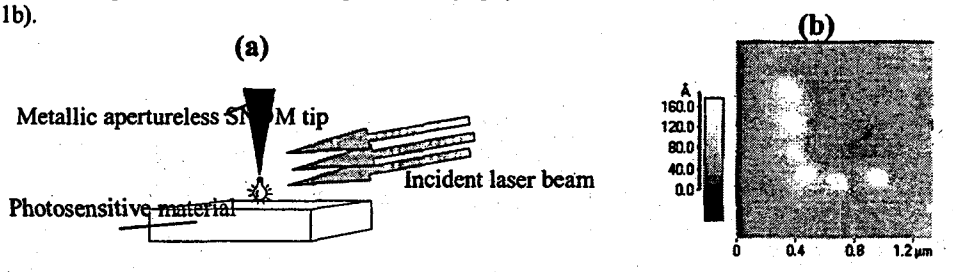

Figure 1 : (a) Principle of the experiment (b) AFM image showing the letter 'L' written by apertureless near-field optical lithography.

References

[1] L. Novotny, R. X. Bian, and X. S. Xie, *Phys. Rev. Lett.* **79**, 645 (1997).
[2] O. J. F. Martin, and C. Girard, *Appl. Phys. Lett.* **70**, 705 (1997).
[3] Y. Martin, H. F. Hamann, and H. K. Wickamasinghe, *J. Appl. Phys.* **89**, 5776 (2001).
[4] G.Wurtz, R. Bachelot, F. H'dhili, P. Royer, C. Triger, C. Ecoffet, and D. J. Lougnot, *Jpn. J. Appl. Phys.* **39**, 98 (2000).
[5] F. H'Dhili, R. Bachelot, G. Lerondel, D. Barchiesi and P. Royer, *Appl. Phys. Lett.* **79**, 4019 (2001).
[6] N. Landraud, J. Peretti, F. Chaput, G. Lampel, J.-P. Boilot, K. Lahlil, and V. I. Safarov, *Appl. Phys. Lett.* **79**, 4562 (2001).

Scanning Near-field Optical Microscopy Using Semiconductor Nanocrystals as a Local Fluorescence and Fluorescence Resonance Energy Transfer Source

G. T. Shubeita, S. K. Sekatskii, G. Dietler, Institut de Physique de la Matière Condensée Université de Lausanne, BSP, CH 1015 Lausanne – Dorigny, Switzerland
I. Potapova, A. Mews, Th. Basché, Institut für Physikalische Chemie Johannes Gutenberg-Universität Mainz, 55095 Mainz, Germany

Semiconductor nanocrystals, especially CdSe ones, are considered as very prospective objects for all kinds of the fluorescence microscopy due to their excellent photophysical properties and for the possibility to tune their fluorescence spectra by changing their sizes through varying their synthesis conditions (see, e. g. [1]). In particular, essentially better photostability in comparison to dye molecules is anticipated for CdSe nanocrystals, which makes them especially suitable to be used in applications aiming the use of a single fluorescence center as a light source. This is very important for the recently proposed [2] Fluorescence Resonance Energy Transfer Scanning Near-field Optical Microscopy (FRET SNOM), where donor fluorescent centers located in the tip apex are used to excite the fluorescence of acceptor centers of the sample (or vice versa). When a single fluorescence center located in the tip apex is used as an excitation source, the spatial resolution can be increased up to 2 – 4 nm (Förster radius) with the sensitivity exceeding that of a usual apertured SNOM [2].

Here we report an experimental realization of the local fluorescent probe based on CdSe nanocrystals. CdSe nanocrystals possessing a narrow size distribution and a high fluorescence quantum yield were synthesized and coated by thin protective ZnS layers in Mainz University (see [3] and references therein for details). Local fluorescent probes were prepared by dipping and extraction of the standard apertured SNOM fiber probe having an aperture of 100 – 200 nm into a solution of CdSe nanocrystals and 1 – 2 vol % of PMMA or polystyrene in toluene. After such a procedure and subsequent rapid drying of the solvent we obtain the SNOM fiber probe coated with a 30 – 100 nm – thick layer of the polymer containing nanocrystals with the concentration of $10^{16} – 10^{18}$ cm^{-3}. The existence of such a layer was confirmed using scanning electron microscopy and experiments with the similarly prepared local fluorescent probes based on dye molecules [4].

Local probes were excited by coupling the 458 nm spectral line of cw Ar ion laser into the opposite end of the fiber probe. They were scanned in the vicinity of the sample in a usual manner using the tuning fork – based shear-force distance regulation. When we record the optical image of a sample in the spectral range of the fluorescence of the CdSe nanocrystals, we exploit our probes as local fluorescent probes. (See, e. g. Ref. [5] for a discussion of local fluorescence probes and their prospectives). These same probes can be exploited as FRET SNOM probes when one records fluorescence from the sample stained with dye molecules capable to work as acceptors for the CdSe nanocrystal donors. Dyes suitable to function as acceptors in a CdSe-dye FRET pair were selected by us earlier.

Different samples were studied using these local probes based on the CdSe nanocrystals, and the corresponding experimental results will be discussed. In particular, the dependence of the fluorescence intensity on the local refraction index of the sample was recorded.

References

[1] A. D. Yoffe, *Adv. Phys.* **50**, 1 (2001).
[2] S. K. Sekatskii and V. S. Letokhov, *Appl. Phys. B.: Laser. Opt.* **63**, 525 (1996).
[3] G. Schlegel, J. Bohnenberger, I. Potapova and A. Mews, *Phys. Rev. Lett.* **88**, 137401 (2002).
[4] G. T. Shubeita, S. K. Sekatskii, G. Dietler and V. S. Letokhov, *Appl. Phys. Lett.* **80**, (2002).
[5] V. Sandoghdar and J. Mlynek, *J. Opt. A. Pure Appl. Opt.* **1**, 523 (1999).

Near-field Raman Imaging of Organic Molecules by an Apertureless Metallic Probe Scanning Optical Microscope

Norihiko Hayazawa[1,2], Yasushi Inouye[2,3,4], Zouheir Sekkat[1,2,3,6], and Satoshi Kawata[1,2,3,5]

1)Department of Applied Physics, Osaka University, Suita, Osaka 565-0871, Japan
2)CREST, Japan Corporation of Science and Technology, Japan
3)Handai FRC, Suita, Osaka 565-0871, Japan
4)School of Frontier Bioscience, Osaka University, Suita, Osaka 565-0871, Japan
5)RIKEN, Wako, Saitama, 351-0198, Japan
6)School of Science and Engineering, Al Akhawayn University in Ifrane, 53000 Ifrane, Morocco.

Near-field Raman Imaging of organic molecules is demonstrated by an apertureless near-field scanning optical microscope [1], the tip of which is a silver-layer-coated cantilever of an atomic force microscope (AFM). The virtue of the enhanced electric field at the tip apex due to the surface plasmon polariton excitations enhances the Raman scattering cross-sections [2, 3]. This phenomenon allows us to reveal from near-field Raman images the molecular vibrational distributions of Rhodamine6G and Crystal Violet molecules beyond the diffraction limit of a light. These molecular vibrations cannot be distinguished by AFM topographic images. Fig. 1 (a) is obtained at 607 cm^{-1} which corresponds to the Stokes-shifted-line of the C-C-C in-plane bending vibration mode of Rhodamine6G, Fig. 1 (b) is obtained at 908 cm^{-1} which corresponds to the Stokes shifted-line of the C-H out-of-plane bending vibration mode of Crystal Violet, and Fig. 1 (c) is a corresponding topographic image in AFM operation.

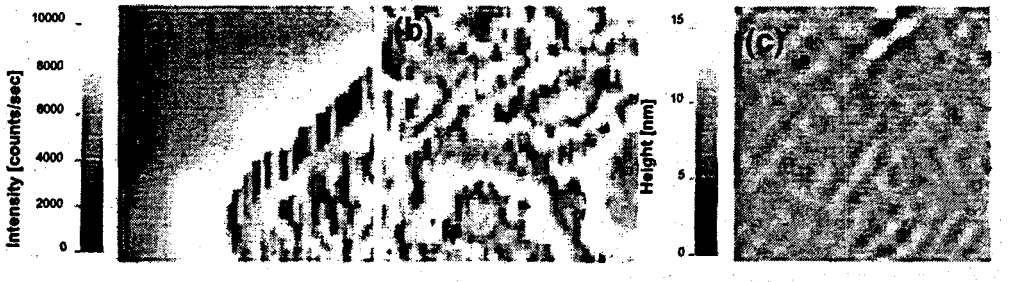

Figure 1 (a) A Near-field Raman image obtained at 607 cm^{-1}; C-C-C in-plane bending mode of Rhodamine6G, (b) A Near-field Raman image obtained at 908 cm^{-1}; CH out-of-plane bending mode of Crystal Violet, and (c) the corresponding topographic image. It took 10 minutes to obtain one image where 1 μm by 1 μm scanning area consisted of 64 by 64 pixels.

References

[1] Y. Inouye and S. Kawata, Opt.Lett., **19**, 159 (1994).

[2] N.Hayazawa, Y. Inouye, Z.Sekkat, and S.Kawata, Opt.Commun., **183**, 333 (2000).

[3] N.Hayazawa, Y. Inouye, Z.Sekkat, and S.Kawata, Chem.Phys.Lett., **335**, 369 (2001).

Real-Space Mapping of Exciton and Biexciton Wave Functions in GaAs Quantum Dot by Near-Field Optical Imaging Spectroscopy

T. Saiki and K. Matsuda
Kanagawa Academy of Science and Technology, Kawasaki, Kanagawa, Japan

S. Nomura
University of Tsukuba, Tsukuba, Ibaraki, Japan

M. Mihara and K. Aoyagi
RIKEN, Wako, Saitama, Japan

The near-field optical studies of semiconductor single quantum dots (QDs) or quantum wires have provided insight into their intrinsic properties by eliminating the ensemble averaging. Beyond such single-constituent spectroscopy, the next challenge of NSOM measurement is to directly illustrate and control the internal features of the quantum confined systems [1]. Theoretical works predict that if the spatial resolution of near-field scanning optical microscopy (NSOM) reaches the length scale of the quantum structures, the NSOM allows a mapping of real-space distribution of eigenstates (wave functions) [2]. In this paper, we demonstrate near-field imaging spectroscopy of a single GaAs island-like QD with a spatial resolution of 35 nm and map out center-of-mass wave functions of exciton and biexciton.

The sample investigated was island-like QDs formed at the interface of a GaAs quantum well structure. An aperture-type NSOM probe was prepared by the chemical etching technique for the tapering and by the impact method for the aperture formation. Photoluminescence (PL) imaging spectroscopy was carried out in illumination-collection mode operation of NSOM at a cryogenic temperature (8K).

Figure 1(a) shows a near-field PL spectrum at one point of the sample. The spectrum exhibits three sharp peaks, which were identified as an exciton (X), a biexciton (XX), and a first-excited exciton (X*). Optical images in Fig. 1(b) and 1(c) were obtained by mapping the PL intensity with respect to the peaks X and XX, respectively. Since the island structure revealed in Fig. 1(b) (~100 nm) is beyond our spatial resolution (35 nm), these images successfully map out the center-of-mass wave functions of the exciton and biexciton states. The difference in the spatial distribution between two images is expected to be associated with the difference in the "dead layer effect". As shown in Fig. 1(d), we also map the emission from first-excited exciton, whose transition to the ground state is inhibited in the far-field regime.

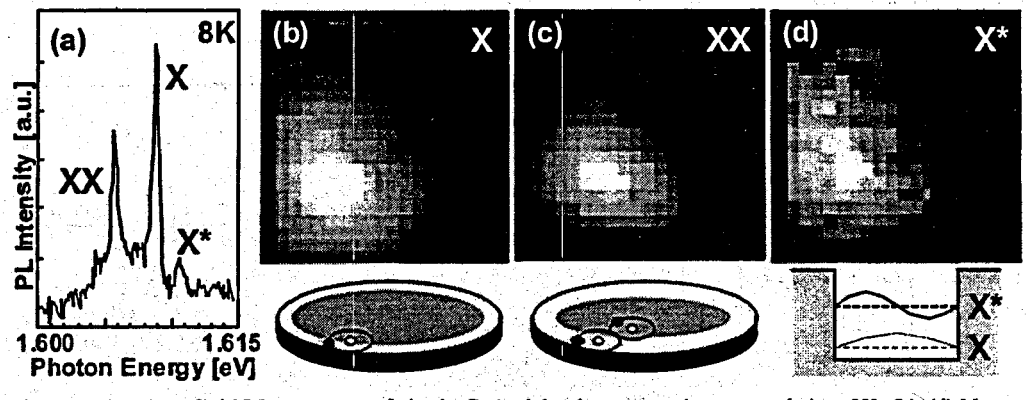

Figure 1: (a) Near-field PL spectrum of single GaAs island structure (quantum dot) at 8K. (b)-(d) Near-field PL images recorded at the energies of exiciton (X), biexciton (XX), and first-excited exciton (X*), respectively. Image size: 200 nm X 200 nm.

References

[1] J. R. Guest, T. H. Stievater, G. Chen, E. A. Tabak, B. G. Orr, D. G. Steel, D. Gammon, and D. S. Katzer, *Science* **293**, 2224 (2001).
[2] G. W. Bryant, *Appl. Phys. Lett.* **72**, 768 (1998).
[3] T. Saiki and K. Matsuda, *Appl. Phys. Lett.* **74**, 2773 (1999).

Plasmon Condenser with a Microscatter for Optical Far/Near field Conversion

T. Yatsui,[a)] T. Abe,[b)] M. Kourogi,[a), b)] and M. Ohtsu[a), b)]
a) ERATO, Japan Science and Technology Corporation, Machida, Tokyo, 194-0004, Japan.
b) Interdisciplinary Graduate School of Science and Engineering, Tokyo Institute of Technology, Yokohama, Kanagawa, 226-8502, Japan.

To realize nanometer-scale photonic devices and their integration [1], coupling them with external conventional diffraction-limited photonic devices is required by using a nanometer-scale optical waveguide for far/near -field conversion. To meet this requirement, we have reported plasmon waveguide using a metallized silicon wedge structure that converts far-field light to optical near field via one-dimensional (1D) plasmon mode [2]. To couple with 1D plasmon mode efficiently, we propose here a plasmon condenser with a microscatter that focus two-dimensional (2D) surface plasmon (SP) and converts to 1D plasmon mode efficiently.

As a plasmon condenser, carbon columns were aligned by focused ion beam. They were positioned on a circumference of a radius *R* in order to compensate for phase-matching of the scattered plasmon waves at the focal point. The angular position of the *n*th column is given by the expression $kR-kR\cos(\alpha_n)=2\pi n$ [see Fig. 1(a)]. Furthermore, to enhance the efficiency of light scattering a microscatter was deposited at focal point of the plasmon condenser. To excite 2D SP mode and increase the near-field optical energy at the microscatter, 50-nm-thickness gold film was coated. In order to investigate the plasmon enhancement due to the microscatter, we compared the spatial distributions of palsmon condenser without and with the microscatter. The spatial distributions of optical near-field energy were observed by the collection mode near-field optical microscope taken at λ = 785 nm and arrangement for 2D SP excitation in Kretschmann configration.

Figures 1(b) and 1(c) show respective topographical and the near-field optical images of the plasmon condenser without the microscatter. Figures 1(d) and 1(e) are for the plasmon condenser with the microscatter. In Fig. 1(f), curves A, B, and C show the cross sectional profiles along dashed white lines A-A', B-B' [in Fig. 1(c)], and C-C' [in Fig. 1(e)], respectively, where the pick-up intensity were normalized by the incident power of 2D SP in front of the plasmon condenser. Note that the peak intensity of curves B and C are twice and 7 times that of curve A, respectively, and full width at half maximum of curve C is 350 nm. These results confirm that plasmon condenser focuses 2D SP and the microscatter enhances the light scattering. By using these structures in the far/near -field conversion device, higher conversion efficiency from 2D SP to 1D plasmon mode is expected.

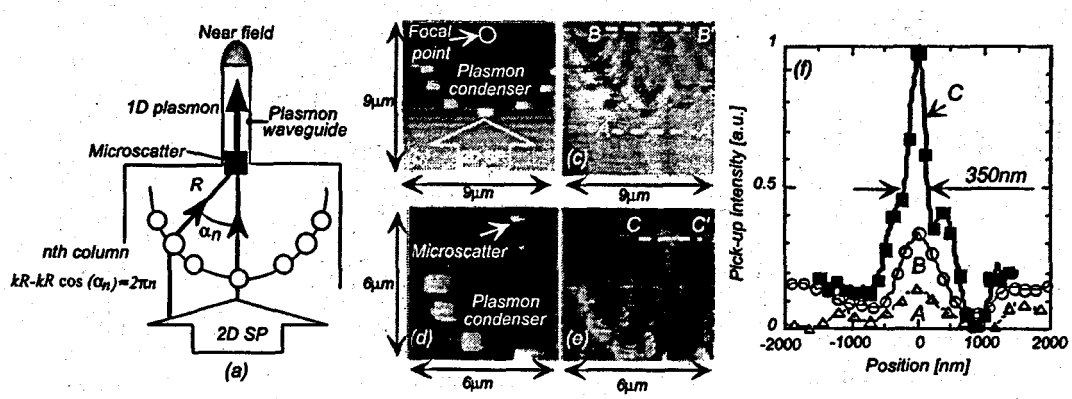

Figure 1: (a) Modeling of plasmon condenser with a microscatter. (b) Topographical image of plasmon condenser. (c) Near-field optical image on (b). (d) Topographical image of plasmon condenser with a microscatter. (e) Near-field optical image on (d). (f) Curves A, B, and C show the cross sectional profiles along the dashed white lines of A-A', B-B', and C-C', respectively.

References

[1] M. Ohtsu, *Proc. of SPIE* 3749, 478 (1999).
[2] T. Yatsui, M. Kourogi, and M. Ohtsu, *Appl. Phys. Lett.* 79, 4583 (2001).

Spontaneous emission of an atom placed near nanobodies

V.V. Klimov

P. N. Lebedev Physical Institute, RAS, 53 Lenin Prospect, Moscow 117924, Russia.

The influence of nanonobodies of different shapes (sphere, cylinder, cone, spheroid) and made of different materials (dielectric, metal, 'left-handed') on decay rate of an atom is considered. The results of calculations performed within the framework of quantum and classical electrodynamics are presented both in analytic and graphical forms and can be readily used for planning experiments and analysis of experimental data. The results obtained show that one can use nanobodies to control effectively the decay rate of spontaneous emission. For example, the decay rate of an excited atom with dipole orientation, which is normal to surface of nanospheroid or nanocylinder, can be enhanced by factor 10 - 100 in comparison with free space rate. More substantial enhancement of decay rate occurs for special (negative) values of permittivity. It corresponds to excitation of surface plasmons inside nanobody. On the other hand, the decay of an excited atom whose transition dipole moment is directed tangentially to the nanobody surface substantially slows down. The probability of nonradiative decay of the excited state is shown to increase substantially in the presence of nanobodies possessing losses.

Let us now consider the observation of an individual molecule with the aid of an apertureless scanning microscope with a needle tip modeled by a prolate nanospheroid wherein plasmon resonances can be excited [1]. We consider that the process of excitation of the object molecule and the process of emission of light by it are separated both in time and frequency. It means that the molecule excitation process is off resonance with the nanoscope needle, whereas the emission band of the molecule falls within the resonance region of the nanospheroid as a needle. With this formulation, the problem reduces to the determination of the rate of the radiative loss suffered by the preexcited molecule in the presence of the nanotip possessing resonance properties due to the plasmons excited therein. In Fig1. one can see scan signal of nanoscope near molecule with different orientations. From these figures one can see that it is possible to achieve space resolution about 2-3 nm. More over it is possible to determine the orientation of dipole through dip in scan image.

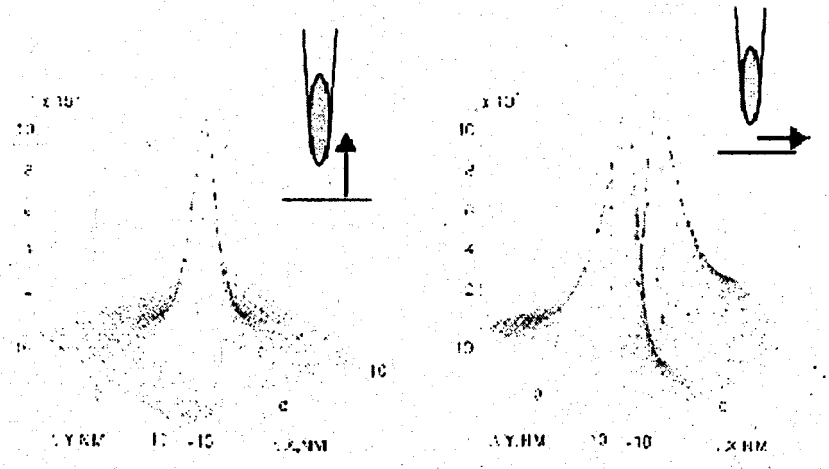

Figure 1. Scan images (relative decay rate) of a molecule for its different orientations. Arrows indicate the position and orientation of the dipole.

References

[1]. Klimov V.V., Ducloy M., Letokhov V.S., A model of an apertureless scanning microscope with a prolate nanospheroid as a tip and an excited molecule as an object, Chem. Phys. Lett., 2002 (in print).

Raman spectroscopy of fullerene- or perylene- filled nanotubes

Débarre A.., Jaffiol R.., Julien C., Nutarelli D., Richard A., Tchénio P.,
Laboratoire Aimé Cotton, C.N.R.S. II, Bât. 505, 91405 Orsay Cedex, France

To improve the spatial resolution in NFO, schemes that take advantage of the field enhancement under an opaque tip, often called apertureless approaches, were proposed[1,2,3,4]. When imaging, resolutions below ten nanometers where obtained. But, for spectroscopic applications in fluorescence, the dynamics of the light emission is strongly affected [5] and for most of the chromophores, the fluorescence is quenched when a high resolution is required. The case of Raman spectroscopy, where the energy is not stored for a long time in an highly excited state seems more favorable and several recent experiments [6, 7] did observed enhanced Raman scattering under metallic tips.

There are close connections between fluorescence or Raman experiments under opaque tips and those that have been performed on rough substrates for more than twenty years. Typical enhanced factors under a tip are still much smaller than those obtained on optimized Surface Enhanced Raman scattering(SERS) substrates. Understanding how nanostructures enhance Raman scattering can lead to a better design of NFO probes for Raman application.

Classical SERS substrate are noble metal (silver, gold usually) films or colloids in solution or deposited on a dielectric substrate. Carbon nanotubes is another kind of nanomaterial that present remarkable electrical and mechanical properties. Their ability to enhance Raman signals has not yet been investigated. Recently, several groups have succeeded in filling these structures with different chemical species[8,9]. In this lecture, we report on Raman scattering of nanotubes filled with fullerenes or perylene molecules. First, we will present the hyperspectral imaging method that allows us to study these very heterogeneous systems. This original method is close to the techniques used in single-molecule spectroscopy. It combines a high spatial resolution Raman imaging (confocal microscope) with sample dilution. In each point of the image, a complete Raman spectrum over a 3000cm^{-1} wide domain is acquired. After processing this 3D image, regions of interest can be selected. Then, we will discuss Raman spectra on nanotubes filled with different chemical species. Preliminary results suggest that strong Raman signals can be obtained with traces of material which supports enhancement of Raman scattering from species inside or near the tube.

References

[1] F. Zenhausern, M.P. O'Boyle, H.K. Wickramasinghe, *Applied-Physics-Letters* **65**, 1623 (1994).
[2] R. Bachelot-R, P. Gleyzes, A.C. Boccara, *Ultramicroscopy* **61**, 111 (1995).
[3] J. Azoulay, A. Débarre, P. Tchénio, *J.of Microscopy* **194**, 486 (1999);
[4] E.J. Sanchez, L. Novotny, X. Sunney-Xie, *Phys. Rev. Letters* **82**, 4014 (1999).
[5] J. Azoulay, A. Débarre, A. Richard, P. Tchénio, *Europhysics-Letters* **51**, 374 (2000).
[6] R.M. Stockle, Yung-Doug-Suh, V. Deckert, R. Zenobi, *Chem. Phys. Letters* **318**, 131 (2000).
[7] N. Hayazawa, Y. Inouye, Z. Sekkat, S. Kawata, *Chem. Phys. Letters* **335**, 369 (2001).
[8] B.W. Smith, M. Monthioux, D.E. Luzzi, *Nature(London)* **396**, 323 (1998).
[9] K. Hirahara and *al*, *Phys. Rev. Letters* **85**, 5384 (2000).

Imaging with a scatter-probe near field optical microscope

V. Ruiz-Cortés, S. Zavala, P. Negrete-Regagnon, E. R. Mndez, H. M. Escamilla
Depto. de Optica, División de Física Apliada
Centro de Investigación Científica y de Educaci ón Suærior de Ensenada (CICESE)
Km. 107 Carr. Tijuana-Ensenada, 22860 Ensenada, B.C., Mexico .

Nano-scale optical technology is currently a highly active area of researc h. Near-field geometoffers opportunities to study optical interactions involving both a propagating optical field and an evanescent field. Near field optical microscopy has been successful in demonstrating the possibility of beating the diffraction limit of conv en tional optical systems. In near field optics the resolution is primarily determined by the size of the probe and resolutions of about $\lambda/10$ or lower are routinely achieved with these instruments.

Most of the near-field optics arrangements employ a tapered optical fiber to illuminate or/and collect the light reflected or transmitted by the sample. The resolution is, in this case, primarily determined by the size of the tip, and efforts are been made to produce sharper ones. T echnology has no w matured to the point where near-field microscopes are employed in a wide variety of applications in biology, material science and surface metrology.

A minor trend in near field microscopy consists of using scatters, rather than tapered optical waveguides employed by more conv en tionalsystems. Using a scanning near-field optical microscope with a metallic probe tip, we investigate the formation of near-field optical images. The scatter-probe is used only for converting an evanescent field to a propagating field and the detection system is in the far-field. This situation models the usual experimental set up employed in scatter-probe near-field microscopy.

We will present a numerical study of a scanning scatter-probe near-field optical microscope. We will describe the numerical technique employed in our studies of the problem and some representativ e results of our findings.

The method of calculation is based on the "in tegral approach" formalism describe by Maradudin *et. al* [1], with some small modifications to be able to deal with multivalued surfaces and multiply connected domains. With this formalism, one is able to calculate the intensity reaching the far field of the sample for a particular position of the probe. By displacing the probe horizontally by small increments, and solving the scattering equations for each one of the positions it is possible to calculate images under various combinations of geometries of incidence and scattering. The image is then formed using the calculated signal for each position of the probe as it is scanned over the sample at constant height.

References

[1] A. A. Maradudin, T. Michel, A.R. McGurn and E.R. Méndez, *A nnals of Physics***203**, 255 (1990).

Dependence of the resolution of a Scanning Near-Field Optical Microscopy Tip on optical fiber parameters.

L. Alvarez, A. Sauceda
Instituto de Ingeniería, Universidad Autónoma de Baja California, CP 21280, Mexicali, Baja California, México.
M. Xiao
Centro de Ciencias de la Materia Condensada, Universidad Nacional Autónoma de México, CP 22800, Ensenada, Baja California, México.

In Scanning Near-Field Optical Microscopy (SNOM) a tapered optical fiber scans a sample surface to obtain resolution beyond the Rayleigh limit. In contrast to conventional microscopy, this particular microscopy does not appear to be diffraction limited and some work has been done with the aim of finding its actual resolution limit. In the case of a metal covered tip, the easier way is to use diffraction theory for a subwavelength aperture pierced in a perfectly conducting metal screen, where the metal screen represents the metal cover of the optical fiber.

Since the optical fiber is not considered in the models, such works are limited to discussing resolution as a function of the aperture size. In a work of Buckland et al. [1], the problem of the resolution of a collection mode SNOM tip, whether metal covered or not, is approached using a modal treatment. In the case of a metal-covered tip, the discussion is based on the analysis of the modes of a conducting wall cylindrical waveguide. In the case of a naked tip, the discussion is based on the analysis of the guided modes of the optical fiber. In both cases, the assumption is made that the aperture size is so small that it was possible to discard all the modes with the exception of the fundamental mode. Therefore, it is an interesting problem to discuss the resolution of a SNOM tip using the complete set of modes. It is desirable that the model includes both the metal cover and the optical fiber.

In a previous article [2], a model for the diffraction through a subwavelength aperture on the top of an optical fiber was developed. Such a model, based on the Direct Moment Method (DMM), uses both the set of modes of the metal wall cylindrical waveguide and the complete orthonormal set of modes of an optical fiber. The model was intended for studying the light transmission through the SNOM tip, taking into account not only the size of the aperture, but also the characteristics of the optical fiber. In this work, the same model will be used to discuss the limit of resolution of a SNOM tip with no restrictions on the size of the aperture. The model will allow discussion of the dependence of the resolution on the radius of the core and the permittivity of both core and cladding.

References

[1] E. L. Buckland, P. J. Moyer and M. A. Paesler, *Journal of Applied Physics* **73**, 1018 (1993).

[2] L. Alvarez, M. Xiao, *Journal of Microscopy* **202**, 351 (2001).

PHOTON INTERACTION BETWEEN TWO ATOMS IN NEAR–FIELD CONTACT

Jacob Broe and Olé Keller,
Institute of Physics, Aalborg University, Pontoppidanstræde 103, 9220 Aalborg Øst, Denmark

In near–field optics a study of the interaction of two atoms (molecules) in near–field contact during the exchange of photons, is of fundamental interest. Concrete problems where such a study is crucial for the understanding could be,

1. the detection of of photon in the near-field of its source. In this situation one atom acts as the source and the other as the detector [1],
2. in a micoroscopic investigation of the resolution problem, where both atoms act as sources,
3. in a study of the optical tunneling problem, which is related to the lack og photon localizability. [2]

A theoretical study of this interaction necessarily must be based upon a microscopic and quantum electrodynamical description. One often used approach is to formulate the problem in the multipole gauge (Power-Zinau-Woolley gauge) [3, 4]. This gauge has the disadvantage that the photon propagation can not be seen directly from the fundamental equations, but this problem can be removed by reformulating the approach in the so-called propagator gauge [5], related in some respects closely to the multipole gauge.

In this presentation we will formulate the two-atom problem in the propagator gauge, and present a closer study of the electrodynamics of a single atom, because many of the problems here also enter the two-atom problem. Because of the close relation between the propagator and multipole gauges, it will further be demonstrated how many of the divergences obtained in many calculations in the multipole gauge [3] are due to the almost universally used assumption that the atom is point-like.

References

[1] E. A. Power and T. Thirunamachandran *Phys. Rev. A* **56**, 3395 (1997).

[2] O. Keller, *J.Opt.Soc.Am. B* **18**, 206 (2001).

[3] R. G. Woolley, *Adv. Chem. Phys.* **33**, 153 (1975).

[4] C. Cohen-Tannoudji, J. Dupont-Roc and G. Grynberg *Photons and Atoms, Introduction to Quantum Electrodynamics* (Wiley Interscience, New York, 1989).

[5] O. Keller, *Phys. Rev. A* **58**, 3407 (1998).

Comment on a controlling method of spins of atoms with optical near fields

A. Shojiguchi, K. Kitahara, International Christian University, Mitaka, Tokyo 181-8585

If two evanescent waves respectively propagating in the direction of the x-axis and of the y-axis are built on top of a dielectric surface, a pattern of circle polarization whose polarization axis is in the z-axis will be made on a straight line on the surface [1]. This is a special circle polarization whose polarization axis is orthogonal with the propagating direction. If an alkali-atom beam runs along with the straight line of this circle polarization pattern, the z-component of angular momentum of the atom increases by 1 due to the induced absorption. If the initial state of the atom is $S_{1/2}$, the valence electron is either in the up-spin state (J, M) = (1/2, 1/2) or in the down-spin state (J, M) = (1/2, -1/2). Atoms in the up-spin state and the down-spin state change to a state $P_{1/2}$ and to a state $P_{3/2}$, respectively. However, if we inhibit the transition to the state $P_{3/2}$ by selecting frequency of the evanescent wave, we can make atoms of the up-spin state (J, M) = (1/2, 1/2) stable. Finally, atoms in the state $P_{1/2}$ relax to the state $S_{1/2}$ of the up or down-spin state. Thus, by repeating the pumping and relaxing processes we can make all the atoms in the up-spin state (see Fig.1). This is a procedure proposed by Kitahara and Hori [2] to arrange the spins of atoms in the same direction.

The probability of the spontaneous emission of atoms near an interface is different from the one in vacuum because the probability depends on the direction of the emitted photon. Moreover, since the atoms are very close to the dielectric surface, the difference cannot be negligible. In order to take account of the surface effect, we expand the electromagnetic waves in terms of the Carniglia-Mandel mode [3], which is a normal mode of the electromagnetic waves with the boundary condition of an infinite plane surface to form a complete orthonormal set. Then we calculate the transition probability from the $P_{1/2}$ state to the up-spin state (w_{up}) or to the down-spin state (w_{down}), perturbatively. The greater the ratio $R(n, z) = w_{up}/w_{down}$ becomes, the faster the up-spin atoms are collected. The ratio $R(n, z)$ depends on the distance from surface to the atoms (z) as well as the refraction index (n) of the dielectric surface. A result on the transition from the state $6P_{1/2}$ to $6S_{1/2}$ of ^{133}Ce atoms is shown in Fig. 2. It follows from the figure that the ratio $R(n, z)$ takes its maximum value at n =1.5 and then monotonically decreases with z. We find that the ratio $R(n, z)$ is enhanced due to the surface effect by 30% than the value estimated in Ref. [2].

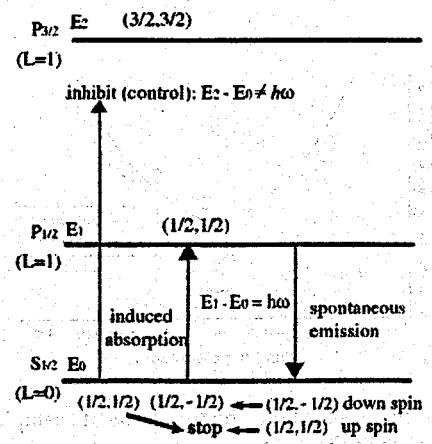

Fig.1: processes of transition

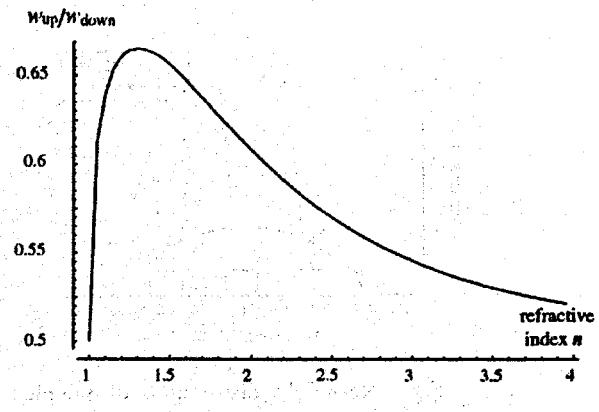

Fig.2: rate of transion probabilities

References

[1] H. Hori, K. Kitahara, and M. Ohtsu, *Abstracts of the 1st AP-NFO* 49 (1996).

[2] Y. Ohdaira, K. Kijima, K. Terasawa, M. Kawai, H. Hori, and K. Kitahara, *J. Microscopy* **202**, 255 (2001).

[3] C.K. Carniglia and L. Mandel, *Phys. Rev. D* **3**, 280 (1971).

Near-firld optical imaging mechanism as a windowed Fourier Transform

Qing Zhou, Hong Dai
Department of Physics, Yunnan University, Kunming 650091, China

Xing Zhu
State Key Lab for Mesoscopic Physics,Peking University, Beijing 100871, China

In near-field optical microscopy, the task of the fiber probe is to capture the radiation from the sample. The process contains two aspects. On the one hand, when the probe is introduced on the sample surface, it disturbs the existed field. It interacts with that field and establishes a new field distribution. The new field distribution contains high frequency information (i.e. evanescent field) from sample because of near field, so high resolution is available. On the other hand, the size of probe tip is finite and constant (infinite impossible), so the tip is seen as a windowed function smoothing the received signal. Therefore, the detected resolution depends on an assembly of the tip size, distance between tip and sample, relative position and material characteristics of both tip and sample.

Computing simulations presented below can show this using three-dimensional FDTD method. The computing model consists of three cubic dielectric blocks whose height and each side is 125nm and 75nm, respectively. The permittivity of the blocks is 12.25 (refractive index=3.5). A plane wave (λ =500nm) illuminates the probe at normal incidence to the bottom (in z-direction). We assume the direction of the incident light polarization is the electric field polarization along the y-axis.

Figure 1 shows near-field distribution of sample without probe. The more distant from the sample surface, the less the part of high frequency.

Figure 2 shows near-field distribution of sample with probe. The tip disturbs the field distribution. The received signal is different from the original field of sample. However the signal contains high frequency information on sample in near-field region. The relation between the undisturbed and disturbed fields is not simple. Therefore, the near-field optical microscopic image must be interpreted carefully.

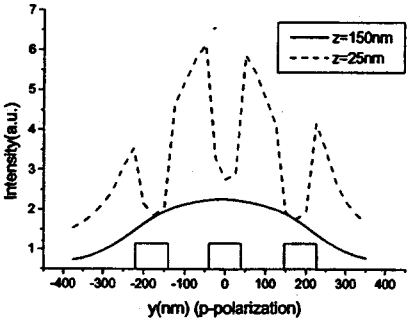

Fig.1 Near-field distribution of sample without probe

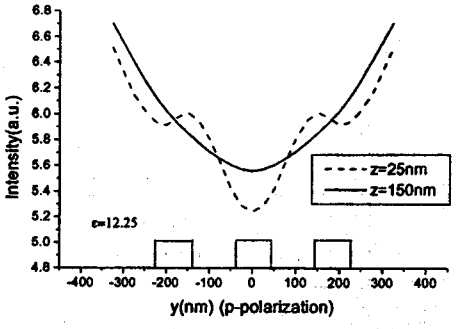

Fig.2 Near-field distribution of sample with probe

Deconvolution Method for Improving Aperture-Scanning Near-Field Magneto-Optical Images

F. Kiendl, G. Güntherodt, II. Physikalisches Institut der RWTH Aachen, 52056 Aachen, Germany.
e-mail: Fabian.Kiendl@physik.rwth-aachen.de

In the aperture mode of magneto-optical scanning near-field microscopy (MO-SNOM) the resolution is determined by the size and geometry of the aperture[1]. Reducing the size of apertures makes their fabrication disproportionally more difficult and curbs the available intensity[2]. Therefore, there is a need to increase the resolution for a given aperture.

We propose a computational image post-processing method[3] to increase the resolution and thereby the contrast of a given magneto-optical near-field image. In many scanning measurement set-ups (e.g., confocal[4] or magnetic force microscopes[5, 6]), the detector is much larger than the structures to be resolved, and the information is recovered by a deconvolution technique. Such a technique, however, requires an appropriate model of the measurement process. In this work we put forward a model for the image acquisition process in our magneto-optical SNOM set-up[7] that allows us to apply a deconvolution technique to our images: We divide the sample into grid squares that are much smaller than the aperture and regard each acquired pixel as a superposition of intensity contributions from many grid squares. While a typical aperture illuminates an area of 50-100 nm diameter at any given time, it can be scanned across the sample with a much higher precision. As most sample grid squares are therefore illuminated more than once during an entire scan, the acquired image can be regarded as a convolution of the true sample information with the aperture geometry. To deconvolve the aperture geometry from a given acquired image, we set up a linear equation system in the intensity contributions from the individual sample grid squares.

We demonstrate the potential benefit and computational feasibility of this method on a test structure. Analyzing the impact of image acquisition disturbances on the deconvolution result, we find that actual images must be de-noised properly before deconvolution. We find that de-noising methods based on wavelet analysis[8] are far superior to Fourier analysis for this purpose. They empower us to deconvolve actual magneto-optical images from our experimental set-up.

Once the sample has been removed from the SNOM, e.g., to change the tip or to acquire reference images using a different magnetic microscope, it is difficult to retrieve the previously imaged area in subsequent measurements. To overcome this problem, we have prepared samples with a topographically visible coordinate system.

References

[1] Michael A. Paesler, Patrick J. Moyer, "Near-Field Optics: theory, instrumentation, and applications", Wiley-Interscience, New York (1996), ISBN 0-471-04311-7.

[2] L. Novotny, D. W. Pohl, B. Hecht, *Ultramicroscopy* **61**, 1-9 (1995).

[3] F. Kiendl, G. Güntherodt, submitted to *J. Appl. Phys.*

[4] M. Schrader, S. W. Hell, H. T. M. van der Voort, *Appl. Phys. Lett.* **69**, 3644-3646 (1996).

[5] J.-G. Zhu, X. Lin, R. C. Shi, Y. Luo, *Appl. Phys. Lett.* **83**, 6223-6225 (1998).

[6] A. Thiaville, L. Belliard, D. Majer, E. Zeldov, J. Miltat, *J. Appl. Phys.* **62**, 3182-3191 (1997).

[7] P. Fumagalli, A. Rosenberger, G. Eggers, A. Münnemann, N. Held, G. Güntherodt, *Appl. Phys. Lett.* **72**, 2803-2805 (1998).

[8] A. Graps, An Introduction to Wavelets, *IEEE Comp. Sci. Eng.* **2** (1995).

Extraordinary Light Transmission through Sub-wavelength Slits: Waveguiding and Optical Vortices

H.F. Schouten, T.D. Visser, D. Lenstra
Dept. of Physics and Astronomy, Vrije Universiteit,
De Boelelaan 1081, 1081 HV Amsterdam, The Netherlands
H. Blok
Dept. of Electrical Engineering, Technische Universiteit Delft,
Mekelweg 4, 2628 CD, Delft, The Netherlands

Using a rigorous scattering model we compute the field around sub-wavelength slits in a metal plate which has both finite conductivity and finite thickness. The transmission through these slits is studied as function of several parameters such as the slit width and the thickness and conductivity of the plate. We found that the recently observed enhanced transmission [1] can also occur for a single slit. We explain this extraordinary behavior in terms of waveguiding and optical vortices. We also study the case of two slits in a metal plate, and investigate the light transmission as a function of their proximity.

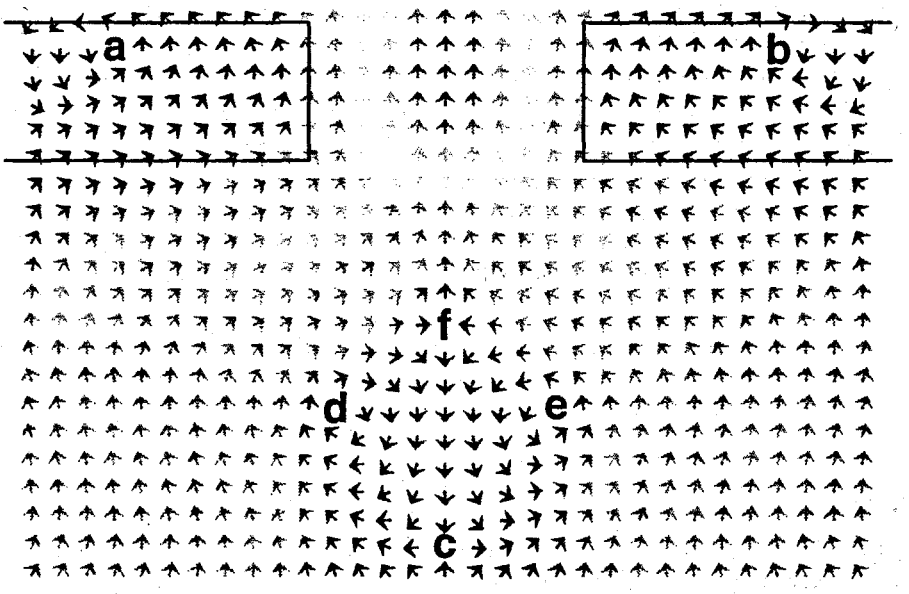

Figure 1: The power flow near a 200 nm wide slit in a 100 nm thick silver plate, illuminated from below by a plane wave with a wavelength of 500 nm and polarized along the slit. Notice the vortices (a, b, d and e) and saddle points (c and f).

References

[1] T.W. Ebbesen *et al.*, Nature (London) **391**, 667 (1998).

Near-field Optical Virtual Probe based on Confinement Field Distribution

Jia Wang Tao Hong Liqun Sun Dacheng Li

Department of Precision Instruments, State Key Laboratory of Precision Measurement Technology and Instruments, Tsinghua University, Beijing 100084, P. R. China

E-mail: wj-dpi@mail.tsinghua.edu.cn

Near-field optical virtual probe is a kind of immaterial tip based on the principle of near-field evanescent wave interference. The evanescent wave interference and the aperture play very significant roles in generating near-field optical virtual probe. Two evanescent waves in opposite direction will interfere to generate the confinement field. The central peak carries most of energy. An aperture can be used to suppress the sidelobe in the optical field distribution to form near-field optical virtual probe. In this paper the optical field distribution of near-field optical virtual probe has been numerically simulated by 3-D finite-difference time-domain (FDTD). The characteristics of near-field optical visual probe have been revealed. The transmission efficiency of optical virtual probe is higher than popular nano-aperture metal-coated fiber probe in near-field scanning optical microscopy. FWHM of the central peak of the confinement field, in other words, the size of optical virtual probe is constant whatever the distance increases in a certain range. It is feasible that the critical nano-separation control in NSOM can be relaxed, so the scratch between the probe and media can be avoided. Some parameters of the optical virtual probe, such as the shape and size of aperture, polarization and etc. have been analyzed. The results also show that sidelobe suppression will depend on optimization of aperture function of optical virtual probe. This kind of probe is likely to be used in near-field high-density optical data storage, nano-lithography, near-field optical imaging and spectral detection, near-field optical manipulation of nano-scale specimen and etc..

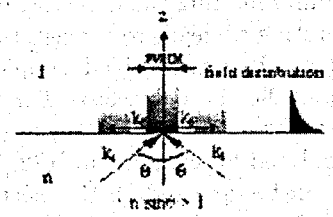

Fig.1 Concept of virtual probe

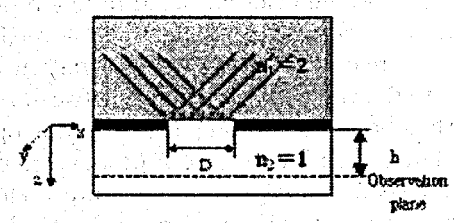

Fig.2 Simulation model

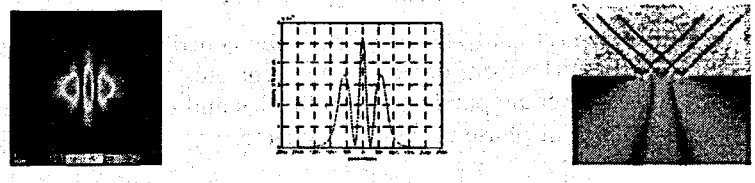

(a) (b) (c)

Fig.3 (a) Intensity distribution ($|E_t|$) on the observation plane (b) section along x direction ($|E_t|^2$) (c) SSEFD of virtual probe

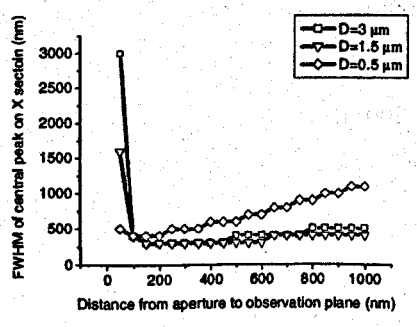

Fig.4 FWHM of central peak vs. distance

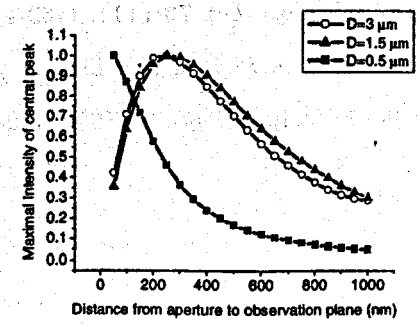

Fig.5 Intensity of central peak vs. distance

Existence of phase modulation phenomena in the light scattered by a vibrating tip in aperturless SNOM

P.-M. Adam, S. Aubert, R. Bachelot, D. Barchiesi, J.-L. Bijeon, A. Bruyant, S. Hudlet, G. Lérondel, P. Royer
Université de technologie de Troyes, Laboratoire de Nanotechnologie et d'Instrumentation Optique 10010 Troyes, France.
A. A. Stashkevich
Université Paris 13, Institut Galilée, 93430 Villetaneuse, France.

The understanding of the image formation in apertureless SNOM is still a big challenge. The purpose of our work is to study the particular influence of the phase modulation of light scattered by the vibrating tip, especially when a background signal exists in experimental set-up.

The scheme of near field experiments that we consider can be described as follows. A monochromatic light wave goes throw a transparent sample. The structures of this sample are responsible for formation of near field and far field. This optical information is thus partially contained in the light diffracted by an AFM vibrating tip. At large distance a fixed photo-sensitive device collected this field eventually in addition to a non-modulated background field.

First, we analyse the field diffracted by the probe and illuminating the detector. The process of diffraction of a plane-wave Fourier component by the vertical vibrating tip leads to a generation of two phase shifts. The first one is created as a result of a variation of distance between a fixed sample and the tip and the second is due to the variation of distance between the tip and the photo-detector. For an evanescent spectral component the phase shift is complex. Thus the optical signal coming from the tip is both -amplitude and phase- modulated. The first aspect of problem as been analysed for example in [1][2][3]. The second aspect of problem is not often analysed in literature because it can be detected on the electrical signal generated by the photo-detector only if a background optical signal (for example created by spurious scattering in the sample) adds to the signal diffracted and modulated by the tip.

Our theoretical and experimental analysis shows that the contribution of the phase modulation is significant. It can noticeably change the form of the curve describing the intensity of signal as a function of the tip modulation amplitude. For some particular amplitudes and detector positions, the signal becoming strictly equal to zero only because of phase modulation effects.

References

[1] Hamann, *Appl. Phys. Let.* **73 (11)**, 1469-1471 (1998).

[2] R. Ladadda, *Eur. J. Phys.* **6 (2)**, 171-178 (1999).

[3] J. N. Walford, *J. Appl. Phys.* **89 (9)**, 5159-5169 (2001).

Nanoscale Environments in Sol-Gel-Derived Silicates by Single Molecule Spectroscopy

D. A. Higgins, M. M. Collinson, Department of Chemistry, Kansas State University, Manhattan, KS, 66506.

Single molecule spectroscopic methods are employed to characterize the nanoscale environments found in thin silicate films prepared by the sol-gel process.[1] A range of organically-modified silicate thin films were prepared by spin casting sols of different chemical composition onto glass substrates. Sols were prepared by cohydrolysis of organically-modified silicate precursors with tetraethyl orthosilicate (TEOS). Others were prepared by separate hydrolysis of these same materials. The organically-modified silicates employed include isobutyltrimethoxysilane (BTMOS) and cyanopropyltrimethoxysilane (CNS). CNS, BTMOS, and TEOS were combined in different ratios during sol preparation to yield films of dramatically different nanoscale properties. The highly solvatochromic dye nile red was doped into these films at nanomolar levels and its fluorescence was used to probe the nanoscale film environments. Single molecule fluorescence spectra obtained from these samples were analyzed using a modified Marcus analysis. Information on the transition energy in the "equilibrium" environment, nominally reflecting the local "polarity", and on the local reorganization energy, nominally reflecting the environmental "rigidity" is obtained. The data show dramatic variations in the molecular-scale properties as a function of preparation conditions and film composition. Films prepared from a series of BTMOS:TEOS mixtures show strong evidence for molecule-scale phase separation. In contrast, those prepared from a range of CNS:TEOS mixtures show gradual variations in environmental polarity and rigidity, consistent with molecular-scale mixing of the precursors throughout the range of samples studied. Overall, all samples show the film environments become dramatically more fluid and less polar with increasing organic content. The temporal emission behavior exhibited by individual molecules is also shown to reflect material phase separation and environmental rigidity. An image obtained from phase-separated TEOS, CNS and BTMOS materials is shown in Fig. 1. Molecules entrapped at fixed locations in the films appear as round spots, those exhibiting substantial dynamics due to translational, rotational, and spectral diffusion appear as "streaks". These image streaks designate film regions of substantially increased fluidity.

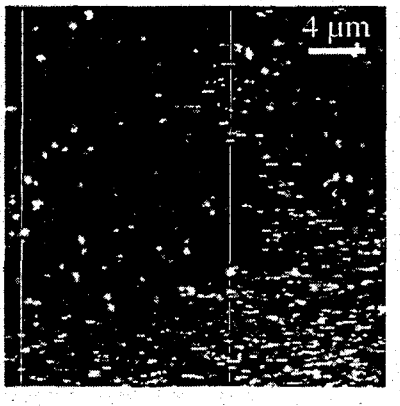

Figure 1: Fluorescence image of a dye-doped, separately-hydrolyzed TEOS:CNS:BTMOS (50:25:25) film.

References

[1] A. M. Bardo, M. M. Collinson, D. A. Higgins, *Chem. Mater.* **13**, 2713 (2001). D. A. Higgins, M. M. Collinson, G. Saroja, A. M. Bardo, *Chem. Mater*, to be submitted.

Single-molecule detection of Rhodamine-6G using cantilever-SNOM-sensors

F. Vargas, G. Tarrach
Facultad de Física, P. Universidad Católica de Chile. Av. Vicuña Mackenna 4860, 6904411 Santiago, Chile
O. Hollricher,
WITec GmbH, Hörvelsinger Weg, D-89081, Ulm, Germany
O. Marti
Abteilung Experimentelle Physik, Universität Ulm, D-89068, Ulm, Germany

In the present work we were able to achieve fluorescent single-molecule detection (SMD) by Scanning Near-field Optical Microscopy (SNOM) using a new kind of tip, namely the "cantilever-SNOM sensor" manufactured by WITec GmbH. These sensors consist of a Si cantilever such as commonly used for Atomic Force Microscopy (AFM), but with a hollow aluminium pyramid as a tip. The pyramid has a small aperture at its apex. The laser light is focused into the backside of the hollow tip and a fraction of the light emerges from the aperture. The cantilever-SNOM sensors were used in an α-SNOM from the same company, which offers the possibility to work simoultaniously in AFM and SNOM mode.

The dye molecules we studied were Rhodamine-6G protected from oxidation by a thin polymer film. The samples were prepared using the following polymers with a layer thickness of 7–10 nm: Polymethyl Methacrilate (PMMA), Polystarine (PS), and Polyvinyl Chloride (PVC). It turned out that PVC gives the most effective protection, but that the protective effect of PMMA is also quite reasonable and more convenient for comparison with the results of other groups. Typically, bleaching still ocurrs at the beginning of exposure, but rapidly reaches a stationary state where the remaining active molecules stay active over a very long time period. Without protection, the bleaching process goes on until there is not a single emitting molecule left.

In a first step, we imaged single molecules with far-field confocal microscopy. Several long-term transitions were observed with dark intervals of up to half a second. During the dark state, the fluorescence intensity dropped to the background level, which means that we can really speak of "on-off" transitions and could not find any "on-dim" transition, like observed in other systems.

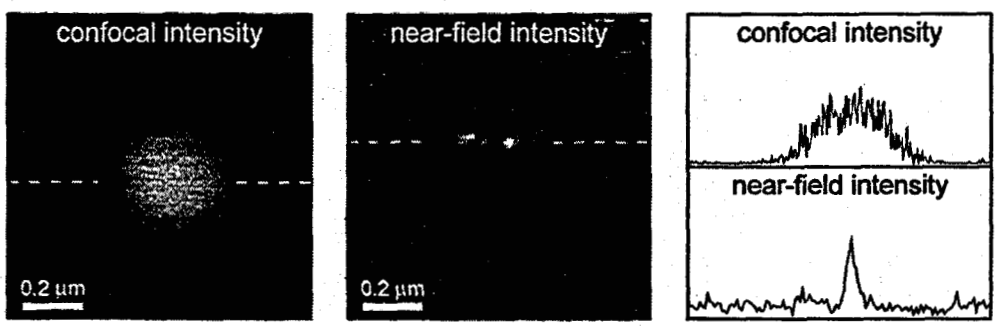

Then we used the SNOM mode in order to obtain high-resolution images with the cantilever SNOM sensor. It turned out that we could achieve similar intensity levels as in the confocal mode, but with about 50 nm spatial resolution on a single fluorescent molecule. Although the images have a superimposed secondary image, a cross section through the intensity map demonstrates, that the secondary spot is of considerably less intensity than the primary spot (see figure). Therefore, the sensors have proved to be useful and to perform well for single-molecule detection.

Towards Near-field Detection of Single Molecules between Nanoelectrodes

A. Drezet, J.-F. Motte, S. Huant, and J. C. Woehl,
Laboratoire de Spectrométrie Physique, Université Joseph Fourier Grenoble et CNRS, 38402 Saint Martin d'Hères, France.
H. B. Weber and H. v. Löhneysen,
Institut für Nanotechnologie, Forschungszentrum Karlsruhe, 76021 Karlsruhe, Germany.

The ultimate goal in molecular electronics is to replace lithographic chip fabrication based on silicon, copper, and aluminum by much smaller building blocks obtained from molecular engineering - the so-called "bottom-up" approach. One possible molecular component for an information processing device consists of a single molecule connected to metallic electrodes. For the interpretation of electronic transport properties of such a setup we need to understand how the molecular electronic structure changes under application of the huge electric fields. While methods in high resolution optical spectroscopy have proven to provide information about electric field effects on the electronic structure with unprecedented detail, it is not evident to use them in strong and inhomogeneous fields. For this purpose, the electrode surfaces have to be very close to each other (on the order of μm), and their position relative to the investigated spot must be known with high accuracy.

Near-field scanning optical microscopy provides just this advantage: the sample can be illuminated with a spot of a size much smaller than the diffraction limit [1], and the geometry of the surrounding nanoelectrode surfaces (and thus the field at the illuminated area) can be determined from the sample topography (force image) which is obtained in parallel. We are therefore applying this technique for the optical detection and, ultimately, Stark spectroscopy at low temperatures of single molecules dispersed between μm spaced nanoelectrodes fabricated by e-beam lithography. Our contribution will outline the various steps taken in order to achieve this goal. The instrumental setup has been tested by using fluorescent microspheres which show a nice correlation between emission and topography. Room temperature detection of single molecules deposited onto a PMMA surface has been achieved, and is currently carried out between a pair of nanofabricated metallic electrodes (thickness: 30 nm) which we were able to image at room temperature in topography mode using our NSOM (see figure).

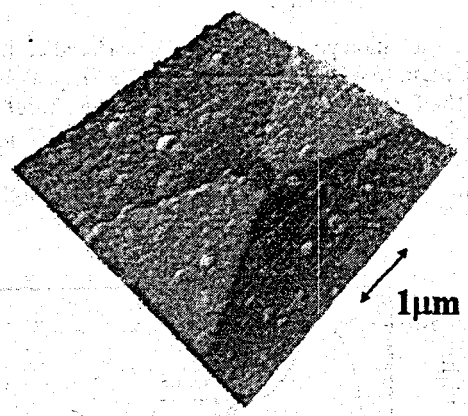

Topographic image of gold nanoelectrodes

References

[1] E. Betzig, J. Trautman, T. Harris, J. Weiner, and R. Kostelak, *Science* **251**, 1468 (1991).

Time-Resolved Quantum Beats in Single InAs Quantum Dots

Young-Jun Yu, Sang-Kee Eah, Han-Eol Noh, and Wonho Jhe
Center for near-field atom-photon technology and Department of Physics, Seoul National University, Seoul 151-742, Korea

Y. Arakawa
Institute of Industrial Science, University of Tokyo, 7-22-1 Roppongi Minato-ku, Tyoko 106-8558, Japan

We report on the observation of quantum beats in single InAs quantum dots (QDs) with a low temperature near-field scanning optical microscope. The sample is self-assembled InAs/GaAs QDs grown by molecular-beam-epitaxy of single layer, lateral size ~20 nm, height ~2 nm, and density ~100 m^{-2}. To do single QDs spectroscopy we covered the sample with 70 nm aluminum using 100 nm diameter polysterene spheres as a mask. The number of quantum dots is ~7 in the 100 nm apertures. To locate an aperture, we used a fiber axicon lens made of uncoated fiber tip sharpened by chemical etching method. We kept the tip ~10 nm above the sample using only a tuning fork and a lock-in-amplifier. Both the tip and sample was cooled down to 5 K using a continuous flow type cryostat.

We used pulses at 1.65 eV from a Ti:sapphire laser to excite carriers at GaAs surrounding InAs QDs. The excitation laser was sent through the fiber, and the luminescence was collected using the same fiber. The luminescence was dispersed by a 0.3-meter spectrometer with spectral resolution of 0.3 meV, and then detected by a charge-coupled device for time-integrated PL spectra. A silicon avalanche photodiode was used for time-resolved spectroscopy with temporal resolution of 250 ps

Figure 1 shows the time integrated PL spectra for excitation power of 100 nW measured at the fiber tip at the temperature of 7 K. The full width at half maximum (FWHM) of each single QD PL peak is 0.25 and 0.3 meV, respectively at 7 K and 0.5 meV at 70 K. The FWHM of single QD PL peak are almost same size at 7 K and 70 K. This result was obtained with uncoated fiber tip sharpened by a chemical etching method, which exhibits a lens effect in the near-field region. Figure 2 shows the time-resolved PL spectra of the single QD, where quantum-beat like oscillations in the time-resolved PL spectra of the single QD are clearly observed.

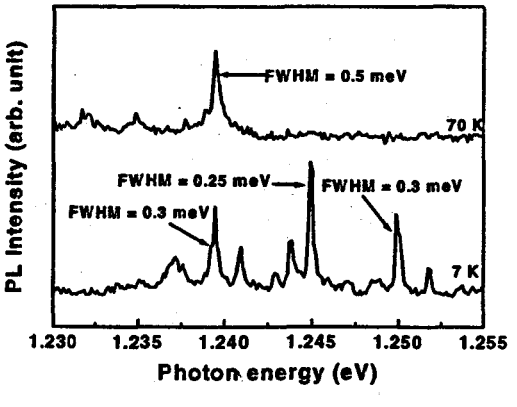

Figure 1. Time-integrated PL spectra of single QDs at 7 K, 70 K.

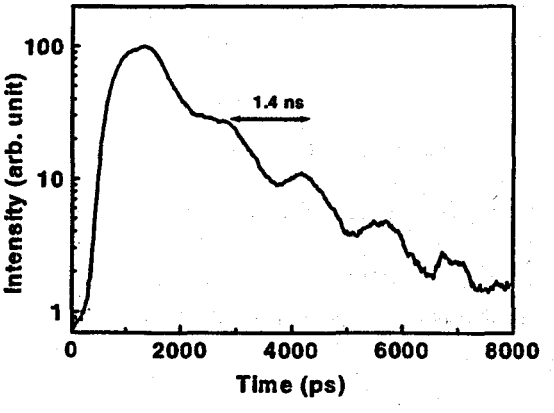

Figure 2. Time-resolved PL spectra of single QD

Optical response of semiconductor quantum dots beyond the electric dipole approximation

Jorge R. Zurita-Sánchez and Lukas Novotny,
University of Rochester, The Institute of Optics, Rochester, NY 14627.

We present a theoretical investigation of a semiconductor quantum dot interacting with a strongly localized optical field as encountered in high-resolution near-field optical microscopy. The strong gradients of these localized fields suggest that higher order multipolar interactions will affect the standard electric dipole transition rates and selection rules. For a semiconductor quantum dot in the strong confinement limit, we calculate the interband electric quadrupole absorption rate and the associated selection rules. It is found that the electric quadrupole absorption rate is comparable with the absorption rate calculated in the electric dipole approximation. This implies that near-field optical techniques can extend the range of spectroscopic measurements beyond the standard dipole approximation. However, we also show that spatial resolution cannot be improved by the selective excitation of electric quadrupole transitions.

Also, we derive the magnetic dipole selection rules and the magnetic dipole absorption rate. We find that electric dipole and magnetic dipole transitions are exclusive and therefore can be spectrally distinguished. The magnitudes of electric and magnetic absorption rates are compared for excitation with a strongly focused azimuthally polarized beam. It turns out that spatial optical resolution can be increased by detecting the ratio of magnetic and electric absorption rates. Resolution is only limited by the purity of the laser mode used for excitation.

Numerical study of the lifetime of an atom close to a lossy nanostructure.

M. Thomas, R. Carminati,
Laboratoire EM2C, Ecole Centrale Paris, CNRS, 92295 Chatenay-Malabry Cedex, France
J.J. Greffet,
University of Rochester, The Institute of Optics, Rochester, NY 14627.
R. Arias, M. Nieto-Vesperinas,
Instituto de Ciencia de Materiales, CSIC, Cantoblanco, Madrid 28049, Spain.

One of the most promising technique in near-field optics uses a sharp tip to enhance locally the electromagnetic field[1]. A major goal for this technique is to achieve spectroscopy of a single molecule. While the tip produces a strong enhancement of the field, it also introduces new channels for the desexcitation of the molecule. The modification of the lifetime of the fluorescence has been well understood since the seminal work of Chance et al. Using an ellipsoid particle as a model for the tip and an electrostatic approximation, it has been shown qualitatively that there is a competition between the enhancement factor and the induced losses in the tip[2]. These phenomena have been studied in detail for the case of an aperture probe by Bian et al.[3] and analysed by Novotny[4]. A quantitative model and a qualitative understanding of these competing processes for apertureless microscopes is still an open question. The purpose of this work is to present a first step towards a quantitative model based on a numerical solution of the problem.

The relevant quantity to study in this context is the Green tensor of the system. On one hand, it yields the lifetime of the molecule. On the other hand, its trace yields the local density of states. From a practical point of view, calculating the Green tensor amounts to computing the electric field scattered by the environment at the location of a dipolar source. From this approach, an energy budget allows to derive a relationship between the power emitted by the dipole source and the power scattered and absorbed by the environment. This amounts to establishing a near-field expression of the optical theorem, from which the influence of both scattering and absorption on the lifetime can be separated.

In order to be able to deal with any possible shape of the scatterer (tip) and to take losses into account, we have used surface-integral equations. The numerical scheme used to solve these equations is the standard moment method. We use this technique to evaluate the influence of both absorption and scattering, i.e. of non-radiative and radiative decay channels. We discuss the effect of the shape and of the dielectric properties of the tip on the lifetime of the emitting atom or molecule. In particular, we study the effect of the coupling with resonant modes inside the tip.

References

[1] E. J. Sanchez, L. Novotny, and X. S. Xie, *Phys. Rev. Lett.*, **82**, 4014 (1999).

[2] J. Azoulay, A. Debarre, A. Richard and P. Tchenio, *Europhys.Lett.*, **51**, 374 (2000).

[3] R.X. Bian, R.C. Dunn, and X. S. Xie, *Phys. Rev. Lett.*, **75**, 4772 (1995).

[4] L. Novotny, *Appl. Phys. Lett.*, **69**, 3806 (1996).

Single Molecular Spectroscopy Using Hybrid SNOM/STM Equipped with ITO/Au-coated Optical Fiber Probe

K. Nakajima, J. G. Noh, T. Isoshima, M. Hara,
Local Spatio-Temporal Functions Laboratory, Frontier Research System, RIKEN, Wako, Saitama 351-0198, JAPAN.
B. H. Lee,
Materials Fabrication Laboratory, RIKEN, Wako, Saitama 351-0198, JAPAN.
D. Fujita,
Nanophysics Research Group, Nanomaterials Laboratory, National Institute for Materials Science, Sengen, Tsukuba 305-0047, JAPAN.

As widely known, the spatial resolution of SNOM is severely limited by its aperture size. However, as reported by the authors [1], hybrid SNOM/STM system with "doubly metal-coated optical fiber probe" could overcome this limitation, with which the gap-distance was decreased down to 1 nm due to STM feedback control, resulting in the high-resolution feature of SNOM imaging (1/50). Meanwhile, the throughput of such a probe was extremely low because of the metal coating on the aperture. Especially in the case of *fluorescence* detection, the problem was not merely the low transmittance but in adittion a "non-radiative energy transfer" from the molecule to the metallized aperture. In order to avoid this problem, we have developed a novel probe, where the metal coating on the aperture was replaced with indium-tin-oxide (ITO) coating.

The SNOM/STM observation was performed firstly on CdSe nano-particles those were dispersed on an ITO thin film. "Illumination-collection mode" was adopted for the SNOM operation. In the obtained fluorescence image, we could observe individual bright spots with FWHM of about 20 nm (Figure 1), which might be assigned as the fluorescence from single nanoparticles. As compared with the actual aperture size of 150 nm (evaluated by SEM pictures), the spot sizes were extremely small. Thus, we can conclude that the high spatial resolution beyond the aperture size was achieved by our new ITO/Au-coated probe as well as single-molecular-level high sensitivity [2].

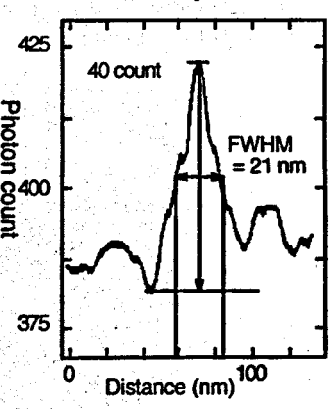

Figure 1: Cross-sectional profile of the fluorescence from a single nanoparticle.

It is a long-term controversial problem in the light-illumination STM that *how photons can reach to tunneling junction* if the light illumination is carried out from the side. Our ITO/Au-coated probe will give some answers against this question because it is possible to excite nm-scale local area by our probe. In this study, we adopted a self-assembled monolayer of GFP-apocytochrome *b*562 molecule which is reconstituted with SH-terminated heme molecule as an appropriate sample system. Preceding an actual application, we performed a conventional light-illumination STS as shown in Figure 2, where the photocurrent generation was observed synchronously with mechanical chopped laser-illumination. In the session, we will give results obtained by combining these two techniques.

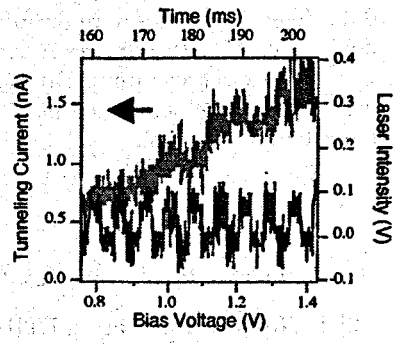

Figure 2: STS measurement on a GFP-cytochrome SAM with light illumination.

References

[1] K. Nakajima *et al.*, *Jpn. J. Appl. Phys.* 38, 3949 (1999).
[2] K. Nakajima *et al.*, to be published in *Jpn. J. Appl. Phys.*

Orientation dependence of fluorescence lifetimes of a dipolar emitter near an interface

M. Kreiter, M. Prummer, B.Hecht†, U.P. Wild*
Physical Chemistry Laboratory, Swiss Federal Institute of Technology, CH-8093 Zurich, Switzerland.

Understanding the behavior of single fluorescent molecules in inhomogeneous media is of importance for Nano-optics since single molecules come very close to ideal dipolar point sources. In this paper we study the excited state lifetime of single molecules embedded in a 20 nm PMMA film as a function of the angle between surface normal and dipole moment. Strong changes in the excited state lifetime of the molecules are expected because their optical near field interacts with the nearby interface with a coupling strength modulated by the dipole orientation. Our experiments are consistent with the behavior predicted by theory [1, 2] as displayed in Fig. 1. The rather large scattering of the data cannot be explained by measurement uncertainties but must be due to local, molecular scale inhomogeneities in the polymer matrix. Experiments were performed with a fluorescence scanning confocal optical microscope [3] using a pulsed, frequency doubled NdYag laser (Antares, Coherent, 532 nm, 150 ps) for excitation. A circular disk with a diameter of 3 mm blocks the inner part of the beam and implements annular illumination geometry [3]. A dichroic mirror directs the light into a microscope objective where it is focused onto the interface. This illumination mode creates strong longitudinal electric field components which are instrumental for probing the out-of plane angle of the dipole moments.

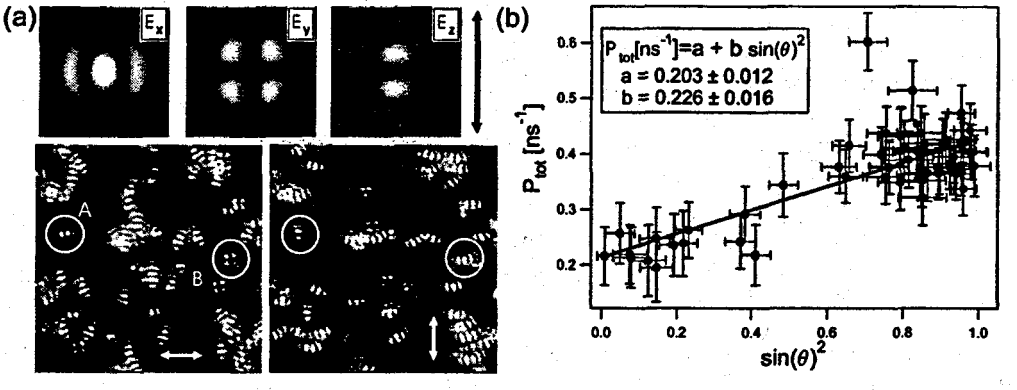

Figure 1: (a) Upper panel: calculated intensity of the electrical field components for annular illumination (1 μm^2). The double arrow indicates the E-field of the incident beam (x-axis). Lower panel: Experimental data. The two images were recorded with linearly polarized light, the double arrows indicate the electrical field vector. The two dipoles A and B are perpendicular and parallel to the sample plane, respectively. (b) Fluorescence decay rate of DiI molecules as a function of $\sin^2\theta$ where θ is the angle between the dipole moment and the surface normal. The straight line is a linear fit to the data, the fitting parameters are indicated in the graph.

References

[1] W. Lukosz, R.E. Kunz, Opt. Commun., **20**, 195 (1976)

[2] L. Novotny, PhD thesis, ETH Zürich (1996)

[3] B. Sick, B. Hecht, L. Novotny, Phys. Rev. Lett., **85**, 4482 (2000)

*present address: MPI für Polymerforschung, Mainz, Germany, email: kreiter@mpip-mainz.mpg.de
†present address: Nano-Optics group, IfP, University of Basel, Basel, Switzerland, email: bert.hecht@nano.optics.ch

A parabolic mirror objective with high numerical aperture for local field enhancement in near-field optical microscopy

M. A. Lieb, A. Drechsler, C. Debus and A. J. Meixner Physikalische Chemie, Universität Siegen, Adolf-Reichwein-Str. 2, 57068 Siegen, Germany.

L. Novotny, University of Rochester, The Institute of Optics, Rochester, NY 14627.

Parabolic mirrors with high numerical aperture (NA) have been used as efficient light collection devices in the early cryogenic single-molecule work [1], but for microscopy and imaging they have been avoided due to poor off-axis imaging properties. However, in a stage scanning confocal setup one can ensure that the light is always focused on the optical axis. It is possible to fabricate a concave parabolic mirror with an aperture close to unity and hence it (1) can produce a tight diffraction limited spot, (2) can efficiently collect the radiation of a point light source in the focal spot, (3) has minimal chromatic aberrations, (4) can be used to illuminate opaque samples without hindering the access and (5) can be cooled down to cryogenic temperatures without loss of performance.

Vector-field simulations for a parabolic mirror illuminated by a radially polarized beam (donut mode) show a strong, highly confined electrical field component along the optical axis which is about 10 times more intensive than the in-plane components, which are also present near the focus [2] (Figure 1, left-hand side). This makes it a well suited tool for local field-enhancement in near-field optics. Simulations (generalized multipole technique) of the electromagnetic fields near a sharp tip, which is placed in the focal spot of the mirror show a field enhancement by a factor in the order of 10^4 (Figure 1, right-hand side).

In excess of these theoretical results the authors have built a parabolic mirror microscope and show single molecule results, which proof very good performance of the confocal setup [3].

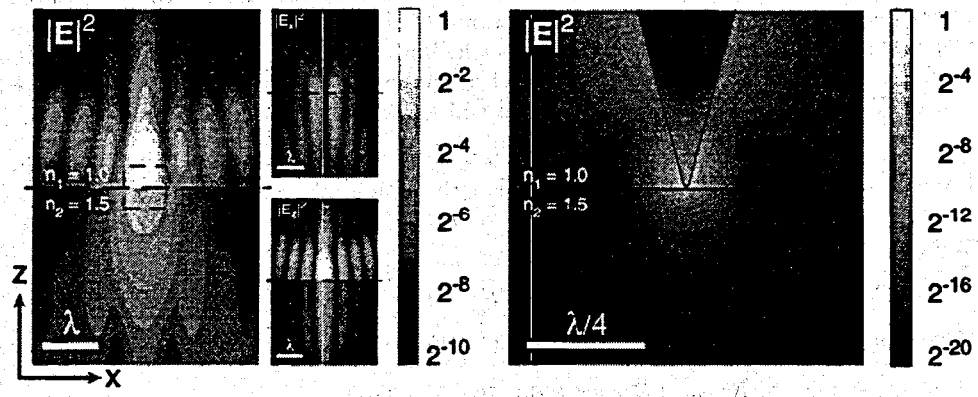

Figure 1. Intensity distribution in the focal region of a high *NA* parabolic mirror illuminated with a radially polarized beam on an air-glass interface. Diffraction limited spot (left) and 10^4 times enhanced field at a Gold tip illuminated with a wavelength $\lambda = 800$ nm (right).

References

[1] T. Basché, W. E. Moerner, M. Orrit, U. P. Wild (eds.) "Single-Molecule Optical Detection, Imaging and Spectroscopy," VCH, Weinheim (1997).

[2] M. A. Lieb and A. J. Meixner, "A high numerical aperture parabolic mirror as imaging device for confocal microscopy," *Opt. Express* 8, 458 (2001).

[3] A. Drechsler, M. A. Lieb, C. Debus and A. J. Meixner, "Confocal microscopy with a high numerical aperture parabolic mirror," *Opt. Express* 9, 637 (2001).

Optics on metal-dielectric films

S. Grésillon, S. Ducourtieux, J.-C. Rivoal,
Laboratoire de spectroscopie en lumière polarisée, ESPCI, 10 rue Vauquelin, 75005 Paris, FRANCE.
P. Gadenne, S. Buil, X. Qulin,
LMOV, Versailles-Saint Quentin University, 78035 Versailles, FRANCE.
V. M. Shalaev,
School of Electrical and Computer Engineering, Purdue University, West Lafayette, IN 47907.

The optical field on a metal-dielectric films is strongly enhanced and highly localized. Because of their composite structures, the surface-plasmons generated by an incident field are localized in subwavelength-size areas called "hot-spots", a processus slightly similar to the localisation of plasmons on the edge of metal particles. The electric field in these resonant hot-spots exceed by several order of magnitude the incident applied field. Finally, the structure of the film shows resonances for any given wavelength, from the visible to the far-infrared when the film metal coverage is close to the percolation threshold [1].

Probing the near-field zone is the best way to investigate the subwavelength properties of these films. The near-field optical microscope with apertureless tip developed in our laboratory was successfully used to verify the theoretical prediction of localization, enhancement and wavelength dependency [2]. Further analysis have shown recently that hot-spot positions changes dramatically with the polarization of the incident light [3], which can be of peculiar importance to address the hot-spot on specific areas, for example to use them to excite single molecules or nanoparticles. Unexpected result of our studies was the observation of a local chirality, which cannot be explained by the 2-D model and implies to take into account the third dimension of the film.

These high enhancements are even stronger in non-linear optics, increasing with the order of non-linearity. In collaboration with the *Photonic and Optoelectronic Group* in Munich (Germany), we have investigated the far field 2nd harmonic emission of metal-dielectric film when illuminated by short laser pulses [4]. This emission shows a broad spatial distribution, which is supposed to be even broader for higher order of the non-linearity. We have also observed a white light emission which is still under investigation.

We are actually improving our near-field set-up to measure non-linear effects in the near-field zone and we will soon study these properties with subwavelength resolution.

References

[1] V. M. Shalaev and A. K. Sarychev, *Physical Review B* **57**, 13265 (1998).

[2] S. Grésillon et al., *Physical Review Letters* **82**, 4520 (1999).

[3] S. Ducourtieux et al., *Physical Review B* **64**, 165403 (2001).

[4] M. Breit et al., *Physical Review B* **64**, 125106 (2001).

Study of Optical Properties of Periodic Array with Carbon with NSOM

Hojin Cho and Wonho Jhe
School of Physics and Center for Near-field Atom-photon Technology
Seoul National University, School of Physics and Center for Near-field Atom-photon Technology,
ShillimDong, KwanakGu,, Seoul, Korea. 151-742

Several studies of the light transmittance enhancement have been reported in periodic hole array. Ref[1] Generally the material used for these experiments are metal like Al, Ag, and etc. There are two candidates for the possible origin of these abnormal phenomena: surface plasmon effect Ref[2] or diffraction effect of the periodical structure.

In our experiments with very elongated periodic carbon nanotubes, we have observed similar remarkable light transmittance in comparison with the existing theory Ref[3]. We expect that nanoscopic study with a near-filed scanning optical microscope exhibits more obvious physics behind this extraordinary phenomena.

References

[1] T. W. Ebbesen et al, Nature, **39**, 667 (1998).
[2] E. Popov et al, Physical Review B, **62**, 1600 (2000)
[3] H. A. Bethe, Physical Review, **66**,163 (1944)

Study of the focused laser spots generated by different laser beam conditions at various interfaces

Yuan Hsing Fu, Fu Han Ho, Din Ping Tsai
Department of Physics, National Taiwan University
1 Sec 4, Roosevelt Road, Taipei 106, Taiwan

Research on the focal region is an interesting topic in both fundamental and applied physics. For optical imaging, confocal microscopy, laser tweezers and optical data storage, the high numerical aperture lens is used to have a small focused laser spot. Understanding of the details of the focused laser spot in various conditions is an important issue. For high numerical aperture systems the effects due to the intrinsic vector characters of the electric fields is no longer trivial, and a vector diffraction theory is needed for the analysis. Experimental probing of the focal region is urgently requested by many theoretical models of the approximation method to demonstrate their validity. In this paper, three-dimensional near-field imaging of the focused laser spot at various conditions was studied both theoretically and experimentally.

The experimental setup shown in Fig. 1(a) is based on a tuning-fork tapping-mode near-field scanning microscope (NSOM) system. High numerical aperture lens (NA 0.85) was used to focus various incident lights, and near-field optical fiber probe was used to measure the intensity of the focal-field. Fig. 1(b) shows the results of the polarization effects in the distribution of the focused field. Changes due to the modification of the incident field and focusing system were observed experimentally. Three-dimensional imaging of the focused laser spots of different incident laser beams and at various interfaces are the focuses of the study as well.

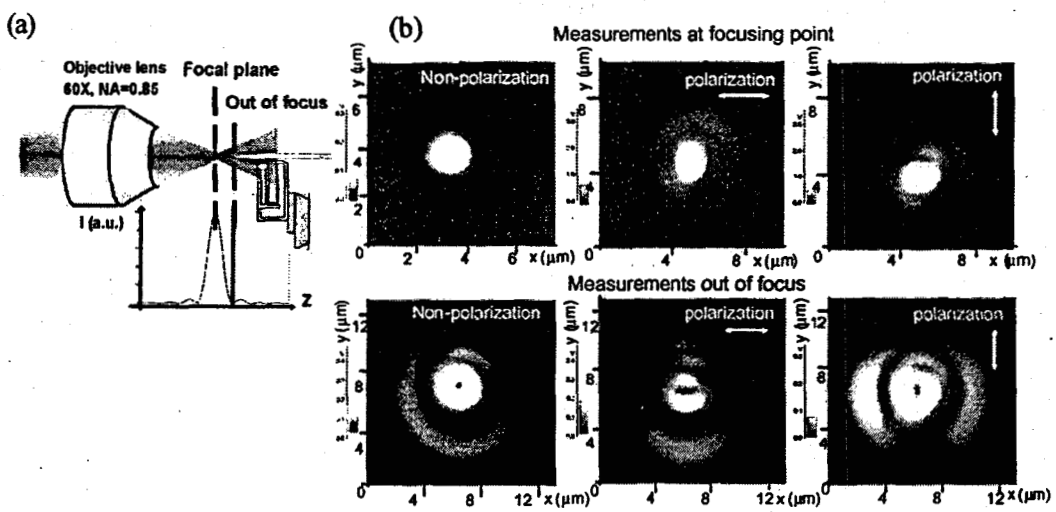

Figure 1: (a) Near-field probing of the focused spot, (b) Experimental results of the images of a focused spot with wavelength of 632.8 nm, and NA = 0.85 in different polarization.

References

[1] M. Born and E. Wolf, "Principles of Optics," 7th ed, Cambridge University Press, Cambridge (1999).
[2] J.J. Stamnes, "Waves in focal regions," Adam Hilger, Bristol (1986).
[3] Min Gu, "Advanced Optical Imaging Theory," Berlin, New York, Springer (1999).
[4] Taco D. Visser, Sjoerd H. Wiersma, J. Opt. Soc. Am. A/Vol. 9, No.11, 2034 (1992).
[5] S. K. Rhodes, A. Barty, A. Roberts, K. A. Nugent, Opt. Commun. 145, 9 (1998).

Near field simulations and measurements of surface plasmons on perforated metallic thin films

Hsia Yu Lin, Din Ping Tsai

Department of Physics, National Taiwan University, Taipei 10617, Taiwan

Wei-Chih Liu

Department of Physics, National Taiwan Normal University, Taipei 116, Taiwan

Manipulating photons by artificial devices is a promising way to control the optical output through metallic or dielectric films. The results reported by Ebbesen et al.[1] showed extraordinary optical transmission of sub-wavelength hole arrays in metallic films. The optical energy can be exchanged in the form of the propagating or evanescent field on these micro or nano structures radiatively or non-radiatively, respectively. The key issue is the dispersion function of the structures which could couple the light into the excited plasmons[2]. In our experiments, an artificial nanolithography performed by an atomic force microscope was used to make hole arrays or periodic grooves on the surface of the metallic thin film. Periodic holes with different depths, diameters, and periods exhibited interesting near-field or far-field optical effects on the interactions between the photons and the nanostructures. Optical transmission spectra of different patterns demonstrated the various surface plasmon excitations. Computer simulations of finite-difference time-domain (FDTD) [3] were used to calculate the near-field distributions and optical transmission on variable nanostructures. Highly enhanced local fields and dispersion relations were studied for surface plasmon polariton and localized surface plasmon of the periodic nanostructures as well.

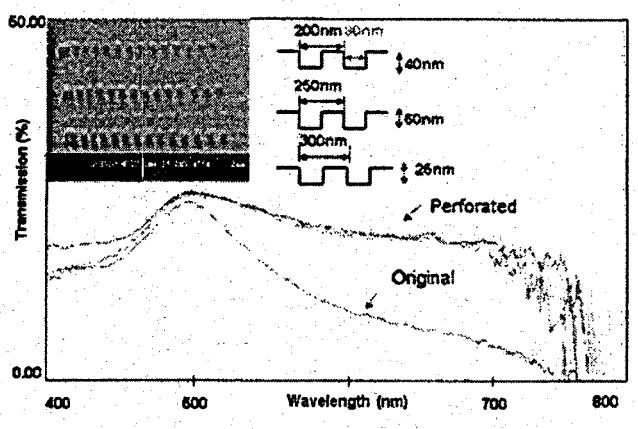

Figure 1: Transmission spectra of the original and perforated 100 nm gold films. Inset is the SEM micrograph of the hole arrays.

References

[1] T. W. Ebbesen, H. J. Lezec, H. F. Ghaemi, T. Thio, P. A. Wolf, Nature **391**, 667 (1998).
[2] H. Raether, Surface Plasmons, Springer-Verlag, Berlin (1988).
[3] W.-C. Liu, D. P. Tsai, Phys. Rev. B (in press).

Local field enhancement at particles on surfaces in nanostructuring and laser cleaning

C. Bartels, O. Dubbers, H.-J. Münzer, M. Mosbacher, P. Leiderer,
Universität Konstanz, Center for Modern Optics, Fach M 676, 78457 Konstanz, Germany.
A. Pack, R. Wannemacher,
Institut für Experimentalphysik II / FKO, Universität Leipzig, Linnstr. 5, 04103 Leipzig, Germany

Local field enhancement at small particles (diameter about the size of the wavelength or below) was used to produce nanostructures on silicon, InSb and glass surfaces by illumination with short and ultrashort laser pulses (FWHM = 8 ns, λ=532 nm/ FWHM = 30 ps, λ=583 nm/ FWHM=150 fs, λ=800 nm/). The investigated particles include dielectric (polystyrene,SiO_2) as well as metallic (gold) colloidal spheres of different size ranging from 50 nm to 3 μm. Additionally to spherical particles we illuminated triangular gold structures as well.

The enhancement of the laser intensity in the near field of the particles results in a local ablation of the substrate material. These ablation sites have been investigated by scanning electron microscopy (SEM) and atomic force microscopy (AFM). We found a strong dependence of the structures' shape on the laser pulse duration which can be ascribed to the heat diffusion during the illumination time.

In addition a comparison with theoretical computations of the near field of the particle-substrate system shows that the shape of the ablated sites in good agreement reflects the field distribution. In order to investigate the origin of certain deviations between calculated field distributions and the shape of the ablated sites we systematically studied the influence of the particle shape on the process.

The results of these experiments facilitate the understanding of the local field enhancement in a systems of (deformed) spherical particles on plane substrates and have important consequences not only as a possible nanostructuring method but also for technically relevant processes such as laser induced particle removal from surfaces.

Optimal Parameters for Raman Spectroscopy by Apertureless Near Field Enhancement

R. Vogelgesang, A. Bek, and K. Kern
Max-Planck Institute for Solid State Research, 70569 Stuttgart, Germany.

Fluorescence, Raman and other types of optical spectroscopy at the single molecule level have attracted considerable attention in recent years. Compared to elastic scattering processes, the cross-sections of the underlying physical processes are exceedingly small and specific measures must be taken to render optical spectroscopy of nanoscopic samples feasible.

To achieve recordable signal levels, taking advantage in a controlled fashion of highly localized and strong field enhancements effects such as those acting at seemingly random surface spots in surface enhanced Raman spectroscopy holds great promise. Not only does a spatially tightly confined field avoid overheating and possibly destroying a large sample volume; the desired spectral signals are also more easily discriminated from spurious signals generated in the nearby environment of a sample region of interest. In this context, near-field optical effects are a natural choice and to date two main approaches have emerged. Based on apertures of sizes down to ≈ 50 nm, scanning near-field optical microscopy (SNOM) has evolved into a well-established method, limited only by the exponentially diminishing throughput of ever smaller apertures. An alternative approach, which holds promise of spatial resolution of ≈ 1 nm, is *apertureless* SNOM which utilizes highly localized near field enhancement effects of laser radiation in the nm-sized volume near the tip apex.[1]

To investigate the potential of controlled Raman spectroscopy of individual molecules by apertureless SNOM, we study carbon nanotubes attached to commercial AFM tips located in the vicinity of another, field enhancing conductive tip. Depending on the relative location of the two tips, the Raman spectrum of the tube is expected to be enhanced, as the tube is subjected to field strengths of varying degree.

In order to determine the optimal experimental parameters for this setup, we study the interactions of the incident exciting radiation and sample holding field enhancing tips theoretically. We solve the three-dimensional vectorial Helmholtz equation using the multiple multipole method. The dependence of the electric field strength on geometry, material and relative location of the two tips as well as direction and polarization of the incident radiation is investigated.

References

[1] L. Novotny, D. W. Pohl, and B. Hecht, Opt. Lett. **20**, 970 (1995).

Local field enhancement on a near-field apertured tip by the use of LOCOS

Ki-Bong Song, Sung-Q Lee, Junho Kim, Jeongyong Kim and Kang-Ho Park*
Basic Research Laboratory, Electronics and Telecommunications Research Institute,
Yu Sung P.O. Box 106, Daejeon 305-600 Korea

To increase the optical throughput of a near field aperture, several fabrication techniques have been proposed so far [1-4]. However, although the enhancement of the throughput of the near field aperture has been realized owing to a geometrical change near the aperture, which has weakened the optical loss at the apex of the aperture, and the optical interaction between incident light and the tip material (such as self focusing effect [3] or the excitation of surface plasmon mode [4]), problems such as simple fabrication flow and higher optical throughput remain.

In this paper we present a simple fabrication process of high throughput near-field apertured tip using local oxidation of Si (LOCOS) [5]. The high throughput structure was fabricated with two key growth mechanisms at a low temperature less than 1050°C. One is that the growth rate of oxide at a flat surface of Si is higher than that at an angled corner due to the compressive stress at the corner structure. Another named a bird's beak (or LOCOS), which is more important mechanism, is that the growth rate of the oxide at a Si/Si_3N_4 interface is lower than that at the air/Si interface because the stress field at the Si/Si_3N_4 interface is stronger than that at air/Si interface. In figure 1(b) (c), we can clearly see the near-field apertured tip as small as 150nm, in which the structure of the bird's beak effect apertured tip at its foot was a parabolic shape for the enhancement of the throughput. Finally, detailed fabrication process and experimental results for the enhanced throughput on the apertured tip will be presented.

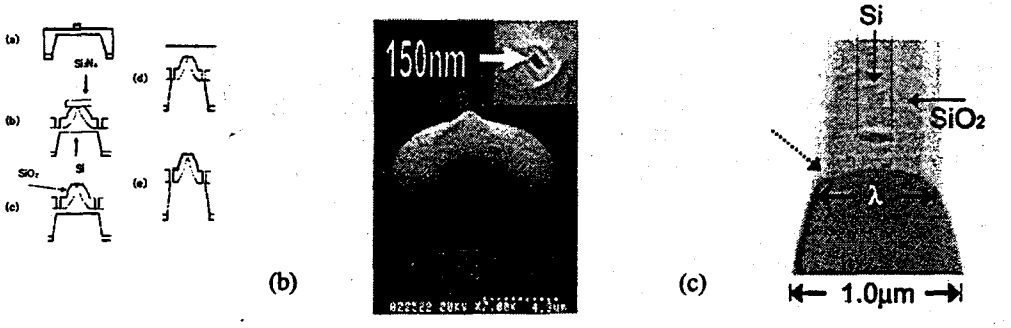

Fig. 1. (a) Fabrication process (b) SEM image of the near-field apertured tip using bird's beak effect (c) Cross-sectional view of the stripe tip.

References

[1] T. Saiki, S. Mononome, M. ohtsu, N. Saito, and J. Kusano, Appl. Phys. Lett., **68**, 2612 (1996).
[2] P. N. Minh, T. Ono, and M. Esashi, Rev. Sci. Instrum. **71**, 3111 (2000).
[3] K. B. Song, J. Kim, and K. H. Park, Appl. Phys. Lett, to be published
[4] K. M. Pellerin, H. J. Lezec, T. W. Ebbesen, R. A. Linke, and T. Thio, IEEE-NANO 2001 293 (2001).
[5] S. Wolf, "Silicon Processing for the VLSI Era, Vol. 3-The Submicron MOSFET" Lattice Pr. 1995.

* Present Address: Department of Physics, University of Incheon, Dowha-dong 177, Nam-ku, Incheon 402-749, Korea.

Plasmon coupled tip-enhanced near-field optical microscopy

A. Bouhelier, M. Beversluis, and L. Novotny,
University of Rochester, The Institute of Optics, Rochester, NY 14627.
J. Renger,
Technische Universität Dresden Institut für Angewandte Photophysik D-01062 Dresden, Germany

Scanning near-field optical microscopy aims at optically resolving subwavelength structures. The most common technique relies on the local excitation of the sample surface by the optical fields near a nano-aperture which is commonly produced at the end of a glass fiber tip[1]. Alternatively, high resolution microscopy can also be achieved by using the local field enhancement produced at the end of a sharp metal tip when illuminated by a highly focused laser beam[2, 3]. By combining these techniques in the form of a sharp metallic tip at the end of an overcoated fiber, we propose a new method that does not require the delicate technologies to produce nano-apertures[4, 5], nor require the intense external focused beam responsible for the field enhancement. Past the cut-off point, the mode inside the fiber no longer propagates, and an evanescent field is created. The large wavevectors of this evanescent field match the resonance conditions for surface plasmon excitation on the surrounding silver layer. The surface plasmons then travel along the metal coating towards the tip apex. If the probe is excited by a radially polarized mode a strongly enhanced field is expected at the tip apex. Figure 1 shows the field calculated at the end of an Au coated glass tip when an dipole situated inside the fiber and oriented along the tip axis is excited. The electromagnetic field associated with surface plasmons can be used as a local optical near-field source to investigate fluorescence samples such as single molecules.

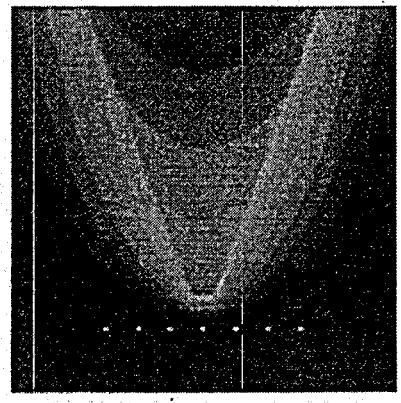

Figure 1: Calculated total field at the end of gold coated glass tip excited by an dipole situated inside the fiber and oriented along the tip axis. The intensity changes by a factor 1.62 between contour lines. Scan is 120×120 nm^2.

References

[1] A. Harootunian, E. Betzig, M. Isaacson, and A. Lewis, *Appl. Phys. Lett.* **49**, 64 (1986).

[2] U. Ch. Fischer, *Scanning tunneling microscopy and related methods*, NATO ASI series (Kluwert, Dordrecht 1989), **184**, Edited by R. J. Behm, N. Garcia and H. Rohrer.

[3] E. J. Sanchez, L. Novotny and X. S. Xie, *Phys. Rev. Lett.* **82**, 4014 (1999).

[4] J. A. Veerman, A. M. Otter, L. Kuipers and N. F. Hulst, *Appl. Phys. Lett.* **72**, 3115, (1998).

[5] A. Bouhelier, J. Toquant, H. Tamaru, H.-J. Güntherodt, D. W. Pohl and G. Schider, *Appl. Phys. Lett.* **79**, 683 (2001).

Phase and Intensity Contrast in Apertureless Scanning Near-Field Optical Microscopy

A.Bruyant, S. Aubert, G. Lérondel, R.Bachelot, S.Hudlet and P.Royer
Université de technologie de Troyes, Laboratoire de Nanotechnologie et d'Instrumentation Optique.
BP 2060 10010 TROYES cedex France

Scanning near-field optical microscopy (SNOM) is an imaging technique that can achieve an optical resolution beyond the diffraction limit. Apertureless scanning near-field optical microscopy [1] [2] [3] (ASNOM), also known as "scattering type" SNOM has numerous potential advantages such as an improved resolution, no wavelength limitation, polarization analysis...

The field scattered by the tip of an ASNOM is generally modulated via a vibrating mode atomic force microscope regulation. However, as pointed out in Ref. [4], a lock-in detection of the signal does not completely remove the influence of the Background Scattered Light (BSL) issued from the whole detection zone since it may interferer with the modulated scattered field.

In our configuration (Fig. 1a) we show that the BSL can be seen as a reference field. The ASNOM behaves then as an interferometer allowing local optical phase measurement (Fig. 1b). The approach curves (Fig. 1c) recorded in the presence or in the absence of BSL lead to a detection of the intensity or the amplitude. A simple numerical model is presented and discussed. This study completes the understanding of imaging in ASNOM

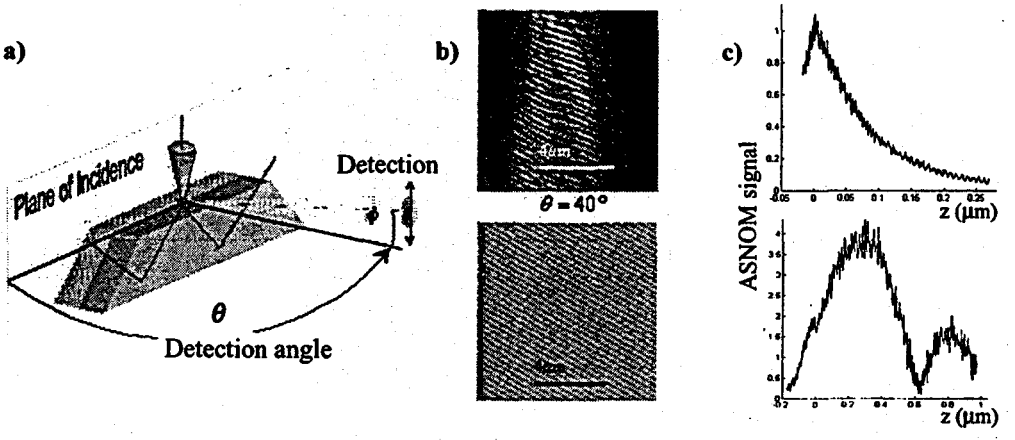

Figure 1: a) Samples are illuminated in total internal reflection b) At the top: image of the demodulated signal obtained when the tip is scanning the prism surface. The fringes are due to the interference between the modulated scattered field and the BSL. Below: numerical simulation of the fringes pattern c) Approach curves in the case of a weak BSL (at the top) and in the case of a strong BSL (below).

References

[1] F.Zenhausern, M.P.O'Boyle and H.K.Wickramasinghe, *App. Phys. Lett.* **65**, 1623 (1994).

[2] Y.Inouye and S.Kawata, *Opt. Lett.* **19**, 159 (1994).

[3] P.Gleyzes, A.C.Boccara, and R.Bachelot, *Ultramicroscopy* **57**, 318 (1995).

[4] B.Knoll and F.Keilmann, *Nature* **399**, 134 (1999).

Near-field distributions and localized surface plasmon of metallic nanostructures in a thin film

Wei-Chih Liu
National Taiwan Normal University, Taipei, Taiwan 116, R.O.C.

Din Ping Tsai
National Taiwan University, Taipei, Taiwan 106, R.O.C.

Surface plasmon polariton and localized surface plasmon resonance of metallic nanostructures were studied with finite-difference time-domain (FDTD) simulations. Enhanced local fields and surface plasmons were found around deep grooves in a metallic thin film and nano-size silver particles. With periodical structures, the surface plasmons have global, extended near-field distributions and the localized surface plasmons are highly concentrated around the nano-structures.[1] Localized surface plasmon exhibits a very broad resonant peak in the transmission spectrum(Fig. 1), which related to its highly localized nature and can be apply to describe optical responses of non-periodic structures.

For randomly distributed nanostructures, the localized surface plasmons are the predominate resonances with incident light. Our simulations showed that enhanced local fields and localized surface plasmons resonances were excited in clusters of silver nanoparticles embedded in a dielectric thin film. The near-field intensity of silver nanoparticle cluster on the thin film surface also exhibits nonlinear behavior with increasing particle densities. Our research has significant implications on applications on near-field optical storages and nanophotonic devices. Especially for the super-resolution near-field structure (Super-RENS)[2], which is a promising high-density near-field optical disk and could generate optical near-field effects without a probe[3-4], our research on localized surface plasmon may indicate its physical mechanism and extend its applications.

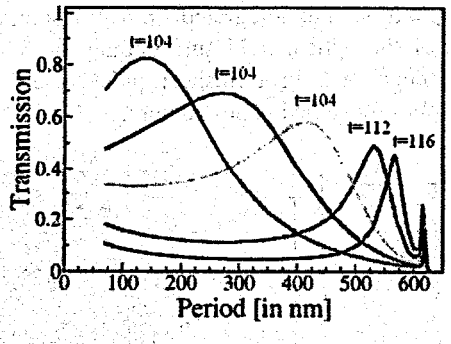

Fig. 1 Transmittance coefficients as functions of the period for a deep-groove grating on a metallic thin film. The thickness of the films is from 104 to 116 nm.

References

[1] W.-C. Liu and D. P. Tsai, Phys. Rev. B (in press).
[2] J. Tominaga, T. Nakano, and N. Atoda, Appl. Phys. Lett. 73, 2078 (1998).
[3] D. P. Tsai, and W. C. Lin, Appl. Phys. Lett. 77, 1413(2000).
[4] W.-C. Liu, C.-Y. Wen, K.-H. Chen, W. C. Lin, and D. P. Tsai, Appl. Phys. Lett. 78, 685 (2001).

Transverse optical field localization in nonlinear periodic optical nanostructures for enhanced second-harmonic generation

W. Nakagawa, G. Klemens, A. Nesci and Y. Fainman, Dept. of Electrical and Computer Engineering
University of California, San Diego, La Jolla CA, 92093

Recent advances in nanofabrication technologies have enabled the construction of a wide range of subwavelength optical nanostructures, facilitating a number of novel applications. In this work, we analyze transverse localization of the optical field in subwavelength periodic optical nanostructures, and investigate the application of this effect to the enhancement of optical nonlinear phenomena.

Previously, we have described transverse field localization in periodic optical nanostructures [1]. These nanostructures can be viewed as a coupled array of waveguides, with localization of the waveguide modes in the high refractive index regions of the structure. An example of such a nanostructure is shown schematically in Fig. 1a. The optical field distribution inside the nanostructure for a TE-polarized normally-incident ultrashort pulse, computed using the Rigorous Coupled-Wave Analysis method [2,3], is shown in Fig. 1b. In the result of Fig. 1b, elevation of the peak intensity due to the temporal localization of the energy in the pulse, as well as the transverse localization of the energy in the nanostructure, is observed. For structures composed of nonlinear optical materials, we expect that significant enhancement of nonlinear optical effects can be achieved through this localization of the field. In addition, using a more complex nanostructure having multiple features in each period, phase matching for SHG can be realized concurrently with field localization. To more rigorously analyze the second harmonic generation process in this nanostructure, we have developed a modeling tool based on the RCWA method [2] extended to analyze SHG in the undepleted pump approximation [4]. Using this tool to analyze an optimized nanostructure, we predict a significant enhancement in the transmitted SHG output as compared to the bulk nonlinear material.

Due to the design degrees of freedom provided by a nanostructure composed of two or more constituent optical materials, it is possible to achieve both transverse localization and phase matching concurrently. An additional benefit of this approach is that the nanostructures are compatible with standard microfabrication techniques, facilitating their incorporation into integrated optical systems. In the future, our goal is to measure the amplitude and phase of the optical field surrounding the nanostructure using a heterodyne scanning near-field optical microscope and an ultrashort pulse laser, as well as to experimentally characterize the SHG output of the phase-matched nanostructure.

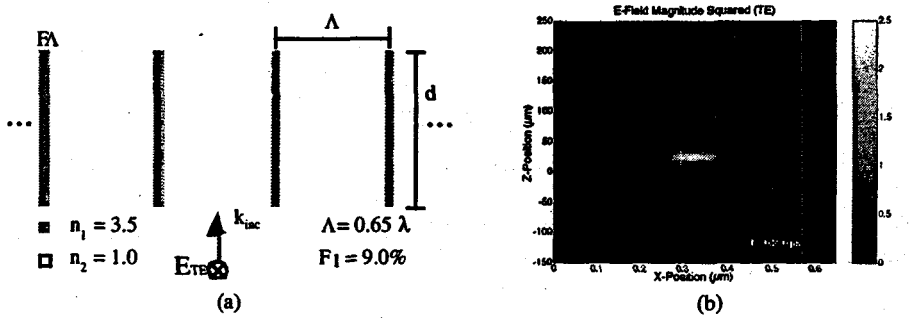

Figure 1: Periodic subwavelength optical nanostructure exhibiting transverse field localization: (a) schematic diagram; (b) modeling results showing a TE-polarized ultrashort pulse propagating in one period of the infinitely periodic structure.

References:

[1] W. Nakagawa, R.-C. Tyan, P.-C. Sun, and Y. Fainman, Optics Express **7**, 123–128 (2000).

[2] M. G. Moharam and T. K. Gaylord, J. Opt. Soc. Am. **72**, 1385–1392 (1982).

[3] W. Nakagawa, R.-C. Tyan, P.-C. Sun, F. Xu and Y. Fainman, J. Opt. Soc. Am. A **18**, 1072–1081 (2001).

[4] W. Nakagawa, R.-C. Tyan, and Y. Fainman, submitted to J. Opt. Soc. Am. A (2001).

Near-Field Observation of the Field Diffracted by Metallic Nanoparticles Excited Near Resonance

Gregory A. Wurtz, Jasmina Hranisavljevic, Jin-Seo Im and Gary P. Wiederrecht,

Chemistry Division, Argonne National Laboratory, Argonne, Illinois 60439-4831.

We report an investigation of the field scattered by isolated metallic nanoparticles on a glass substrate by apertureless near-field optical microscopy. The experimental configuration used is depicted in Fig. 1. The studied sample (gold or silver particles) is illuminated in total internal reflection at a wavelength of 400 nm and the resulting scattering diagram is far-field radiated using a silicon tip. The near-field contrast (both distribution and intensity) is shown to be strongly sensitive to the polarization of the incident light (see Fig.2). A large field enhancement has been observed for Ag in TM polarization (Fig.2(a)). Complementary experiments made on Au particles suggest that the particle plasmon resonance contributes strongly to the intensity of the field around the particle for Ag. The interaction of this intense field (mainly polarized along the probe axis) with the near-field probe leads to coherent scattering of the two local light sources (i.e. the Ag particle and the probe extremity) affecting dramatically the near-field contrast as shown in Fig. 2(a) [1]. Furthermore, by analyzing the polarization state of the unexpected spatially extended scattering pattern shown in Fig.2 it is found that, regardless of the incident polarization, Fig.2 contains a spatially confined component of the field that vibrates perpendicularly to the substrate.

This work was supported by the Division of Chemical Sciences, Office of Basic Energy Sciences, U.S. Department of Energy under contract W-31-109-Eng-38.

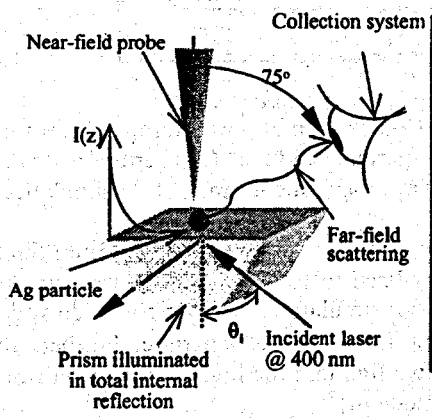

Fig.1: Schematic of the experimental set-up.

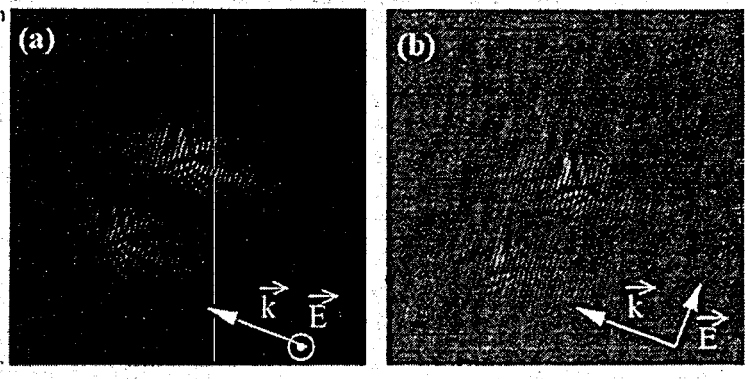

Fig. 2: SNOM images of isolated Ag nanoparticles (27 and a 40 nm in diameter) illuminated in total internal reflection at λ=404 nm on a glass substrate. (a) TM polarization and, (b) TE polarization. The scan size in the images is 15 μm.

References

[1] G. A. Wurtz, N. M. Dimitrijevic and G. P. Wiederrecht, Japanese Journal of Applied Physics **41**, L1331 (2002).

Greatly Enhanced Light Transmission Through a "C"-shaped Metallic Nano-aperture for Near Field Optical Applications

Xiaolei Shi, Lambertus Hesselink, Stanford University, Department of Electrical Engineering, Palo Alto, CA 94305

Robert Thornton, Siros technologies, Inc., San Jose, CA 95134

Conventional tapered fiber near field optical probe [1] uses an aperture at a fiber tip to provide a high spatial resolution beyond diffraction limit. However, this probe has very low power transmission due to propagation mode cutoff [2]. By studying how an aperture's geometry affects its power transmission, we find a very exciting "C"-shaped aperture geometry that shows ~1000× higher transmission efficiency than a conventional square aperture of size λ/10 while maintaining a comparable near field spot size.

Our study started with a Finite difference time domain (FDTD) [3] numerical simulation. The incident light is a planewave linearly polarized in the *x* direction of wavelength 1μm. Aperture is in a planar metallic screen. Fig.1 shows near field intensity distribution of the "C"-aperture at 48nm in comparison with that of a 100nm square aperture. The aperture geometries are overlaid on the intensity distribution. About 3 orders field enhancement from the "C"-aperture is clearly shown in Fig.1 and the near field spot sizes from the two apertures are comparable. By optimizing the "C"-aperture geometry, even smaller spot size and higher near field intensity have been achieved.

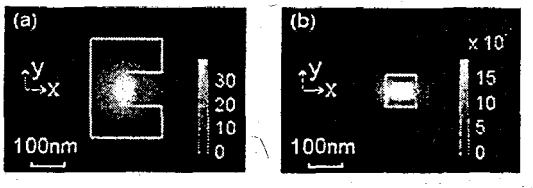

Fig. 1. Comparison of intensity ($|E|^2$) distribution at 48nm away from (a) "C"-aperture; (b) 100nm square. The lines show the aperture geometry. Incident light is a planewave linearly polarized in the x direction.

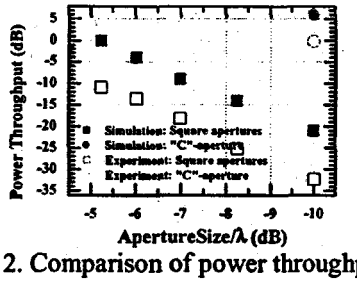

Fig. 2. Comparison of power throughput from square apertures and the "C"-aperture from both microwave experiments and FDTD simulation.

Microwave experiments were carried out at wavelength 5cm. Apertures were fabricated in 1.5mm thick copper plates. Power throughput, *i.e.*, total transmitted power normalized to total incident power over an aperture's physical area, is measured and plotted in Fig.2 together with simulations results. The microwave experiments confirms the ~1000× power throughput enhancement from the "C"-aperture. Further, by measuring copper plate's thickness effect on the power throughput, we find that the high transmission from the "C"-aperture is mainly due to the existence of propagation TE_{10} mode [4].

In summary, based on both FDTD simulation and microwave experiment, we report a unique "C"-aperture design that provides ~1000× higher transmission than a λ/10 sized square aperture. The high transmission is mainly due to propagation TE_{10} mode. The "C"-aperture is expected to play an important role in future high capacity data storage and other near field optical applications.

References

[1] E. Betzig, J. K. Trautman, E. D. Harris, J. S. Weiner, and R. L. Kostelak, *Science* **251**, 1468 (1991).
[2] L. Novotny and C. Hafner, *Phys. Rev. E* **50**, 4094 (1994).
[3] A. Taflove, S. C. Hagness, *Computational Electrodynamics: the Finite-Difference Time-Domain Method* (Artech Hourse, Boston, ed. 2, 2000).
[4] R. S. Elliott, *An Introduction to Guided Waves and Microwave Circuits* (Prentice Hall, 1993), p. 116.

Near-field Imaging of Magnetic Domains: Linear and Nonlinear Approaches

W. Dickson, S. Takahashi, A. V. Zayats,
School of Mathematics and Physics, The Queen's University of Belfast, BT7 1NN, United Kingdom.

Magnetic properties of thin films, multilayered structures, and related magnetism of surfaces and interfaces attract enormous interests owing to their numerous applications as well as from a fundamental point of view. Ultimately, the performance of magnetic materials is determined by their properties at the microscopic level, particularly by the sizes of magnetic domains and their motion in applied fields. Because of the rapid improvements in the areal density and performance of the magnetic materials and devices, it is important to develop high-resolution techniques to characterise the micromagnetic and magneto-optical properties of these materials in order to adopt a bottom-up approach in the search for new materials with improved characteristics.

Scanning near-field optical microscopy is a promising technique for both non-contact imaging of magnetic materials and magneto-optical applications such as data writing and reading. It opens up a new avenue of research in the future of high-density data storage. Optical approaches to characterisation of magnetic materials rely on the magneto-optical Kerr (or Faraday) effects which manifest themselves in a rotation of polarisation of reflected (or transmitted) light [1]. Significant enhancement of the contrast can be obtained using the nonlinear magneto-optical effects based on observation of magnetisation induced second-harmonic generation [2].

We present here the detailed experimental studies of near-field magneto-optical resolution of domain imaging with linear and second-harmonic generation techniques. Image formation mechanisms in the case of magnetic films of different thicknesses and magnetisation directions (in-plane and out-of-plane) are investigated in different polarisation configurations.

The diffraction effects on the domain walls are visible even in the near-field proximity to the surface of the thick magnetic films limiting the resolution of linear magneto-optical measurements in agreement with the theoretical predictions [3]. The resolution depends not only on the measured light polarisation component but also on the orientation of the incident light polarisation with respect to the domain wall. Since in many cases domain patterns exhibit complex geometrical structures, the optical resolution of the domain imaging is different depending on the domain wall orientation with respect to the polarisation of the incident light. This leads to complex images and difficulties in the magneto-optical image interpretation. Domain wall structure itself also influences the diffraction on the domain wall. As domain walls structure changes even along the same domain, it additionally complicates the near-field images. Nevertheless, in the case of thin magnetic films, the optical resolution is comparable to the resolution obtained with magnetic force microscopy. Combination of linear and second-harmonic imaging of magnetic domains could allow easy discrimination between in-plane and out-of-plane components of the domain magnetisation.

References

[1] E. Betzig, J. K. Trautman, R. Wolfe, E. M. Gyorgy, P. L. Finn, M. H. Kryder and C. H. Chang, *Appl. Phys. Lett.* **61**, 142 (1992).

[2] I. Smolyaninov, A. V. Zayats and C. C. Davis, *Opt. Lett.* **22**, 1592 (1997).

[3] A. A. Stashkevich and S. Hudlet, *Opt. Commun.* **199**, 305 (2001); J. N. Walford, J.-A. Porto, R. Carminati and J.-J. Greffet, *J. Opt. Soc. Am. A* **19**, 572 (2002).

Cold atoms manipulation with optical near-field modulated by high index nanostructures

G. Lévêque, C. Meier, R. Mathevet, C. Robilliard, J. Weiner
Laboratoire de Collisions, Agrégats et Réactivité
UMR 5589 du CNRS et l'Université Paul Sabatier
31062 Toulouse Cedex 4 France
C. Girard
Centre d'Elaboration de Matériaux et d'Etudes Structurales
29, rue Jeanne Marvig, BP 4347
31055 Toulouse Cedex 4 France
J. C. Weeber Laboratoire de Physique de l'Université de Bourgogne
9 avenue A. Savary, F-21078
Dijon, France

The coherent manipulation of neutral atoms by confined optical near-fields is a growing field of research with possible applications ranging from atomic interferometry to "integrated atom optics". In this poster, we expose a numerical study of the interaction of cold cesium atoms with an optical near-field acting as a periodically modulated atomic-optic grating (Fig. 1). Repulsive and diffractive effects are obtained by the confinement of an evanescent wave by a nanometric array of high index dielectric objects [1, 2]. In the first part, the main steps of the calculation are presented. This general approach permits a precise study of different aspects of atom-field interaction. In particular, different atomic models of increasing sophistication can be employed. A full calculation of several polarization components of the light field is necessary to study influence of the atomic fine structure. A comparison of different illumination polarization modes is presented.

We have carried out a systematic study of the effect of various realistic parameters on the diffraction figure. This study is in support of an experimental program now under development in our laboratory in Toulouse.The results of these simulations together with a description of the experiment will be presented.

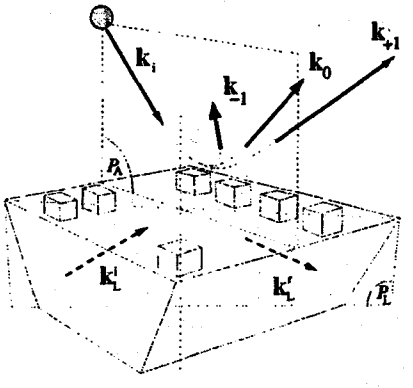

Figure 1: Diffraction of cold atoms by periodic optical potential modulated by dielectric nano-objects.

References

[1] G. Lévêque, G. Colas des Francs, C. Girard, J-C.Weeber, C. Meier, C. Robilliard, R. Mathevet, and J. Weiner, *Phys. Rev. E* **65**, 036701 (2002).

[2] G. Lévêque, C. Meier, R. Mathevet, C. Robilliard, J. Weiner, C. Girard, J-C.Weeber, *Phys. Rev. A* (in press)

Snom and Leed study of the 3C-SiC growth on Si(100) with improved interface quality

C. Cepek[1,4], E. Magnano[1], P. Schiavuta[2], M. Sancrotti[1,3], S. Prato[4], B. Troian[4], M. Bressanutti[4]
[1]Laboratorio Nazionale TASC-INFM, Trieste, Italy.
[2]Universita' di Padova, Italy
[3]Universita' Cattolica, Brescia, Italy.
[4]A.P.E. Research s.r.l., Area Science Park, Trieste, Italy

Silicon carbide is one of the most promising materials for many electronic and opto-electronic applications. In spite of all the efforts done by the scientific community, nowadays only few SiC-based semiconductors are realized, because of the high difficulties to grow single-crystals and single-polytypes with sufficient quality for electronic applications. Particular attention has been focused on the possibility to grow epitaxially 3C-SiC single crystals on Si surfaces, in order to open a way to Si-SiC device integration. In this case, it is crucial to control both, the cristallinity and the SiC-Si interface morphology after the growth of the SiC film.

We performed a systematic structural-morphological (LEED and SNOM) investigation of the early stages of growth of SiC films on Si(100)-(2x1) by co-deposition of C_{60} molecules and Si atoms. We spanned over a wide range of parameters that influence the growth process, including substrate deposition and post-deposition annealing temperature and relative effusion fluxes of C_{60} and Si. The long range order of the grown sample have been checked *in situ* by LEED, while the interface quality *ex situ* by SNOM.

Here we will present the results obtained by SNOM microscopy. Due to the SiC transparency in the visible light, this technique has the unique capability to study at the same time the morphology of the SiC-Si interface and the topography of the grown film. In particular in reflection mode at 650 nm the optical image reveals the presence of some micron sized defects. The figure 1b shows enhanced reflectivity with interference fringes due to the presence of the pits at the interface.

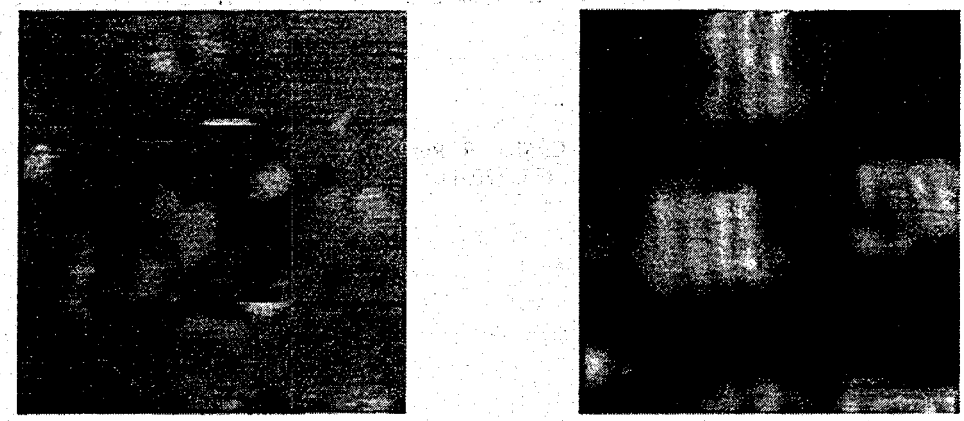

a b

Figure 1: SNOM topographic image (a) and reflection image (b) of SiC film on Si (100). The scan area is 10μm x 10μm.

Our results show that it is possible to find out the right grown conditions in order to obtain well ordered samples (3x1 LEED pattern) in which negligible pits are present at the interface and negligible holes are visible on the surface (SNOM).

Applications of SNOM in the material science: the case of SnO_2 thin films deposited by Sol-Gel

B. Troian, S. Prato
A.P.E. Research s.r.l., Area Science Park, s.s. 14, Km 163,5 Basovizza I-34012 Trieste (Italy)

E. Bontempi, L. E. Depero
INSTM and Laboratorio di Strutturistica Chimica, Dipartimento di Ingegneria Meccanica, Università di Brescia, Via Branze 38, I- 25123 Brescia (Italy)

D. Barreca, L. Armelao and E. Tondello
Centro di Studio sulla Stabilità e Reattività dei Composti di Coordinazione del CNR – Dipartimento di Chimica Inorganica, Metallorganica ed Analitica - Università di Padova, Via Marzolo 1, I-35131 Padova (Italy)

C. Canevali, R. Scotti and F. Morazzoni
Dipartimento di Scienza dei Materiali, Università degli Studi di Milano-Bicocca, Via Cozzi 53, I-20125 Milano (Italy)

Thin films are nowadays employed in many fields, from sensors to electronics, from magnetic to polymeric applications. Due to the strong influence of interfaces, layer thickness, density and morphology on the efficiency of thin films based devices, a careful structure characterisation involving complementary techniques is mandatory. The main aspects to investigate in the thin films are structure, microstructure, morphology and interfaces quality.

In this work samples of tin oxide films, for sensing applications, were deposited with the aim of investigating their structural and morphological properties. Nanostructured (3-6 nm) thin films were obtained by sol-gel route using tetra(tert-butoxy)tin(IV) and bis(acetylacetonato)platinum(II) as metal precursors [1].

The structural characterisation was performed by means of Glancing Incidence X-ray Diffraction (GIXRD), while the morphological characterisation by Atomic Force Microscopy (AFM) and Scanning Near-Field Optical Microscopy (SNOM).

In particular, in this poster, we will discuss SNOM results in order to characterise the surface topography, the average roughness of the films, and, in particular, the defects buried into the thin film.

The film interface quality will be evaluated by the comparison between SNOM and AFM: the SNOM images will show the presence of nanoclusters and "bubbles" with sub-micron diameter. These results show the potentiality of SNOM in the interface characterisation.

References

[1] F. Morazzoni, C. Canevali, N. Chiodini, C. Mari, R. Ruffo, R. Scotti, L. Armelao, E. Tondello, L. E. Depero, E. Bontempi, *Chemistry of Materials* **13** (11), 4355 (2001).

Near-field Observation of Carrier Diffusion in GaAs Quantum Structures under High Magnetic Fields

T. Tokizaki [a,b], H. Yokoyama [a,b],
[a] National Institute of Advanced Industrial Science and Technology, Tsukuba, Ibaraki 305-8568, Japan.
[b] Core Research for Evolutional Science and Technology (CREST), Wako, Saitama 351-0198, Japan.
T. Onuki, T. Tsuchiya,
Science University of Tokyo, Noda, Chiba 278-8510, Japan.

In modulation-doped single hetero-structures, two-dimensional electron gas (2DEG) systems have been investigated for novel quantum phenomena such as quantum Hall effects. The high mobility of the 2DEG is expected to show new phenomena related to the carrier diffusion. In this paper, the photo-luminescence has been observed for the 2DEG system using a scanning near-field optical microscope (SNOM) under high magnetic fields. The luminescence intensity strongly depends on the field, and the behavior is understood by the suppression of the carrier diffusion in the magnetic field.

In the sample, the 2DEG ($n_e \cong 2\times10^{11}$ cm^{-2}) is confined on the hetero-interface between the GaAlAs and the GaAs layer. The SNOM is operated in the illumination-collection mode at the temperature >5 K and the magnetic field <6 T, which is applied perpendicular to the 2DEG layer. The sample is excited using 633-nm-laser light. Figure 1 shows the luminescence spectra concerned with the 2DEG under the several magnetic fields. The data are measured at 8 K using Probe A with the aperture diameter D ~300 nm. We observe the magnetic-field induced peak energy shift, which is originated from the magnetic interaction of the excitons. Moreover, the luminescence intensity is strongly enhanced with the magnetic field. Figure 2 shows the field and the temperature dependence of the luminescence intensity measured with Probe A and B with D ~200 nm. While the intensity is significantly increased below 2 T for both probes at <10 K, the maximum intensity depends on the aperture size. On the other hand, at the higher temperature of 77 K, the field dependence becomes gentler. These behaviors are understood by taking account of the carrier diffusion. Since the diffusion length is ~μm for this sample, most of carriers excited under the probe are diffused out of the aperture area, and it causes the decrease of the luminescence intensity. However, when the magnetic field is applied, the carriers receive the Lorentz force and the diffusion is suppressed. If the carriers are confined in the cyclotron orbit with the diameter of 51 nm for 1 T, we can expect more than hundred-times enhancement of the intensity inside the aperture area, and the enhancement is more effective for the smaller aperture. At higher temperatures, thermal phonons scatter the carriers in the cyclotron orbit, and weaken the confinement effect under lower magnetic fields.

The authors would like to thank Dr. K. Suzuki and Dr. Y. Hirayama of NTT Basic Research Laboratories for the discussion and the preparation of the samples.

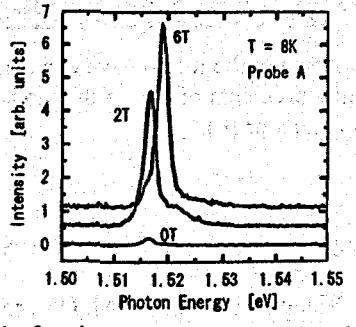

Fig.1: Luminescence spectra concerned with 2DEG under several magnetic fields.

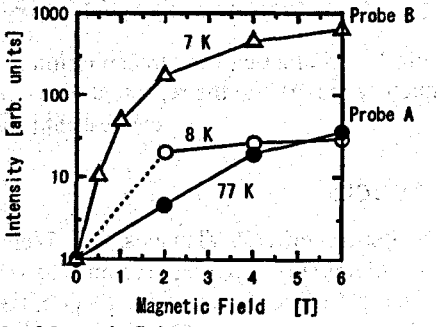

Fig.2: Magnetic field dependence of the luminescence intensity measured by Probe A and B.

Scanning Near-field Dielectric Microscopy at Microwave Frequencies for Materials Characterization

S. J. Stranick, S. A. Buntin, and C. A. Michaels

National Institute of Standards and Technology, Gaithersburg, MD 20899.

One of the common characteristics of recently developed, advanced dielectric materials is that they possess critical dimensions on short length scales (sub-micrometer) and that the components with these dimensions must be homogeneous and of high quality (defect free) for the intended dielectric performance to be achieved. Given that these critical dimensions are well below that of the radiation wavelength, analysis by conventional dielectric probes, which look at materials on a macroscopic dimension, is no longer sufficient. Alternatively, a near-field microscope takes advantage of the non-propagating electromagnetic fields (evanescent fields) present at a sample's surface when exposed to an electromagnetic wave. This results in an improvement in the spatial resolution below that of the radiation wavelength.

In our near-field microwave probe, radiation up to 20 GHz is coupled evanescently to the sample surface using a sharp proximal probe that is part of a resonant cavity/transmission line structure, Fig. 1a. Analysis of reflected and transmitted signals is performed using an HP8510 C Network Analyzer allowing the extraction of dielectric response information, Fig. 1b. The probe-sample separation is controlled using shear-force feedback giving the microscope the ability to map out the topographic structure of the sample surface. The importance of going to microwave frequencies is to gain access to information concerning the dielectric nature of materials. Additionally, valid measurements of a dielectric response should be made at the intended operational frequency: 1-40 GHz for wireless communications. Our current focus is on the validation of this form of microwave microscopy and dielectric spectroscopy. Geometric effects, organic contamination, and resonant effects can mask the true dielectric properties of a sample. These effects will be magnified when moving to smaller and smaller sample volumes/sizes.

This form of dielectric microscopy represents both a significant advance in the achievable spatial resolution [1] and more importantly a dramatic increase in the speed at which dielectric characterizations can be made (higher throughput measurement) [2]. Characterize of the dielectric response of variable-composition oxide and polymeric samples will be highlighted.

(a) (b)

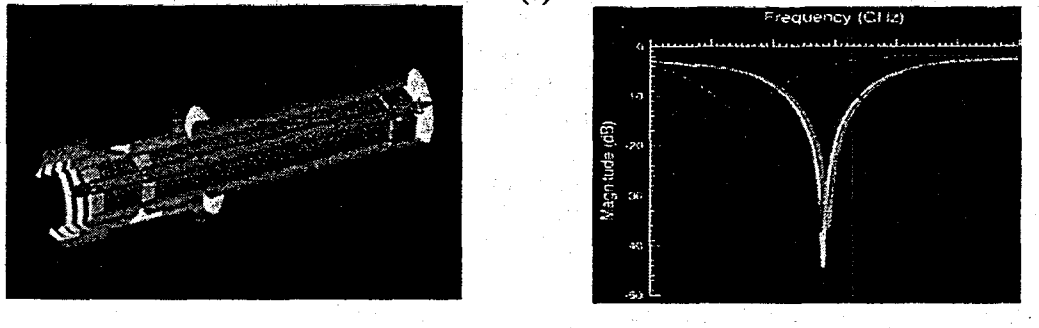

Figure 1: Schematic of the transmission line cavity structure used in the microwave evanescent probe microscope (a) and the representative network analyzer measurements of one of the modes of the evanescent probe microscope's resonator (b).

References

[1] D.E. Steinhauer, C.P. Vlahacos, F.C. Wellstood, S.M. Anlage, C. Canedy, R. Ramesh, A. Stanishevsky and J. Meingailis, Appl. Phys. Lett. **75**, 3180 (1999).

[2] H. Chang, C. Gao, I. Takeuchi, Y. Yoo, P.G. Schultz, X.D. Xiang, R.P. Sharma, M. Downes, M.T. Venkatesan, Appl. Phys. Lett. **72**, 2185 (1998).

Near-field photoconductivity and fluorescence imaging on blends of conjugated polymers

R. Riehn, R. Stevenson, J.J.M. Halls,
Cavendish Laboratory, University of Cambridge, Cambridge CB3 0HE, UK.
D. Richards,
Department of Physics, King's College London, London WC2R 2LS, UK.
D.-J. Kang, M. Blamire,
Department of Materials Science and Metallurgy, University of Cambridge, Cambridge CB2 3QZ, UK.
F. Cacialli,
Department of Physics, University College London, London WC1E 6BT, UK.

The field of conjugated polymer devices has reached a level of maturity such that they may now be considered as viable alternatives to other, more traditional optoelectronic technologies. The performance of these devices may be further improved by fabricating a compositionally and structurally optimized blend for the active layer, which can either create relatively large interfacial surface areas for efficient photovoltaics, or enable independent optimization of the electronic transport and luminescence properties of polymer light-emitting diodes. Blending does not produce a homogeneous film; instead, phase separation occurs on length scales from tens of nanometers to several microns, depending on the preparation conditions adopted. Understanding the optoelectronic properties of these blends at the length-scale of the phase separation is highly desirable for both a quantitative description of device operation, and further performance optimization.

We report combined scanning near-field optical microscopy (SNOM) and near-field photocurrent (NPC) imaging of a binary conjugated polymer blend; we find phase separation on a scale of about 5 μm, with a good correspondence between topographic, fluorescence, and photocurrent images. The photocurrent was measured for field strengths up to 12 kV/cm with the field applied between gold electrodes thermally evaporated on top of the polymer film, and spaced approximately 150 μm apart. Measurements were performed with near-field illumination, through 100 nm apertures fabricated in aluminium coated etched optical fibre probes using focused ion beam (FIB) milling, with excitation at 488 nm, a wavelength at which only one of the two polymers absorbs light. Under this illumination regions that are high in the topography image show high luminescence and photocurrent.

The photoluminescence (PL) efficiencies in the different regions of the sample were determined by calculating the absorbed energy using the Bethe-Bouwkamp model, to describe the electromagnetic radiation from the near-field probe, and the known chemical compositions of the different phases of the polymer blend. The calculation also allowed us to conclude that the photocurrent generation efficiencies (current/absorbed photons) of the different polymer phases are comparable within the limits of confidence of this experiment (±10 %).

Observation of Dye-containing Nano-domains by near-field optical microscope

Noritaka Yamamoto, Toshiko Mizokuro, Hiroyuki Mochizuki, and Takashi Hiraga,
,Photonics Research Institute, National Institute of Advanced Industrial Science and Technology (AIST)
KANSAI, 1-8-31Midorigaoka, Ikeda, Osaka 563-8577, Japan,
Shin Horiuchi
Macromolecular Technology Center, National Institute of Advanced Industrial Science and Technology (AIST)
1-1-4 Higashi, Tsukuba, Ibaraki 305-8562, Japan

Most polymers are immiscible with each other; so heterogeneous blends organize themselves into large-scale structures when they are cast into thin films. The blending of polymers is a useful means of combining and improving the properties of already existing polymers in the development of new materials. The properties of such blends are strongly determined by the properties of the interphase. The polymer alloy system, which has two immiscible polymers, is more interesting because it forms ordered nano-structure. The attractive material, which has a novel property, is often related to optical material and nano structure. We also deal with a vacuum technique, termed the "vapor transportation method", as a promising technique for preparing a novel class of polymeric organic thin films. The purpose of this study is to give an overview of the present status and the future prospects of the development of organic thin films both in fundamental understanding and in industrial technology.

Figure 1 shows a micro phase separation structure in thin solid films with Polystyrene (PS)/Polymethyl methacrylate (PMMA) alloy system by TEM. PS (diameter of several tens of nm) was dispersed in the PMMA matrix. In this case, amounts of PS are smaller than PMMA. Adding a PS with lower molecular weight than the alloy and a PMMA of the same controls the domain size and distances between the domains, respectively. Then the films were treated by the previously reported technique under vacuum condition, where an organic dye was dispersed into the PS selectively [1].

Furthermore, a SNOM technique was developed to study interdiffusion between films of PS/PMMA with a thickness of a few nanometers, which is in the range of the interphase thickness of any heterogeneous blends. Finally, simultaneous SNOM spectroscopic and AFM measurements were used to study the molecular orientation in the dispersed phase in compatibilized PS/PMMA blends. The technique was found to be useful in studying interfacial optical interactions in compatibilized blends. Photoexcited energy transfers between domains are promises well for the molecular optoelectro devices.

References

[1] T.Hiraga et al. Mol. Cryst. Liq. Cryst., Vol344, 211-216.. (2000),

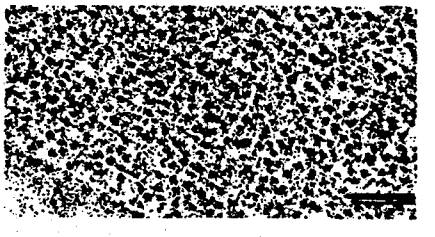

Fig.1 TEM image of a sample.

Magnetic Characterization of Microscopic Particles by MO-SNOM

J. Schoenmaker, M. S. Lancarotte, L. N. Nobrega and A. D. Santos, Instituto de Física, Universidade de São Paulo, São Paulo, Brazil, CP 66318, ZIP 05315-970.

Y. Souche, Laboratoire Louis Néel-CNRS, Grenoble, France.

The magnetic material technical applications are progressively being miniaturized. As a consequence, the research community needs to develop new instrumentation to study the magnetic properties in a sub-micron or nanoscopic scale. In this paper we present the development of a Scanning Near-Field Optical Microscope (SNOM) devoted to the study of magnetic thin films. We have incorporated the capability of analyzing the light polarization to get magnetic information by means of the transverse magneto-optical Kerr effect (MO).

The MO-SNOM operates basically as a tuning fork AFM, where the tip is made of a tapered optical fiber. The fiber is laterally Al coated, in order to have a sub-micron aperture at its end. The light source is a diode-laser. The sample's diffracted light is collected by an avalanche photodiode, giving us a near-field optical image, simultaneously to the topographic one. The lateral optical resolution is better than 100 nm.

By the light polarization analysis we can either measure the hysteresis loops with sub-micron spatial resolution (Fig. 1a) or to construct the image point-by-point for some particular magnetic properties, as p.e., the differential susceptibility (Fig. 1b). Here, we will present experimental results for magnetic particles of $Co_{70.4}Fe_{4.6}Si_{15}B_{10}$ amorphous thin films prepared by magnetron sputtering over electron lithographic mask. The particles ranged from 32x32 to 1x1 μm^2. Although the transverse Kerr effect is not quantitative for magnetic measurements, the sensitivity of the MO-SNOM for hysteretic properties is high and the MO-SNOM can become a powerful instrument to study the magnetic properties of thin films in a sub-micron spatial scale.

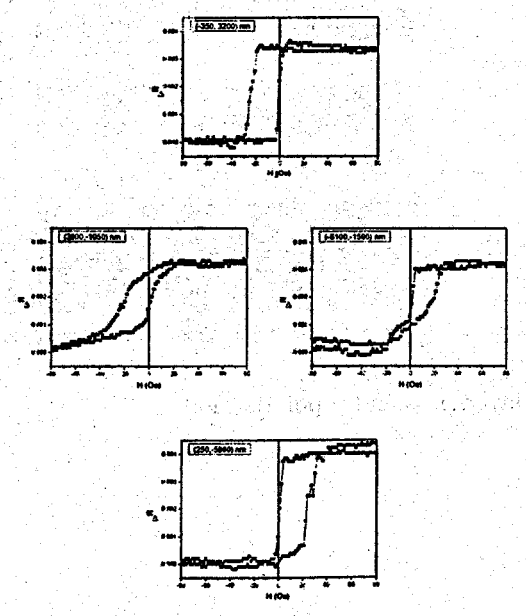

a)

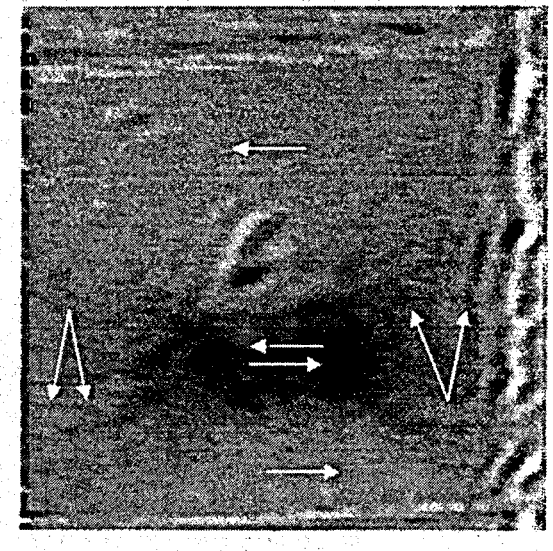

b)

Figure 1) TMOKE Hysteresis loops (a) and Differential Susceptibility image (b) obtained by the MO-SNOM on a 16x16 μm^2 amorphous $Co_{70.4}Fe_{4.6}Si_{15}B_{10}$ particle.

This work was supported by the Brazilian Agency FAPESP.

Super-RENS: field inhomogeneities in the readout layer and plasmons

R. Fikri, D. Barchiesi, P. Royer
Université de Technologie de Troyes, Nanotechnology and Optical Instrumentation Laboratory (LNIO)
12 rue Marie Curie - BP 2060 - FR-10010 Troyes cedex

Phase-Change (PC) ultra-thin layers provide a very promising family of re-writable media for the industry of high density storage. Indeed the phase transition between the amorphous and the crystalline states due to the temperature gradient in the PC layer occurs rapidly (a few nanoseconds) and reversibly. Moreover, as the two states present well distinct optical indices, such materials enables a high speed optical writing and reading of the information. One of the most exciting solution to overpass the diffraction limit has been proposed by J. Tominaga et al [1], called super-RENS. In this technique, a Sb readout layer is placed in the optical near field just below the PC recording layer. The Sb film locally melts when illuminated by a focused laser beam, providing an optical nano-aperture (window) in the Sb opaque film.

The size of the aperture is very small compared to the laser spot (typically 10 to 20 times smaller in diameter). The origin and the shape of the aperture are not completely understood, but it has been explained in terms of local and surface plasmon [2], which have been put in evidence theoretically by the FDTD method [3]. We analyze the plasmon resonance by crystalline nano-structures inside the amorphous layer, by a method based on the Born approximation [4] and the diffraction by the whole multilayer by finite element method [6]. The finite element method with adaptive mesh is able to describe both nanometric bit and micrometric multilayer of the super-RENS with low cost gridding. Both method are complementary and can lead to a better understanding of the super-RENS and the thermal effects could be introduced in this description, to get a realistic description of the setup and therefore to an improvement of the structures.

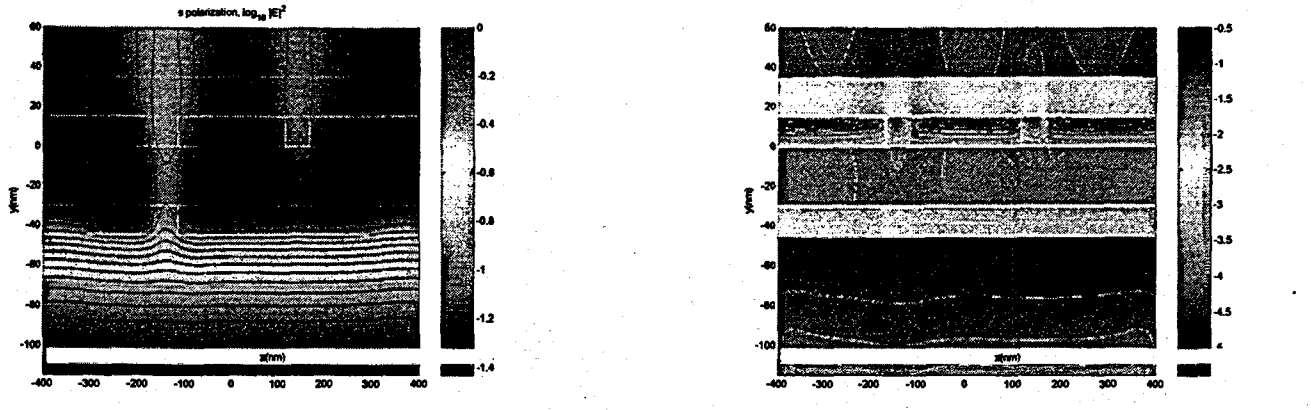

Figure 1: Intensity in the superRENS layers in s and p polarization.

References

[1] J. Tominaga et al, *Appl. Phys. Lett.* **73**, 2078 (1998).

[2] D. P Tsai et al, *Jpn. J. Appl. Phys.* **39**, 982 (2000).

[3] J. Tominaga et al, *Jpn. J. Appl. Phys.* **40**, 1831 (2001).

[4] D. Barchiesi, *Opt. Commun.*, **126** 7 (1996) and V. I. Tatarskii, *J. Opt. Soc. Am. A*, **12** 1254 (1995).

[5] J. Jin, *The Finite Element Method in Electromagnetics* (John Wiley and Sons, New York, 1993).

Near-field Pump-probe Luminescence Spectroscopy of CuCl quantum cubes in ultraviolet region

T. Kawazoe, K. Kobayashi, S. Sangu,
Japan Science and Technology Corporation (JST), 687-1 Tsuruma, Machida, Tokyo 194-0004, Japan
M. Ohtsu,
Japan Science and Technology Corporation (JST), and also
Tokyo Institute of Technology, 4259 Nagatsuta, Midori-ku, Yokohama 226-8502, Japan

The coupled quantum-dots system exhibits more unique properties in contrast with the single quantum-dot system. The optical near-field interaction [1] is interesting, as it can govern the coupling strength among quantum dots. Recently, we observed optically forbidden energy transfer between CuCl quantum cubes (QCs) via optical near-field interaction [2]. We consider that a nanometric optical switch based on a new operation principle can be realized by controlling this energy transfer.

The quantized exciton energy levels of (1,1,1) in a 4.6 nm CuCl QC and (2,1,1) in a 6.3 nm QC resonate with each other, as shown in Fig.1 (a) [3]. For this type of resonant condition, the energy transfer between QC via the optical near-field occurs for less than 100 ps, assuming that the separation between two QCs is equal to 10 nm. This energy transfer time is much shorter than the exciton lifetime and is longer than the inter-sub-level transition time. Therefore, most of the exciton in a 4.6-nm CuCl QC transfers to the neighboring 6.3-nm QC. Thus, a 4.6-nm QC, located close to a 6.3-nm QC cannot emit light. However, when (1,1,1) level in a 6.3-nm QC is pumped by a laser, the energy transfer form a 4.6-nm QC to a 6.3-nm QC is obstructed due to the state filling effect of 6.3-nm QC.

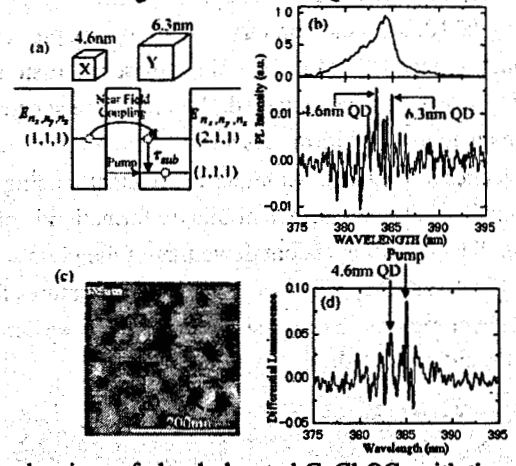

Figure 1: (a) Schematic drawings of closely located CuCl QCs with the effective side lengths of 4.6 nm and 6.3 nm. (b) Far- and near- field luminescence spectra of CuCl QCs embedded in a NaCl matrix. (c) Spatial distributions of the near-field luminescence intensity. (d) Differential luminescence spectrum.

The luminescence from a 4.6 nm and 6.3 nm QCs are shown in the near-field luminescence spectrum in the lower part in Fig.1 (b). For the experiment of the near-field pump-probe luminescence spectroscopy, SH of Ti-sapphire laser (385nm) and He-Cd laser (325nm) are used as pump and probe light source, respectively. The experimental result, observed at the position indicated broken circle in Fig. 1 (c), is shown in Fig. 1 (d) as a differential luminescence spectrum. The luminescence from a 4.6 nm QC increased by the pump of 6.3 nm QC (wavelength of 385 nm), as shown by an allow in Fig. 1 (d). This is the first demonstration of the control of the energy transfer between QCs.

References

[1] K. Kobayashi, S. Sangu, H. Ito, and M. Ohtsu, Phys. Rev. A **63**, 013806 (2000).
[2] T. Kawazoe, K. Kobayashi, J. Lim, Y. Narita and M. Ohtsu, Phys. Rev. Lett. **88**, 6, 067404 (2002).
[3] N. Sakakura and Y. Masumoto, Phys. Rev. B **56**, 4051 (1997).

Fluorescent Polyelectrolyte-Surfactant Complexes Studied by Near-Field Optical and Atomic Force Microscopies

X. Liao, D. A. Higgins, Department of Chemistry, Kansas State University, Manhattan, KS, 66506.

Near-field scanning optical microscopy (NSOM) and atomic force microscopy (AFM) are used to study nonstoichiometric polyelectrolyte-surfactant complexes (PSCs).[1] Fluorescent thin films prepared by complexation of poly(vinyl sulfate) (PVS) and a cationic indocarbocyanine surfactant dye (DiI) are investigated. The results are compared to those obtained from more common PSC films prepared using PVS and alkyltrimethylammonium bromide (C_nTAB). The latter samples were doped with a hydrophobic dye (nile red) for NSOM fluorescence imaging and spectroscopy. In both systems, local film morphology and chemical composition were studied as a function of surfactant:anionic-site stoichiometry. In the PVS-C_nTAB system, film characteristics were also investigated as a function of surfactant alkane chain length (for n=12, 14, 16, 18). AFM and NSOM images obtained from these samples show a clear evolution of PSC film morphology with surfactant content and chain length. PVS alone forms a "porous" film containing polymer "network" structures. Pore formation is attributed to film shrinkage and substrate dewetting during drying in this case. At low surfactant content (i.e., 1:100 stoichiometry), the films become much more uniform, having root-mean-square roughnesses of < 0.5 nm, despite the fact that the surfactant concentrations in each solution employed were all above the critical aggregation concentration (CAC). At moderate surfactant loading (≤ 10:100 stoichiometry), small topographic protrusions (10-40 nm in height) appear across the films. Fluorescence NSOM images show these protrusions incorporate both dye and surfactant. Fig. 1 shows representative images obtained. Fluorescence spectroscopy on the PVS-DiI system shows the dye is present in an aggregated form. As a result, the protrusions are concluded to be polymer-surfactant micelles and/or micelles aggregates. At highest surfactant loading (25:100 and 50:100 stoichiometries), clear evidence for lamellar polymer-surfactant bilayer formation is obtained. The bilayers exhibit heights on the order of 4-5 nm. Surfactant-dependent dewetting of the glass substrate surface is also observed at these high loadings. Finally, AFM images of the lamellar structures for 50:100 films show the presence of interesting, defected bilayer regions. The possible origins of these defected regions and their associated bilayer height variations are discussed.

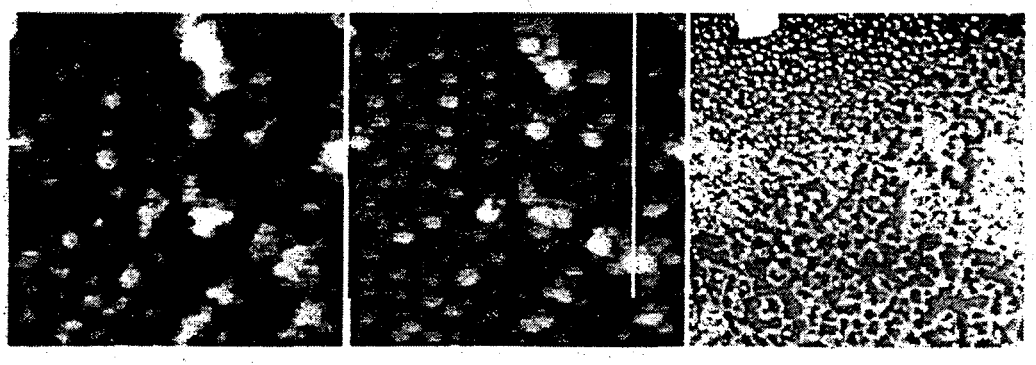

Figure 1: NSOM fluorescence (A) and topography (B) of a PVS-C_{16}TAB (1:100) thin film. AFM image (C) of a PVS-C_{16}TAB (10:100) thin film.

References

[1] X. Liao, D. A. Higgins, *Langmuir* **17**, 6051 (2001). X. Liao, D. A. Higgins, *Langmuir*, submitted.

NEAR-FIELD UV LITHOGRAPHY OF A CONJUGATED POLYMER

Robert Riehn,
Cavendish Laboratory, University of Cambridge, CB3 0HE Cambridge, UK
Ana Charas, Jorge Morgado,
Instituto Superior Engenharia Quimica, Lisbon, Portugal
Franco Cacialli
Department of Physics, University College London, London, UK
Cavendish Laboratory, University of Cambridge, CB3 0HE Cambridge, UK

We prepared nanoscopic features of the conjugated polymer poly(p-phenylene vinylene) (PPV) by near-field optical lithography of its soluble precursor. We used a scanning near-field optical microscope (NSOM/SNOM) of our own design and construction to illuminate thin films with the 325 nm line of a HeCd laser. The irradiation renders the precursor polymer insoluble, which allows the development of features by subsequent wash-off of the unexposed precursor in methanol. Following thermal conversion of the precursor, the process results in fully conjugated features of the semiconducting polymer surrounded by air.

The resolution achieved for a 40 nm thick precursor film is about 160 nm. We demonstrated the fabrication of functional 2-dimensional patterns, including photonic crystals with artificial defects and templates for surface energy induced phase separation of a conjugated polymer blend. We also showed specific properties of patterning a negative resist using near-field optical lithography.

We conclude our discussion by comparing the experimentally obtained shapes and sizes of lithographic features with those predicted by a Bethe-Bouwkamp simulation. We find that highest resolution can only be obtained for films that are thin compared to the aperture size.

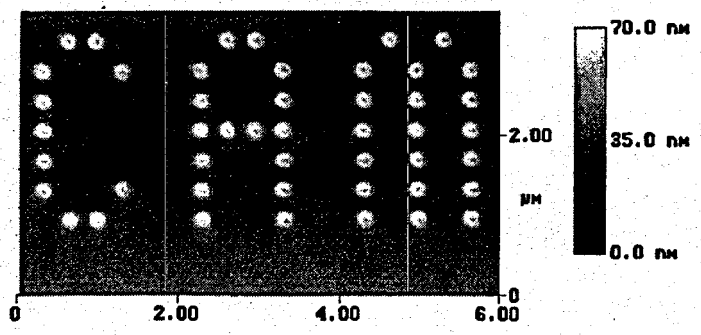

Figure 1: Pattern prepared by near-field UV lithography of the precursor of the conjugated polymer poly(p-phenylene vinylene) (PPV). The underlying grid has a spacing of 300 nm, and the polymer film was about 40 nm in thickness.

Near-Field Scanning Optical Microscopy and Near-Field Photocurrent Analysis of Nickel-Silicon Carbide Contacts

M.P. Ackland, P.R. Dunstan,
Dept. of Physics, University of Wales Swansea, Singleton Park, Swansea, SA2 8PP, UK

W.Y. Lee, S.P. Wilks,
Dept. of Electrical &Electronic Engineering, University of Wales Swansea, Singleton Park, Swansea, SA2 8PP, UK

An aperture near-field scanning optical microscope has been used in the study of nickel contacts on the wide band-gap semiconductor, silicon carbide. Shear-force topological maps have been recorded simultaneously with detailed photo-response images of both the reflected and transmitted light, to clearly reveal the differing surface structure of various types of contact.

Samples of both Schottky and Ohmic nature were studied, where the underlying interface dictates the electrical properties. Initial comparisons have been made between the different surface structures and photo-response of the samples, with efforts made to decouple the topographic and optical data. We performed near-field photoelectric (photocurrent) experiments to probe a Schottky diode whilst under bias to characterize the variation in structure, photo-response and photo-induced current simultaneously across a contact. By stimulating the photocurrent directly using the evanescent field of the NSOM tip, we have observed localized variations in the contact properties on the nanoscale.

Development of "nano-FISH" method for DNA and Chromosome analyses using SNOM/AFM

T. Ohtani, J. M. Kim, T. Yoshino, S. Sugiyama, S. Hagiwara,
National Food Research Institute, Tsukuba, Ibaraki 305-8642 Japan
T. Hirose,
Japan Atomic Energy Research Institute, Takasaki, Gunma 370-1292 Japan
H. Muramatsu
Seiko Instruments Inc. Matsudo, Chiba 270-2222, Japan

The locations of genes on a genome as well as DNA sequences seem to play a principal role in gene expression. Detecting the precise location of a gene transfer is a major factor for guaranteeing transduction by gene modification or mutation. There is a need for a novel method, which would enable the location of a specific gene on a given genome to be directly and precisely detected. The final objective of this study is to establish a novel method, termed "nano-FISH", that directly defines the location of a specific gene on a DNA fiber and a chromosome with a high resolution using a scanning near-field optical microscope/atomic force microscope (SNOM/AFM). The method exceeds the limited resolution of conventional FISH (Fluorescence *in situ* hybridization) achieved using an optical microscope. Specifically, the novel method should break through the optical limit of the conventional method. The high-resolution fluorescent images of DNA fibers and chromosomes were observed using a SNOM/AFM in the first step.

Simultaneous topographic and fluorescent imaging of a DNA fiber was succeeded for the first time using our experimental set up. And a double-stranded and a denatured single-stranded DNA molecules can be distinguished comparing with topographic and fluorescent images, because, YOYO-1 dye stains only double strand DNA fibers. Very small quantity of YOYO-1 is possible to be intercalated or externally bonded in the single-stranded DNA [1].

Figure 1 shows topographic and fluorescent images of barley chromosomes stained with YOYO-1. Topographic image (c) showed that the surface was relatively flat and no significant height difference between the high-fluorescent region and the low intensity region of the chromosome was detected. Thus the high fluorescent intensity of the region is not the effects of chromosome thickness but considered to reflect internal structure of the chromosome [2].

Images of the specific genes on DNA fibers and chromosome will be demonstrated in NFO-7.

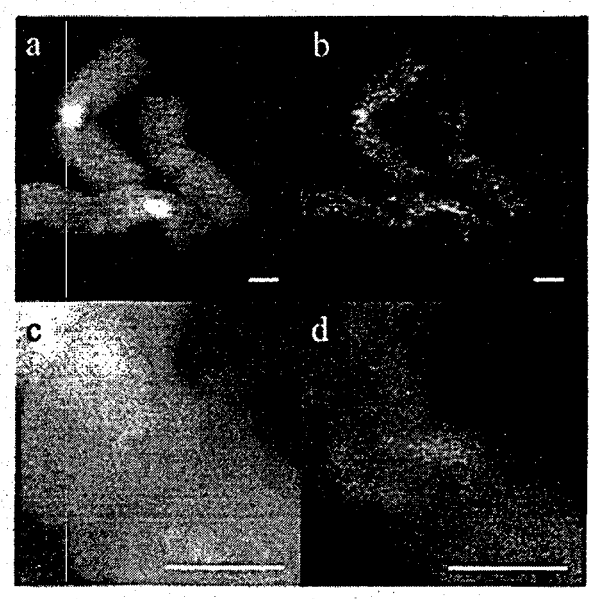

Figure 1: SNOM/AFM images of the barley chromosomes stained with YOYO-1 dye.
(a) Topographic image. The height range is 200 nm.
(b) Fluorescent image in the same portion of (a). The height range is 5.0×103 mV.
(c) Topographic image of a part of a chromosome (a). 200 nm.
(d) Fluorescent image of (c). 300 mV. Bars = 1μm

References

[1] J. M. Kim, T. Ohtani, S. Sugiyama, T. Hirose and H. Muramatsu, *Anal. Chem* **73**, 5984-91 (2001).

[2] T. Yoshino, S. Sugiyama, S. Hagiwara, T. Ushiki and T. Ohtani, J. Electron Microsc. **55**, in press (2002).

Acknowledgements
The author greatly appreciate the financial support given to the present study by BRAIN (Bio-oriented Technology Research Advancement Institution) and Special Coordination Funds of the Ministry of Education, Culture, Sports, Science and Technology of the Japanese Government.

Abstract for the 7th International Conference on Near-field Optics and Related Techniques

Scanning near field optical microscopy of cells in liquid

R. Januskevicius, D. J. Arndt-Jovin, T. M. Jovin,
Department of Molecular Biology, Max Planck Institute for Biophysical Chemistry,
Am Fassberg 11, Goettingen, D-37077, Germany.

A scanning near field optical microscope has been constructed and applied to fluorescence imaging of biological samples in liquid, including live cells. Our homemade SNOM is mounted on a Zeiss Axiovert135 TV fluorescence microscope. For feedback we use tuning fork shear force and a RHK controller. The scanning tip is produced from a 125 μm optical fiber (Siecor, 8.3 μm core diameter) by a heating and pulling sequence in a commercial Sutter P-2000 pipette puller and coating with Al. A PI nanostage is used. The X-Y scanning of the sample Coarse Z axis adjustment is hydraulic and fine positioning with pz tube units. The depth of liquid is maintained very small in order to minimize the loss in Q factor. We have designed a simple and stable construction with a liquid depth of 40 μm. Near-field images of fixed and living cells obtained in liquid are presented. Human epithelial A431 cells, stably transfected with a GFP fusion protein of the epidermal growth factor transmembrane receptor protein, were scanned for topography and sitribution of membrane fluorescence.

An apertureless near-field microscope and its advantages in unraveling the structure of the photosynthetic membrane

C. C. Gradinaru, G. A. Blab, P. Martinsson, Th. Schmidt, T. J. Aartsma
Department of Biophysics, Huygens Laboratory, Leiden Universiyt, 2333 CA Leiden, The Netherlands

T. Oosterkamp
Interface Physics Group, Kamerlingh Onnes Laboratory, Leiden University, 2300 RA Leiden, The Netherlands

A widespread trend nowadays is to combine two or more scanning probe techniques in order to shed light into the relationship between structure and function of various samples under study: atoms, molecules, polymers, proteins, etc. The system we are investigating is the photosynthetic apparatus of plants and (some) bacteria, which is constituted of protein complexes embedded in a lipid membrane and is responsible for the conversion of light into chemical energy. While the individual proteins have been extensively characterized (for many of them the crystal structure is available), the way they are distributed in the membrane, interact with each other, or react to external factors is still largely unknown.

The combination of atomic-force microscopy (AFM) and apertureless scanning near-field optical microscopy (SNOM) looks like a natural choice for investigating this system, as many of its units are light sensitive and have lateral sizes in the order of 5-15 nm (unreachable by "classic" SNOM). A commercial instrument, the Digital Instruments Bioscope, was adapted to allow simultaneous acquisition of topography and fluorescence data from the sample. Several AFM tips were tested for the enhancement effect, including narrow multi-wall carbon nanotubes and whisker-type, gold-coated tips. The test samples were monolayers of quantum dots and electro luminescent polymers; their fluorescence was detected using two-photon excitation conditions with femtosecond laser pulses in the near infrared (700-1000 nm). Preliminary results on fragments of the thylakoid membrane found in the chloroplasts of the green plants are also presented, thus opening the way for a direct, straightforward visualization of the architecture and function of the photosynthetic machinery.

High-Resolution Near-Field Optical Imaging of a Cell Membrane in Aqueous Solution

C. Höppener, D. Molenda, H. Fuchs, and A. Naber,
Physics Institute, Wilhelm-Klemm-Str. 10, D-48149 Münster, Germany.

Over the past 10 years several distance control techniques for SNOM have been developed from which today the shear-force method in conjunction with a piezoelectric quartz tuning fork as force sensor is the most popular one. For soft samples under liquid, however, this method turned out to be not as well-suited as under ambient conditions. Up to now, SNOM measurements of biological samples under liquid are very rare due to the lack of a sensitive distance control.

Recently it has been shown that a tuning fork can also be used for a force feedback configuration in which the attached probe oscillates in a direction normal to the surface (tapping mode like force feedback) [1, 2]. We have shown that such a technique is especially well-suited for a distance control under liquid since in this mode there is no need to immerse the force sensor in the liquid [2]. The preserved high force sensitivity of the tuning fork enabled us to image reliably even soft biological material [2] or double-stranded DNA (Figure 1) under liquid.

By means of this technique, we are able to show for the first time high-resolution near-field optical images of a cell membrane, the nuclear envelope, in an aqueous solution. The nuclear envelope encloses the nucleus of a eukaryotic cell and is perforated by supramolecular protein complexes, so-called nuclear pore complexes (NPCs), which regulate the transport of molecules in and out of the nucleus. Since the distance of neighboring NPCs is only ~120 nm, conventional optical microscopes are not able to resolve single NPCs in their native environment. In contrast to that, our near-field fluorescence measurements of ~60 nm resolution clearly show fluorescence signals of single dye-labeled NPCs embedded in the nuclear envelope.

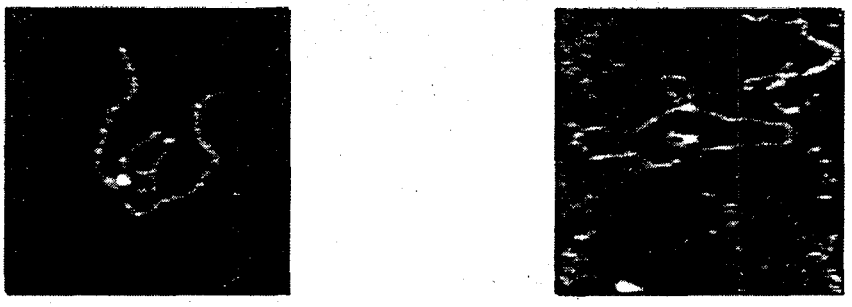

Figure 1: Topographic images of double-stranded DNA on mica under ambient conditions (left) and under liquid (right) measured with a tapping mode like distance control on the basis of a tuning fork as force sensor and an bare tapered glass fiber as force tip. Only the fiber tip was immersed in the liquid (~1 mm). Size of images: 500 nm x 500 nm; Grayscale: 2 nm.

References

[1] D. P. Tsai and Y. Y. Lu, *Appl. Phys. Lett.* **73**, 2724 (1998).
[2] A. Naber, H.-J. Maas, K. Razavi, and U.C. Fischer, *Rev. Sci. Instrum.* **70**, 3955-3961 (1999).

Spectroscopic Imaging of Nanoscale Rafts in Biomimetic Lipid Bilayers Using Near-field Scanning Optical Microscopy

Jeeseong Hwang[1], Fuyuki Tokumasu[2], Takayuki Arie[2], Albert J. Jin[3], Paul D. Smith[3], Gerald W. Feigenson[4], Lori S. Goldner[1], and James A. Dvorak[2]

[1]Optical Technology Division, National Institute of Standards and Technology, Gaithersburg, MD 20899.
[2]Biophysical Parasitology Section, Laboratory of Malaria Research, National Institute of Allergy and Infectious Disease, National Institutes of Health, Bethesda, MD 20892.
[3]Division of Bioengineering and Physical Science, ORS, Office of the Director, National Institutes of Health, Bethesda, MD 20892.
[4]Department of Molecular Biology & Genetics, Cornell University, Ithaca, NY 14853.

We used near-field optical microscopy to image nanoscale domains in biomimetic lipid membranes composed of bilayers of binary or tertiary mixtures of 1, 2-dipalmitoyl-*sn*-glycero-3-phosphocholine (DPPC), 1, 2-dilauroyl-*sn*-glycero-3-phosphocholine (DLPC), and cholesterol. At room temperature, the membranes displayed phase separations indicative of nanoscale domain structures that are thought to have relevance to functional cell-surface rafts. We labeled the lipids with the fluorescent lipid analogs Bodipy-PC and diI:C_{20} to identify unambiguously the presence and distribution of specific membrane components. Simultaneous multicolor imaging at the wavelengths of the emission maxima of the fluorescent analogs revealed a non-correlated patchy distribution of Bodipy-PC and diI:C_{20} indicative of a domain separation of the lipid bilayer. The 100-300 nm size distribution of these patches is consistent with both the size of lipid domain clusters and thermodynamic parameters estimated by atomic force microscopy (AFM). Energy transfer studies of the fluorescent lipid analogs are also in progress to elucidate phase mixing in the domain boundary regions. Our studies were performed either on a homebuilt wet cell NSOM or on a prototype NSOM/AFM we are developing for biomedical research. Simultaneous detections of topography and fluorescence information of nanoscopic membrane domains by NSOM will also help better understandings of the raft structure in native membranes.

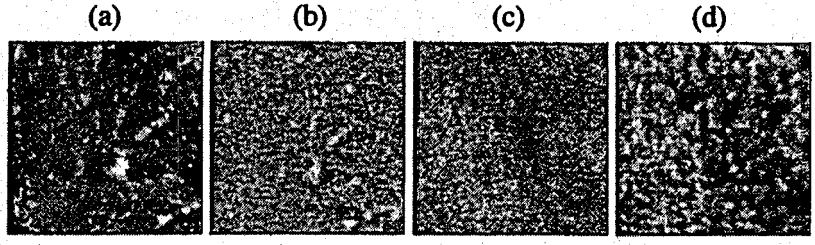

Figure 1: Near-field images of a DLPC(30%)/DPPC(70%) bilayer doped with Cholesterol(18 mol%), Bodipy-PC (0.1 mol%), and diI:C_{20} (0.1 mol%). All images 6 μm square. (a) topography (b) transmission at λ=488±5nm (b) fluorescence at 515nm<λ<530nm (d) fluorescence at λ>560nm.

Size and distribution of lipid rafts: atomic force and near field microscopy study of G_{M1} domains in model membranes

P. Burgos [a,b], R. S. Taylor [c], Z. Lu [a], M. L. Viriot [b], L. J. Johnston [a]

[a] *National Research Council of Canada, Steacie Institute of Molecular Science SIMS, Ottawa, Ont., K1A 0R6*
[b] *Centre National de la Recherche Scientifique, ENSIC-DCPR, Nancy, France*
[c] *National Research Council of Canada, Institute for Microstructural sciences, Ottawa, Ont., K1A 0R6*

Recent work has given rise to a fundamentally new way of thinking about biological membranes. Contrary to earlier views, lipids don't always mix homogeneously in membranes, but are organized into domains and microdomains of different sizes. Characterization of these domains is essential to understand their role in membrane processes. Glycolipids, such as ganglioside G_{M1}, are receptors for numerous biologically active agents and are likely to be involved in the formation of specialized microdomains, «rafts», which are enriched in sphingolipids and cholesterol, and exhibit properties similar to a liquid ordered phase. Since specific proteins have the propensity to be included or excluded from rafts, these domains are proposed to play an important role in membrane transport and signal transduction [1].

Determination, at the mesoscopic scale, of raft distribution in lipid mixtures has been performed based on indirect techniques (AFM, FRET, epifluorescence microscopy) and has led to conflicting results [2,3,4,5] : membrane models provide evidence of raft micron-sized domain, although in natural membranes, their sizes are postulated to be far beyond the resolution of conventional optical microscopy.

Langmuir-Blodgett (LB) films are a useful membrane model and have provided information on lipid-lipid and lipid-protein interactions. Our LB films are prepared from equimolar mixtures of cholesterol/sphingomyelin/dioleoylphosphatidylcholine as a mimic for the natural rafts found in membranes [4]. The characterization of the structure of LB films with near field fluorescence microscopy and atomic force microscopy offers the possibility of obtaining topographic and optical information ranging from nanometer to micrometer resolution. We developed methods for making bent, doubled etched probes that have transmission efficiency (close to 10^{-2}) suitable for fluorescence applications.

The results show that the addition of 1% G_{M1} to the monolayer leads to the formation of glycolipid enriched domains that mimic rafts. They are localized in the more ordered sphingomyelin/cholesterol rich phase and are heterogeneously distributed in this phase. The lipid properties are sufficient to direct the formation of these rafts in membranes without requiring the presence of protein. For the first time, our recent data suggest that sub-micron domains raft-like domains are found in model membranes and adopt a circular shape with a diameter around 100-200 nm.

References

[1] K. Simons and E. Ikonen, *Nature*, **387**, 567-572 (1997)
[2] C. Dietrich, L. A. Bagatolli, Z. N. Volovyk, N. L. Thompson, M. Levi, K. Jacobson and E. Gratton, *Biophysical Journal*, **80**, 1417-1428 (2001)
[3] V. Vié, N. Van Mau, E. Lesniewska, J. P. Goudonnet, F. Heitz, C. Le Grimellec, *Langmuir*, **14**, 4574-4583 (1998)
[4] C. Yuan, J. Furlong, P. Burgos, L. J. Johnston, *Biophysical Journal*, **82**, 2526-2535 (2002)
[5] S. N. Ahmed, D. A. Brown, E. London, *Biochemistry*, **36**, 10944-10953 (1997)

Single molecule spectroscopy of autofluorescent proteins

J. Hofkens, M. Cotlet, S. Habuchi, F.C. De Schryver,
K.U.Leuven, Department of Organic Chemistry, Laboratory for Photochemistry and Photophysics
Celestijnenlaan 200 F, 3001 Heverlee Belgium.

In recent years, the Green Fluorescent Protein (wild-type GFP) from the Pacific jellyfish *Aequorea victoria* has become one of the most widely studied and exploited proteins in cell and developmental biology. Due to the brilliant intrinsic green fluorescence that can be enhanced or even spectrally shifted from blue to yellow by mutagenesis, GFP technology has established a universal method for introducing a fluorescent tag into nearly any biological structure without affecting the native function.

Recently, the emission color palette offered by GFPs has extended to higher wavelengths by the discovery in the reef coral *Discosoma genus* of a red fluorescent protein (DsRed) with similar structure compared to GFP and with the capacity to be cloned and expressed in vivo. However, biophysical and biochemical studies revealed several drawbacks of DsRed when has to be used as a fluorescent marker. Analytical ultracentrifugation and time-resolved fluorescence anisotropy experiments revealed the occurrence of DsRed as a tetramer at dilute concentrations [1,2]. Moreover, the final red emitting chromophore appears through a slow and incomplete maturation process, resulting in tetramers containing one or more green precursor chromophores even for the so called mature DsRed samples and, as a result, energy transfer can occur between the above mentioned chromophores [1].

Single molecule spectroscopy (SMS) experiments performed on 543-nm CW excitation point to the existence of DsRed as a tetramer and reveal the presence of a blinking phenomenon in the ms time range [3]. Collective effects involving the red chromophores within the individual tetramers were observed. Time-resolved data reveal the presence of a population of 25 % of the immature green chromophores which relates to tetramers containing only this immature green form and which is responsible for the weak fluorescence emitted by DsRed at 500-nm when excited at 460-nm [4]. The remaining 75 % of the immature green chromophores are involved in an energy transfer process to the red chromophores within the tetramers that contain them. Time-and spectrally resolved detection at single molecule level reveals, upon 543-nm excitation of individual DsRed tetramers, the existence of a photoconversion process of the red chromophore emitting at 583-nm into a super red species that emits weakly at 595-nm. The same phenomenon is further corroborated at the ensemble level with the observation of the creation of a super red form and a blue absorbing species upon irradiation with 532-nm pulsed light at high excitation power [4].

References

1]. Baird, G.S., Zacharias, A.A., Tsien, R.Y. *P.N.A.S.* USA. **97**, 11984 (2000)
[2]. Heikal, A., Hess, S., Baird, G., Tsien, R.Y. & Webb, W.W. *P.N.A.S.* USA **97**, 11996 (2000).
[3]. Cotlet M., Hofkens J., Kohn F., Michiels J., Dirix G., Van Guyse M., Vanderleyden J. and De Schryver F.C. *Chem. Phys. Lett.* **336**, 415, (2001).
[4]. Cotlet, M., Hofkens, J., Kohn, F., Michiels, J., Dirix, G., Van Guyse, M., Vanderleyden, J. and De Schryver F.C. *P.N.A.S.* USA **98**, 14398, (2001).

Tracing of secretory vesicles of PC12 cells using total internal reflection fluorescence microscopy

De-Ming Yang
Department of Medical Research & Education, Taipei Veterans General Hospital, Taipei 112, Taiwan
Chien-Chang Huang, Lung-Sen Kao
Institute of Biochemistry, Department of Life Science, National Yang-Ming University, Taipei 112, Taiwan
Hsia Yu Lin, Din Ping Tsai
Department of Physics, National Taiwan University, Taipei 10617, Taiwan
Chung-Chih Lin
Department of Life Sciences, Chung Shan Medical University, Taichung 402, Taiwan

The secretory vesicles and organelles near the cell surface of a neuroendocrine PC12 cell were monitored by total internal reflection fluorescence microscopy (TIRFM) [1]. The secretory vesicles were labeled by over-expressing one of the small G proteins that is involved in the fusion of secretory vesicles to plasma membrane, GFP-Rab3 fusion protein, in PC12 cells. Mitochondria were monitored by a specific indicator MitoTracker Green [2]. The images acquired from a fast cooled CCD were compared and analyzed. Time-dependent changes of fusion events and fluorescence intensity of a defined area were analyzed. Within the small evanescent range (about 200 nm), the movement of vesicles near the cell surface was monitored. Figure 1 shows an example of the movement of the secretory vesicle of PC12 cell upon high K^+ stimulation and the fusion between one vesicle with another vesicle which already docked on the membrane. The TIRFM provides an opportunity to specifically trace and analyze the exocytotic events and vesicle dynamics near cell membrane without interference of signals from other parts of the cell.

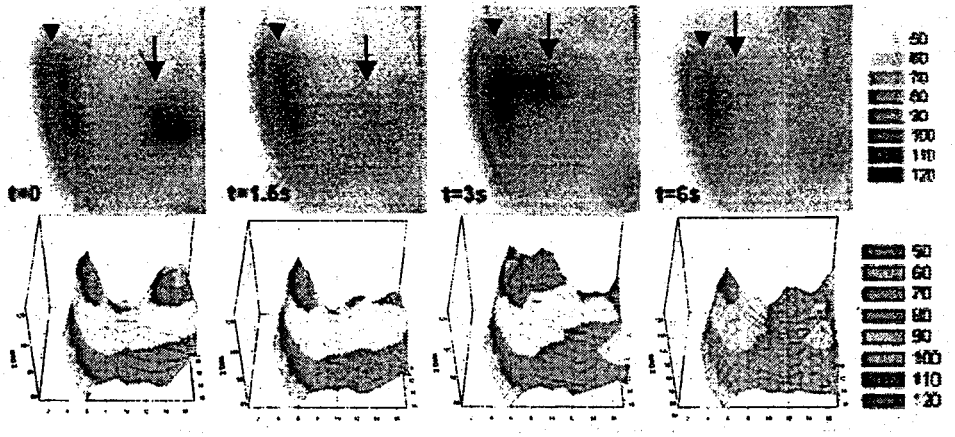

Figure 1: The vesicle fusion event occurred after high K^+ stimulation. GFP-Rab3A fusion protein was overexpressed in PC12 cells. Upon high K^+ stimulation, one secretory vesicle (arrows) first moved away from the focal plan, then back to the focal plan and fused with the vesicle (arrowheads) on the plasma membrane.

References

[1] J. A. Steyer, H. Hostmann and W. Almers, Nature **388**, 474 (1997).
[2] D. M. Yang and L. S. Kao, J. Neurochem. **76**, 210 (2000).

Simulation and Experiments on Trapping Biological Molecule by Near-field Optical Probe

Jia Wang, *Zhaohui Hu*, *Jinwen Liang*
State Key Laboratory of Precision Measurement Technology and Instruments,
Department of Precision Instruments, Tsinghua University, Beijing 100084, P. R. China
* *E-mail: wj-dpi@mail.tsinghua.edu.cn*

Near-field Optics has been developed and used in various fields, such as optical imaging at resolution beyond the diffraction limit, fluorescence detection in the local field, optical data storage, and so on. Research on near-field optical manipulation has attracted attention of scientists. The theories of near-field optical manipulation for atom[1] and dielectric particle[2,3] have been discussed. Some experimental results of trapping and moving the Mie particles in an evanescent field along a channeled waveguide have been shown[4].

In this paper, we calculate the distribution of electromagnetic field near a taper optical fiber probe by the method of 3-D finite-difference time-domain (FDTD). From the distribution of field, the distribution of optical force to particle can be calculated. Interaction between the optical near-field and dielectric and biological particle will be discussed based on the simulation results. Then we discuss the different distribution of optical force to different size of the optical fiber probe and the particle on scale of micrometers to nanometers. The result shows the possibility to spatially trap a nanometer-size particle with nanometer-size optical fiber probe in the optical near-field and to 2-D trap a particle with micrometric optical fiber probe. Some experimental results on manipulation of different-size dielectric particles and biological molecule by near-field optics will be provided. The experimental results show that the optical forces on the dielectric particle agree with the simulation results and it is also possible to trap a biological particle.

Reference:

[1] M.Ohtsu. *Near-field nano/atom optics and technology.* Springer-Verlag Tokyo, (1998)
[2] L.Novotny L., R.X.Bian, X.S.Xie. *Physical Review Letters*, 79 (4): 645-648, (1997)
[3] M.Tanaka, K.Tanaka. *Journal of the Optical Society of America A*, 15 (1): 101-105, (1998)
[4] S.Kawata, T.Tani. *Optics Letters*, 21 (21): 1768-1770, (1996)

Near Field Photo-fabrication of Thin Film Using Locally Enhanced Field at a Metallic Tip

Y. Inouye[1,2,3] A. Tarun[4], N. Hayazawa[3,4], and S. Kawata[2,3,4,5]
1) Osaka University, School of Frontier Bioscience, Suita, Osaka 565-0871, Japan
2) Handai FRC, Suita, Osaka 565-0871, Japan
3) CREST, Japan Science and Technology Corporation, Japan
4) Osaka University, Department of Applied Physics, Suita, Osaka 565-0871, Japan
5) RIKEN, Wako, Saitama, 351-0198, Japan

An apertureless-metallic-tip of near field scanning optical microscopy (NSOM) enhances the electric field strongly at the tip apex besides achieving ultimate spatial resolution that is as small as the size of the tip apex [1,2]. Due to these features, we attained 15 nm spatial resolution in near field Raman spectroscopy and imaging of aggregated molecules [3-5]. The locally enhanced field can also induce photochemical reaction at nanometric scale.

In this presentation, we report on near field lithography on a photoresist film using a platinum-covered cantilever and a blue semiconductor laser [6]. The metallized cantilever (tip radius: ~20 nm) was brought onto positive g-Line photoresist film (thickness: 110 nm) which was coated on a cover slip using a spinner. Then, a focused beam from a blue semiconductor laser (λ = 405 nm) was irradiated on the tip-film contact point.

Figure 1 shows a topographic image of the developed photoresist film obtained with an atomic force microscope. Structures of 100 nm-width trench were obtained with energy dose of 6.3 mJ/cm^2. Considering that the threshold of energy dose was 28.5 mJ/cm^2 in far-field process, energy dose in near–field process exceeds the threshold locally due to the local field enhancement of the tip, and photoresist film was exposed at nanometric scale. Figure 2 shows dependence of linewidth of the fabricated trench on energy dose irradiated on a film. The experimental result shows that apertureless-metallic-tip NSOM is one of the promising technologies for next generation of photofabrication.

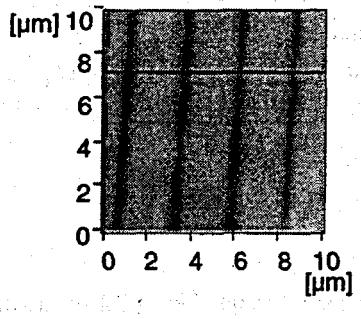

Fig. 1 AFM image of photoresist film exposed in the near field.

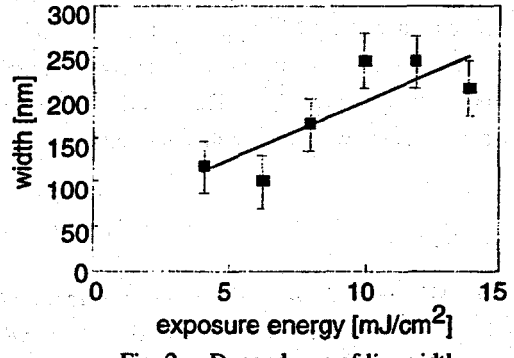

Fig. 2 Dependence of linewidth on energy dose.

References

[1] Y. Inouye and S. Kawata, Opt. Lett., **19**, 159 (1994).
[2] S. Kawata ed., Near-field Optics and Surface Plasmon Polariton, (Springer-Verlag, Berlin Heidelberg, 2001).
[3] Y. Inouye, N. Hayazawa, K. Hayashi, Z. Sekkat and S. Kawata, Proc. SPIE, **3791**, 40 (1999).
[4] N. Hayazawa, Y. Inouye, Z. Sekkat, and S. Kawata, Opt. Commun., **183**, 333 (2000).
[5] N. Hayazawa, Y. Inouye, Z. Sekkat, and S. Kawata, Chem. Phys. Lett., **335**, 369 (2001).
[6] A. Tarun, M.R.H. Daza, N. Hayazawa, Y. Inouye, and S. Kawata, Appl. Phys. Lett. (in press).

Optical detection of nano-particles.

F.Ignatovitch, A.Hartschuh, L.Novotny,
University of Rochester, The Institute of Optics, Rochester, NY 14627.

The methods of detection and recognition of particles more than half a wavelength are well established. However as particle size enters nanometer region, the sensitivity of those methods decreases rapidly. This is due to the fact, that as particles gets smaller, they exhibit dipole-like light scattering pattern and thus become indistinguishable.

We developed a method of nano-particles recognition, which is based on detecting optical gradient forces [1, 2], exerted on a particle by a tightly focused laser beam.

Our optical setup resembles one used in a basic optical tweezers experiment [3, 4]. Nanometer sized particles under test are guided in a microfluidic channel through a tightly focused laser beam. The particle's position with respect to the focus is monitored by detecting the scattered light. A feedback loop permanently adjusts the laser intensity and thereby ensures that the particle's path remains unaffected by the gradient force of the trap. The feedback signal provides a unique fingerprint for the particle's size and shape.

This method was developed in application to a virus recognition biosensor program. In the near future the above scheme will be integrated in a chip-scale device, allowing real-time bio-warfare sensing in a battlefield.

References

[1] A. Ashkin, *Science* **210**, 1081 (1980).

[2] A. Ashkin, J.M. Dziedzic, J.E. Bjorkholm, S. Chu, *Opt. Lett.*, **11**, 288 (1986).

[3] S.P.Smith, S.R.Bhalotra, A.L.Brody, B.L.Brown, E.K.Boyda, M.Prentiss, *Am. J. Phys.*, **67**, 26 (1999).

[4] Z.Ulanowski and I.K.Ludlow, *Meas. Sci. Techol.*, **11**, 1778 (2000).

Tunnel-Electron-Induced Oxygen Movement in $YBa_2Cu_3O_{7-\delta}$ Measured with Near-Field Optical Microscopy

S. H. Huerth and H. D. Hallen
North Carolina State University
Raleigh, NC 27695

The movement of atoms induced by electron motion, electromigration or electron-induced-motion (EIM), has been studied in many systems. In the case of the classic electron-wind mechanism, the atom motion is in the same direction as the current. We show here that this is not necessarily the case when few-eV electrons are used in an electron-excitation mechanism. In this case, the local electron interaction enhances the diffusion of the atoms. Naively, this localization of an electron interaction in a conductor seems unlikely, but it will occur when the electron can excite a carrier from a localized state on the atom rather than from the extended conduction states. The excitation places the atom in an unstable configuration, a Franck-Condon excitation, and it may move before relaxation if a vacancy is adjacent. Excitation from a localized state entails a threshold energy for the injected electron, which we measure for the case of oxygen motion in Yttrium barium cuprate (YBCO) and will present here. To better understand the mechanism of oxygen movement in YBCO while avoiding complications due to grain boundaries, we use a near-field scanning optical microscope (NSOM). The metal cladding of the NSOM probe provides a scanning tunneling microscope (STM) tip to pull (inject) electrons from (into) an industrial quality sample of YBCO. This induces movement of oxygen. We have shown that reflection-mode near-field scanning optical microscope can be used to image oxygen movement in YBCO. [1,2] Optical NSOM images taken before and after EIM are compared to eliminate the native background oxygen concentration variations and determine the amount of oxygen moved in the lattice and where the movement occurred, Fig. 1. It is interesting that the motion of oxygen described here shares many of the same qualitative features as the motion of vacancies in gold films with injection of few-eV tunnel electrons. [3,4] Both have *energy thresholds*, related to their respective band structures. The EIM is limited to a single grain in both cases, indicating that *few-eV electrons are scattered strongly at grain boundaries* in quite disparate materials. There are differences, however. The topographies of the gold films change as the atoms move, whereas the oxygen atoms in YBCO move in a fixed lattice with no detectable topographic change. The EIM of oxygen in YBCO changes in its superconducting properties, since they depend on the oxygen concentration. [5,6] We thank Brian Moeckly of Conductus for providing the YBCO.

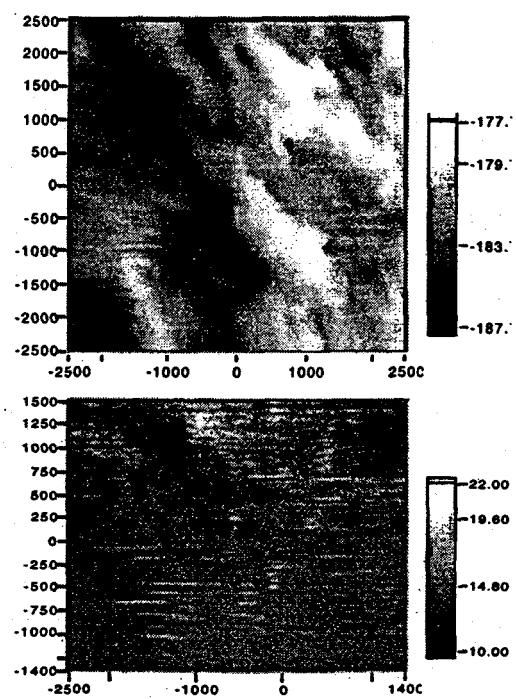

Figure 1: Top: background oxygen variation. Bottom: Drift-corrected difference image showing the change in oxygen concentration after electromigrating at 2 nA, 1 eV for 36 min.

References

[1] S. H. Huerth, M. P. Taylor, H. D. Hallen and B. H. Moeckly, Appl. Phys. Lett. 77, 2127 (2000).

[2] Suzanne Huerth, Michael Taylor, Michael Paesler and Hans Hallen, Proceedings of the Second Asia-Pacific Workshop on Near-field Optics, Beijing, China, (1999)

[3] H.D. Hallen, A. Fernandez, T. Huang, R.A. Buhrman and J. Silcox, Phys. Rev. Lett. 69, 2931 (1992).

[4] H.D. Hallen and R.A. Buhrman, in *Atomic nd Nanometer-Scale Modification of Materials: Fundamentals and Applications*, Edited by P. Avouris (Kluwer, Dordrecht, 1993)

[5] B.H. Moeckly, D.K. Lathrop and R.A. Buhrman, Phys. Rev. B 47, 400 (1993).

[6] B.H. Moeckly, R.A. Buhrman and P.E. Sulewski, Appl. Phys. Lett. 64, 1427 (1994).

Atom optics with nanostructured near-field light potentials: theory and applications

G. Lévêque, C. Meier, R. Mathevet, C. Robilliard, J. Weiner
Laboratoire de Collisions, Agrégats et Réactivité
UMR 5589 du CNRS et l'Université Paul Sabatier
31062 Toulouse Cedex 4 France
C. Girard
Centre d'Elaboration de Matéiaux et d'Etudes Structurales
29, rue Jeanne Marvig, BP 4347
31055 Toulouse Cedex 4 France
J. C. Weeber
Laboratoire de Physique de l'Université de Bourgogne
9 avenue A. Savary, F-21078
Dijon, France

As a first step in the development of atom and molecule manipulation by optical near fields, we develop a versatile calculational approach to the study of ultracold atom diffractive scattering from light-field gratings. We combine computation of the optical near field generated by evanescent waves close to the surface of periodic nanostructured arrays with advanced atom wavepacket propagation techniques. Nanometric 1-D and 2-D arrays with subwavelength periodicity deposited on a transparent surface and optically coupled to an evanescent wave source exhibit intensity and polarisation gradients [1] on the length scale of the object and can produce strong near-field periodic modulation in the optical potential above the structure. As a specific and experimentally practical example [2] we calculate the diffraction of cold Cs atoms dropped onto a periodic optical potential crafted from a 2-D nanostructured array. For an "out of plane" configuration we calculate a wide diffraction angle($\simeq$ 2 degrees) and about 60% of the initial atom flux in diffraction orders ± 1, an encouraging result for future experiments. Calculated simulations over a wide range of experimental parameters indicate that positive experimental results should be robust.

References

[1] G. Lévêque, G. Colas des Francs, C. Girard, J-C. Weeber, C. Meier, C. Robilliard, R. Mathevet, and J. Weiner, Phys Rev E **65**, 036701 (2002).

[2] G. Lévêque, C. Meier, R. Mathevet, C. Robilliard, J. Weiner, C. Girard, J. C. Weeber, Phys. Rev. A (in press)

Photopolymers for nanofabrication in the near optical field

Carole Ecoffet r(2), Renaud Bachelot(2), Fehkra H'dilli(2) Pascal Royer(2), Gregory A. Wurtz (4),

Département de Photochimie Génerale CNRS UMR7525-ENSCMu ; 3, rue Alfred Werner ; F-68093 Mulhouse-Chrystelle Triger
Département de Photochimie Génerale CNRS UMR7525-ENSCMu ; 3, rue Alfred Werner ; F-68093 Mulhouse-Renaud Bachelot, Fehkra H'dilli, Pascal Royer,
Laboratoire de Nanotechnologie et d'Instrumentation Optique, Université de Technologie de Troyes ; 12, rue Marie Curie ; F-10010 Troyes
Photosynthesis / Nanophotonics Group Chemistry Division Argonne National Laboratory Building 200 - 9700 South Cass Avenue - IL 60439-4831

Photopolymers are interesting material that can be easily patterned by light. When the illumination is made trough a classical optics set-up, the resolution is limited by diffraction.

But this limitation can be over passed when illumination is made trough near optical field set-up. Thus, ultra thin polymer spots were obtained by photopolymerization by evanescent waves. In this procedure, the area of interaction of the actinic light with the reactive formulation is confined within a layer of few hundreds of nanometers. The confinement of the light is achieved by Total Internal Reflection (TIR) of the light at the interface between the material and a high index prism [1]. This method is particularly suitable for the fabrication of micro parts and thin films (30 to 800 nm).

The concept of photopolymerization by evanescent waves is interesting from a technical point a view beacause it makes possible the fabrication of smaller structures than the one available by classical optical set-up. Besides, from a fundamental physical point of view, it is possible to make a copy of the near optical field and then to study it by other microscopy methods such as AFM. And finally the fact that illumination occurs over a very small volume allows studying the influence of diffusion processes during photopolymerisation.

Process of photopolymerisation was also applied to polymerization under a SNOM tip [2] and polymerization under metallic layers is under achievement. Results concerning different systems will be given.

References

[1] A. Espanet, G. Dos Santos, C. Ecoffet, D.J. Lougnot, *Applied Surface Science*, **138-139**, 87-92 (1999)

[2] G. Wurtz, R. Bachelot, F. H'Dhili, P. Rroyer, C. Triger, C. Ecoffet, D.J. Lougnot, *Jpn. J. Appl. Phys*, **39**, 98-100 (2000)

Local Fluorescent Probes for the Fluorescence Resonance Energy Transfer Scanning Near-Field Optical Microscopy

G. T. Shubeita, S. K. Sekatskii, G.Dietler, Institut de Physique de la Matière Condensée Université de Lausanne, BSP, CH 1015 Lausanne – Dorigny, Switzerland

V. S. Ltokhov, Institute of Spectroscopy, Russian Academy of Sciences, Troitsk, Moscow Region, 142190 Russia

While the resolution of Scanning Near-field Optical Microscopy (SNOM) is limited by the size of the aperture for light collection or transmission to about 100 nm, other approaches to near-field imaging are necessary. Fluorescence Resonance Energy Transfer (FRET) – based SNOM was proposed [1] to enhance both the resolution and the sensitivity of the method. It exploits the dipole-dipole energy transfer between a donor and an acceptor in a FRET chromophore pair where the donor is incorporated at the apex of the scanning probe and the acceptor is labeling the sample (or vice-versa). When imaging using the acceptor fluorescence resolution is no longer limited by the size of the aperture but rather by the Förster radius for energy transfer, which is typically of the order of 2-5 nm.

Nanolocal FRET SNOM measurements [2] and FRET SNOM images [3] based on this idea have been reported. Here, the first FRET-SNOM images with sub-aperture-size resolution will be presented [4]. Islands of the donor dye DCM deposited on a glass slide were imaged using the fluorescence of the donor dye OM57 deposited by dipping a fiber tip having an aperture of 200 nm in a solution of both the dye and the polymer PMMA which served both as a photobleaching inhibitor and a medium for better mechanical stability. Moreover, the "self-sharpening pencil" behavior could be realized for such a probe: the apical layers of the FRET-active tip coating are mechanically worn out and hence an active apex containing fresh acceptor molecules is continuously exposed to continue imaging. That the probe contains acceptor rather than donor molecules guarantees that only the molecules lying within a few nanometers of the apex are excited by FRET and are hence eventually photobleached. Exactly these molecules are continuously refreshed by the "pencil self-sharpening" mechanism.

From the geometry of the tip one estimates that some tens of acceptor molecules are involved in imaging, which, allowing for the experimental conditions, leads to an expected collected signal of ~750-2250 s^{-1}. This is in an order of magnitude agreement with the measured signal of 1000 photon/s. Moreover, good reproducibility of small details of the light intensity distribution along the DCM "clusters" (see the inset in Fig. 1) can be considered as an indication of a spatial resolution exceeding the size of the probe aperture.

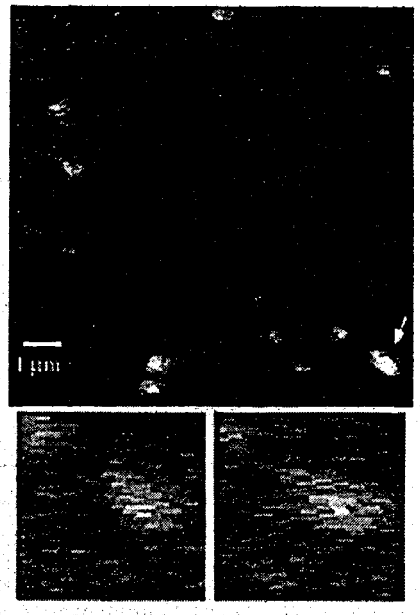

Fig.1. FRET SNOM image of donor molecule "clusters" on a glass slide surface. In the insert we show details of the raw images of one of the clusters (indicated by an arrow) recorded for the left-to-right and right-to-left movements of the tip. The size of one pixel is 43 nm, the minimal size of a structure in the scan direction (determined by the photon integration time) is ~170 nm.

References

[1] S. K. Sekatskii and V. S. Letokhov, Appl. Phys. B 63, 525, (1996). JETP Lett. 63, 319 (1996)

[2] G. T. Shubeita, S. K. Sekatskii, M. Chergui, G. Dietler, and V. S. Letoknov, Appl. Phys. Lett. 74, 3453, (1999)

[3] S. A. Vickery and R. S. Dunn, Biophys. J. 76, 1812 (1999); J. Microsc. 202, 408 (2001).

[4] G. T. Shubeita, S. K. Sekatskii, G. Dietler, and V. S. Letoknov, Appl. Phys. Lett. 80, (2002)

Super-Resolution Near-field Cover Glass Slip or Mount, a Novel Application of the Localized Surface Plasmon For Near-field Imaging

Yu Hsuan Lin, , Yuan Hsin Fu, Hsia Yu. Lin, Wei Chi Lin, Hsun Hao Chang, Din Ping Tsai

Department of Physics, National Taiwan University, Taipei 10617, Taiwan

A novel application of localized surface plasmon (LSP) has been developed to made a new type of cover glass slips or mounts with the near-field super-resolution imaging capability for use with a laser scanning microscope (LSM). An active layer of AgOx was prepared on the normal cover glass slips or mounts, and protected by a thin (less than $\lambda/10$) layer of dielectric film. This innovation allows an easy usage of the common laser scanning optical microscope to achieve near-field super-resolution imaging of nano-structures on the slips or mounts. Fig. 1 is the optical imaging results of this innovative method. Reflection images of the latex particles with diameters of 500 nm, 200 nm and 100 nm, respectively, were measured by using our super-resolution near-field cover glass slip. Features of the 100 nm standard latex particle can be clearly resolved. This novel innovation is expected to be used in various near-field imaging of medical and bio-samples in different environments with great simplicity, fast speed of laser scanning, and very low cost.

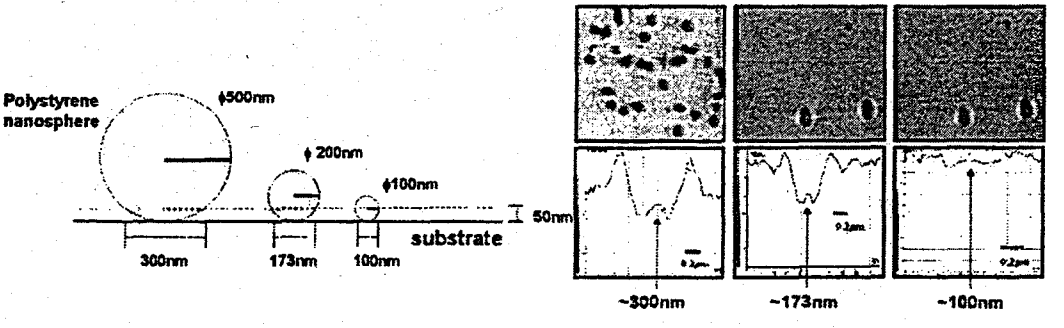

Fig 5. Near-field images of the standard latex particles with diameters of 500 nm, 200 nm and 100 nm, respectively, by using our innovative near-field super-resolution cover glass slip.

References

[1] James. B. Pawley, "Handbook of Biological confocal microscopy," Plenum Press, New York, London, 2nd edition 1995.

[2] M. Born and E. Wolf, "Principles of Optics," Cambridge University Press, Cambridge, 7th edition 1999.

[3] H. Fuji, J. Tominaga, L. Men, T. Nakano, H.Katayama, and N. Atoda, Jpn. J . Appl. Phys., Part 1 39, 980 (2000).

[4] J. Tominaga, J. Kim, H. Fuji, D. Buchel, T. Kikukawa, L. Men, H. Fukuda, A. Sato, T. Nakano, A. Taghibana, Y. Yamakawa, M.Kumagai, T.Fukuya and N. Atoda, Jpn . J. Appl. Phys., Part1 40 1831 (2001).

Near-field optical properties of a thin-film photonic transistor

Wei Chih Lin, Chien Wen Huang, Yu Hsuan Lin, Din Ping Tsai
Department of Physics, National Taiwan University, Taipei 10617, Taiwan

Wei-Chih Liu
Department of Physics, National Taiwan Normal University, Taipei 116, Taiwan

Super-resolution near-field structured photonic transistor was reported by Tominaga et al.[1] recently. Intensity of the incident signals could be amplified by the other input light at the focused spot of PC/ZnS-SiO_2/AgOx/ZnS-SiO_2/GeSbTe/ZnS-SiO_2 structure. h this paper, we investigate the near-field optical properties of the super-resolution near-field structured photonic transistor. Samples of glass/ZnS-SiO_2/AgOx/ZnS-SiO_2 and glass/ZnS-SiO_2/AgOx /ZnS-SiO_2/GeSbTe/ZnS-SiO_2 have been experimentally studied by a tapping-mode near-field scanning optical microscope. Near-field nonlinear optical effects of the transmitted light on both samples were found. Strong enhancement was observed in near field as well. Results show both surface plasmon (SP) and localized surface plasmon (LSP) should be active in the enhanced effects we found. Images of the near-field scanning optical microscope clearly illustrate the effects of the short and long-range interactions of the plasmons. The working mechanism of the super-resolution near-field structured photonic transistor is studied. Fig. 1(a) is the micrograph of the ZnS-SiO_2(20nm)/AgOx(15nm)/ZnS-SiO_2(20nm). The nano-composites are believed to be the nano-scatters shown in the Fig. 1(b), and the FDTD simulation indicates that these Ag scatters are sources of the enhancement at the focused spot.

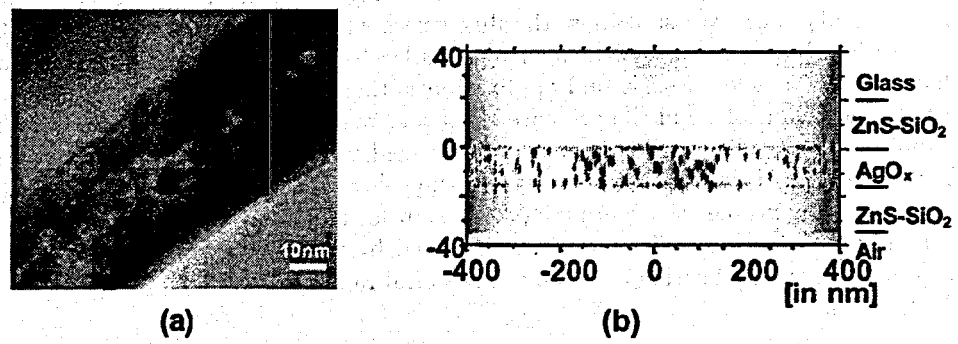

Figure 1. (a) TEM micrograph of the ZnS-SiO_2(20nm)/AgOx(15nm)/ZnS-SiO_2(20nm) super-resolution near-field structure. (b) Two-dimensional FDTD simulation of a ZnS-SiO_2(20nm)/AgOx (15nm)/ZnS-SiO_2 (20nm) super-resolution near-field structure under a focused laser beam.

References:

[1] J. Tominaga, C. Mihalcea, D. Bu¨chel, H. Fukuda, T. Nakano, and N. Atoda, H. Fuji, T. Kikukawa. Appl. Phys. Lett. **78**, 2417(2001).
[2] D. P. Tsai, W. C. Lin, Appl. Phys. Lett. **77**, 1413 (2000).
[3] D. P. Tsai, C. W. Yang, W. C. Lin, F. H. Ho, H. J. Huang, M. Y. Chen, T. F. Tseng, C. H. Lee, C. J. Yeh, Jpn. J. Appl. Phys., Part 1 **39**, 982 (2000).
[4] W. C. Liu, C. Y. Wen, K. H. Chen, W. C. Lin, D. P. Tsai, Appl. Phys. Lett. **78**, 685 (2001).
[5] T.Fukaya, D. Buechel, S. Shinbori, J. Tominaga, N. Atoda, D. P. Tsai, W. C. Lin, J. Appl. Phys. **89**, 6139 (2001).

Radiative heat transfer in the near-field.

J.P.Mulet, K.Joulain, R. Carminati,
Laboratoire EM2C, Ecole Centrale Paris, CNRS, 92295 Chtenay-Malabry Cedex, France
J.J. Greffet,
University of Rochester, The Institute of Optics, Rochester, NY 14627.

It has been shown recently by Carminati et al.[1] and Shchegrov et al.[2] that the field emitted by a thermal source made of a polar material at a distance of the order of 10 to 100 nm is enhanced by more than four orders of magnitude and is partially coherent. The reason for this large enhancement is that close to the interfaces, the local density of states increases dramatically due to the presence of surface-phonon polaritons. These are composite particles composed of a phonon and a photon bounded to the interface. Whenever a material supporting these excitations is heated, surface phonon-polaritons are emitted.

The purpose of this paper is to discuss the implications of this phenomenon for the radiative heat transfer between objects separated by distances in the range of the nanometer. It has been known for many years that radiative heat transfer can be enhanced across small distances due to evanescent waves (or tunneling photons). We have recently pointed out that this enhancement is strongly amplified when surface-phonon polaritons are excited to the extent that they are responsible for almost all the radiative heat transfer. The heat transfer mechanism can be viewed as an electromagnetic coupling of phonons across the gap.

We will consider two different geometries. First, we study the heat transfer between two half spaces as a function of the distance. We show how the flux varies with the distance. It will also be shown that most of the radiative flux is exchanged at some particular frequency. A behaviour completely different from what happens in far field. The second application is the study of the heat transfer between a small spherical particle and an interface in the presence of surface phonon-polaritons[3]. This can be viewed as a first model describing the radiative flux between a near-field probe tip and an interface. We examine the distance dependence of the power exchanged between the sphere and the interface. We have found that the radiative heat transfer overcomes the conductive heat transfer in air for spacings lower than 100 nm. This means that the radiative heat transfer has been enhanced by more than four orders of magnitude. This opens the possibility of locally heating or cooling a material radiatively.

References

[1] R. Carminati and J.J. Greffet*Phys.Rev.Lett.* **82**, 1660 (1999).

[2] A.V. Shchegrov, K. Joulain, R. Carminati and J.J. Greffet, *Phys.Rev.Lett.* **85**,1548 (2000).

[3] J.P. Mulet, K. Joulain, R. Carminati and J.J. Greffet*Appl. Phys. Lett.* **78**, 2931 (2001).

Intensity vs. Amplitude Detection in Scattering-type Near-field Optical Microscopy

M. Labardi, M. Allegrini
INFM and Dipartimento di Fisica, Universita' di Pisa, Via Buonarroti 2, 56127 Pisa, Italy

S. Patanè, E. Cefalì,
INFM and Dipartimento di Fisica MTFA, Universita' di Messina, Salita Sperone 31, 98166 Messina, Italy

P.G. Gucciardi
CNR - Istituto per i Processi Chimico-Fisici, Sez. di Messina, Via La Farina 237, I-98123 Messina, Italy

Sharp dielectric or metallic tips are used in scattering (or apertureless) NSOM as nanometer-size scatterers of the optical field produced by laser light in the vicinity of the surface. Scattering properties are strongly sensitive to nanoscale features of the surface when the mutual distance is of the order of a few nm. Near-field optical microscopy in the visible region has been performed with artifact-free resolution in the 10-nm range [1,2]. Two-photon fluorescence in biological samples has been evidenced [3], on the scale of 20-30 nm. Single molecule emission has been also used as the near-field source [4].

High resolution, obtained with the elastic scattering experiment, requires the detection of small light intensities with a poor signal to background ratio and result in a challenging task. Such light can be extracted from the background light since, if a small modulation is superimposed to the tip-sample distance, the signal presents terms at the second and higher harmonics of the modulation frequency [5], detectable by lock-in techniques. This point is a crucial one in order to obtain genuine near-field contrast, not affected by topographical artifacts due to the surface tracking of the probe, performed in order to maintain a constant distance from the surface. Optical interferometry provides the key to enhance the sensitivity of the system. Interference of the scattered light with a reference beam, detected with a Michelson [6] or a Mach-Zehnder (heterodyne) [2] configuration, provides a signal that scales with the electric field amplitude instead of its square (light intensity). Within the Mie's approximation, this leads to a scattering signal that scales with the third power of the size of the scattering center instead of the sixth power, that is the case of the intensity detection.

We have explored and characterized different illumination and collection geometries as well as different modulation techniques and interferometric configurations. In particular, on-axis illumination and collection with a Nomarski interferometer has provided 15 nm resolution (10%-90% criterion) [1], while grazing illumination looks more promising for obtaining high fields required for spectroscopy experiments.

Fischer patterns fabricated with 500 nm diameter spheres have been imaged by our scattering-NSOM. The current status of our apparatus will be described. The system allows simple positioning and monitoring of tip, sample and laser spot as well as ease of detection mode (amplitude vs. intensity) switching. Results of comparison between the latter two detection modes will be discussed in terms of contrast, resolution, and artifact content. One important conclusion is that axial configuration setups [1,3,6,7] (when used in elastic scattering mode) are inherently concerned by the interference between the reflected light and the photons scattered by the tip. This could explain the unexpectedly high performance that can be attained with no additional interferometer setup.

References

[1] M. Labardi, S. Patanè, and M. Allegrini, *Appl. Phys. Lett* **77**, 621 (2000).
[2] R. Hillenbrand, and F. Keilmann, *Appl. Phys. Lett.* **80**, 25 (2002).
[3] E.J. Sanchez, L. Novotny, and X. Sunney Xie, *Phys. Rev. Lett.* **82**, 4014 (1999).
[4] J. Michaelis, C. Hettich, J. Mlynek, and V. Sandoghdar, *Nature* **405**, 325 (2000).
[5] N. Maghelli, M. Labardi, S. Patanè, F. Irrera, and M. Allegrini, *J. Microsc.* **202**, 84 (2001).
[6] J. Azoulay, A. Debarre, A. Richard, and P. Tchenio, *Appl. Opt.* **39**, 129 (2000).
[7] R. Bachelot, P. Gleyzes, and A.C. Boccara, *Appl. Opt.* **36**, 2180 (1997).

MMP Calculation of the electromagnetic field enhancement at sharp noble metal tips for tip-enhanced Raman scattering

V. Deckert, J. Renger, and L.M. Eng
Institut für Angewandte Photophysik, TU Dresden, D-01062 Dresden, Germany
deckert@iapp.de, www.iapp.de

Scattering near-field optical microscopy (S-SNOM) has the potential to become an alternative to aperture SNOM (A-SNOM). The method is especially promising in combination with Raman spectroscopy to obtain chemical information. As Raman scattering already suffers from a very low cross-section in standard setups, the light restrictions imposed by an A-SNOM instrument are a major limitation. Only selected molecules with a comparably high Raman scattering yield have been investigated by SNOM. However, the Raman signal can be enhanced by several orders of magnitude in the neighborhood of small metal particles - the so-called surface enhanced Raman scattering (SERS) [1]. The concept of S-SNOM with Raman enhancing metal particles combines the advantages of S-SNOM techniques, easier instrumental implementation without the need of delicate near-field probes and a somewhat higher lateral resolution, and the advantages of SERS with its high signal intensities.

Important for an optimum Raman signal enhancement is knowledge on the tip material and geometry. Clearly the noble metals like Ag and Au are the candidates of choice when inducing electromagnetic field enhancement via local plasmon excitation. For a fixed excitation wavelength λ, the major challenges therefore are to find both the optimal tip geometry providing the highest Raman enhancement, and the most suitable illumination/detection arrangement.

Several groups already proved the successful use of massive metal tips to enhance Raman scattering with a resolution of down to ~20 nm[2,3]. However, no theoretical investigation has been reported yet, calculating the strength and orientation aspects of the local field enhancement for a specific tip geometry and material. Both these two parameters are important when optimizing the collection of the Raman scattered light.

We present theoretical investigations based on the multiple multipole (MMP) approach [4] in order to calculate the electromagnetic field enhancement at sharp noble metal tips, mostly Ag, for different optical geometries as well as a broad spectral range. Excitation is done for different illumination geometries (sidewise, bottom, etc.) allowing also the modeling of objectives with both high and low numerical apertures. Also the incident beam shape, whether being a plane wave or having a Gaussian shape, seems to severely affect the local field enhancement. Furthermore, calculations are presented for different polarization orientations.

This approach allows us either to estimate the optimal optical resonance frequency for a given tip shape or, vice versa, to optimize the tip geometry and material for a given set-up and laser excitation wavelength λ. Therefore theoretical results have to be compared with tip shapes being experimentally realizable.

References

[1] See for instance: Kerker, M., Selected papers on surface enhanced Raman scattering, ed. Thomson, B. J. (Spie Optical Engineering Press, Bellingham), 1990.
[2] R. M. Stöckle, Y. D. Suh, V. Deckert, and R. Zenobi, *Chem. Phys. Lett.* **318**, 131 (2000).
[3] N. Hayazawa, Y. Inouye, Z. Sekkat, and S. Kawata, *Opt. Comm.* **183**, 333 (2000).
[4] L. Novotny, D. W. Pohl, and P. Regli, *J. Opt. Soc. Am. A* **11**, 1768 (1994).

Transient optical elements: application to near-field microscopy

D. Simanovskii, D. Palanker, K. Cohn, T. Smith
Stanford University, Hansen Experimental Physics Laboratory
Stanford, CA 94305

We present two new methods of near-field infrared microscopy based on transient optical elements. Photoinduced carrier generation in semiconductors is used to create 2- and 3-dimensional reflecting and refracting structures that can provide infrared light confinement on subwavelength scale. Both methods use short pulse Ti:S laser as a pump source to generate electron-hole plasma in semiconductors and picosecond OPA as an infrared light source.

The first technique – transient aperture (TA) resembles a fundamental near-field configuration when light is squeezed through a subwavelength aperture in a nontransparent screen. To generate the TA subpicosecond, laser pulse illuminates a large area of the semiconductor film except for a small region in the middle that is shadowed. This illumination results in creating a large transient mirror (TM) with a small transparent aperture that acts as a near-field probe [1]. We studied the optical properties of the TM and TA experimentally and performed initial experiments on near-field imaging with the TA.

The second technique is based on a concept of a solid immersion microscopy [2]. Many solids have refractive index much higher than 1, providing diffraction limited resolution several times better than in air. To benefit from using of high refractive index material, focusing element must be incorporated in this material. We used photoinduced reflectivity to generate a transient Fresnel lens on the surface of semiconductor wafer to focus infrared light on the other side of the wafer, where a sample was positioned. Two materials were tested: GaP and Si with refractive indices 3 and 3.4 respectively. In both cases second harmonic of Ti:S laser (400 nm) was used to generate a lens, that was optimized to focus infrared radiation at a specific wavelength in a spectral range from 6 to 10 μm. Test images of polystyrene microbeads were obtained that demonstrate resolution better than $\lambda/5$.

We will discuss such issues as ultimate resolution, contrast parameters and chromatic aberrations typical for both systems we present. Other new applications of transient optical elements will be also considered.

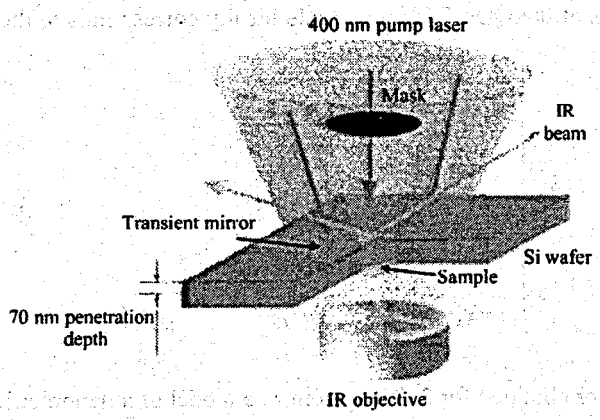

Figure 1: Layout of a near field microscope with a photoinduced aperture

References

[1] D. Simanovskii, D. Palanker, K. Cohn, T .Smith, Applied Physics Letters, 79, #8, p. 1214 (2001)
[2] D. Fletcher, K. Crozier, C. Quate, et al., Applied Physics Letters, 77, #14, p. 2109 (2000)

Localized Photon Picture vs. Effective Interaction Picture: Towards a Nanometric Photonic Device

K. Kobayashi, S. Sangu, T. Kawazoe, ERATO Localized Photon Project, Japan Science and Technology, 687-1 Tsuruma, Machida, Tokyo 194-0004, Japan
A. Shojiguchi, K. Kitahara, Division of Natural Sciences, International Christian University, 10-2 Osawa 3-chome, Mitaka-shi, Tokyo 181-8585, Japan
M. Ohtsu, Japan Science and Technology, and also Interdisciplinary Graduate School of Science and Engineering, Tokyo Institute of Technology, 4259 Nagatsuta-cho, Midori-ku, Yokohama, Kanagawa 226-8502, Japan

In near-field optical microscopy and spectroscopy, localization and tunneling of photons have played essential roles, and are now realized as key issues for nanometric photonic devices. For example, the principles of operation of our proposed device [1] are based on excitation energy transfer induced by localized optical near fields between nanometric quantum dots (QDs) [2], and irreversible signal transmissions are guaranteed by the exciton-phonon coupling. Here we report on two alternative approaches: localized photon picture and effective interaction picture to discuss physics behind the devices.

When we explicitly include localized photonic degrees of freedom, we can describe dynamics of a relevant system that are governed by localized photons. The theory predicts, for example, a coherent dipole oscillation of a linear chain of two-level QDs, after local manipulation of initial states of some of the QDs [3]. We find that this kind of phenomenon originates in the fermionic nature and nonlinear effects of excitons. In order to understand such phenomenon more deeply, we use an effective interaction picture [4]. Taking the trace with respect to localized photonic degrees of freedom, we can derive an effective optical near-field interaction between QDs as $\hat{H}_{\text{eff}} = -\sum_{<i,j>} J_{ij}\hat{\vec{P}}(i)\cdot\hat{\vec{P}}(j)$, where $\hat{\vec{P}}(i)$ and J_{ij} are the dipole operator of the i-th QD and the coupling strength between the nearest neighbor QDs, respectively. It follows from this Hamiltonian that the dipole moments of the system tend to align parallel or antiparallel, depending on the sign of the coupling J_{ij}.

The above approaches can be extended to include exciton-phonon coupling in addition to the optical near-field coupling. Using the density operator method, we obtain equations of motion for such a system, and estimate a time scale of exciton population tunneling as a few to 100 picoseconds for CuCl QDs, depending on the sizes and the separation distances of the QDs. This time scale ideally corresponds to the switching speed of our proposed nano-switch.

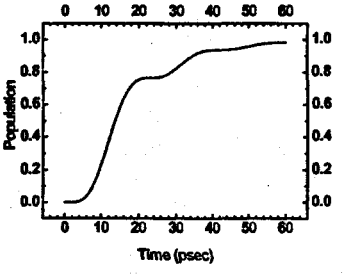

Figure 1: Typical switching behavior obtained for 3-QD system as a model of a nanometric photonic switch.

References

[1] M. Ohtsu, K. Kobayashi, T. Kawazoe, S. Sangu, and T. Yatsui, *to be published in IEEE J.*
[2] T. Kawazoe, K. Kobayashi, J. Lim, Y. Narita, and M. Ohtsu, *Phys. Rev. Lett.* **88**, 067404 (2002).
[3] A. Shojiguchi, K. Kobayashi, K. Kitahara, S. Sangu, and M. Ohtsu, *Proc. 3rd Asia Pacific Workshop on Near Field Optics*, 82 (2001).
[4] K. Kobayashi, S. Sangu, H. Ito, and M. Ohtsu, *Phys. Rev. A* **63**, 013806 (2001).

NSOM probes with strongly enhanced optical transmission

G.D. Lewen, K.m. Pellerin and Tineke Thio, NEC Research Institute, Princeton NJ 0854.

The optical transmission of a single, subwavelength aperture in a metal film is strongly enhanced when the metal surface surrounding the aperture has a periodic corrugation. [1] The transmission enhancement is mediated by a resonance of the incident light with surface plasmon polaritons. The resonance leads to a strong enhancement of the electric fields at the entrance of the hole. Since the interaction occurs through grating coupling at the corrugated surface, the resonant wavelengths are proportional to the corrugation periodicity P, and are thus tunable. At the transmission peak, three times more light is transmitted through the hole than is directly falling onto its area. This is independent of aperture size, so the total throughput scales as $T \sim d^2$ (where d is the hole diameter), rather than the $T \sim d^6$ dependence predicted by the Bethe-Bouwkamp model. So the relative transmission enhancement (the ratio of the transmission with and without the enhancement) grows as d becomes smaller.

The optimal corrugation geometry consists of a set of concentric circular grooves around the central aperture, equally spaced in the radial direction and with a depth corresponding to about three times the skin depth fo the metal. The reason is that for the unpolarised light we have used in our experiments, the Huygens wave associated with the small aperture has axial symmetry, and is therefore best matched to the surface plasmon modes on a cylindrically symmetric surface corrugation rather than one with translational symmetry. Such a "bullseye" pattern is well suited for fabrication at the tip of an optic fiber, for use in near-field microscopy.

We present results on a fiber tip with an enhanced device, of which the resolution is determined by the exit diameter of the aperture. For NSOM use on rough surfaces, it is useful to have a device with a very small footprint. From our preliminary measurements on the minimum corrugated area necessary to obtain the enhanced transmission, we find that at least four rings are required to obtain the full enhancement: as the number of rings is increased from one to four, the enhanced transmission peak becomes both higher and narrower. This size effect confirms again the importance of the periodicity of the surface corrugation. We discuss other strategies to minimise the device footprint.

References

[1] T. Thio, K.M. Pellerin, R.A Linke, H.J. Lezec and T.W. Ebbesen, *Optics Letters* **26**, 1972 (2001).

More information at http://www.neci.nj.nec.com/homepages/thio/

Z-scan analysis for the optical nonlinearity of the AgO_x-type super-resolution near-field structure

Hsun Hao Chang, Fu Han Ho, Pei Wang[a], Din Ping Tsai
Department of Physics, National Taiwan University, Taipei, Taiwan, 10617
[a]Department of Physics, University of Science and technology of China, Hefei, Anhui, 230026

Near-field optical storage using AgO_x-type super-resolution near-field structure (Super-RENS) attracts many attentions recently[1]. One of the key issues of the AgO_x-type Super-RENS is the working mechanism and optical properties of the sandwiched AgO_x thin film. Tsai et al. [2] have reported the strongly enhanced near-field intensities measured by a tuning-fork tapping-mode near-field scanning optical microscope (TFTM-NSOM). Ensemble of the excited localized surface plasmons at the focused spot was proposed for the origin of the enhancement of the near-field intensity, and the nano marks size beyond the diffraction limit.

In this paper, the nonlinear optical properties of the AgO_x-type Super-RENS thin films were studied using Z-scan technique[3-4] with a 0.7ns, 532nm laser pulse. The changes of the transmission, and the nonlinear absorption properties were observed and studied. Nonlinear refractive index n_2 can be obtained through close-aperture Z-scan as well. The causes of these changes come from photochemical reaction, thermal effects and optical response. Results shown in Fig. 1 indicated that the transmittance of Z-scan at the focal position had a strong enhancement at proper incident laser power

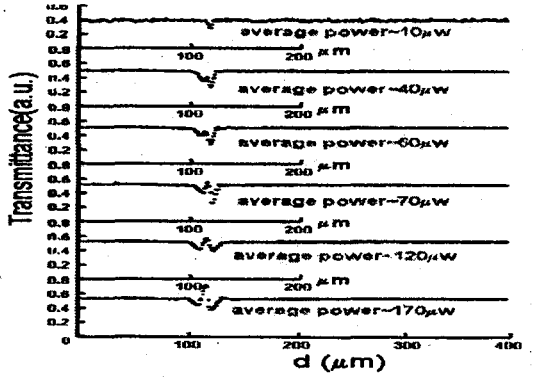

Figure. 1 Z-scan normalized transmittance of the AgO_x layer at different incident pulse laser power.

References

[1] H. Fuji, J. Tominaga, L. Men, T. Nakano, H.Katayama, and N. Atoda, Jpn. J . Appl. Phys., Part 1 **39**, 980 (2000).

[2] D. P. Tsai, W. C. Lin, Appl. Phys. Lett. **77**,1413(2000).

[3] F. H. Ho, W. Y. Lin, H. H. Chang, Y. H. Lin, W. C. Liu, D. P. Tasi, Jpn. J. Appl. Phys. **40** ,134 (2001).

[4] Toshio Fukaya, Dorothea Buchel, Shunichiro Shinbori, Junji Tominaga, and Nobufumi Atoda, Din Ping Tsai and Wei Chi Lin, J. Appl. Phys. **89**, 6139 (2001).

Numerical Studies of Optical Switching and Optical Bistability Phenomena of Mesoscopic scale-spheres

T. Okamoto, M. Haraguchi, M. Fukui, University of Tokushima, Faculty of Engineering, Tokushima, JAPAN 770-8506.

It is apparent that an enhancement of light intensity can be expected to occur in and around spheres coated by Kerr-materials in which the so-called whispering gallery modes (WGM's) are excited. This enhancement may lead to the realization of optical switching and optical bistable devices in mesoscopic scale. It is well known that when the real part of the dielectric constant of spheres is negative, even if the size of spheres is considerably smaller than a wavelength of an incident light, the WGM's are readily excited and then there exists a strong near-field light in the surrounder of spheres. We are, therefore, concerned with CuCl whose dielectric function has the abnormal dispersion based on a Z_3-exciton. Namely, it has a negative real part of the dielectric constant around a characteristic wavelength of the Z_3-exciton. The structure employed here is shown in Fig.1. The first aim of this study is to numerically calculate nonlinear responses of CuCl-spheres by using the Mie-theory modified to analyze nonlinear phenomena. The second one is to examine optical switching and optical bistability due to the WGM's excited in such spheres.

We employ the Lorentz model as the dielectric function in trems of the Z-exciton of CuCl. For the CuCl-sphere, the WGM is a surface mode of 1S-type and its characteristic wavelength is 410.154 nm. Figure 2 shows a typical result on the ratio of $|E|^2/|E_i|^2$ as a functions of the incident light intensity I_i measured at point A in Fig.1, where E is electric field at point A in Fig.1 and E_i is electric field of the incident light . At λ=410.154 nm, where λ is the wavelength of the incident light, the optical switching occurs. At λ=410.204 nm, we can observe the optical bistability. These results suggest that fundamental optical devices related to optical information processing can be realized by employing Kerr-nonlinear spheres in a mesoscopic scale.

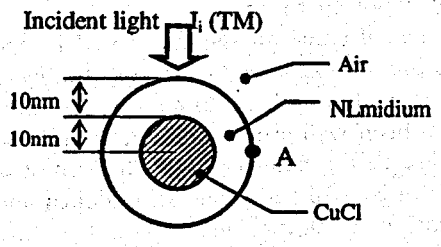

Fig.1 The structure for the calculation.

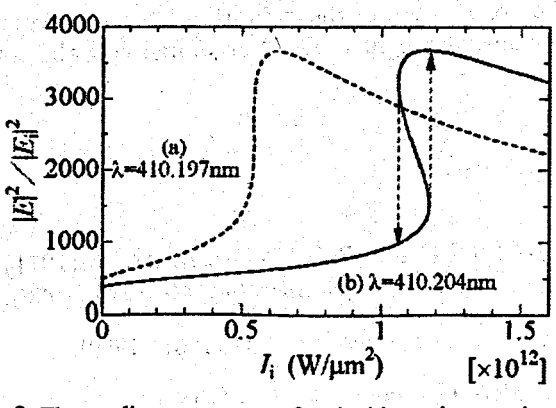

Fig.2 The nonlinear response of optical intensity at point A in Fig.1.

Two-photon Excitation of Excitons in CuCl in Total Reflection Geometry

M. Hasuo, A. Shimamoto and T. Fujimoto,
Kyoto University, Graduate School of Engineering, Kyoto, 606-8501, Japan.

It is well-known that the evanescent light accompanying the totally reflected light at an interface of dielectric mediums with a high refractive index n_1 and a low refractive index n_2 has interesting features: One is its small penetration depth of the order of wavelength of the light that is given as

$$\eta = \frac{1}{k_0\sqrt{n_1^2 \sin^2\theta - n_2^2}} \tag{1}$$

where k_0 is the wavenumber of the light in vacuum and θ is the incident angle of the light. Another feature of the evanescent light is its wavenumber parallel to the surface that is determined by n_1 and θ as

$$k = k_0 n_1 \sin\theta. \tag{2}$$

In linear spectroscopy, electronic excitations such as surface plasmons and surface polaritons, which can not be excited by usual propagating light wave, have been examined by using these features [1]. On the other hand, systematic study of the second harmonic generation at an interface was done by N.Bloembergen et.al [2]. The wavenumber of the evanescent field plays an essential role in the nonlinear optical phenomena through the phase matching condition. In principle, these situations may be applicable to the two-photon excitation of excitons. However, as far as we know, two-photon spectroscopy on exciton systems with evanescent light field has not been reported so far.

Here, we report the measurement of emission spectra of CuCl deposited on a TiO_2 (rutile) prism surface(110) associated with the two-photon excitation of the exciton system in total-reflection geometry. We choose CuCl as a nonlinear optical medium with a low refractive index because characteristics of the excitons and exciton-polaritons have been well studied by linear and nonlinear spectroscopy [3, 4, 5]. As a medium with a high refractive index TiO_2 single crystal is chosen not only by its very high refractive index but also by its birefringence. We can control the penetration depth and the wavenumber of the evanescent field by only changing the polarization of the incident light.

As the experimental result, the I_1 bound exciton luminescence which resonantly appears at the two-photon excitation of the Z_3 and $Z_{1,2}$ excitons was observed. The dependence of the intensities of the I_1 bound exciton luminescence on the polarization of the excitation light was explained by the field intensity and the penetration depth of the evanescent light in CuCl accompanying the totally reflected light at the CuCl/ TiO_2 interface.

References

[1] N. Marschall, B. Fischer and H. J. QUeisser, *Phys. Rev. Lett.* **27**, 95 (1971). I. Hirabayashi, T. Koda and Y. Tokura, J.Murata and Y.Kaneko *J. Phys. Soc. Jpn.* **40**, 1215 (1976).

[2] N.Bloembergen, H. J.Simon and C.H.Lee, *Phys. Rev* **181**, 1261 (1969).

[3] T.Mita and N.Nagasawa, *Solid State Commun.* 44, 1003 (1982).

[4] D.Fröhlich, P.Kohler, W.Nieswand and E.Mohler, , *Phys.stat.sol.(b)* **167**, 147 (1991).

[5] K.Saito, M.Hasuo, T.Hatano and N.Nagasawa, *Solid State Commun.* **94**,33 (1995).

White light continuum generated by gold tips.

M. R. Beversluis, A. Hartschuh, and L. Novotny
University of Rochester, The Institute of Optics, Rochester, NY 14627.

Non-linear optical interactions can be used to increase resolution in near-field microscopy, but can also introduce new sources of unwanted background signal. In the presence of highly non-linear materials, such as gold, a white-light continuum can be generated. Because the origin is not yet well understood, we have measured the spectral, spatial, and temporal properties of this white light generated by a sharp gold tip in a focused ultrashort laser pulse. We found a continuous spectrum from the excitation wavelength to its second harmonic. Furthermore, characteristic of its nonlinear origin, the total white light intensity has a quadratic dependence on the excitation power. Unexpectedly the temporal behavior is slow, in contrast to white light continuum generation due to self-phase modulation [1]. We measured an exponential decay of the white-light intensity with a lifetime of 800 ps, which suggests that another mechanism is responsible.

We also found that the white light is excited by light polarized along the tip axis, and when the tip is scanned through a highly focused laser beam, the white light intensity maps out the longitudinally polarized component, as shown in Figure 1.

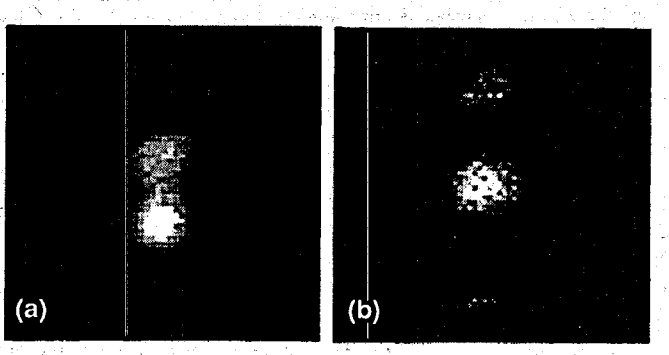

Figure 1: White light intensity as a function of tip position within the focus of Gaussian (a) and Hermite-Gaussian (b) excitation beams (1.5 by 1.5 micron area).

References

[1] A. L. Gaeta *Phys. Rev. Lett.* 84, 3582 (2000).

Action of Ultra-Short Laser Pulses on Surface in the Near Field

M.Libenson, G.Martsinovsky,
S.I. Vavilov State Optical Institute, Birzhevaya Liniya 12, St.-Petersburg, Russia

Scanning near-field optical microscope (SNOM) excels as a unique instrument for investigation of optical properties of a surface with lateral resolution of several hundredths of the wavelength used. Using of ultra short laser pulses (USLP) supplements SNOM with high temporal resolution, thus achieving the maximum localization of the light both in space and time [1-3]. The light action of the above conditions has a number of peculiarities that were the subject of the present paper.

To analyze the light action it is necessary to know the field structure and its characteristics in the immediate vicinity of the probe when its output aperture d is much smaller than the light wavelength λ. In these conditions the concept of near-field is associated with the region where non-propagating waves exist. The amplitudes of these waves fade out exponentially with the distance z from the probe aperture. The exponential decay straightforwardly follows from the Heisenberg principle of uncertainty applied to a photon-like particle. The angular spectrum of such a source in the near field contains both propagating and non-propagating components. The non-propagating components carry information about geometrical features of the radiating aperture, which are smaller than $\lambda/2$, and rapidly vanish at distance $z > d$ from the probe aperture [4]. Only propagating components of a solitary probe can be registered in the far field. However, these components do not transfer any information about high spatial frequency portion of the spectrum that corresponds to configuration and features of a sub-wavelength object. As the result, it is impossible to reconstruct these parameters the way it was proposed in some recent papers (see, for examples, [5, 6]).

The most interesting aspect of USLP action in the case of high spatial localization is related to the peculiarities of photoexcitation of nonequilibrium carriers in metals and semiconductors. In particular, it results from small duration of the light pulse ($t_p < 1$ ps), which is not enough for the excited carriers to transfer their excessive energy to the lattice. Under this condition the electron temperature can reach tens and hundreds of kK which results in considerable thermal additive to the carrier photoemission from the medium surface. When the pulse ends the thermo-emission becomes the only mechanism of the electron liberation. The uniqueness of the near-field action in this case is determined by the submicron size of the subsurface region from which the emission takes place. For the laser pulse duration of 100 fs the characteristic diffusion length of the excited nonequilibrium carriers amounts to about 30 nm. The Arrenius type dependence of the emission current density on the temperature can noticeable reduces the effective size of the emitting area. The emission current is also influenced by local relief of the surface, its electro-physical properties and presence of adsorbed layers.

We have developed a simple theory for pulsed laser local photoexcitation in metals and semiconductors by a single ultra short pulse and analyzed isolated heating of free electrons in the metal. It allowed estimation of emission current density in the area of the near-field interaction. By registering the emission signal with optical or electrical methods and using the opportunity for application of an electrical potential to the metal cladding of the near-field probe the combination of USLP and SNOM makes it possible to acquire additional information about the surface local properties and achieve "emission" contrast.

The work was supported by the Russian Foundation for Basic Research grants 00-02-16716 and 01-02-16872.

References:

[1] A. Vertikov, M. Kuball, A. V. Nurmikko, and H. J. Maris, *Appl. Phys. Lett.* **69** 2465 (1996)
[2] S. Smith, N.C. Holme, B. Orr, R. Kopelman, T. Norris, *Ultramicroscopy*, **71**, 213, (1998)
[3] B.A. Nechay, U. Siegner, M. Achermann, H. Bielefeldt, U. Keller, *Rev.Sci.Inst.* **70**, 2758 (1999)
[4] G. S. Zhdanov, M. N. Libenson, G. A. Martsinovsky, *Uspekhi Fizicheskikh Nauk (Physics - Uspekhi)* **41**, 719 (1998).
[5] M. Xiao, *J. Mod. Optics*, 46, p.729 (1999)
[6] V. P. Veiko, N. B. Voznessenski, V. M. Domnenko, A. E. Goussev, T. V. Ivanova, S. A. Rodionov, *Proc. SPIE* **3736** 341 (1998)

Surface Plasmon enhanced Second-Order Nonlinear Optical Study on Monomolecular Layers

K. Kajikawa, Ryo Naraoka and T. Iiyama,
Tokyo Institute of Technology, Yokohama 226-8502, Japan

In these years, much attention has been directed towards the surface plasmon resonance (SPR). Since SPR yields considerable enhancement of the electric field, the nonlinear optical (NLO) effect is clearly observed if the NLO medium is very thin such as a monomolecular layer[1,2]. In this paper, we will report our recent results on large second-order NLO effects in a monomolecular layer adsorbed on a gold thin film with the SPR enhancement. The second-order nonlinear susceptibility obtained by the linear electro-optic measurement with enhancement of the electric field by SPR was compared with that by second-harmonic generation (SHG) study. The optical geometry used for the linear electrooptic measurement is depicted in Figure 1(a). The electric field was applied between the electrodes with the gap of 12 μm. The reflectivity difference ΔR due to the electric field was plotted as a function of the angle of incidence as shown in Figure 1(b). Best fit to the theoretical expression (solid line) gives the susceptibility value $\chi^{(2)}_{zzz}$=33 pm V^{-1} , which is in good agreement with that obtained from SHG measurement $\chi^{(2)}_{zzz}$=58 pm V^{-1} for the monomolecular layer[2].

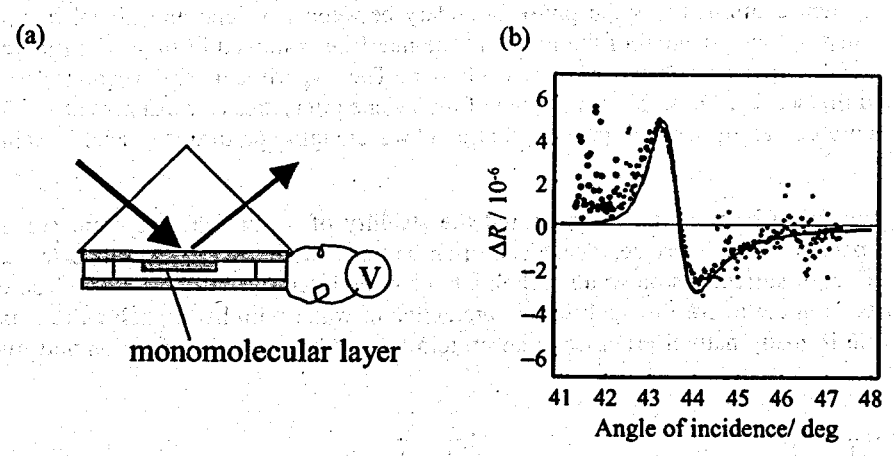

Figure 1: Optical geometry (a) and ΔR as a function of the angle of incidence (b).

References

[1] R. Naraoka, K. Kajikawa , H. Okawa, H. Ikezawa, K. Hashimoto, submitted to Chem. Phys. Lett.
[2] K. Kajikawa , R. Naraoka, T. Iiyama, submitted to Jpn. J. Appl. Phys.

Chemical analysis of the phase boundary between two liquids through near-field optical microscopy

M. De Serio, A. Bader, R. Zenobi, Laboratory of Organic Chemistry, ETH Hönggerberg, CH-8093 Zürich, Switzerland.
V. Deckert, Institut of Applied Photophysics, Technische Universität Dresden, Germany.

Scanning near-field optical microscopy has already been successfully applied in combination with Raman spectroscopy [1]. In this way the improved resolution is combined with spectroscopic analysis to provide chemical information for the sample of interest.

Our attempt aims at applying this technique to the study of the boundary between two liquids. An important property of near-field probes is the high resolution or small depth of focus in tip direction. This means that the interface can be approached in small steps over a wide range. Gradual structural changes at variable distances from the interface can be spectrally analysed. Traditionally the investigation of the interface is based on methods that differ from the above; they exploit second order optical effects such as Sum Frequency Generation (SFG) or Second Harmonic Generation (SHG) [2]. These processes are forbidden in media that have inversion symmetry and thus they are only sensitive to the interface where this symmetry is, by definition, broken.

The first binary system examined was the phase boundary between p-xylene and glycol in order to investigate the feasibility and the potential of the method. The interface is moved in steps of 3 μm towards the near-field probe and a spectrum is recorded at each step. The experiment was performed with an uncoated and a coated tip (see fig. 1). An abrupt change of the xylene intensities (for example at 1200 cm^{-1}) is observed only when a coated tip is used, proving that a subwavelength aperture is crucial in achieving higher resolution.

The exchange phenomena between two liquids and the stability of a multiphase system are mainly controlled by the properties of the interface. These can often be tuned with the addition of surface-active molecules [3]. The effect of surfactants on water/carbon tetrachloride interface will be studied. The choice of these liquids comes from the interest to analyse the interaction of water with hydrophobic fluid surfaces which plays a key role in many natural processes like protein folding, membrane formation and micellar assembly.

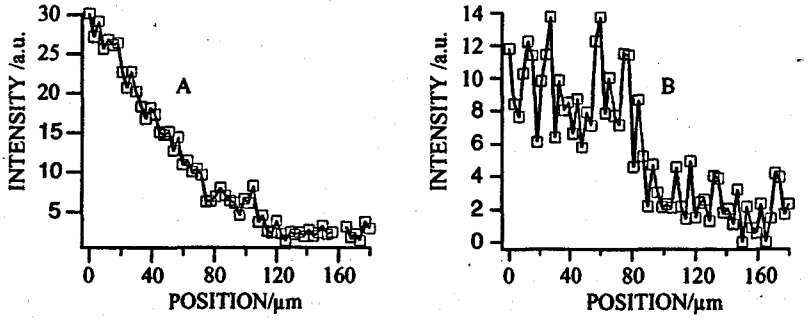

Fig.1 : Intensity plot of the Raman signal (1200 cm^{-1}) during the approach of an uncoated (A) and a coated (B) tip to the p-xylene/glycol interface.

References

[1] Y. Narita, et al., Appl. Spectrosc. **52**(9), 1141 (1998)
[2] L. F. Scatena, et al., Science **292**, 908 (2001)
[3] F. Ravera, et al., Adv. Coll. Int. Sci. **88**, 129 (2000)

Tip-Enhanced Raman Spectroscopy for Nanoscale Analytical Applications

J. E. Melanson, M. Gerunda, V. Deckert, and R. Zenobi
Department of Chemistry, ETH Hönggerberg
CH-8093 Zürich, Switzerland

Surface enhanced Raman scattering (SERS) has emerged as a highly sensitive analytical technique, offering signal enhancements of several orders of magnitude over conventional Raman scattering. However, the inherent heterogeneity of metallic SERS substrates creates variable electromagnetic field enhancement across the surface. This shortcoming limits the utility of the technique and renders quantitative measurements highly speculative. As an alternative to conventional SERS, a metallized AFM tip can be brought very near a sample surface, providing highly localized signal enhancement[1-3]. This technique provides a more homogenous enhancement across the sample, allowing for quantitative analysis and even Raman imaging. This presentation will discuss recent advances in instrumentation, including the incorporation of a scanning fluorescence microscope for rapid optical alignment of the laser focus with the AFM tip. Further, an external scanning stage is now being employed to scan the sample relative to the tip and optics, ensuring constant alignment of the laser beam and collection optics with the AFM tip. Finally, this presentation will describe the application of tip-enhanced Raman scattering for the characterization of carbon nanotubes.

References:

1. R. M. Stöckle, Y. D. Suh, V. Deckert, R. Zenobi, *Chem. Phys. Lett.* 318 (2000) 131-136.
2. M. S. Anderson, *Appl. Phys. Lett.* 76 (2000) 3130-3132.
3. N. Hayazawa, Y. Inouye, Z. Sekkat, S. Kawata, *Chem. Phys. Lett.* 335 (2001) 369-374.

Single Polymer Chain in Two-Dimensions Observed by Scanning Near-Field Optical Microscopy

Hiroyuki Aoki, Makoto Anryu, and Shinzaburo Ito

Department of Polymer Chemistry, Graduate School of Engineering, Kyoto University, Sakyo-ku, Kyoto 606-8501, Japan

Poly(alkyl methacrylate) is known to form a stable monolayer, and the polymer chain is extremely constrained in a two-dimensional plane. Since the morphology and dynamics of polymer materials are greatly dependent on the entropy for the individual chain, i.e., the degree of freedom, the properties of the polymer in a monolayer are expected to be largely different from those in the bulk state. However, little is known about the polymers in two-dimensional systems. Recently, we have shown that scanning near-field optical microscopy (SNOM) is a versatile tool for investigating the structures of polymer ultra-thin films [1]. In the current study, the conformation of a single polymer chain in two dimensions is discussed with the images taken by SNOM.

Poly(isobutyl methacrylate) (PiBMA) was used as the sample, and the small amount of the isobutyl groups was substituted to perylene in order to observe using the fluorescence SNOM. A monolayer of the mixture of the labeled and unlabeled PiBMAs was deposited on a cover slip by the Langmuir-Blodgett technique. The excitation wavelength was 442 nm and the fluorescence of perylene at 470 – 550 nm was detected.

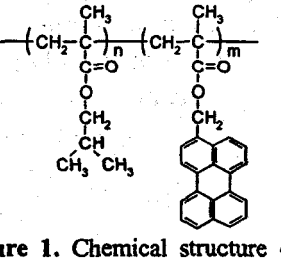

Figure 1. Chemical structure of perylene labeled PiBMA.

The fluorescence SNOM image for single PiBMA chains is shown in Figure 2. The fluorescence intensity from each chain was proportional to molecular weight. The histogram of the intensity was in good agreement with the molecular weight distribution obtained by size exclusion chromatography (SEC). This indicates that the fluorescent spots in the SNOM image are attributed to the individual perylene-labeled PiBMA chains dispersed in the unlabeled polymer monolayer. Comparing the fluorescence intensity histogram with the SEC trace, the molecular weight of each polymer can be determined. The polymer chain with molecular weight of 4.8×10^6, indicated by an arrow in Figure 2, was observed as a circular fluorescence spot with a diameter of 200 nm. This value was similar to the diameter for the ideally collapsed conformation. This indicates that the polymer chain in two dimensions takes a contracted conformation and has no entanglement with the other chains [2].

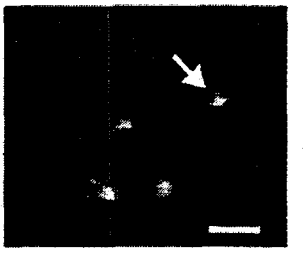

Figure 2. Fluorescence SNOM image of single PiBMA chains. The scale bar indicates 1 μm.

References

[1] (a) H. Aoki, Y. Sakurai, S. Ito, and T. Nakagawa, *J. Phys. Chem. B*, **103**, 10553 (1999); (b) H. Aoki and S. Ito, *J. Phys. Chem. B*, **105**, 4558 (2001).

[2] P. G. de Gennes, *Scaling Concepts in Polymer Physics*, Cornell University Press, Ithaca, New York, 1979.

Phase separation in polyfluorene - polymethylmethacrylate blends studied using UV near-field microscopy

J. Chappell, D.G. Lidzey,
Dept. of Physics & Astronomy, University of Sheffield, Hounsfield Road, Sheffield, S3 7RH, UK

We present ultra-violet near-field microscopy investigations of blends of poly(9,9-dioctylfluorene) [PFO] and polymethylmethacrylate [PMMA]. A scanning near-field optical microscope (SNOM) was employed to study the distribution of blue-emitting PFO in a blend with PMMA. The samples investigated contain between 1%-50% PFO in PMMA and were spin coated onto glass to give films less than 100nm thickness. The films were excited through the SNOM probe with the 352nm line of an argon ion laser and transmission SNOM was used to map the spatial distribution of the PFO fluorescence. We observe phase separation in the shear force images on length scales between 250nm to 2μm which allow us to identify the distribution of the PFO.

The Influence of Local Environment on the Optics of Nanosources and Nanocavities

A. Rahmani, G. W. Bryant,
National Institute of Standards and Technology, Gaithersburg, MD 20899-8423.
P. C. Chaumet,
Institut Fresnel, Faculté des Sciences et Techniques de St Jérôme, F-13397 Marseille cedex 20, France.

The influence of local environment on the optics of nanosources and cavities is crucial in near-field microscopy, nanooptics and optoelectronics and must be modeled accurately. We present a formulation of the coupled dipole method (CDM) that accounts for the effects of environment on local-field corrections.

The CDM has been used to study light scattering by arbitrary objects, near-field microscopy, optical forces, and nanosources, such as atoms, molecules and quantum dots, in cavities. The versatility of the CDM resides in its simplicity. However, typical implementations of the CDM are based on a dipole polarizability that reduces to the Clausius-Mossotti (CM) bulk polarizability in the long wavelength limit. This approach can break down because it relies on the assumption that all dipoles have the same optical response, irrespective of their environment. Near interfaces, one must account for the local environment of each dipole. We present a new formulation of the CDM[1] that is *exact* in the long-wavelength regime by deriving a self-consistent local-field correction that accounts for the particular environment of each dipolar subunit. To illustrate the method we consider a slab. This configuration has an analytic solution that will be a reference. As shown in Fig. 1, the conventional CDM predicts nonphysical oscillations of the field inside the slab that result from the assumption of a bulk local-field correction for each subunit. The new form of the CDM reduces drastically the oscillations of the macroscopic field inside the slab. Reflected and transmitted fields and the convergence of the CDM are improved as well. The new local-field correction is most important at interfaces. In general the new polarizability differs from the CM value only for a few layers near an interface.

We conclude by showing that the CDM can be used to derive the local-field factors for nanosources in arbitrary microcavities[2] and interstitial nanosources[3].

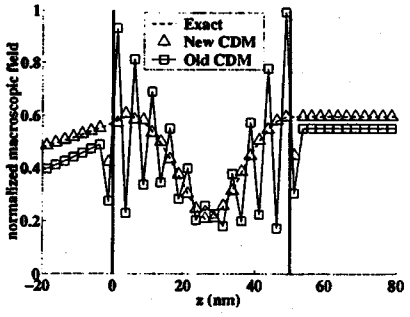

Figure 1: Macroscopic field outside and inside a 50 nm dielectric slab delimited by the vertical lines. A plane wave is incident from the left.

References

[1] A. Rahmani, P. C. Chaumet and G. W. Bryant, *Optics Letters* (submitted).

[2] A. Rahmani and G. W. Bryant, *Phys. Rev. A* **65**, 033817 (2002).

[3] A. Rahmani, P. C. Chaumet and G. W. Bryant, *Optics Letters* **27**, 430 (2002).

Probing the emission pattern of a near-field aperture in three dimensions

M. Wellhöfer, O. Hollricher,
WITec GmbH, Hörvelsinger Weg 6, D-89081 Ulm, Germany.
O. Marti,
University of Ulm, Dept. Exp. Physics, Albert-Einstein-Allee 11, D-89069 Ulm, Germany.

Resolution in near-field optical microscopy is a point of intensive discussion. The maximum resolution in a near-field image is determined by aperture size, probe-sample distance and the sample itself.

We present near-field optical x-y-scans at different tip-sample distances and x-z-scans of a single nanohole in an opaque metal layer. While the detection unit is fixed and focused on the SNOM aperture, the z-position of the sample was sucessively changed by the scanning table of our microscope. The nanoscopic pinhole was used to examine the emission pattern of the aperture probe in three dimensions.

Every line of the x-z-scans represents a cross section through the emission pattern at a different tip-sample distance, while the y-coordinate is fixed at the position of the maximum value of the x-y-profile. Reflection and scattering from the sample surface and the probe metallization produce interference undulations in the approach curve.

To investigate the influence of the tip-sample distance on resolution, every line has been fitted with a gaussian profile function by the Levenberg-Marquardt method. The full width at half maximum value (FWHM) has been determined and shows a linear trend superimposed by oscillations with a period of exactly half of the used wavelength.

Direct Measurement of the Absolute Value of the Interaction Force between a Fiber Probe and a Sample in a Scanning Near-field Optical Microscope

S. K. Sekatskii, G. T. Shubeita, G. Dietler, Institut de Physique de la Matière Condensée Université de Lausanne, BSP, CH 1015 Lausanne – Dorigny, Switzerland

D. A. Lapshin, V. S. Letokhov, Institute of Spectroscopy Russian Academy of Sciences, Troitsk Moscow region 142190 Russia

When closely approaching the surface with a laterally dithered fiber tip of a Scanning Near-field Optical Microscope (SNOM), a decrease in the dither amplitude is observed. This effect is by far the most popular to control the distance between the fiber tip of the microscope and surface of the sample and is often referred to as shear force control. Surprisingly, and despite all its popularity, to the best of our knowledge the absolute values of the shear force have never really been *measured*, so researchers are obliged to rely on model – dependent estimations. This is unsatisfactory both because of the great importance of the question (for example, not to destroy soft and fragile biological samples, the value of the force must be known, low and well controlled) and the fact that the nature of the shear force is still unclear. Here, we present the measurements of the shear force made by means of a reasonably stiff (to avoid the jump to- or out of- contact problems) Atomic Force Microscope (AFM) cantilever. The experiments were performed for the most popular shear force detection methods currently in use: in resonance and out of resonance optical detection, and tuning fork – based detection.

The experimental setup combines a home made SNOM with a home built AFM and is presented in the self – explanatory Fig. 1. The interaction force value is determined from the measured cantilever deflection using the known spring constant. Two components of this force are clearly distinguishable: mainly a static one (this is nothing but the standard signal of the AFM exploited in contact mode) and a component oscillating at the dithering frequency of the tip. The latter was recorded using an additional lock-in amplifier and named "dither force". The main results of our study are the following. 1. For tuning fork – based and optical in-resonance detection, the shear force signal decreases until permanent contact between the fiber and the lever (=sample) is established, after what this signal is no more detected. 2. For optical out-of resonance detection, the shear force signal continues to decrease and is detectable well after permanent contact is established. 3. *Absolute values of the interaction force were measured* for different detection schemes and dither amplitudes a_{dith}. For example, the maximal attainable values of the dither force are 6 nN for tuning-fork-based detection, a_{dith} = 3.5 nm; 13 nN for optical in resonance detection, a_{dith} = 6 nm, and so on. These values are small and much less than the usually neglected static interaction force, which, for the same conditions, was measured to be 100 – 300 nN. 4. The dither force can be sensed as far as 100 nm from the surface due to the long – range electrostatic tip – sample interaction. 5. The width of the shear-force transition (i.e. the change of the tip – sample distance during which all the noticeable changes in the shear force signal occur; this was especially well seen analyzing dither force approach curves) essentially exceeds the value of $a_{dith}.sin\theta$ expected for the fiber having a dither amplitude a_{dith} and tilted by θ with respect to the surface normal. These results and their interpretation will be discussed.

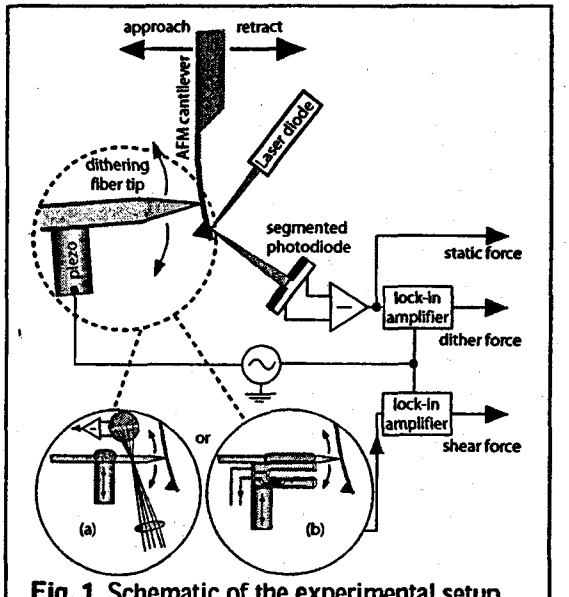

Fig. 1. Schematic of the experimental setup.

Tuning-fork-based apertureless SNOM for visible and infrared studies

Y. De Wilde, F. Formanek, L. Aigouy,
Laboratoire d'Optique, ESPCI - CNRS UPR A0005,
10 rue Vauquelin, 75 005 Paris, France.

Recent studies have shown that sharp apertureless probes can be used to scatter the evanescent field at the sample surface, revealing optical contrast on a subwavelength scale. The main interest of the use of an apertureless probe in a scanning near field optical microscope (SNOM) is that it does not require any waveguiding towards the detector, providing the possibility to perform optical studies at any wavelength. Hence, apertureless SNOMs (aSNOMs) have successfully been used with visible and infrared illumination, producing optical images with a resolution of a few tens of nanometers [1],[2]. Most aSNOMs are based on a metallic tip, which is either a tungsten tip or the metal-coated tip of a commercial AFM cantilever.

Published aSNOM designs use an optical detection to monitor the tip's movement, which requires a secondary laser source, besides that used to excite the evanescent field, and additional optical access. Here, we describe a homemade setup in which the tip's movement is monitored via the piezoelectric signal of a quartz tuning fork. As shown on Fig.1, a tungsten tip is glued on one tine of the tuning fork. The tuning fork is excited close to the resonance by means of a PZT piezoelectric plate, producing an AC voltage whose amplitude is proportional to the tip's vertical displacement. A laser source is focused on the tip at the sample surface. The near-field periodically scattered by the tip is collected by a large numerical aperture objective and focused on the detector, where it is extracted from the far-field background using lock-in detection. The system has been used to investigate near-field optical images of subwavelength holes in a chromium thin film and of a twinned YBCO crystal. Preliminary testing in a liquid environment have also been performed. Results obtained both with a visible (λ=655 nm) and an infrared (λ=10μm) illumination will be presented. As shown on Fig.1c in some cases we achieve a resolution of the order of 20 nm.

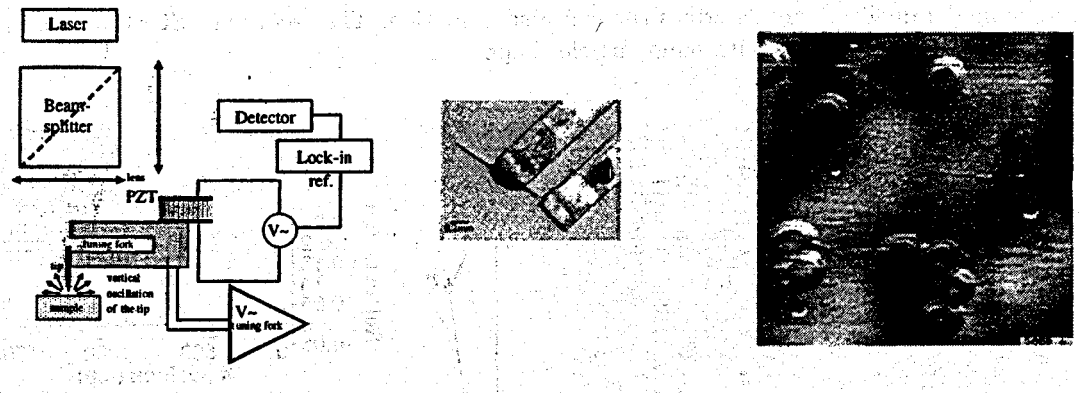

(a) (b) (c)

Figure 1: a) Setup of the tuning-fork-based aSNOM. (b) Image showing the tip mounting on the tuning-fork. c) Near-field optical image (3 μm x 3 μm) of subwavelength holes in a chromium thin film using a 655 nm laser source.

References

[1] R. Bachelot, P. Gleyzes, and A.C. Boccara, *Opt. Lett.* **20**, 1924 (1995). A. Lahrech, R. Bachelot, P. Gleyzes, and A.C. Boccara, *Opt. Lett.*, **21**, 1315 (1996).
[2] B. Knoll and F. Keilmann, *Nature* **399**, 134 (1999).

Phase-sensitive Imaging of Metal Nanoparticles Using an Aperture-type Near-field Microscope

J. Prikulis, H. Xu, L. Gunnarsson, M. Käll, Chalmers University of Technology, Applied Physics, Göteborg, Sweden SE-41296.

H. Olin, Chalmers University of Technology, Experimental Physics, Göteborg, Sweden SE-41296.

We report on the development of an aperture-type near-field scanning optical microscope (NSOM) for phase-sensitive imaging. The NSOM was used to analyze phase properties of localized surface plasmons (SP) in colloidal silver nanoparticles. Nanoparticles and small particle-clusters are imaged as interference patterns, due to far-field superposition of the optical fields emitted from the tip and elastically scattered from the SP.

Fig. 1a and 1b show simultaneously recorded AFM and NSOM images of colloidal Ag particles with average diameter $\approx$ 90 nm. The illumination wavelength was 633 nm. The key observation is that particles with similar height appear with dark or bright central intensity. Fig. 1c shows the optical profile and NSOM image (inset) of a single Ag particle. The optical contrast can be understood from a simple model (fig. 1d). We approximate the NSOM probe with a point source: $E_{tip}(r) \propto \exp\big(i(kr-\omega t)\big)\Big(\frac{A}{kr}+B\exp\big(-r/\eta\big)\Big)$. The constants A and B define the amplitudes of the far-field and near-field contributions, respectively, r is the distance from the light source, k is the wave number, ω is the angular frequency, and η is the near-field decay length. A dipole moment $P = E_{tip}(r)\alpha$ is induced in the particle. The oscillating dipole emits scattered waves $E_s(r_1)$ which superimpose with the far-field emission from the probe. The measured intensity is thus approximately given by: $I \propto \int_0^{\frac{2\pi}{\omega}} \Re\{E_{tip}(\ell)+E_s(r_1)\}^2 dt$ where $\Re$ denotes the real part and ℓ is the distance between the light source and the detector. The phase of the complex nanoparticle polarisability $\alpha = |\alpha|e^{i\phi}$ determines whether the particle appears with a dark or a bright center in the NSOM image, as shown in fig. 1e and 1f.

This simple model qualitatively describes the contrast formation. The recorded NSOM images indicate strong SP coupling phase variation with nanoparticle shape.

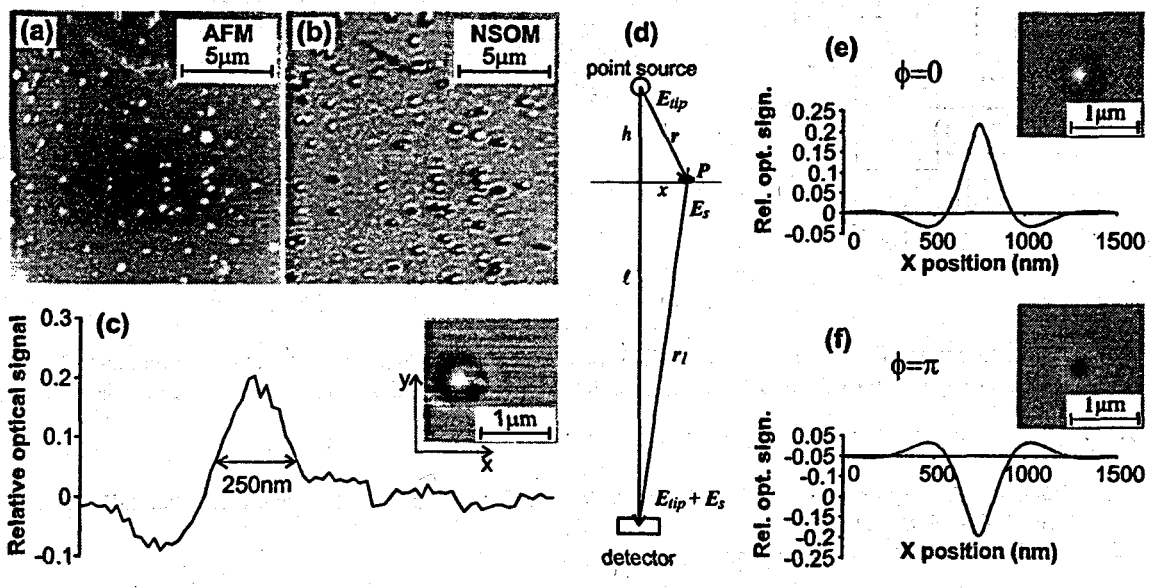

Figure 1: Phase-sensitive near-field imaging of colloidal Ag nanoparticles.

A Versatile Multipurpose Scanning Probe Microscope

E. Cefalì, S. Patanè
Università di Messina, Dipartimento di Fisica MTFA and INFM, Unità di Messina
Salita Sperone 31, I-98166 Messina, Italy
P.G. Gucciardi
CNR - Istituto per i Processi Chimico-Fisici, Sez. di Messina
Via La Farina 237, I-98123, Messina, Italy
M. Labardi, M. Allegrini
Università di Pisa, Dipartimento di Fisica and INFM, Unità di Pisa-Università,
Via F. Buonarroti 2, I-56127 Pisa, Italy

We report on the realization of a multipurpose scanning probe microscope derived from the combination of Scanning Tunneling Microscopy [1], Atomic Force Microscopy [2] and apertureless Scanning Near-Field Optical Microscopy techniques [3,4].

The instrument has been developed starting from a commercial optical microscope (AXIOTECH Vario ZEISS) in order to take advantage of the facilities provided by the framework. The probes are homemade and consist of tungsten tips, produced by means of electrochemical etching. This process, starting from a 50 micron tungsten wire, is able to produce a sharp apical radius of less than 100 nm with a considerable reproducibility degree and low cost. The sample is scanned in tapping mode, stabilizing the tip-surface distance by means of a tuning fork detection system [5]. A solid-state laser source is focused on the tip apex by using a long working distance microscope objective (Nikon 50X plan-apo]. The back-reflected optical signal, providing information about the sample's refractive index, is collected through the camera port of the AXIOTECH Vario and is detected in phase with the tapping frequency by means of lock-in techniques. Simultaneous measurements of the sample's electrical properties can be carried out by biasing the tip with respect to the sample surface, and detecting the current by means of an ultra low noise preamplifier mounted on the sample holder. Once again the signal is detected by means of a lock-in amplifier in phase with the tapping frequency. Test measurements have been performed on homemade sample consisting of Aluminum nanostructures deposited on a Si p-doped substrate [Fig. 1].

The technique results in a non-invasive tool able to image simultaneously the morphology, the optical and electrical properties of the sample. It provides information on the quality of the surfaces by mapping the local optical and electrical properties with a lateral resolution on the nanometer scale.

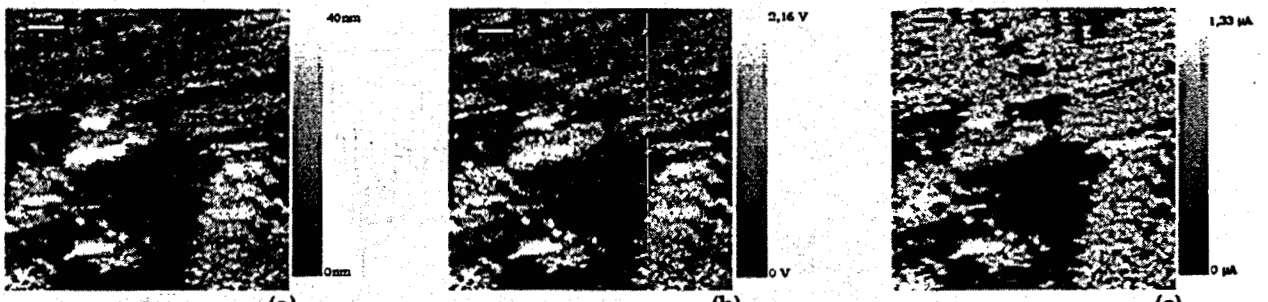

(a) (b) (c)

Fig 1. Topographic (a), optical (b) and current images of a sample showing Al islands on a Si p-doped substrate. The images have been acquired simultaneously within a single scan. Scan area 10 µm × 10 µm; Scale bar = 1 µm.

References

[1] G. Binnig and H. Rohrer, Helv. Phys. Acta **55**, 726 (1982)
[2] G. Binnig, C.F. Quate, and Ch. Gerber, Phys. Rev. Lett. **56**, 930 (1986)
[3] F. Zenhausern, Y. Martin, H.K. Wickramasinghe, Science **269** 1083 (1995)
[4] R. Bachelot, P. Gleyzes, A.C. Boccara, Opt. Lett. **20**, 1924 (1995)
[5] K. Karrai and R.D. Grober, Appl. Phys. Lett. **66**, p. 1842 (1995)

Development of Dual-probe Scanning Near-field Optical Microscope [1]

T. Sigehuzi,
National Institute of Advanced Industrial Science and Technology, Tsukuba, 305-8568 Japan.

We have developed a dual-probe scanning near-field optical microscope – a pair of SNOM probes resting on mutually independent piezoelectric tubes, the tips of which are located within the vicinity of each other (illustrated in Fig. 1) – to observe the spatio-temporal correlations in optical phenomena in the sub-wavelength area. It could also be used to stimulate and observe some unit processes in nano-scale structures, e.g. quantum dots.

Not only in the image resolution but also in the relative positioning of the two probes we must overcome the diffraction limit. We introduced probe-specific wavelength light (633nm and 532nm) into each of the probes and observed the light emitted from its tip using a far-field microscope with a color CCD camera. We identified the position of a probe apex with the center of gravity of the imaged light spot in the corresponding color plane (red or green). The accuracy of this positioning scheme could be made on the nanometer level, since the light wave diffraction dose not change the position of the intensity peak but its dispersion.

In each of the following experiments we kept the relative position of the probe pair constant and drove the samples rather than the probes for scanning, which made the above positioning procedure necessary only occasionally. Except for that we could use the instrument for SNOM measurements. We injected light only into one of the probes for illumination/collection mode imaging, while the other probe collected the near field from this probe-sample system.

We imaged an optical grating surface (1μm period) with this microscope. Basically we got two grating images horizontally shifted by the interprobe distance. In Fig. 1 we show a cross section (single scan signal) of a obtained pair of images. Each of the images, especially one from the collection mode probe, seems to be rather noisy. These "noises" in the two signals, however, are mutually related and contain information about the probes-sample system. Even without any sample the illuminating field will be repeatedly "reflected" between the probe pair, while of course the sample will influence this interaction.

The experimental results will be compared to the three dimensional finite-difference time-domain method calculations.

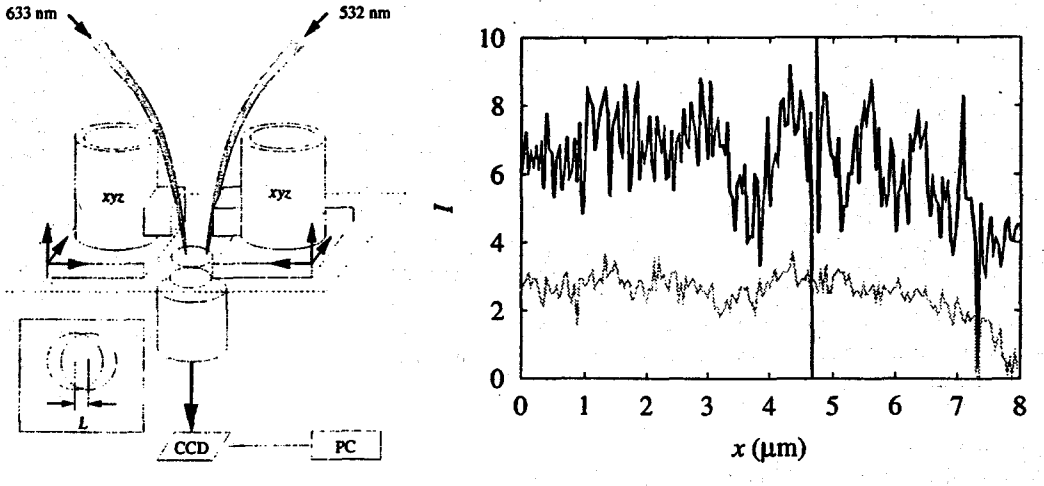

Figure 1: (Left) Schematic picture of the experimental setup. (Right) The intensity cross sections of optical grating images from the two probes, the distance between which is 200 nm. The black line represents the signal from the illumination/collection mode probe, while the gray one corresponds to the collection mode probe.

[1] This study is a part of the "Function Evolution of Materials and Devices based on Electron / Photon Related Phenomena" (FEMD) research project of Core Research for Evolutional Science and Technology (CREST), sponsored by Japan Science and Technology Corporation (JST).

Apertureless near-field optical microscopy of fluorescent sub-micron structures

A. Fragola and L. Aigouy
Laboratoire d'Optique, ESPCI, CNRS UPR A0005,
UPMC, 10 rue Vauquelin, 75005 Paris, France
tel : 33 1 40 79 45 91 - fax : 33 1 43 36 23 95 - e-mail : fragola@optique.espci.fr

Apertureless near-field optical microscopy has proven its efficiency to image objects with a sub-wavelength resolution [1, 2, 3]. In this method, the probe is not an usual optical fiber but a sharp metallic tip, whose extremity scatters the electromagnetic field located on the surface of a structure. This technique has enabled us to study various fluorescent objects such as latex spheres doped with organic molecules and erbium-doped crystals.

Fluorescence images of 200 nanometers latex spheres are displayed in the figures below. Excitation is performed at $\lambda = 488$ nm and fluorescence is detected around $\lambda = 550$ nm. An improvement of the lateral resolution is clearly visible between the far field and the near field image. As it can be seen, the two latex spheres that are very closed to each other are barely separated on the far-field image whereas they are clearly resolved in the near-field optical image. In this case, the apparent lateral resolution is around 100 nanometers.

We will also present results on Erbium-doped vitroceramic. In this case, the excitation process is a two-photon process : excitation is made at $\lambda = 780$ nm and fluorescence is detected around $\lambda = 550$ nm. For all kind of samples, we will show the influence of various experimental parameters like the oscillation amplitude of the tip. Besides, the analysis of approach curves performed on the fluorescent structures will allow us to understand how the fluorescence images are formed with this technique.

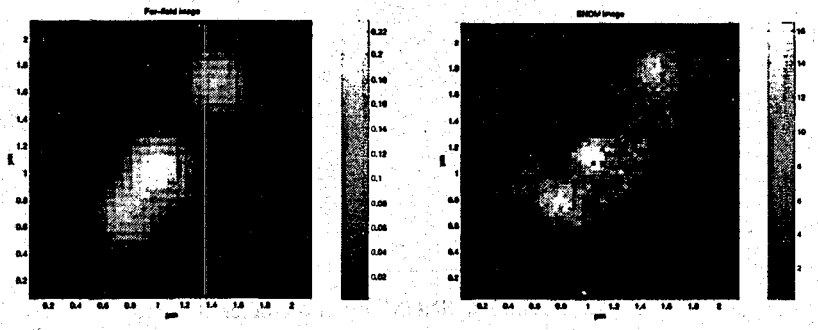

Far-field image Near-field image

References

[1] E. J. Sanchez, L. Novotny and X. S. Xie, *Physical Review Letters* **82**, (1999).

[2] H. F. Hamann, A. Gallagher and D. J. Nesbitt, *Applied Physics Letters* **76**, (2000).

[3] T. J. Yang, G. A. Lessard and S. R. Quake, *Applied Physics Letters* **76**, (2000).

The MagSNOM project

B. Ressel, G. Biasiol, L. Sorba, and M. Lazzarino,*
INFM-TASC Laboratory, Strada Statale 14, km 163.5 Basovizza 34012 Trieste, Italy.

M. Bressanutti, D. Orani, B. Troian, and S. Prato,
A.P.E. Research srl, Strada Statale 14, km 163.5 Basovizza 34012 Trieste, Italy.

Due to the increasing demand of investigating semiconductor devices, we developed a SNOM (Scanning Near Field Optical Microscope) suitable to operate at low temperature (down to 1.4 K) and in presence of magnetic fields (up to 7 T). Main aim of this instrument is to study the optical properties of low dimensionality semiconductor systems, like InAs/GaAs or GaAs/AlGaAs quantum dots.

This project is the result of a collaboration between the INFM, the Italian National Institute for the Physics of Matter, and A.P.E. Research, a company operating in the production and development of SPM microscopes.

In order to fit inside the superconducting magnet, a standard Maglab 2000 from Oxford Instruments, we developed a novel design of SNOM with an overall outer diameter of 29 mm. In figure 1 the prototype of the microscope is shown. The instrument can host 100 mm^2 square samples, up to 8 mm thick. Maximum scan area at RT is 85 μm x 85 μm. The SNOM tip is mounted on an asymmetric piezoelectric sensor in order to control the tip-sample relative position. In this way it is also possible to operate the instrument in non-contact AFM (Atomic Force Microscopy) mode. Moreover an independent optical excitation-collection signal is provided to perform photoluminescence and photoluminescence excitation spectroscopy, in addition to the standard reflection mode.

In order to exploit the capabilities of the instrument, we investigated the optical properties of InAs/GaAs quantum dots in presence of magnetic field.

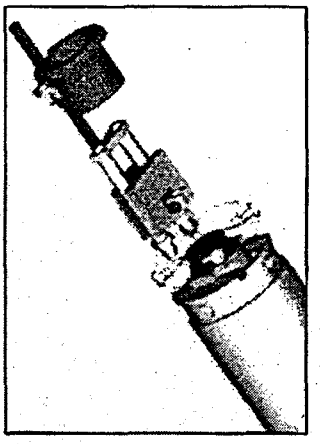

Figure 1: The MagSNOM, outer diameter 29 mm.

also at: "Università di Modena e Reggio Emilia", Via Campi 213/a, 49100 Modena, Italy.

Near-field optical microscopy with a STM metallic tip

A. Barbara, T. López-Rios,
Laboratoire d'Etudes des Propriétés Electroniques des Solides, CNRS, 25 avenue des Martyrs, BP 166, 38042 Grenoble Cedex, France.

We present the first results obtained with a homemade experimental set up. The latter is an apertureless near field optical microscope essentially based on a scanning tunneling microscope (STM) of Besocke type coupled to a laser source and an optical detection system. We use gold tips electrochemically prepared from a $250\mu m$ wire on which a Kr^+ laser is focused. The scattered light is collected by a microscope objective. One part of the tip image, provided from the objectif, is selected by a $150\mu m$ optical fiber connected to a photomultiplier. In order to selectively detect the light diffused by the neighborhood of the tip, a periodic oscillation of the vertical position of the tip is performed, applying to the piezo-tube supporting the tip a $9kHz$ sinusoidal voltage. The scattered light is then synchronously detected. The optical signal, corresponding to the synchronous signal, is about 0.1 percent of the overall scattered light. Good quality images can be realized with a laser power as low as 0.1 mW but powers as high as several hundred of mW can also be used. Optical images providing from the elastic scattering signal are currently obtained, simultaneously with the topographic (STM) images, with a resolution of a few nm and with an optical contrast different from the topographic one, when materials with different dielectric constant are present on the same sample. This is shown in Fig. 1, where gold colloids of typical size $10nm$ were deposited on a flat graphite substrate. The topographic contrast is thus only induced by the colloids (right bottom of the image) and corresponds to an opposite optical contrast.

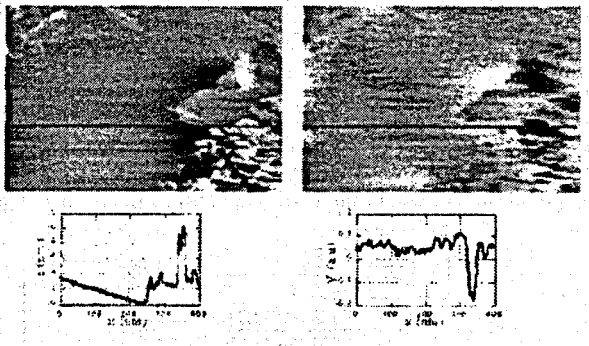

Figure 1: $400 \times 270nm^2$ STM (left) and near-field optical (right) images of gold colloids deposited on HOPG graphite surface showing i) a nanometer resolution of the optical image and ii) an optical contrast between gold and graphite different from the topographic one. Incident laser wavelength is $647.1nm$

The goals of our current research are i) to take advantage of the experimental set-up enabling to achieve nanometer resolutions to perform local spectroscopy analysis at this scale and ii) to understand the physical origins of such high resolutions and the link between the measured scattered field and the electromagnetic interaction existing between the tip and the sample. The on-going experiments aim in determining the optical responses at a nanometric scale. We focus in particular on the possible field amplification in the sub-wavelength metallic cavity formed by the tip and the sample, the behaviour of the optical signal as a function of the incident wavelength and the inelastic scattering. Results on theses experiments will also be presented.

The Apertureless Scanning Near-field Optical Microscope: Transmission and Reflection scattering Geometry

J. J. Wang[1], D. N. Batchelder[1], D. A. Smith[1], J. Kirkham[2], C. Robinson[2], Y. Saito[1], K. Baldwin[1] and B. Bennett[3]

[1]Department of Physics and Astronomy, University of Leeds, Leeds, LS2 9JT, UK; E-Mail: phyjjw@phynov.leeds.ac.uk

[2]Dental Institute, University of Leeds, Leeds, LS2 9JT, UK

[3] Spectroscopy Products Division, Renishaw plc, Wotton-under-Edge, Gloucestershire,UK; E-Mail: bob.bennett@renishaw.com

The scanning near-field optical microscope overcomes the optical diffraction limit by using a nanometer sized local probe to illuminate or to scatter light from the sample. The apertureless approach avoids the technically challenging that manufacture of nanometer sized apertures at the apex of an optical waveguide. Instead a solid probe, which may take the form of a metal wire or an AFM tip, is used as the local probe which interacts with the near-field of the sample. The tip end can be viewed as a collection of dipoles which, interacting locally with the sample surface, are excited by the optical near-field of sample and radiate homogeneous waves which can be detected far from the sample surface using conventional optics. The signal depends on the local optical properties of the sample just beneath the tip end.

By combining a Topometrix Explorer AFM with a Physik Instrumente PI-730.20 XY stage (Resolution ~1 nm) and Renishaw Raman spectrometers, we built an apertureless SNOM setup as show in Figure 1. The RM1000 Raman spectrometer is used to take transmission spectra and enhancement Raman images and RA200 is used to collect reflection spectra for opaque samples studying. Two scan modules - AFM scanning and PI XY stage scanning - can be chose for different purpose. In-house software integrates all of the instruments and permits topographical and either Raman or fluorescence spectra and images to be simultaneously acquired.

The apertureless metallic probes are commercial AFM tips coated with gold or silver by vacuum evaporating or simple mirror reaction [1]. A special designed device which used to transfer 514.5nm laser mode of an argon ion from TEM00 to TEM10 provides the p-polarization along tip axis for near-field enhancement. A tip enhancement Raman spectrum of C60 was measured with this setup. The other samples such as carbon nanotubes and single molecule film will be studied in near future.

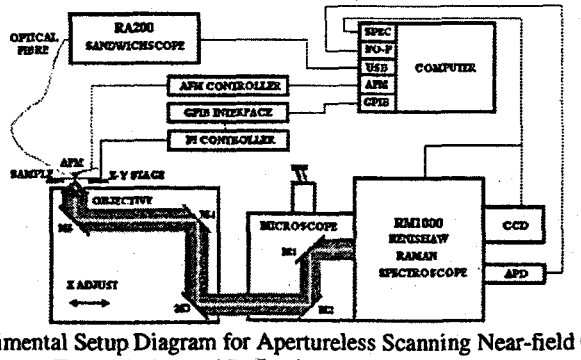

Figure 1: The Experimental Setup Diagram for Apertureless Scanning Near-field Optical Microscope: Transmission and Reflection scattering Geometry

References

[1] Y. Saito, J. J. Wang, D.A. Smith, D.N. Batchelder *LANGMUIR* (2002).(accepted)

The Excitation and The Propagation of Resonant Cylindrical Surface Polaritons

M. N. Libenson, G. A. Martsinovsky,
S. I. Vavilov's State Optical Institute, Saint-Petersburg, Russia.

D. S. Smirnov,
State Institute of Fine Mechanics and Optics, Saint-Petersburg, Russia.

In order to localize an electromagnetic field within a subwavelength area near-field devices typically exploit tapered fiber waveguides or probes that have an output aperture of much smaller size as compared to the light wavelength. Development of new principles for near-field probe design has been crucial for near-field technology progress for the last ten years. Employing surface polaritons gives new opportunity for near-field probe development [1, 2]. This paper considers excitation of cylindrical surface polaritons (CSPs) upon a harmonic grating formed at the surface of two-layer metal cylindrical waveguide in the framework of the approach suggested in [3]. Existence of resonant polariton modes in three-layer waveguide has been also investigated.

The electromagnetic problem of diffraction of incident electromagnetic wave converging to longitudinal axis of a cylindrical waveguide has been analyzed. This analysis has shown existence of field component propagating along the surface of a cylindrical wavegiude. Its amplitude is maximum when the wave numbers of the incident radiation and CSP are equal at a given light frequency. The expression for the transformation coefficient in the case of normal incidence of radiation on the waveguide surface "corrugated" by harmonic grating has been also obtained. This coefficient connects the amplitude of longitudinal component of electric vector of surface wave at the boundary with resulting field of light wave on the surface. The coefficient dispersion with respect to the wave number of surface wave and the frequency has been investigated.

It has been shown that in the case of resonant excitation of CSP the transformation coefficient is limited only by dissipative and radiation losses when of phase synchronism condition is observed. At non-resonant excitation of CSP the wave amplitude is limited and decreases quickly with disarrangement growing. The possibility of significant amplification of light field on surface as a result of CSP's excitation doesn't conflict with any conservation principles. From the one side it's the consequence of coherent energy pumping of 3D wave into CSP at its propagation along resonant grating. From the other side it can be explained by high localization of energy distribution in CSP. Numerical estimations show that in the typical case of resonant grating with height of the ripples about 0.1 of the wavelength the electric fields of CSP and incident wave are equal. As far as efficient transformation of laser light into SEW may take place, this effect can be used for the needs of near field optics.

The propagation parameters and their relation with the medium properties were investigated for surface polaritons excited in coated cylindrical waveguide. It has been shown that in a cylindrical three-layered waveguide with metal core or metal cladding the CSP has no cut-off even when core and cladding radiuses tending to zero. In this case the coefficient of non-dissipative attenuation of the fields is growing infinitely and the CSP (TM_0-mode) can be localized, theoretically, within an arbitrary small space. Existence of two types of polaritons modes with symmetrical and antisymmetrical field distribution has been shown. The conditions for total localization of the near field of the TM_0-mode were determined by numerical simulation for three-layered waveguide with a metal core. The proposed approach for light localization has practical benefits for IR radiation (in particular CO_2-laser radiation) for which the propagation-length of the CSP along probe exceeds 1 – 10 cm and the probes can be fabricated with existing technologies.

References

[1] V. S. Gurevich and M. N. Libenson, *Ultramicroscopy* **57**, 277 (1995).
[2] J. Takahara, S. Yamagishi, H. Taki, A. Morimoto and T. Kobayashi, *Optics Letters* **22**, 475 (1997).
[3] M. N. Libenson, *Soros educational journal* **10**, 92 (1996).

Scanning Near-Field Optical Microscope with a small protrusion probe

Noritaka Yamamoto ,Kazuo Ohtani, and Takashi Hiraga,
Photonics Research Institute, National Institute of Advanced Industrial Science and Technology (AIST)
KANSAI
1-8-31Midorigaoka, Ikeda, Osaka 563-8577, JAPAN.

Near-Field Optical Microscope has been developed to overcome the lateral resolution limit of conventional optical microscope. Although interesting results have been obtained using aperture probes, near-field optics is not sufficiently applied industrial fields. One reason of this may come from the less reproducible production. Recently, some groups made microfabricated probes using microelectromechanical systems (MEMS) technique [1,2], and photoplastic technology [3]. But, many researcher use fiber probe even now, actually.

On the other hand, a small particle or a sharpen tip are used in apertureless SNOM and they have the advantage of resolution [4,5,6]. Practically a scattering center as probe is needs to hold by support body in these approaches unless otherwise used laser manipulation technique. When the probe (scattering center) breaks into evanescent field, bottom of the support body has an effect on the near-field measurements.

In this work, we propose a simple novel probe for SNOM. The probe consists of a small protrusion on optical flat glass surface. Laser beam illuminates it from the backside by total internal reflection angle. The small protrusion combines with the evanescent field and may acts as a sensitive probe. This tip is set on an objective lens, which has high numerical aperture and it is attached by matching oil. Probe-sample distance is controlled by optically. Beginning, we try to use a small Polystyrene sphere on flat substrate as a probe. Tip height is only 500-nm, so it is not allowed a slight inclination of both (tip and sample) substrate. The position between the tip substrate and the sample stage keep to precisely paralleling during approach and scan. In order to resolve this point, we will to design a small sample stage. PZT scanner only has a scan area of 20-30um at most, so the sample stage is enough large at 30umX30um area. Furthermore, it has to point out that low concentration samples, for example single molecule measurements and DNA sample, are difficult to find the objects. For the purpose to save sample and effort, small sample stage is desired. We fabricate a small sample stage from an optical fiber.

References

[1] R.Eckert, J.M.Freyland, H.Gersen, H.Heinzelmann, G.Schurmann, W.Noell, U.Staufer, and N.E.De rooij, J. Microscopy, **202** ,7, 2001.
[2]P.N.Minh, T.Ono, S.Tanaka, and M.Esashi, J.Microscopy. **202**, 28, 2001.
[3]B.J.Kim, J.W.Flamma, E.S.Ten Have, M.F.Garcia-Parajo, N.F.Van Hulst, and J.Bruggerr, J.Microscopy, **202**, 16, 2001.
[4] UC.Fischer and D.W.Pohl, Phys. Rev. Lett. **62**, 458 (1989).
[5]F.Zenhausern, M.P.O'Boyle, and H.K.Wickramasinghe, Appl.Phys. Lett. **65**, 1623 (1994).
[6]T.Kataoka, K.Endo, Y.Oshikane, H.Inoue, K.Inagaki, Y.Mori, H.An, O.Kobayashi, and A.Izumi, Ultramicroscopy, **63**, 219 (1996).

Simultaneous Topographical and Optical Characterization of Near-Field Optical Aperture Probes

C. Höppener, D. Molenda, H. Fuchs, and A. Naber,
Physics Institute, Wilhelm-Klemm-Str. 10, D-48149 Münster, Germany.

The quality of probes for SNOM is normally routinely checked with different, relatively fast characterization methods prior to their use in a near-field optical measurement. The main purpose of a characterization is to obtain a first clue of the optical resolution capability of the probe. For the characterization of aperture type probes, e.g., metal coated tapered optical fibers, the most frequently applied methods are e-beam microscopy and optical far-field measurements of the light transmitted through the aperture. These methods can provide important information and are especially useful for sorting out ill-defined probes. In our experience, however, they are not able to predict the actual optical resolution in a near-field optical experiment. The optical characteristics of the aperture as light source depends strongly on the random structure of the grainy metal film in the direct vicinity of the aperture, so that a reliable statement about the resolution capability is probably only possible by means of a near-field optical characterization technique.

We introduced recently a method for a simultaneous topographical and optical characterization of near-field aperture probes which is based on imaging of small sized fluorescent nanospheres (~20 nm) [1]. As a sample for the characterization, a strongly diluted solution of dyed nanospheres is spread on a smooth glass substrate (< 1 sphere/μm). The fluorescence intensity of the randomly distributed dye molecules contained by a single polystyrene nanosphere corresponds to an equivalent of ~180 fluorescein molecules. The diameter of a nanosphere is much smaller than the typical size of an aperture (~50–100 nm) so that a nanosphere takes on the role of an optical probe which maps the electric field intensity at the end of the SNOM tip. Similar to this, a simultaneously taken force image of a single nanosphere can be interpreted in such a way that the nanosphere acts as a force tip and probes the end face of the SNOM tip. A comparison of optical and height images enables us to assign the aperture to a certain position on the end face of the probe.

We are routinely using this method to control a mechanical modification of aperture fiber probes. By squeezing a probe repeatedly against a smooth glass substrate and thereby removing obstructing protrusions the aperture is brought as close as possible to the sample surface which results in a strongly improved optical resolution. Furthermore, we applied this method for the near-field optical characterization of a new type of probe with a triangular aperture [2].

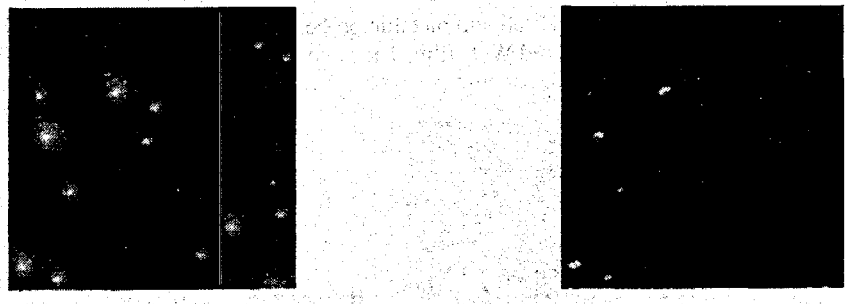

Figure 1: Topographical (left) and near-field fluorescence image (right) of (20±4) nm sized nanospheres taken by means of an aperture probe with a flat end face. Size of images: 3 μm x 3 μm.

References

[1] C. Höppener, D. Molenda, H. Fuchs, and A. Naber, *Appl. Phys. Lett.* 80, 1331 (2002).
[2] D. Molenda, U. C. Fischer, H.-J. Maas, C. Höppener, H. Fuchs, and A. Naber, "Enhanced light confinement in a near-field optical probe with a triangular aperture", this communication.

Current Sensing Scanning Near-Field Optical Microscopy for Nanometer-Scale Observation of Electrochromic Films

F. Iwata, K. Mikage, H. Sakaguchi*,
M. Kitao* and A. Sasaki

Faculty of Engineering, Shizuoka University, Johoku Hamamatsu 432-8561, Japan
Fax: 81-53-478-1072, e-mail: tmfiwat@ipc.shizuoka.ac.jp
*Research Institute of Shizuoka University, Johoku Hamamatsu 432-8011, Japan

A novel scanning near-field optical microscopy (SNOM) capable of point-contact current sensing has been developed to investigate the nanometer-scale electrochromic (EC) behaviors of EC thin film. In order to detect the current and the optical signal at a local point on the surface, a cantilever type metal probe was fabricated. The near-field optical property can be detected by using the local field enhancement effect generated at the edge of the metal probe under p-polarized laser illumination[1]. The current signal can be detected with a high-sensitive current amplifier connected with the metal probe[2]. As the performance of the novel microscope, EC thin films of WO_3 were observed. Using the current sensing SNOM, the surface topography, conductive image and optical distribution of the colored EC thin film were observed (Fig. 1). Nanometer-scale EC properties accompanied with local bleaching behaviors was also investigated using the current-sensing SNOM (Fig. 2).

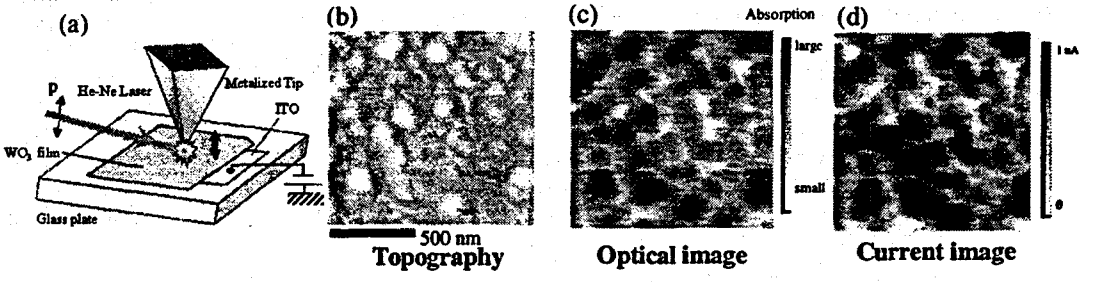

Figure 1 (a) Set up of the EC cell and metallic probe. (b)Topography, (c) optical image and (d)current image of the colored WO_3 film. Those images were obtained, simultaneously.

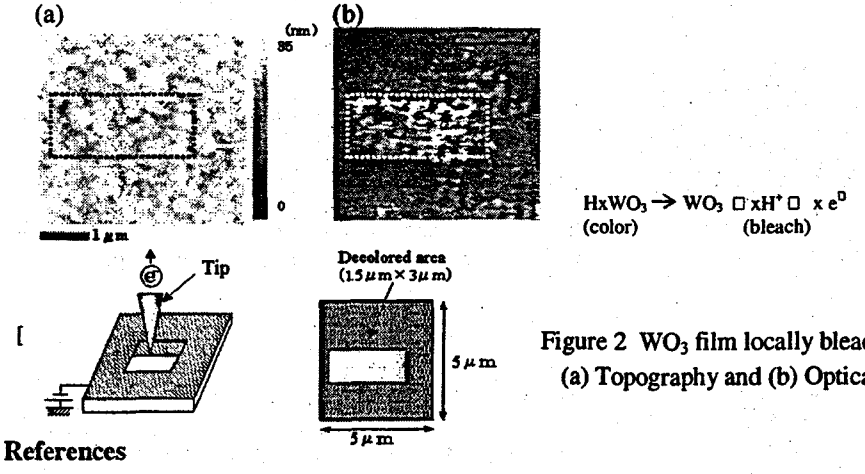

Figure 2 WO_3 film locally bleached with metal probe. (a) Topography and (b) Optical image.

References

[1] Y. Inouye and S. Kawata, *Opt. Lett.*, **19**, 159 (1994).
[2] F. Iwata, D. Someya, H. Sakagchi, Y. Igasaki, M. Kitao, T. Kubo and A. Sasaki, *J. Microscopy*, **202**, 188 (2001).

Design, Fabrication and Characterization of a Diffractive Solid Immersion Lens

Sung Chul Hohng, Jeffrey O. White
University of Illinois, Frederick Seitz Laboratory, Urbana, IL 61801.
Margret Ferstl,
Heinrich-Hertz-Institut für Nachrichtentechnik Berlin GmbH
Einsteinufer 37, 10587 Berlin, Germany

Alexander Pesch, Matthias Burkhardt, and Robert Brunner
Carl Zeiss Jena GmbH, 07745 Jena, Germany

Compared to a tapered optical fiber with a subwavelength aperture, a Solid Immersion Lens (SIL) has the advantage of high light throughput. This is particularly important for applications, e.g., lithography, data storage, and Raman spectroscopy. Up until now, the Solid Immersion Lenses (SIL) described in the literature are either refraction based superspheres (rSIL), or simple hemispheres (hSIL), in which the incident rays propagate through the upper interface without deviation. Here, we report on diffractive Solid Immersion Lenses (dSIL) based on the concentric rings of a Fresnel zone plate. Here, inside the medium the propagation angles of the first order diffracted waves point in the same direction as the incident angles from outside the SIL. Compared to the hSIL and rSIL, dSILs can be lighter in weight and offer more flexibility in the design of the optical system to adapt the SIL to the objective lens.

We realized two types of dSILs. Binary phase elements were fabricated in a highly refracting glass (LaSF35) by direct e-beam writing and successive reactive ion etching (Fig. 1). dSILs with a blazed profile were manufactured in photoresist by holographic lithography. The minimum distance between adjacent zones in the diffracting structure is in the range of one wavelength. Polarization dependencies and phase impacts have to be considered in the design of an optical element with features this small. In comparison to the lithographically realized binary phase grating, the holographic elements have the advantage of high diffraction efficiency. Near-field optical measurements of the point spread function of both types of dSIL will be presented.

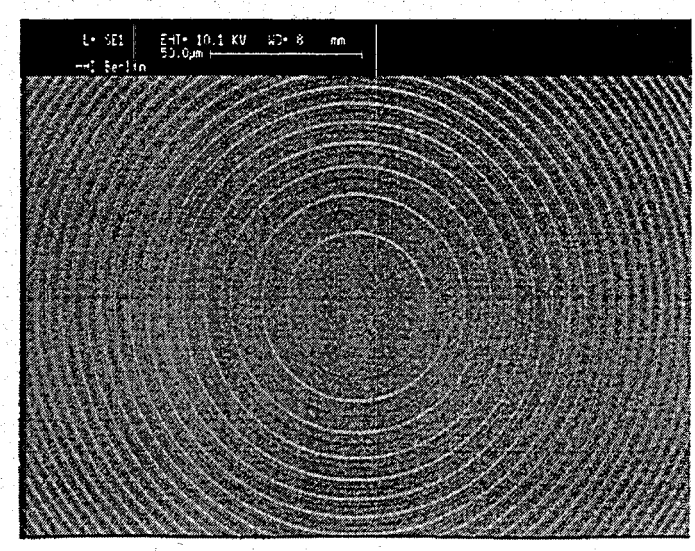

Fig. 1 SEM-picture of a two level dSIL etched into LASF35; the structure depth is 200 nm.

Enhanced Resolution of NSOM by using a Fiber Coupler

Seongjin Chang , Yongho Seo, Wonho Jhe
Seoul National University , Center for Near-field Atom-Photon technology, Seoul Korea .

We have developed several schemes to enhance the resolution of near-field scanning optical microscopy, for example , by using the second harmonic detection or the fiber coupler detection. As an application, we have obtained the optical image of carbon nano tube (CNAT), which has a periodic hole array structure. The hole diameter of CNT is 40nm and the gab between each hole is 100nm. As we mesure the topographical image of CNT as well as the optical image , we can discuss the characteristics of light transmission in such a nanometric structure of CNT.

A tapping-mode tuning fork with a short fiber probe sensing for near-field scanning optical microscopy

Chien Wen Huang, Tsung Sheng Kao, Din Ping Tsai,
Department of Physics, National Taiwan University, Taipei, Taiwan 10617
Pei Wang,
Department of Physics, University of Science and Technology of China, Hefei, Anhui, 230026

Near-field scanning optical microscopy (NSOM) is an instrument that can provide a detailed view of the optical fields and topography of materials with high spatial resolution beyond the diffraction limits. NSOM are widely used in nanometer technology, biological technology, high density optical storage and measurements of local spectrum, photonic devices, etc. A typical NSOM uses a fiber probe to form a point light source, and shear force or tapping-mode tuning fork force feedback to keep the probe in proximity with the sample's surface. At fist, tuning fork with a fiber probe must own stable and high Q at tapping frequency of the tuning fork, the NSOM can work well.

In this paper, a tapping-mode tuning fork with a short fiber probe sensing for near-field scanning optical microscopy is reported. The method is demonstrated that how to fabricate the short fiber probe. A schematic of our tapping-mode tuning fork with a short fiber probe setup is shown in Fig. 1 (a). First a short near-field optical fiber probe was fixed on one tine of the tuning fork , then we glue a multi-mode fiber on another tine of tuning fork to receive the light signal which are from the short probe, there is a very sma ll split between the short fiber and multi-mode fiber, they are non-contacted. All these were performed under optical microscopy. This type tapping-mode tuning fork with a short fiber probe can provide stable and high Q at tapping frequency of the tuning fork as shown in figure 1 (b), and give high quality NSOM and AFM images.

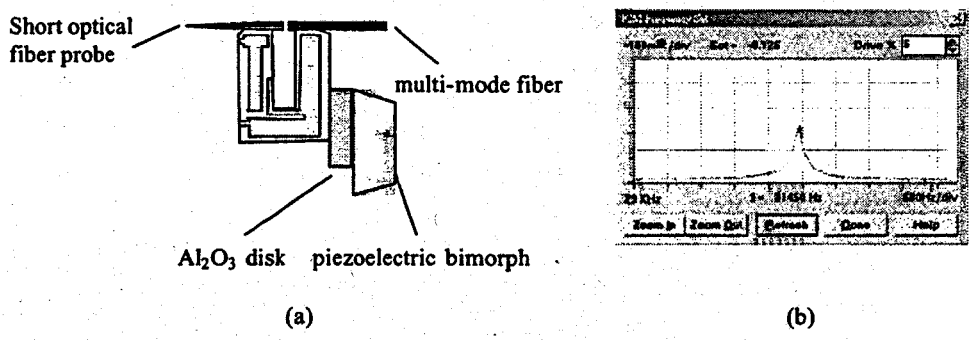

Figure 1: (a) schematic construction of the tapping-mode tuning fork with a short fiber probe, (b) the tapping frequency and amplitude of the fork of figure 1(a) stucture.

References

[1] Din Ping Tsai and Yuan Ying Lu, *Apply Physics Letters* 73, 2724 (1998)

Nanoparticles for Use in Förster Transfer Microscopy

S.C. Hohng, J.O. White, J.M. Therrien, M. Nayfeh, I. Rasnik, B. Stevens, T. Ha,
University of Illinois, Frederick Seitz Laboratory and Dept. of Physics, Urbana, IL 61801

Förster transfer microscopy (FTM) relies on non-radiative energy transfer between a probe containing a donor and a sample containing an acceptor, or vice versa. The short range interaction has the potential to yield a spatial resolution of 5-10 nm. Acceptors and donors consisting of semiconductor or metallic nanoparticles have the advantage of being less susceptible to bleaching and blinking than dye molecules. We have recently developed a technique for fabricating 1-nm silicon nanoparticles with excellent size uniformity and fluorescence efficiency.[1] Chemically-synthesized, high quantum yield, CdSe nanoparticles of diameter 4-8 nm are also excellent candidates.[2] We will present results on the characterization of both types of nanoparticle, including quantum efficiency and lifetime. Recent progress in the development of a cantilever-based NSOM probe incorporating such particles will also be presented. This probe is particularly well suited to studying samples under water, e.g. living cells.

References

[1] M.H. Nayfeh, N. Barry, J. Therrien, O. Akacir, E. Gratton, and G. Belamoin, *Appl. Phys. Lett.* **78**, 1131 (2001).

[2] X. Peng, M.C. Schlamp, A.V. Kadavanich, A.P. Alivisatos, *J. Am. Chem. Soc.* **119**, 7019 (1997).

Fabrication of Si_3N_4 Film Covered Si Planar Near-field Optical Probe: A Nano-*slide* Integrated Nano-*probe*

Sang-Youp Yim, Moongoo Choi, Seung-Han Park,
Department of Physics, Yonsei University, Seoul 120-749, Korea.

The near-field optical probe is the heart of the near-field scanning optical microscopy (NSOM). A number of probes have been developed and adopted, although the metal coated tapered optical fiber tip, fabricated either by pulling or etching process, is the most commonly used probe in the NSOM imaging [1]. Each probe, including the tapered optical fiber tip, exhibits specific advantages that may enlarge the capabilities of NSOM. However, the need of complicate distance regulation system makes most of the probes difficult to be employed for the study of nanostructure materials in low temperature environment and device applications.

We designed a new type of near-field optical probe for the nanostructure material studies, accessible by standard photolithographic techniques. A few tens of nanometer thick film, covered on the nano aperture, acts as a 'slide (glass)' for the samples. The fabrication of the nano-*slide* integrated nano-*probe* was made possible due to the Si anisotropic etching characteristics and the Si_3N_4 film deposition during the Si processing. Because {111} planes of Si serve as etch stops, the width of an etched {100} plane decreases along depth, forming an inverted pyramid [2]. Subwavelength apertures may be formed routinely by means of standard photolithography techniques with properly selected mask [3].

To reduce photolithographic errors, as narrow as 15 μm thick (100) Si layer of SOI (Silicon On Insulator) wafer was prepared. On the both sides, PECVD Si_3N_4 layers were deposited, which the upper Si_3N_4 layer was used as a mask film, and the lower one, 30nm thickness, was preserved to be the nano-*slide*. Patterning on the mask film was processed by photolithography, and subsequently the Si layer was dipped into a KOH aqueous solution.

As shown in Fig. 1, a 300nm width nano-*slide* integrated nano-*probe* and Au particles placed on top of the nano-*slide* were imaged by scanning electron microscopy (SEM). It is clearly shown that the nano-*slide* serves as a supporting base for the few tens of nm diameter Au particles.

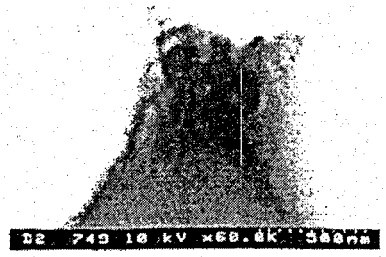

Figure 1: Au particle coated nano-*slide* integrated nano-*probe* (SEM image).

References

[1] E. Betzig, J. K. Trautman, T. D. Harris, J. S. Weiner and R. L. Kostelak, *Science* **251**, 1468 (1991).
[2] H. Seidel, L. Csepregi, A. Heuberger and H. Baumgärtel, *J. Electrochem. Soc.* **137**, 3612 (1990).
[3] M. B. Lee, M. Kourogi, T. Yatsui, K. Tsutsui, N. Atoda and M. Ohtsu, *Appl. Opt.* **38**, 3566 (1999).

Novel design of a low temperature scanning near-field optical microscope using a parabolic mirror

P. Anger, A. Feltz, T. Berghaus
OMICRON Nanotechnology,
65232 Taunusstein, Germany
A.J. Meixner
Physikalische Chemie, Universität Sie gen,
57068 Siegen, Germany

Starting with a design of a low temperature confocal microscope using a parabolic mirror with high numerical aperture as focusing element [1], a scanning near-field optical microscope was developed. The system consists of an UHV-chamber, a lift and a helium bath cryostat for variable temperatures (300 K – 8.5 K). The head of the microscope, which is inserted in the cryostat is built up completely nonmagnetic and can be used in a magnetic environment. The sample is illuminated with an aperture fiber tip. For controlling the tip - sample surface distance, a new shear force based sensor was designed. The optical emission generated at the surface is collected by the mirror and reflected out of the cryostat. This radiation can either be spectrally analyzed or focused on a photodetector (avalanche photo diode). Both, the sample and the fiber tip module can be changed without breaking the vacuum or heating up the microscope. For scanning the sample a UHV compatible and nonmagnetic x, y, z-scanning stage was developed in cooperation with PI (Physikinstrumente GmbH, Waldbronn, Germany). The scanning stage consists of a compact setup with a scan range of 25 μm × 25 μm × 2 μm at 6 K. The three axes of the stage are linearized with capacitive sensors. For the positioning of the sample, coarse motors for use in UHV and under magnetic conditions were designed. First near-field optical investigations of surface-enhanced resonance Raman scattering (SERRS) of rhodamine 6G on Ag-colloids at several temperatures down to 8.5 K will be presented.

References

[1] A. Drechsler, M. A. Lieb, C. Debus, and A.J. Meixner, *Optics Express* **9**, 637 (2001).

Active and passive photonic devices studied by near-field scanning optical microscopy

Chien Wen Huang, Tsung Sheng Kao, Din Ping Tsai

Department of Physics, National Taiwan University, Taipei, Taiwan 10617

Pei Wang

Department of Physics, University of Science and Technology of China, Hefei, Anhui, 230026

The active and passive photonic devices are widely used in optical switches, transceivers, modulators, signal processors, and arrays of laser sources in the optical communication. Small size and high integration of the photonic devices are the current trend. Imaging and measurements of these photonic devices are the important tasks to characterize the functions, and to understand the details of structure problem during the fabrication processes. Near-field scanning optical microscopy (NSOM) can provide a detailed view of the optical fields and topography of photonic devices with high spatial resolution beyond the diffraction limit. The measured light intensity distributions can be an important clue for the comparison and evaluation of the theoretical modeling to improve the design and process of these devices.

In this paper, we present results of a tapping-mode tuning fork with a short fiber probe sensing for near-field scanning optical microscopy measurements performed on single mode fiber (Newport, FSV), 8 channels silica waveguide and multiquantum-well semiconductor diode lasers. The tapping-mode tuning fork with a short fiber probe was used for stable and high Q at tapping frequency of the tuning fork, and provide high quality NSOM and AFM images of active and passive photonic devices. The optical intensity distributions at the endface of single mode fiber, 8 channels silica waveguide and multiquantum-well semiconductor diode lasers have been measured. Useful near-field information were used to understand and characterize these novel photonic devices. Figure 1 shows an example of the NSOM and AFM images at the endface of one of the 8 channel silica waveguide.

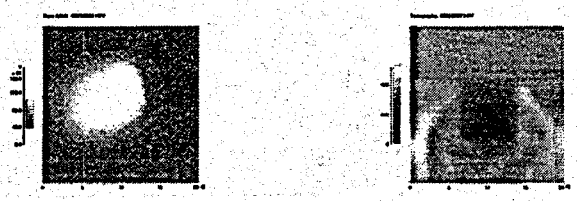

(a) (b)

Figure 1: (a) 20um x 20um NSOM image, (b) AFM image of the endface of one of the 8 silica channel waveguide.

References

[1] D. P. Tsai, Y. L. Chung, A. Othonos, Optical and Quantum Electronics **28**, 1563 (1996).

[2] D. P. Tsai, W. K. Li, J. Vac. Sci. Technol. A **15**, 1427 (1997).

[3] D. P. Tsai, C. W. Yang, S. Z. Lo, H. E. Jackson, Appl. Phys. Lett. **75**, 1039 (1999).

[4] N. H. Lu, D. P. Tsai, C. S. Chang, T. T. Tsong, Appl. Phys. Lett. **74**, 2746 (1999).

[5] S. H. Chen, D. P. Tsai, Y. F. Chen, P. M. Ong, Rev. Sci. Instrum. **70**, 4463 (1999).

Mapping of the longitudinal component responsible for the field enhancement

A. Bouhelier, M. Beversluis, and L. Novotny,
University of Rochester, The Institute of Optics, Rochester, NY 14627.

It was suggested that longitudinal field components, created by a tightly focused higher-order laser mode, provide favorable conditions for creating a local field enhancement at the end of a sharp metal tip [1]. Understanding how the field responsible for this enhancement effect is distributed at the interface is therefore important. We demonstrate an experimental method to map the spatial distribution of such on-axis fields.

We show that information on the spatial field distribution can be obtained by detecting the light scattered from the tip while it is scanned through a laser focus. We investigate laser focii of two different modes: the fundamental Gaussian mode HG_{00} and the Hermite-Gaussian mode HG_{10}. We find that no matter what the material of the tip is, the scattered signal provides information about the on-axis component of the electric field (longitudinal field). For a gold tip, the regions with strong longitudinal field yield a strong scattering signal. However, by replacing the gold tip with a glass tip we observe contrast reversal, i.e. regions with strong longitudinal field attenuate the scattering signal. We compare these experimental findings with calculated images of the field distribution and explain the origin of the observed contrast reversal.

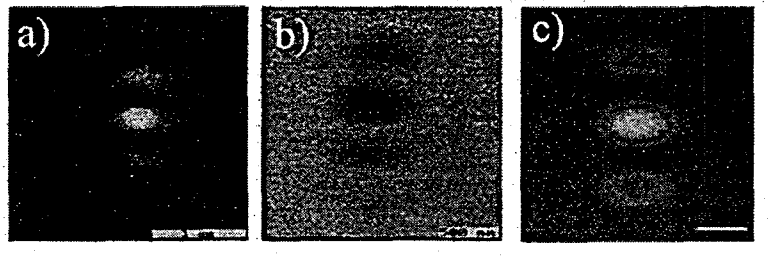

Figure 1: Spatial field distribution of the longitudinal field created in the focus of a Hermite-Gaussian HG_{10} mode. (a) Probed by a gold tip and (b) probed by a glass tip. (c) represents the calculated pattern of the longitudinal field at the glass/air interface. Scale bar: 500nm

References

[1] L. Novotny, E. J. Sànchez, and X. Sunney Xie, *Ultramicroscopy* **71**, 21 (1998).

Optical transmission through sub-wavelength metallic gratings

*P. Quémerais, A. Barbara, E. Bustarret, T. Lopez-Rios and T. Fournier**

*LEPES and *CRTBT*
Centre National de la Recherche Scientifique
BP 166X, 38042 Grenoble Cedex 9, France.

We present experimental evidence in the 1.5 to 7 μm spectroscopic range for an enhanced resonant optical transmission through metallic gratings of period 1.75 μm with 0.6 μm-wide rectangular slits. Such high-aspect ratio structures were obtained by e-beam lithography of a 1 μm-thick SiO_2 film deposited on a silicon substrate and by subsequent oblique incidence evaporation of Ti and then Au, the thickness of the Au layer remaining superior to the skin depth in that spectroscopic range.

By comparing the experimental results at normal incidence spectrum (see fig.1) to appropriate calculations using the modal approach, we show that the transmission can be attributed to the existence of a non-vanishing field at the mouth of the groove. This situation was obtained either when a resonant waveguide mode was excited in the rectangular cavity or when the field was large enough above the slit, in particular close to surface plasmon excitation conditions. The corresponding 2D-maps of the near-field intensity in air and in the silicon substrate showed that coupling between plasmons on both sides of the grating was not necessary to observe an enhanced transmission [1].

After presenting and discussing in terms of the same EM modes the additional evidence provided by polarized transmission measurements performed at oblique incidence on these metallic microstructures, we make some concluding remarks about the fundamental difference between transmission though such 1D array of slits and a periodic 2D array of holes as measured by Ebbesen in Ref. [2].

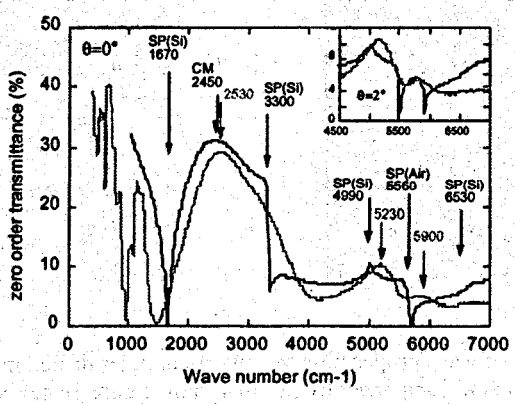

Figure 1: Experimental and calculated zero-order transmittance at normal incidence with features associated to surface plasmons (SP) and cavity modes (CM). Insert : same spectra for a 2° incidence.

References

[1] A. Barbara, P. Quémerais, E. Bustarret, T. Lopez-Rios, submitted for publication.
[2] T.W. Ebbesen, H.J. Lezec, H.F. Ghaemi, T. Thio, P.A. Wolff, *Nature* **391**, 667 (1998).

Coupling waveguides to planar photonic crystals : FDTD modeling and near-field probing

F. Lacour, M. Spajer, A. Sabac
Université de Franche-Comté, Laboratoire d'Optique P. M. Duffieux
UMR 6603 CNRS – 25030 Besançon cedex - France

We report experimental results and theoretical analysis of a system composed by two strip loaded waveguides coupled by an array of holes drilled between them. This array can be described as planar photonic crystal. The validity of such structures as a bandpass filter has been demonstrated in a recent work [1].

Because of the confinement of optical field in such photonic devices, one of the more efficient way to characterize them experimentally is to use near-field microscopy as shown in other works ([2], [3]). A stand-alone near-field scanning optical microscope is used to ease the probing of evanescent light at the surface of the structure without misalignment of the injection into the waveguides. Different wavelengths of injected light are delivered by a Titanium-Sapphire laser in the range 700 - 950 nm.

The waveguide is a multilayer structure (SiO_2 / $SiON$ / SiO_2) deposited by PECVD method on silicon substrate. PECVD deposition provides good control of the thickness and refractive index of the layers. The rib is then structured on the cladding layer (SiO_2) using RIE method. Focused Ion Beam ensures a periodic etching in the interval of two waveguides. The efficiency of light transfer is studied experimentally as a function of the period of array, the diameter, the depth and the shape of holes.

The use of modern simulation methods (BPM and FDTD) have afforded the analysis of each elements of the structure (waveguides and hole matrix, see Fig. 1) to find appropriate parameters. Different structures have been plahed like simple holes array or resonating photonic devices to increase coupling efficiency.

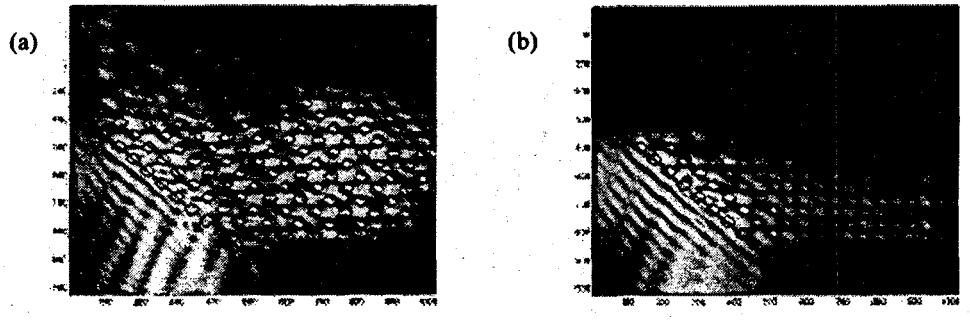

Figure 1: 2D FDTD simulation of wave propagation in a matrix of holes drilled in the proximity of a waveguide. Hole size 300 nm. Component Ey (normal to the figure plane) is represented. Influence of wavelength : (a) l = 760nm (b) : l = 810nm.

References

[1] D. Mulin, C. Girard, G. Colas des Francs, M. Spajer and D. Courjon, *Journal of Microsopy* **202** (2000).
[2] M. L. M. Balestreri, D. J. W. Klunder, F. C. Blum, A. Driessen, H. W. J. M. Hoekstra, J. P. Korterik, L. Kuipers and N. F. van Hulst , *Optic Letters* **24**, 24 (1999).
[3] D. Gérard, L. Berguiga, F. de Fornel, L. Salomon, C. Seassal, X. Letartre, P. Rojo-Romeo and P. Viktorovitch, *Optics letters* **27**, 3 (2002).

A new structure for enhanced transmission through a 2D metallic grating

*Fadi Baida, Daniel Van Labeke**
Institut des Microtechniques de Franche Comté
Laboratoire d'Optique P.M. Duffieux
Université de Franche Comté
CNRS, UMR 6603
Route de Gray, 25030 Besançon Cedex, France

**Email :daniel.vanlabeke@univ-fcomte.fr*

The aim of our communication is to show that the light transmission through arranged nanostructures can be largely increased compared to what was observed three years ago by Ebbesen et al. [1]. FDTD-3D simulation were performed in order to obtain the spectral response of a metallic periodic structure in the visible domain. We have tested our code by studying published examples of enhanced transmission [2]. The results obtained by Ebbesen et al. with gold metallic structure are also confirmed [3]. A new design is suggested in order to enhance the light transmission. The grating structure is modified by filling the central region of each hole with a concentric cylinder of smaller diameter. The grating now consists of a periodic array of coaxial cylinders. Theoretical simulations were performed with a sub-wavelength silver grating made with submicronic annular apertures. The grating is illuminated in normal incidence with a linearly polarized pulsed plane wave. The mean wavelength is 600nm and the pulse temporal width is adjusted in order to cover all the visible spectrum. It is shown that the transmission efficiency of the coaxial grating can reach 80%. An interpretation of this extraordinary transmission will be suggested and clarified by near-field images. A quantitative study of the influence of grating parameters on the transmission spectrum will be presented.

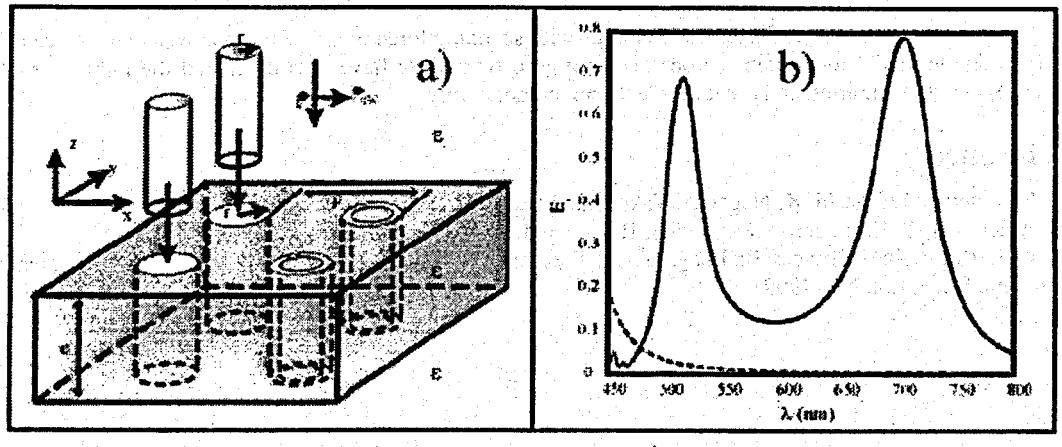

Figure: (a) schematic of the proposed structure. (b) Spectrum of zero order transmission efficiency. Solid line: annular aperture array. Dashed line: circular aperture array

References

[1] T.W. Ebbesen et al., Nature, 391 pp667-669 (1998).
[2] S. Astilean, Ph. Lalanne and M. Palamaru, Optics Commun. 175 pp265-273 (2000).
[3] A. Krishnan et al. Optics Commun. 200 pp1-7 (2001).

Anisotropic lateral resolution in external reflection and collection mode optical scanning probe microscopy

B. Levine, C. Caumont, W.S. Bacsa,
Laboratoire Physique des Solides, Université Paul Sabatier, 31062 Toulouse, France
B. Dwir,
Department of Physics, IMO, EPFL CH-1015 Lausanne. Switzerland

We use the external reflection collection mode which is characterized by the overlap zone of an incident, a reflected and a scattered beam from the surface topography [1-3] to image lithographic micro-gratings. While the asymmetric configuration helps to circumvent aperture limitations, interference of incident and reflected beams in the overlap zone (Wiener fringes) is used to orient the image plane with respect to the substrate and to select the region of interest at large distances from the surface. The fringe pattern of the incident field with the scattered field from a single sub-wavelength particle is used to estimate the probe-sample distance.

We have recorded constant height images of micro-gratings created by electron beam lithography where we have observed asymmetric lateral resolution in the direct image, a superimposed indirect image (due to the finite size of the grating structure and coherence of the scattered light) and a displaced shadow image. We have attributed these effects to the finite penetration depth of the incident beam. This indicates that the recorded two-dimensional image contains depth or three-dimensional information, which can be exploited by systematic imaging at different heights.

We have compared our experimental findings with scanning force microscopy images and have used an analytic dipole model to explain the observed fringe patterns. We have thus estimated the image sample distance, image orientation and the local electronic polarizability.

References

[1] N. Umeda, Y.Hagashi, K. Nagai, A. Takayanagi, Appl. Opt. 31 (1992) 4515
[2] A. Kramer, T. Hartmann, S.M. Stadler, R. Guckenberger, Ultramicroscopy 61 (1995) 191
[3] W.S. Bacsa, in Advances In Imaging and Electron Physics by P.W. Hawkes, Vol. 110 Chapter 1, Academic Press, London (1999)

Near-field Optical Transmission of Surface Polaritonic Crystals

A. V. Zayats,
School of Mathematics and Physics, The Queen's University of Belfast, BT7 1NN, United Kingdom.
L. Salomon, F. de Fornel,
Laboratoire de Physique de l'Université de Bourgogne, CNRS UPR 5027, B. P. 47870-21078, Dijon Cedex, France.

Current progress in photonics requires novel approaches to light manipulation on the nanoscale. One of the promising approaches is based on photonic crystals allowing to control dispersion and propagation of light. In analogy to photonic crystals for light waves, polaritonic crystals for surface plasmon polaritons (SPPs) can be created using periodically nanostructured metal films. Nanostructuring modifies not only in-plane properties of SPPs but also conventional optical properties of a metal film such as reflection and transmission. One of the prominent examples of this effect is the so-called "extraordinary" enhancement of the optical transmission of a periodic hole array in a metal film [1, 2].

Here we shall discuss the mechanisms of the enhanced optical transmission through periodically nanostructured metal films due to resonant light tunnelling via states of surface polaritonic crystals formed on the metal film interfaces [2]. The optical properties of such nanostructured films are governed mainly by in-plane surface polariton behaviour on a periodic two-dimensional surface structure.

The SPPs propagation on a periodic structure results in the changes of the SPP dispersion relations due to the interaction with the structure. This interaction leads to scattering of SPPs in SPPs as well as to scattering of SPPs in light. The latter process results in the appearance of transmitted light. The former process followed by the multiple SPP beam interference leads to the formation of the SPP band-gap and SPP Bloch waves on a periodic structure. Only surface polaritons satisfying the Bloch wave condition can be excited and subsequently contribute to transmission. The role of the periodic surface structure is three-fold, namely, (i) excitation of surface polaritons, (ii) polaritonic crystal selecting the wavelength of SPPs which are allowed to propagate on a periodic structure, and at the same time, (iii) scattering of SPPs into bulk waves that gives rise to transmitted light. As at different wavelengths the surface polariton Bloch waves propagate in different directions, the transmitted light intensity above the surface exhibits specific near-field distributions depending on the orientation of the surface scatterers with respect to the SPP Bloch wave propagation. The variation of the structure periodicity leads to the changes of the SPP resonant conditions and thus modification of the enhanced transmission spectrum. The scatterer size has smaller effect on the spectrum as it influences the resonant conditions indirectly via the efficiency of SPP scattering.

Periodically nanostructured metal films provide a possibility to efficiently control the spectrum and intensity of optical transmission and can find numerous applications in novel photonic and optoelectronic devices.

References

[1] T. W. Ebbesen, J. Lezec, H. F. Ghaemi, T. Thio and P. A. Wolff, *Nature* **391**, 667 (1998).

[2] L. Salomon, F. Grillot, F. de Fornel and A. V. Zayats, *Phys. Rev. Lett.* **86**, 1110 (2001).

[3] L. Salomon, G. Bassou, J. P. Dufour, F. de Fornel and A. V. Zayats, *Phys. Rev. B* **65**, 125409 (2002).

Probing highly confined optical fields in the focal region of a high NA parabolic mirror with sub-wavelength spatial resolution

C. Debus, M. A. Lieb, A. Drechsler, S. Vierbücher and A. J. Meixner,
Physikalische Chemie, Universität Siegen,
57068 Siegen, Germany

Parabolic mirrors with a high numerical aperture can be conveniently used to produce highly confined optical fields in the focal region[1]. Furthermore, these fields can have interesting polarization behavior due to the high numerical aperture. In particular, if the mirror is illuminated with a size matched radially polarized or azimuthally polarized doughnut mode, the electric field has in the focal region almost exclusively a longitudinal or a transverse polarization component. Such field distributions are interesting for application in confocal or near-field optical microscopy [2,3].

Here we present experimental results where we have probed some of these field distributions by raster scanning a very fine gold tip in nanometer steps through the focal region and compare the results with vector-field calculations.

References

[1] M.A. Lieb and A. J. Meixner, Opt. Express **8**, 458 (2001).
[2] A. Drechsler, M. A. Lieb, C. Debus, and A.J. Meixner, Opt. Express **9**, 637 (2001).
[3] L. Novotny, M.R. Beversluis, K.S. Youngworth, and T.G. Brown, Phys. Rev. Lett. **86**, 5251 (2001).

Author Index

List of Participants

Mathew Ackland
University of Wales Swansea, Dept. of Physics, Singleton Park, Swansea, West Glamorgan, UK SA2 295402
156108@swan.ac.uk

Laurie Aeschimann
Institute Of Microtechnology, University of Neuchatel, Jaquet-Droz 1, CH-2007, Neuchatel, Switzerland
laure@aeschimann@unine.ch

Lydia Alvarez
Instituto de Ingenieria, Blvd. Bentio Juarez esq. Calle de la Normal, Meicali, Baja California, Mexico
lydia@iing.mxl.uabc.mx

Eric Ammann
Nanonics Imaging Ltd., Manhat Technology Park, Malacha, Jerusalem 914877, Israel
info@nanonics.co.il

Neil Anderson
Institute of Optics, University of Rochester, Rochester, NY, 14627, USA
neanders@optics.rochester.edu

Steven Anlage
University of Maryland, MRSEC and CSR, Physics Department, College Park, MD, 20742-4111, USA
anlage@squid.umd.edu

Hiroyuki Aoki
Department of Polymer Chemistry, Kyoto University, Yoshida Honmachi, Sakyo, Kyoto 606-8501, Japan
aoki@polym.kyoto-u.ac.jp

Sebastien Aubert
University of Technology of Troyes, 12, rue Marie Curie B.P. 2060, 10 000 Troyes, France
sebastien.aubert@utt.fr

Aude Barbara
CNRS-LEPES, 25 abenue des Martyrs BP 166, 38042 Genoble Cedex 9, France
abarbara@labs.polycnrs-gre.fr

Christof Bartels
University of Konstanz, Universitaetsstr. 10, Konstanz, Baden-Wurttemberg, Germany
christof.bartels@uni-konstanz.de

Alpan Bek
Max-Planck-Institut fur FestKorperforschung, Heisenbergstrasse 1, 70569, Stuttgart, Germany
bek@fkf.mpg.de

Michael Beversluis
Institute of Optics, University of Rochester, Rochester, NY, 14627, USA
beversmr@optics.rochester.edu

Robert Bloksberg Fireovid
NIST- Advanced Technology Program, 100 Bureau Drive MS 4730, Gaithersburg, MD, 20899-3571, USA
robert.b-f@nist.gov

Sergey Bozhevolnyi
Institute of Physics, AAU, Pontoppidanstraede 103, DK-9220, Aalborg Ost, Denmark
sergey@physics.auc.dk

Alexandre Bouhelier.
Institute of Optics, University of Rochester, Rochester, NY, 14627, USA
bouhelie@optics.rochester.edu

William Brocklesby
University of Southhampton, Optoelectronics Research Centre, Southhampton, Hampshire, England
wsb@orc.soton.ac.uk

Jacob Broe
Institute of Physics, Aalborg University, Pontoppidanstraede 103, DK-9220, Aalborg Ost, Denmark
broe@physics.aus.dk

Aurelin Bruyant
University of Technology of Troyes, 12 rue Marie Curie, BP 2060, 10000 Troyes, France
aurelien.bruyant@utt.fr

Garnett Bryant
National Institute of Standards and Technology, 100 Bureau Drive, Mail Stop 8423, Gaithersburg, MD, USA
garnett.bryant@nist.gov

Ahmad Bsiesy
Laboratoire de Spectrometrie Physique, University of Grenoble and CNRS – France, Rue de la Physique, Saint Martin d'Heres, France
ahmad.bsiesy@ujf-grenoble.fr

Pierre Burgos
National Research Council Canada, 100 Sussex Drive, Ottawa, Ontario, Canada
Pierre.burgos@nrc.ca

Andrea Callegari
University of Lausanne, BSP-Dorigny, Lausanne, VD, Switzerland
Andrea.Callegari@ipmc.unil.ch

Paul Carney
University of Illinois at Urbana-Champaign, 3009 BI/MC251, 405 N. Mathews Ave., Urbana, IL, 61801, USA
schappel@uiuc.edu

William Challener
Seagate Technology, 1251 Waterfront Place, Pittsburg, PA, USA
william.a.challener@seagate.com

Sungchin Chang
Seoul National University, Shillim-dong, Kwanak-gu, Seoul, South Korea
sjchang62@phya.snu.ac.kr

John Chappell
University of Sheffield, Department of Physics and Astronomy, Hicks Building, Hounsfield Road, Sheffield, S3 7RH, UK
John.Chappell@sheffield.ac.uk

Hojin Cho
Seoul National Unviersity, Shillim-dong, Kwanak-gu, Seoul, South Korea
mpbs@phya.snu.ac.kr

Keith Cohn
Stanford University, 1221 S El Camino Real # 309, San Mateo, CA, USA
kcohn@stanford.edu

Alexander Connor
King's College London, Strand, London WC2R 2LS, UK
Alexander.Connor@Kcl.ac.uk

Haim Cory
Technion-Electrical Engineering Dept., Technion City, Haifa 32000, Israel
cory@ee.technion.ac.il

Hans Danzebrink
PTB, Bundesallee 100, 38116, Braunschweig, Germany
Hans-Ultich.Danzebrink@ptb.de

Barbel de Bakker
University of Twente, Faculty of Applied Physics, Applied Optics Group, PO Box 217, 7500 AE, Enschede, The Netherlands
b.I.debakker@tn.utwente.nl

Martina De Serio
ETH Honggerberg, ETH Honggerberg HCI D 325, CH-8093, Zurich, Switzerland
martina.deserio@org.chem.ethz.ch

Yannick De Wilde
ESPCI/CNRS UPRA0005, Laboratoire d'Optique, 10, rue Vauquelin, Paris, 75005, France
dewilde@optique.espci.fr

Volker Deckert
TU Dresden, George-Bahr-Str.1, Dresden, Germany
deckert@iapp.de

Wayne Dickson
Queen's University Belfast, University Road, Belfast, CO Antrim, Northern Ireland
w.dickson@qub.ac.jk

Severine Diziain
University of Technology of Troyes, 12 rue Marie Curie, BP 2060, 10000 Troyes, France
severine.dizian@utt.fr

Jeff Doran
Digital Instuments, Veeco, 112 Robin Hill Road, Sata Barbara, CA, 93117, USA
infor@di.com

Aurelien Drezet
University of Grenoble, BP 87, St. Martin d'Heres, France
aurelien.drezet@ujf-grenoble.fr

Carole Ecoffet
DPG-CNRS UMR7525, 3, rue A Werner, F-68093 Mulhouse, France
cecoffet@uha.fr

Valentine Emiliani
LENS, Via N. Carrara 1, Sesto Fiorentino, Firenze, Italy
emiliani@lens.unifi.it

Jeorg Enderlein
IBI-1, Forschungszentrum Juelich, D-52425 Juelich, Germany
j.enderlein@fz-juelich.de

Lukas Eng
TU Dresden, Mommsenstr. 13, Dreseden, Sazony, Germany
eng@ispp.de

Wunshain Fann
Academia Sinica, P.O. bopx 23-166, Taipei, Taiwan
fann@gate.sinica.edu.tw

Frederic Festy
King's College London, Strand, London WC2R 2LS, UK
frederic.festy@kcl.ac.uk

Radouane Fikri
University of Technology of Troyer, 12 rue Marie Curie, BP 2060, 10000 Troyes, France
radouane.fikri@utt.fr

Ulrich Fischer
Physikalischer Institu, Universitat Muenster, Wilhelm Klemmstr. 10, 48149, Muenster, Germany
fischeu@nwz.uni-muenster.de

Mark Flowers
RHK Technology, Inc, 1050 East Maple Road, Troy, MI, 48083, USA
green@rhk-tech.com

Alexandra Fragola
Optics Group-ESPCI-CNRS-UPMC, Laboratoire d' Optique Physique ESPCI, 10 rue Vanquelin 75005, Paris, France
fragola@optique.espci.jr

Yuan Hsing Fu
Department of Physics, National Taiwan University, 1 Sec 4, Roosevelt Road, Taipei, Taiwan, R.O.C
murphy@phys.ntu.edu.tw

Masanori Fujinami
The University of Tokyo, 7-3-1 Hongo, Bunkyo-ku, Tokyo, Japan
fujinami@k.u-tokyo.ac.jp

Masuo Fukui
University of Tokushima, 2-1 Minami-josanjima, Tokushima, Japan
fukui@opt.tokushima-u.ac.jp

Anselm Gademann
Trinity College Dublin, Physics Department, Trinity College, Dublin, Ireland
gademana@tcd.ie

Kristin Galbally
Colorado School of Mines, Physics Department, Golden, CO, 80401-1887, USA
kgalball@mines.edu

Henkjan Gersen
MESA Research Institute, University of Twente, PO Box 217, 7500 AE, Enschede, The Netherlands
H.Gersen@tiv.utwente.nl

Jordan Gerton
Caltch, 1200 E. California Blvd, Pasadena, CA, USA
jgerton@caltech.edu

Lerondel Gilles
University of Technology of Troyer, 12 rue Marie Curie, B.P. 2060, 10,000 Troyes, France
gilles@lreondel@utt.fr

Bennett Goldberg
Boston University, Physics Department, 590 Commonwealth Ave., Boston, MA, USA
goldberg@bu.edu

Lori Goldner
NIST, Stop 8441 100 Bureau Drive, Gaithersburg, MD, 20899, USA
lori.goldner@nist.gov

Claudiu Gradinaru
Leiden University, Niels Bohrweg 2, Leiden, The Netherlands
claudiu@biophys.leidenuniv.nl

Jean-Jacques Greffet
Ecole Voie des Vignes, Grande Voie des Vignes, Chatenay-Malabry, F-92295, France
greffet@em2c.ecp.fr

Samuel Gresillon
Optics GroupUPMC & CNRS, ESPC 1, 10 Rue Vauquelin, 75231 Paris, France
gresillon@optique.espri.fr

Thierry Grosjean
University of Franche-Comte, 16, route de Gray, Besancon, Franche-Comte, France
thierry.grosjean@univ-fcomte.fr

Pietro Gucciardi
CNR-IPCF sez. Messina, Via La Farina 237, Messina, Italy
gucciardi@me.cnr.it

Jay Gupta
UC Santa Barbara
gupta@qi.ucsb.edu

Rob Gutierrez
Eastman Kodak, ATD: Research Labs Bldg 82, Rochester, NY, 14650-2105, USA
rob.gutierrez@kodak.com

Daniel Haefliger
Nonotechnology Group, Swiss Federal Institute of Technology Zurich, Tannenstrasse 3, CH-8092, Zurich, Switzerland
haefliger@nano.mavt.ethz.ch

Hans Hallen
North Carolina State University, Campus Box 8202, Raleigh, NC, USA
Hans_Hallen@ncsu.edu

Masanobu Haraguchi
University of Tokushima, 2-1 Minami-josanjima, Tokushima, Japan
haraguti@opt.tokushima-u.ac.jp

Achim Hartschuh
University of Rochester, The institute of Optics, Rochester, New York 14627, USA
harschu@optics.rochester.edu

Masahiro Hasuo
Kyoto University, Sakyou-ku Yoshidahonmachi, Kyoto, Kyoto, Japan
hasuo@kues.kyoto-u.ac.jp

Norihiko Hayazawa
2-1Yamada-oka, Suita, Osaka, Japan
hayazawa@ap.eng.osaka-u.ac.jp

Fekhra H'Dhili
University of Technology of Troyes, 12 rue Marie Curie, B.P. 2060, 10 000 Troyes, France
fekhra.hdhili@utt.fr

Alan Heaney
Institute of Optics, University of Rochester, Rochester, NY, 14627, USA
Heaney@earthlink.net

Bert Hecht
University of Basel, Physics Institute, Klingelbergstr. 82, Basel, Switzerland
bert.hecht@nano-optics.ch

Ahmed Heikal
Cornell University, 213 Clark Hall, Ithaca, New York, USA
aah14@cornell.edu

Fred Henn
Omicron Nanotechnology USA, 1226 Stoltz Road, Bethel Park, PA, 15102, USA
infor@omicronus.com

Daniel Higgins
Kansas State University, 111 Willard Hall, Manhatten, KS, USA
higgins@ksu.edu

Rainer Hillenbrand
MPI Biochemie, D-82152, Martinsried, Germany
hillenbr@biochem.mpg.de

Fu Han Ho
Department of Physics, National Taiwan University, 1 Sec 4, Roosevelt Rd, Taipei 106, Taiwan, R.O.C.
fuhanho@phys.ntu.edu.tw

Christiane Hoeppener
Westfaelische-Wilhelms-Universitaet Muenster, Physikalisches Institut, Wilhelm-Klemm-Str. 10, Muenster, 48149 Muenster, Germany
hoppenc@uni-muenster.de

Johan Hofkens
Kuleuyen, Department of Physics, Lelestijnenlaan 200 F, 3001, Heverlze, Belgium
johan.hofkens@chem.kulzuven.ac.be

Sung Chul Hohng
Univ. of Illinois at Urbana-Champaign, 1110 West Green Street, Urbana, IL
shohng@uius.edu

Thomas Huser
Lawrence Livermore National Laboratory, 7000 East Ave, Livermore, CA
huser1@llnl.gov

Filipp Ignatovich
Institute of Optics, University of Rochester, Rochester, NY, 14627, USA
philipp@optics.rochester.edu

Shinzaburo Ito
Kyoto University, Sakyo, Kyoto, Japan
sito@polym.kyoto-u.ac.jp

Futoshi Iwata
Shizuoka Univ., 3-5-1 Johoku, Hamamatsu, Shizuoka, Japan
tmfiwat@ipc.shizuoka.ac.jp

Torsten Jaehnke
JPK Instruments, Bouchestrasse 12, 12435 Berlin, Germany
Jaehnke@jpk.com

Catherine Jahncke
St. Lawrence University, Physics Department, Canton, NY, 13617,USA
cjah@stlawu.edu

Wonho Jhe
Seoul national University, Shillim-dong, Kwanak-gu, Seoul, South Korea
whje@snu.ac.kr

Karl Joulain
Ecole Centrale Paris, Grande Boie Des Bigres, Chatenay-Malabry, Paris, France
joulain@em2c.fr

Cecile Juekens
HFML/NSRIM, University of Nijmegen, Toernooiveld 1, 6525 ED, Nijmegen, Gelderland, The Netherlands
cecilej@sci.kun.nl

Thomas Kalkbrenner
Universitat Konstanz, Universitatsstr. 10, 78464 Konstanz, Baden, Germany
Thomas.Kalkbrenner@uni-konstanz.de

Tsung Sheng Kao
Department of Physics, National Taiwan University, 1 Sec 4, Roosevelt Road, Taipei, Taiwan, R.O.C.
sheng@phys.ntu.edu.tw

Peter Karageorgiev
University of Potsdam, Germany, Am Neuen Palais 10, Potsdam, Potsdam 14469, Germany
ppkara@rz.uni-potsdam.de

Satoshi Kawata
Osaka University, 2-1 Yamadaoka, Suita, Osaka, Japan
kawata@ap.eng.osakak-u.ac.jp

Yoshimasa Kawata
Shizwoka University, Department of Mechanical Engineering, Johoku, Hamamatsu 432-8561, Japan
kawata@eng.shizwoka.ac.jp

Fritz Keilmann
MPI Biochemie, D-82152, Martinsried, Germany
keilmann@biochem.mpg.de

Ole Keller
Bente Keller, Institute of Physics, Aalborg University, Pontoppidanstraede 103, DK-9220, Aalborg Ost, Denmark
okeller@physics.auc.dk

Fabian Kiendl
Aachen University of Technology, Templergraben 55, 52056 Aachen, NRW, Germany
Fabian.Kiendl@physik.rwth-aachen.de

Gyu Man Kim
EPFL, STI-IMM, EPFL, Lausanne, CH 1015 Lausanne, Switzerland
gyuman.kim@epfl.ch

Jeongyong Kim
University of Incheon, Dowha-dong 177, Nam-ku, Incheon, Kyoungki, South Korea
jeongyong@incheon.ac.kr

Tae-Won Kim
Japan Science and Technology Corporation (JST), Tsuruma, Tenko 17 bldg., 687-1, Machida City, Tokyo, Japan
twkim90@ohtsu.jst.go.jp

Vasily Klimov
P.N. Lebedev Physical Institute, Leninsky prospect, 53, Moscow, Russia
klimov@rim.phus.msu.su

Rajiv Kohli
RK Associates, 2450 Airport Road, #D-238, Longmont, CO, 80503, USA
kohlirkassoc@hotmail.com

Marjolein Koopman
University of Twente, Faculty of Applied Physics, Applied Optics Group, PO Box 217, 7500AE, Enschede, The Netherlands
m.koopman@tn.utwente.nl

Patrick Kramper
Universitat Konstanz, Universitatsstr. 10, 78457 Konstanz, FB Physik, Germany
patrick.Kramper@uni-konstanz.de

Joachim Krenn
Karl-Franzens-University, Universitatsplatz 5, Graz, Stmk, Austria
joachim.krenn@kfunigraz.ac.at

John Krug
Harvard University Dept. of Chemistry and Chemical Biology, 12 Oxford Street, Cambridge, MA, USA
jkrug@fas.harvard.edu

Kobus Kuipers
MESA Research Institute, University of Twente, PO Box 217, 7500 AE, Enschede, The Netherlands
L.Kuipers@Utwente.nl

Andreas La Rosa
Portland State University, Physics Department, Portland, Oregon, USA
andres@pdx.edu

Marc Lamy
University of Technology of Troyes, 12, rue marie Curie, B.P. 2060, 10 000 Troyes, France
marc.lamydelachapelle@utt.fr

Gilles Lerondel
University of Technology of Troyes, 12, rue Marie curie of Troyes, B.P. 2060, 10 000 Troyes, France
gilles.lerondel@utt.fr

Gaetan Leveque
Universite paul Sabatier IRSAMC/LCAR, 118 route de Narbonne, Toulouse, Haute Garonne, France
gaetan.leveque@irsamc.ups-tlse.fr

Geoffrey Lewen
NECI, 4 Independence Way, Princeton, NJ, USA
geoff@research.nj.nec.com

Mikhail Libenson
S. I. Vavilov State Optical Institute, 12, Birzhevaya Liniya, St. Petersburg, 199034,-Russia
libenson@beam.ifmo.ru

Andreas Lieb
Institute of Optics, University of Rochester, Rochester, NY, 14627, USA
lieb@optics.rochester.edu

Christoph Lienau
Max-Born Institut, Max-Born-Str. 2A, Berlin, Germany
lienau@mbi-berlin.de

Hsia Yu Lin
National Taiwan University, No. 1, Sec 4, Roosevelt Road, Taiwan
hyling@phys.ntu.edu.tw

Wei-Chih Liu
National Taiwan Normal University, 88 Sec. 4 Ting Chou Rd., Taipei, Taiwan
wcliu@phy.ntnu.edu.tw

Nien Hua Lu
De Lin Institute of Technology, No.1, Lane 380, Ching-Yun Road, Tu-Cheng City, Taiwan
nhlu@sitc.edu.tw

Alfred Meixner
University of Siegen, Adolf-Reichwinstr. 2, Siegen, NRW, Germany
meixner@chemie.uni-siegen.de

Jeremy Melanson
Swiss Federal Institute of Technology, ETH Honggerberg, Department of Chemistry, HCL D 325, CH 8093, Zurich, Switzerland
melanson@org.chem.ethz.ch

Gereon Meyer
Freie Universitat Berlin, Fachbereich Physik, Arnimallee 14, 14195 Berlin, Berlin, Germany
meyerg@physik.fu-berlin.de

Brun Mickael
Laboratoire de Spectometrie Physique, CNRS/UJF Grenoble, BP87 38402 Saint Martin d'Heres cedex, Grenoble, France
mickael.brun@ujf-grenoble.fr

Katsunari Mikage
Shizuoka Univ., 3-5-1 Johoku, Hamamatsu, Shizuoka, Japan
f0130065@ipc.shizuoka.ac.jp

Daniel Molenda
Muenster University, Wilhelm Klemmstr. 10, 48149 Muenster, NRW, Germany
molenda@uni-muenster.de

Andreas Naber
Physics Institute, Wilhelm-Klemm-Str.10, Munster, NRW, Germany
naber@uni-muenster.de

Wataru Nakagawa
Univ. of California, San Diego, 9500 Gilman Drive ECE 0407, La Jolla, CA, USA
wnakagaw@ucsd.edu

Ken Nakajima
RIKEN, 2-1 Hirosawa, Wako, Saitama, Japan
knakaji@local.riken.go jp

Antonello Nesci
University of California, San Diego, Department of Electrical and Computer Engineering, 9500 Gilman Drive, Mail Code 0407, La Jolla, CA, 92093-0407, USA
nesci@ece.ucsd.edu

Toshio Ohtani
National Food Research Institute, Kannondai 2-1-12, Tsukuba, Ibaraki 305-8642, Japan
ohtani@affrc.go.jp

Takayuki Okamoto
RIKEN, Hirosawa, Wako, Saitama 351-0198, Japan
okamoto@optsun.riken.go.jp

Toshihiro Okamoto
University of Tokushima, 2-1 Minami-jyosanjima, Tokushima 770, Japan
okamoto@opt.tokushima-u.ac.jp

Teppei Onuki
Tokyo University of Science, 1-1-1 Umezono, Tsukuba, Ibaraki, Japan
onuki-t@aist.go.jp

Tobias Otto
University of Technology-Dresden, George-Baehr-Strasse 1, D-01069 Dresden, Saxony, Germany
otto@iapp.de

Mi-Young (Molly) Park
Institute of Optics, University of Rochester, Rochester, NY, 14627, USA
mp002i@mail.rochester.edu

Seung-Han Park
Yonsei University, 134 Shinchondong Seodaemoongu, Seoul, Seoul, Republic of Korea
shpark@phya.yonsei.ac.kr

Royer Pascal
University of Technologie of Troyes, 12, rue Marie Curie, B.P. 2060, 10,000 Troyes, France
pascal.royer@utt.fr

Dieter Pohl
University of Basel, Physics Institute, Klingelbergstr.82, Basel, Switzerland
Dieter.Pohl@unibas.ch

Helmut Port
University of Stuttgart, Pfaffenwaldring 57, 70550 Stuttgart, Baden-Wuertt, Germany
h.port@physik.uni-stuttgart.de

Juan Porto
Chalmers University of Technology, Department of Applied Physics, Gothenburg, SE-412 96 Goteborg, Sweden
jporto@fy.chalmers.se

Jurius Prikulis
Chalmers University of Technology, Fysikgrand 3, Gothenburg 41296, Sweden
prikulis@fy.chalmers.se

Nicole Putnam
Institute of Optics, University of Rochester, Rochester, NY, 14627, USA
np002i@mail.rochester.edu

Huihe Qiu
Hong Kong University of Science and Technology, Department fo Mechanical Engineering, Clear Water Bay, KLN, Hong Kong
mequi@ust.hk

Romain Quidant
Submicron Optics Group/University of Burgundy, 9 Avenue Alain Savary, Dijon, France, 21000
rquidant@u-bourgogone.fr

Fikri Radouane
University of Technology of Troyes, 12, rue Marie Curie B.P. 2060 10000 Troyes , France
radouane.fikri@utt.fr

Michael Rappaport
Weizman Institute of Science, Physics Services, Rehovot, Israel
michael.rappaport@weizmann.ac.il

Januskevicius Regimantas
Max-Planck Institiute for Biophysical Chemistry, Department of Molecular Biology
Am Falsberg 11, Gottingen, D-37077, Germany
zjanusk@gwdg.de

Bachelot Renaud
University of Technology of Troyes, 12, rue marie Curie, B.P. 2060, 10 000 Troyes, France
renaud.brachelor@utt.fr

Jan Renger
University of Technology-Dresden, George-Baehr-Strasse 1, D-01069 Dresden, Saxony, Germany
renger@iapp.de

Barbara Ressel
TASC Laboratory - INFM, Strada Statale 14 km. 163.5, Basovizza, Trieste, Italy
ressel@tasc.infm.it

Robert Riehn
University of Cambridge, Madingley, Cambridge, Cambridgeshire, UK
rr242@cam.ac.uk

Karsten Rottwitt
Technical Univ. of Denmark, Building 345v, 2800 Lyngby, Denmark
kar@com.dtu.dk

Pascal Royer
University of Technologie of Troyes, 12, rue Marie Curie, B.P. 2060, 10 000 Troyes, France
pascal.royer@utt.fr

Toshisharu Saiki
KAST, 3-2-1 Sakado, Takatsu, Kawasaki, Kanagawa, Japan
saiki@net.ksp.or.jp

Erik Sanchez
Harvard University Dept. of Chemistry and Chemical Biology, 12 Oxford Street, Cambridge, MA, USA
esanchez@fas.harvard.edu

Antonio Santos
Universidade de Sao Paulo, C.P. 66318, Sao Paulo, Brazil
adsantos@if.usp.br

Hannes Schniepp
Swiss Federal Institute of Technology (ETH), Laboratorium fur Phyikalische Chemie, ETH Zurich, Zurich, CH-8093, Switzerland
hannes.schniepp@ethz.ch

Hugo Schouten
Free University Amsterdam, Boelelann 1081, 1081 HV, Amsterdam, The Netherlands
hfschout@nat.vu.nl

Jan Seidel
University of Technology-Dresden, George-Baehr-Strasse 1, D-01069, Saxony, Germany
jseidel@iapp.de

Kursat Sendur
Seagate Research, 1251 Waterfront Place, Pittsburgh, PA, 15222, USA
kursat.sendur@seagate.com

Yongho Seo
Seoul National Unviersity, Shillim-dong, Kwanak-gu, Seoul, South Korea
yonghoseo@phya.snu.ac.kr

Sekatskii Sergey
Inst. Phys. Mat. Cond., Universite de Lausanne, BSP, CH 1015 Lausanne, Switzerland
sergey.sekatskii@ipmc.unig.ch

Tero Setala
Helsinki University of Technology, Optics and Molecular Materials, Univ. Of Technology P.O. Box 2200, Fin-02015, HUT, Finland
tsetala@focus.hatifi

Diziain Severine
University of Technology of Troyes, 12, rue Marie Curie, BP 2060, 10 000 Troyes, France
serverine.dizian@utt.fr

Xiaolei Shi
Stanford University, CISX Bldg, Rm 133, Department of Electrical Engineering, Stanfrod, CA, 94305-4075, USA
xiaolei@stanford.edu

Akira Shojiguchi
JST/ERATO, 687-1 Tsuruma, Machida, Tokyo, Japan
akirasho@ohtsu.jst.go.jp

Tomoo Sigehuzi
National Institute of Advanced Industrial Science/T, Umezono 1-1-1, Tsukuba, Ibaraki, Japan
sigehuzi.tomoo@aist.go.jp

Dmitrii Simanovskii
Stanford University, 445 Via Palou str., Stanford, CA, USA
simanovski@stanford.edu

Urs Staufer
Inst. Of Microtechnology, University of Neuchatel, Jaquet-Droz 1, CH-2007, Neuchatel, Switzerland
urs.staufer@unine.ch

Junichi Takahara
Osaka University, Machikaneyama 1-3, Toyonaka, Osaka, Japan
takahara@ee.osaka-u.ac.jp

Satoshi Takahashi
Queen's University of Belfast, University Road, Belfast BT 7 1NN, Northern Irelane, UK
s.takahashi@qub.ac.uk

Naoto Tamai
Kwansei Gakuin University, 2-1, Sanda, Hyogo, Japan
tamai@ksc.kwansei.ac.jp

Hiroharu Tamaru
The University of Tokyo, Komaba 4-6-1, Meguro-ku, Tokyo 153-8904, Japan
tamaru@myn.rcast.u-tokyo.ac.jp

Kazuo Tanaka
Gifu University, Yanagido, Gifu City, Gifu Prefecture, Japan
tanaka@tnk.info.gifu-u.ac.jp

Shu-Guo Tang
Optical Sciences Center, University of Arizona, Tucson, AZ, 85721, USA
tangs@u.arizona.edu

Thomas Taubner
MPI Biochemie, D-82152, Martinsried, Germany
taubner@biochem.mpg.de

Paul Tchenio
CNRS, Laboratoir Aime Colton, 91405 Orsay Ledex, , France
paul.tchenio@lac.u-psud.fr

Tineke Thio
NEC Research Institute, 4 Independence Way, Princeton, NJ, 08540, USA
tineke@research.nj.nec.com

Marjorie Thomas
Ecole Centrale Paris-Laboratoire EM2C, Grande Voie des Vignes, Chatenay-Malabry, 92 295, France
marjorie@em2c.ecp.fr

Satoshi Tojo
Kyoto University, Sakyoku, Yoshidahommachi, Kyoto, Japan
tojo@pianica.mbox.media.kyoto-u.ac.jp

Takashi Tokizaki
National Institute of Adv. Industrial Sci. & Tech., AIST Tsukuba Central 2, Tsukuba, Ibaraki 305-8568, Japan
t-tokizaki@aist.go.jp

Pavel Tomanek
Brno University of Technology, Department of Physics, Technicka 8, Brno, Czech Republic
tomanek@feec.vutbr.cz

Julien Toquant
Institute for Physics, Klingelbergstrasse, 82, CH-4056 Basel, Switzerland
julien.toquant@unibas.ch

Pierpasquale Tortora
IMT University of Neuchatel, Rue A.-L. Breguet 2, Neuchatel, CH, Switzerland
piero.tortora@unine.ch

Sven Trogisch
University of Technology-Dresden, George-Baehr-Strasse 1, D-01069 Dresden, Saxony, Germany
trogisch@iapp.de

Din Ping Tsai
National Taiwan University, Department of Physics, Taipei, Taiwan
dptsai@phys.ntu.edu.tw

Selim Unlu
Boston University, 8 Saint Mary's St., Boston, MA, USA
selim@bu.edu

Luciana Vaccaro
Institute of Microtechnics, Universisty of Neuchatel, Rue A.-L. Breguet 2, Neuchatel, CH, Switzerland
luciana.vaccaro@unine.ch

Erik Van Dijk
University of Twente, PO Box 217, 4500 AE, Enschede, The Netherlands
E.M.H.P.VanDijke@an.ufwenke.ne

Nick van Hulst
University of Twente, PO Box 217, 7500 AE, Enschede, Netherlands
n.f.vanhulst@tm.utwente.nl

Daniel Van Labeke
Laboratoire P.M. Duffieux, University of Besancon, route de Gray, Besancon, Doubs, France
daniel.vanlabeke@univ-fcomte.fr

Fernando Vargas
Pontificia Universidad Catolica de Chile, Vicuna Mackenna 4860, Santiago, RM, Chile
fvargas@fis.puc.cl

Taco Visser
Free University, De Boelelaan 1081, Amsterdam, Netherlands
tvisser@nat.vu.nl

Ralf Vogelgesaug
Max Plauck-Institut fur Festkorperforschung, Heisenberg str. 1, 70569, Stuttgart, Germany
r.vogelgesaug@fkf.mpg.de

Valentyn Volkov
Institute of Physics, AAU, Pontoppidanstraede 103, DK-9220, Aaeborg Ost, Denmark
volkov@physics.auc.dk

Ian Walmsley
University of Oxford, Clarendon Laboratory, Oxford, England, UK
walmsley@physics.ox.ac.uk

Jing Jing Wang
Dept of Physics & Astronomy, University of Leeds, Leeds, LS2 9TT, UK
phyjjw@phynov.leeds.ac.uk

Cheng-Hung Wei
National Taiwan University, No. 1, Roosevelt Road, Section 4, Taipei, Taiwan
shauhong.tw@yahoo.com.tw

PeiKuen Wei
Caser, Academia Sinica, 128, Sec.2, Academic Rd. Nankang, Taipei, Taiwan
pkwie@gate.sinica.edu.tw

John Weiner
Universite Paul Sabatier IRSAMC/LCAR, 118 route de Narbonne, Toulouse, France
jweiner@irsamc.ups-tlse.fr

Klaus Weishaupt
WITec Wissens Instruments and Technology Gmbh, Hoervelsinge Weg 6 D-89081, Ulm, Germany
info@witec.de

Matthias Wellhoefer
University of Ulm, Albert-Einsteing-Allee 11, Ulm, 89069 Ulm, Germany
matthias.wellhoefer@witec.de

Jeffrey White
University of Illinois, Frederick Seitz Materials Research Laboratory, Urbana, Illinois, 61801, USA
white5@vive.edu

Gary Wiederrecht
Argonne National Laboratory, 9700 South Cass Avenue, Bldg. 200, Argonne, Illinois, USA
wiederrecht@anl.gov

Jorg Woehl
University of Grenoble, BP 87, Saint Martin d'Heres, France
jorg.woehl@ujf-grenoble.fr

Emil Wolf
Institute of Optics, University of Rochester, Rochester, NY, 14627, USA
ewlupus@pas.rochester.edu

Gregory Wurtz
Argonne National Lab, Chemistry Division 9700 S. Cass Avenue, Argonne, IL, 60439, USA
wurtz@anl.gov

Xiaoliang (Sunney) Xie
Harvard University, Dept. of Chemistry & Chemical Biology, 12 Oxford St., Cambridge, MA, USA
xie@chemistry.harvard.edu

Noritaka Yamamoto
National Institute of Advanced Industrial Science, (AIST), 1-8-31Midorigaoka, Ikeda, Osaka 563-8577, Japan
noritaka.yamamoto@aist.go.jp

De-Ming Yang
Department of Medical Research 7 Education, Taipei Veterans General Hospital, No. 201, Sec. 2, Shih Pai Road,, Taipei 11271, Taiwan
dmyang@vghtpe.gov.tw

Takashi Yatsui
ERATO, JST, 687-1 Tsuruma, Machida, Tokyo, Japan
yatsui@ohtsu.jst.go.jp

Yossi Yayon
Weizmann Institute, Condensed Matter Physics, Rehovot, 76100, Israel
hyayon@wisemail.weizmann.ac.il

Sang Youp Yim
Yonsei University (Dept. of Physics), 134 Shinchondong Seodaemoongu, , Seoul, Rep of KOREA
syim@phya.yonsei.ac.kr

Youngjun Yu
Seoul National University, Shillim-dong, Kwanka-gu, , Seoul, South Korea
exciton@phya.snu.ac.kr

Anatoly Zayats
The Queen's University of Belfast, University Road, Belfast, UK
a.zayats@qub.ac.uk

Renato Zenobi
ETH Zurich, HCI E 329, CH-8093 Zurich, Switzerland
zenobi@org.chem.ethz.ch

Qiwen Zhan
University of Minnesota, 4-174 EE/Csci Building, 200 Union St SE, Minneapolis, MN, USA
qzhan@ece.umn.edu

Jorge Zurita-Sanchez
Institute of Optics, University of Rochester, Rochester, NY, 14627, USA
jzurita@optics.rochester.edu

Additional information

Emergency

In case of emergency while on-campus, you may use one of the outside emergency phones marked with a blue light. Dial 13. You may also dial 13 from any on-campus phones. If you are using off-campus phone, dial 911 (no money is required to call 911 from a payphone).

In case you are left behind during an excursion or get lost, you may call one of the local organizing committee members at 585-305-1516.

Where to check your email

There are few places to check your e-mail. The closest place is Carlson library (see map). You may also use Rush Rhees library terminals. However telnet is not available on the library's terminals. If you use telnet, go to CLARC computer center located in the same building as Rush Rhees library, northern entrance (see map).

Going to and from hotels

A list of shuttle times have been provided in the Conference Schedule. Busses will depart every 1/2 hour during the allotted times.

In case you you need to go from a hotel to the University during the time when conference shuttles do not operate, ask for a free shuttle ride at the reception desk. The hotels you are staying in have a complimentary shuttle service within a certain mile radius from the hotel (12 miles for Holiday Inn, 5 miles for Radisson). The University, as well as downtown Rochester, is located within this distance.

In case you need to go from the conference to a hotel while no conference shuttles are available, the easiest way is to call a cab. "Checker cab" 325-2460. "Associate cab" 232-3232.

Post-office

On campus post office is located in Todd Union building. Working hours are 10am to 5pm.

Campus parking

Daily parking permits are available at the Information Booth at the entrance to the University for $3.25.